

FUNCTIONAL CHARACTERIZATION OF PEROXISOMES AND PATHOLOGICAL CONSEQUENCES OF PEROXISOMAL DYSFUNCTION IN THE LUNG

SRIKANTH KARNATI

INAUGURAL DISSERTATION

submitted to the Faculty of Medicine
in partial fulfilment of the requirements
for the PhD-degree of the
Faculties of Veterinary Medicine and Medicine
of the Justus Liebig University Giessen



édition scientifique
VVB LAUFERSWEILER VERLAG

Das Werk ist in allen seinen Teilen urheberrechtlich geschützt.

Jede Verwertung ist ohne schriftliche Zustimmung des Autors oder des Verlages unzulässig. Das gilt insbesondere für Vervielfältigungen, Übersetzungen, Mikroverfilmungen und die Einspeicherung in und Verarbeitung durch elektronische Systeme.

1. Auflage 2009

All rights reserved. No part of this publication may be reproduced, stored in a retrieval system, or transmitted, in any form or by any means, electronic, mechanical, photocopying, recording, or otherwise, without the prior written permission of the Author or the Publishers.

1st Edition 2009

© 2009 by VVB LAUFERSWEILER VERLAG, Giessen
Printed in Germany



édition scientifique
VVB LAUFERSWEILER VERLAG

STAUFENBERGRING 15, D-35396 GIESSEN
Tel: 0641-5599888 Fax: 0641-5599890
email: redaktion@doktorverlag.de

www.doktorverlag.de

**Functional characterization of peroxisomes and
pathological consequences of peroxisomal
dysfunction in the lung.**

Inaugural Dissertation
submitted to the
Faculty of Medicine
in partial fulfilment of the requirements
for the PhD-degree
of the Faculties of Veterinary Medicine and Medicine
of the Justus Liebig University Giessen

by

Srikanth Karnati

of

Suryapet, India

Giessen 2009

From the Institute for Anatomy and Cell Biology II
of the Faculty of Medicine of the Justus Liebig University of Giessen
Director / Chairperson: Prof. Dr. Eveline Baumgart-Vogt

First Supervisor and Committee Member: Prof. Dr. Eveline Baumgart-Vogt
Second Supervisor and Committee Member: Prof. Dr. Peter Gehr (Bern)
Examination chair and Committee Member: Prof. Dr. Martin Diener
Committee Member: Prof. Dr. Ralph Brehm

Date of Doctoral Defense
14th Aug 2009

Declaration

"I declare that I have completed this dissertation single-handedly without the unauthorized help of a second party and only with the assistance acknowledged therein. I have appropriately acknowledged and referenced all text passages that are derived literally from or are based on the content of published or unpublished work of others, and all information that relates to verbal communications. I have abided by the principles of good scientific conduct laid down in the charter of the Justus Liebig University of Giessen in carrying out the investigations described in the dissertation."

Date: 14th Aug 2009

(Srikanth Karnati)

Place: Giessen, Germany

My parents

Karnati Swarajya Laxmi, Karnati Sathyanarayana

My wife

Porwal Manvi

And

My family

Table of Contents

| | |
|---|-----------|
| 1 INTRODUCTION | 1 |
| 1.1 DISCOVERY OF PEROXISOMES AND PEROXISOMAL ENZYMES | 1 |
| 1.2 GENERAL FUNCTIONS OF PEROXISOMES | 2 |
| 1.2.1 <i>The peroxisomal β-oxidation system</i> | 4 |
| 1.2.1.1 Peroxisomal β -oxidation enzymes | 5 |
| 1.2.2 <i>Biosynthetic pathways of cholesterol and ether-phospholipids in peroxisomes</i> | 7 |
| 1.3 BIOGENESIS OF PEROXISOMES..... | 7 |
| 1.3.1 <i>Peroxisomal targeting signals</i> | 8 |
| 1.3.2 <i>Docking of the cargo-receptor complex to the peroxisomal membrane</i> | 9 |
| 1.3.3 <i>Translocation, dissociation and receptor cycling</i> | 10 |
| 1.3.4 <i>Import and assembly of peroxisomal membrane proteins</i> | 10 |
| 1.3.5 <i>Peroxisome growth and division</i> | 11 |
| 1.3.6 <i>Peroxisomal diseases</i> | 12 |
| 1.4 PATHOLOGICAL CONSEQUENCES OF PEX11 β DEFICIENCY | 13 |
| 1.5 ANIMALS MODELS FOR GENERAL PEROXISOMAL BIOGENESIS DISORDERS (PEX5, PEX2 AND PEX13 KNOCKOUT MICE) | 14 |
| 1.6 CONTROL OF PEROXISOME ABUNDANCE AND COMPOSITION BY THE ACTION OF NUCLEAR RECEPTORS | 14 |
| 1.6.1 <i>Functions of PPARγ in organ systems</i> | 15 |
| 1.6.2 <i>PPARs in the lung</i> | 16 |
| 1.6.3 <i>Molecular mechanisms of PPAR transcription</i> | 16 |
| 1.7 RESEARCH SO FAR DONE ON PEROXISOMES IN MOUSE AND HUMAN LUNGS | 17 |
| 1.8 PEROXISOMES IN DEVELOPMENT AND MATURATION OF THE LUNG | 18 |
| 1.9 PEROXISOMAL METABOLIC CHANGES DURING TRANSITION OF AECII TO AECl | 18 |
| 1.10 PEROXISOMES IN HUMAN LUNG DISEASES | 19 |
| 2 AIMS OF THE STUDY | 20 |
| 3 MATERIALS & METHODS | 22 |
| 3.1 EXPERIMENTAL ANIMALS, INSTRUMENTS AND MATERIALS | 22 |
| 3.1.1 <i>Experimental animals and patient characteristics</i> | 22 |
| 3.2 LABORATORY INSTRUMENTS, GENERAL MATERIALS, PROTEINS AND CHEMICALS..... | 23 |
| 3.2.1 <i>Kits</i> | 25 |
| 3.2.2 <i>Buffer solutions</i> | 26 |
| 3.2.3 <i>Antibodies</i> | 27 |
| 3.2.4 <i>Primers</i> | 27 |
| 4 METHODS | 30 |
| 4.1 TECHNIQUES FOR LIGHT AND FLUORESCENCE MICROSCOPY | 30 |
| 4.1.1 <i>Fixation of mouse lungs for light microscopy by tracheal instillation</i> | 30 |
| 4.1.2 <i>Immersion fixation of human lungs</i> | 31 |
| 4.1.3 <i>Immunohistochemistry (IHC) with the ABC-peroxidase method</i> | 31 |
| 4.1.4 <i>Indirect immunofluorescence on paraffin sections of wildtype and PEX11β^{-/-} mouse and human and lung tissue</i> | 32 |
| 4.1.5 <i>Indirect immunofluorescence on freshly isolated or cultured AECII</i> | 33 |
| 4.2 TECHNIQUES FOR ELECTRON MICROSCOPY..... | 33 |
| 4.2.1 <i>Fixation and embedding for routine electron microscopy</i> | 33 |

| | | |
|----------|---|-----------|
| 4.2.2 | <i>Cytochemical localization of the catalase activity with the alkaline DAB-method...</i> | 34 |
| 4.2.3 | <i>Post-embedding immunoelectron microscopy.....</i> | 34 |
| 4.2.4 | <i>Illustrations.....</i> | 35 |
| 4.3 | BIOCHEMICAL TECHNIQUES..... | 35 |
| 4.3.1 | <i>Isolation of enriched peroxisomal fractions from frozen lung and liver tissue by differential centrifugation.....</i> | 35 |
| 4.3.2 | <i>Subcellular fractionation of primary AECII for enriched peroxisomal fractions.....</i> | 35 |
| 4.3.3 | <i>Subcellular fractionation of adult mouse liver for enriched peroxisomal fractions..</i> | 36 |
| 4.3.4 | <i>Western blotting.....</i> | 36 |
| 4.3.5 | <i>Catalase activity assay.....</i> | 37 |
| 4.4 | MOLECULAR BIOLOGICAL TECHNIQUES..... | 37 |
| 4.4.1 | <i>RNA isolation.....</i> | 37 |
| 4.4.2 | <i>cDNA synthesis.....</i> | 38 |
| 4.4.2.1 | <i>DNase I digestion.....</i> | 38 |
| 4.4.2.2 | <i>Reverse Transcription.....</i> | 38 |
| 4.4.3 | <i>Primer design.....</i> | 39 |
| 4.4.3.1 | <i>Exon-specific primers.....</i> | 39 |
| 4.4.3.2 | <i>Intron-spanning primers.....</i> | 39 |
| 4.4.4 | <i>Reverse transcription-polymerase chain reaction (RT-PCR).....</i> | 40 |
| 4.4.5 | <i>Gel electrophoresis.....</i> | 41 |
| 4.4.5.1 | <i>Formaldehyde agarose gel electrophoresis for analysis of RNA integrity.....</i> | 41 |
| 4.4.5.2 | <i>Agarose gel electrophoresis for the analysis of RT-PCR products.....</i> | 41 |
| 4.5 | CELL CULTURE METHODS..... | 41 |
| 4.5.1 | <i>Isolation of AECII from adult mouse lungs.....</i> | 41 |
| 4.5.2 | <i>Primary Culture of AECII.....</i> | 42 |
| 5 | RESULTS..... | 43 |
| 5.1 | CHARACTERIZATION OF PEROXISOMES IN MOUSE AND HUMAN LUNG TISSUE WITH VARIOUS MORPHOLOGICAL TECHNIQUES..... | 43 |
| 5.1.1 | <i>Catalase- and Pex14p are detectable in individual peroxisomes of various cell types in mouse and human lungs by immunohistochemistry with the ABC-peroxidase technique.....</i> | 43 |
| 5.1.2 | <i>Double-immunofluorescence labelling reactions confirm the presence of peroxisomes in all pulmonary cell types and reveal the heterogeneity in peroxisomal protein content.....</i> | 46 |
| 5.1.3 | <i>Peroxisomes in AECI contain lower levels of catalase, but high levels of β-oxidation enzymes and the lipid transporter ABCD3.....</i> | 48 |
| 5.1.4 | <i>Peroxisomes in mouse AECII are often tubular, larger in size than in other cell types and show a close association with lamellar bodies.....</i> | 50 |
| 5.1.5 | <i>Post-embedding protein A-gold immunocytochemistry for catalase localization revealed exclusive labelling of peroxisomes.....</i> | 51 |
| 5.1.6 | <i>Peroxisomes are present in all cell types of human donor lungs, are most abundant in AECII and macrophages and show heterogeneity of their enzyme content.....</i> | 53 |
| 5.1.7 | <i>The difference in the distribution and expression of distinct peroxisomal proteins in samples of human and mouse lungs are also revealed in Western blotting experiments.....</i> | 54 |
| 5.2 | CHARACTERIZATION OF PEROXISOMES IN HIGHLY PURIFIED FRESHLY ISOLATED OR CULTURED MOUSE AECII..... | 57 |

| | |
|---|-----------|
| 5.2.1 Immunofluorescence analysis revealed the high purity of the isolated AECII preparations | 57 |
| 5.2.2 Subcellular fractionation of primary AECII revealed a high enrichment of AECII peroxisomes with ACOX1..... | 58 |
| 5.2.3 Downregulation of peroxisomal enzymes during transition of AECII to AECI..... | 60 |
| 5.3 CHARACTERIZATION OF PEROXISOMAL PROTEINS DURING THE NEONATAL DEVELOPMENT OF THE LUNG ... | 64 |
| 5.3.1 The mRNA expression levels of peroxisomal docking complex proteins decrease during the postnatal development of the lung. | 64 |
| 5.3.2 The mRNA level of the peroxisomal lipid transporter, ABCD3 exhibited the biggest differences in expression levels during the postnatal development. | 64 |
| 5.3.3 The mRNA levels for peroxisomal peroxiredoxins are lower expressed in newborn mouse lungs compared to adult animals..... | 65 |
| 5.3.4 Differential mRNA expression levels of ROS metabolizing enzymes of different subcellular compartments..... | 67 |
| 5.3.5 No changes in the mRNA levels of cell-type-specific differentiation markers and of surfactant proteins were noted..... | 67 |
| 5.3.6 Downregulation of catalase activity during the postnatal development of the lung..... | 67 |
| 5.4 PATHOLOGICAL CONSEQUENCES OF PEROXISOME-DYSFUNCTION IN THE LUNG. A STUDY WITH PEX11 β KO MICE | 68 |
| 5.4.1 Upregulation of peroxisomal biogenesis proteins in PEX11 β deficient mouse lungs..... | 68 |
| 5.4.2 Increased mRNA and protein levels of peroxisomal lipid transporter and β -oxidation enzymes of pathway 1..... | 70 |
| 5.4.3 Imbalance of peroxisomal antioxidative enzymes in PEX11 β deficient lungs..... | 70 |
| 5.4.4 Alterations of antioxidant enzymes in other subcellular compartments..... | 70 |
| 5.4.5 Alterations of cell type-specific marker proteins in the PEX11 β KO lungs..... | 74 |
| 5.4.5.1 A severe downregulation of the Clara cell protein CC10 occurred in the lung of PEX11 β -KO mice. | 74 |
| 5.4.5.2 Distinct alterations of surfactant proteins due to PEX11 β deficiency..... | 75 |
| 5.4.5.3 Alterations of the type I cell marker T1 α /podoplanin | 75 |
| 5.4.6 Semi-quantitative RT-PCR analysis of WT, PEX11 β HZ and KO lungs | 78 |
| 5.4.6.1 Severe alterations of expression levels of multiple mRNAs encoding for peroxisomal biogenesis, and lipid metabolic proteins in PEX11 β KO mouse lungs | 78 |
| 5.4.6.2 Imbalance of mRNA levels for ROS metabolizing enzymes of distinct subcellular compartments..... | 78 |
| 5.4.6.3 Alterations of expression levels of the mRNAs encoding for peroxisomal proliferator activated receptors in PEX11 β KO mouse lungs..... | 79 |
| 5.4.6.4 Regulation of Wnt5a in PEX11 β KO mouse lungs | 79 |
| 5.4.6.5 Alterations of mRNA levels for cell type-specific marker proteins and targeting signalling molecules in PEX11 β deficient mouse lungs..... | 79 |
| 5.5 UPREGULATION OF PEROXISOMAL PROTEINS (CATALASE AND PEX14P) IN ALVEOLAR EPITHELIAL CELLS IN LUNG TISSUE OF PATIENTS WITH IDIOPATHIC PULMONARY FIBROSIS. | 81 |
| 6 DISCUSSION..... | 83 |
| 6.1 CATALASE AS MARKER FOR PEROXISOMES IN DIFFERENT PULMONARY CELL TYPES | 83 |
| 6.2 PEROXISOMES CAN BE BEST VISUALIZED IN MOUSE OR HUMAN LUNGS AT THE LIGHT-MICROSCOPICAL LEVEL WITH PEX14P AS MARKER | 85 |
| 6.3 PEROXISOMAL β -OXIDATION ENZYMES ARE UBIQUITOUSLY EXPRESSED IN DISTINCT CELL TYPES OF MOUSE AND HUMAN LUNGS | 86 |

| | |
|--|------------|
| 6.4 POSSIBLE FUNCTIONS OF PEROXISOMAL β -OXIDATION IN THE LUNG – CONNECTION TO PPAR REGULATION | 87 |
| 6.5 PEROXISOMAL β -OXIDATION MAY PROVIDE ACETYL-CoA UNITS FOR BIOSYNTHETIC PATHWAYS IN PEROXISOMES, SUCH AS PUFA-, PLASMALOGEN- AND CHOLESTEROL SYNTHESIS..... | 88 |
| 6.6 COUPLING OF LIPID AND ROS METABOLISM | 89 |
| 6.7 ALTERATIONS OF THE PEROXISOMAL COMPARTMENT DURING TRANSDIFFERENTIATION OF AECII INTO AECI – EFFECTS OF THE KERATINOCYTE GROWTH FACTOR (KGF) ON THIS PROCESS..... | 90 |
| 6.8 WHICH SIGNALLING MECHANISMS COULD BE TRIGGERED BY KGF ADMINISTRATION?..... | 91 |
| 6.9 KGF AND NRF2-SIGNALLING IN THE PROTECTION AGAINST ROS-MEDIATED OXIDATIVE LUNG INJURY..... | 92 |
| 6.10 INTERFERENCE OF KGF-MEDIATED SIGNALLING WITH PULMONARY LIPID METABOLISM..... | 93 |
| 6.11 ROLE OF KGF AND PPARs IN LUNG MATURATION (DIFFERENTIATION) | 95 |
| 6.12 TECHNICAL PITFALLS INFLUENCING THE COMPARATIVE ANALYSIS OF LUNG TISSUE IMMUNOFLUORESCENCE PREPARATIONS OF WILD TYPE AND PEX11 β KO MICE..... | 96 |
| 6.13 PATHOLOGICAL CONSEQUENCES OF PEX11 β DEFICIENCY IN THE LUNG WITH SPECIAL EMPHASIS ON ALTERATIONS IN CLARA CELLS | 97 |
| 6.13.1 <i>Significant alterations of secretory proteins in Clara cells of PEX11β KO animals .</i> | 97 |
| 6.13.2 <i>PPAR-mediated signalling in the Clara cells of PEX11β KO animals</i> | 100 |
| 6.13.3 <i>Oxidant and antioxidant imbalance in the Clara cells of PEX11β deficient mouse lungs</i> | 101 |
| 6.13.4 <i>Failure of iNOS regulation in the Clara cells of PEX11β deficient mouse lungs...</i> | 103 |
| 6.14 HYPOTHESIS FOR THE MOLECULAR PATHOGENESIS OF THE PATHOLOGICAL ALTERATIONS DUE TO PEX11 β DEFICIENCY | 103 |
| 6.15 PRELIMINARY DATA ON THE ALTERATIONS OF PEROXISOMES IN THE ALVEOLAR EPITHELIUM IN PATIENTS WITH IDIOPATHIC PULMONARY FIBROSIS | 105 |
| 6.16 CONCLUSIONS AND FUTURE PERSPECTIVES | 106 |
| 7 SUMMARY..... | 107 |
| 8 ZUSAMMENFASSUNG..... | 109 |
| 9 REFERENCES | 111 |
| 10 INDEX OF ABBREVIATIONS | 123 |
| 11 ACKNOWLEDGMENTS..... | 124 |
| 12 CURRICULUM VITAE | 126 |

1 Introduction

1.1 Discovery of peroxisomes and peroxisomal enzymes

Peroxisomes were first identified by electron microscopy in proximal tubular epithelial cells of the mouse kidney and described as small, single-membrane bound organelles, which were called at first “microbodies” (Rhodin, 1954). These “microbodies” were also described two years later in rat liver cells (Bernhard and Rouiller, 1956). Ten years later, de Duve and his colleagues used cell fractionation experiments to characterize lysosomes during which they detected another enzyme-containing organelle. With these isolated fractions, De Duve and Baudhuin performed biochemical and electron microscopic characterization in parallel. In their fractions they found organelles that resembled the described microbodies and proposed the name “peroxisome” for this organelle, due to its involvement in the metabolism of hydrogen peroxide (H_2O_2) (De Duve, 1965; De Duve and Baudhuin, 1966): with oxidases, generating H_2O_2 and catalase, involved in the degradation of this toxic molecule. Peroxisomes possess a large number of oxidases producing H_2O_2 during metabolization of a variety of heterogeneous compounds such as D-amino acids, uric acid (non-primates) and α -hydroxy acids (Purdue and Lazarow, 2001; Subramani et al., 2000). Peroxisomes were detected cytochemically on the light- and electron microscopical level by the introduction of the alkaline 3, 3'-diaminobenzidine (DAB) reaction, visualizing the peroxidatic reaction of catalase (Fahimi, 1968, 1969; Novikoff and Goldfischer, 1969) (see Fig. 10). With this method it was possible to show that peroxisomes vary in their size (diameter ranging from 0.2 to 1 μm) and shape (angular, tubular, elongated, or networks of interconnected peroxisomes), depending on the organ and cell type investigated.

Almost at the same time peroxisomal β -oxidation was discovered in plants (endosperm of the germinating castor bean enzymes) (Cooper and Beevers, 1969) and subsequently also in animals (rat liver) (Lazarow, 1977; Lazarow and De Duve, 1976). The importance of peroxisomes in lipid metabolism was further substantiated by the localization of ether lipid and cholesterol synthesizing enzymes, such as glycerone-phosphate O-acyltransferase (Gnpat = previously called as DHAPAT) (Hajra et al., 1979; Keller et al., 1985) and 3-hydroxy-3-methylglutaryl-coenzyme A reductase (Hmgcr), in rat liver peroxisomes (Keller et al., 1985). Recent proteomic analysis of liver

or kidney peroxisomes suggest that these organelles contain over 130 different proteins, involved in various metabolic pathways, such as synthesis of cholesterol and plasmalogens, degradation of various toxic, bioactive pro-inflammatory and signalling lipid derivatives and metabolism of reactive oxygen species (ROS) (Islinger et al., 2006; Wiese et al., 2007). In addition to the various oxidases producing H_2O_2 , in recent years several other enzymes involved in the metabolism of distinct ROS and reactive nitrogen species (RNS) have been described in these organelles, including the antioxidant enzymes Cu, Zn-SOD, glutathione peroxidase and peroxiredoxin I and V (Heijnen et al., 2006; Immenschuh and Baumgart-Vogt, 2005; Schrader and Fahimi, 2004).

1.2 General functions of peroxisomes

In addition to the biochemical analyses of organelle fractions, several metabolic pathways were first detected by analysis of blood or organ biopsy samples of patients with peroxisomal disorders, such as deficiency in plasmalogen biosynthesis, the reduction in common C24 bile acids and the increased formation of C27 bile acid precursors as well as the reduced cholesterol levels and accumulation of very-long chain fatty acids (VLCFA) in body fluids, which highlighted the importance of peroxisomal metabolism for human health (see figure 1B).

Fig 1A

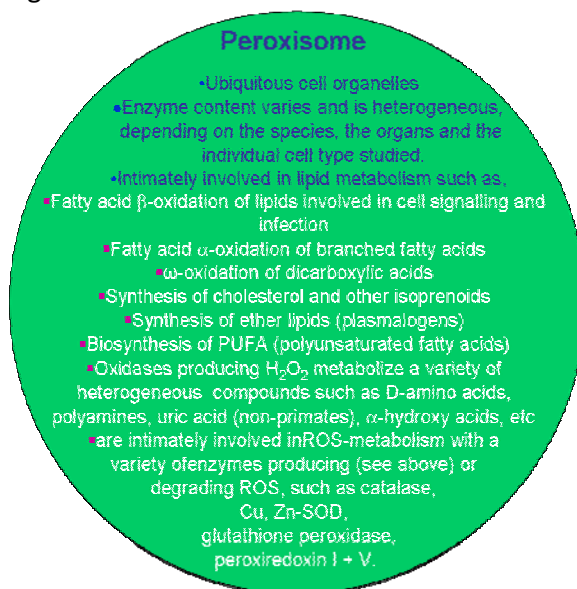


Fig 1B

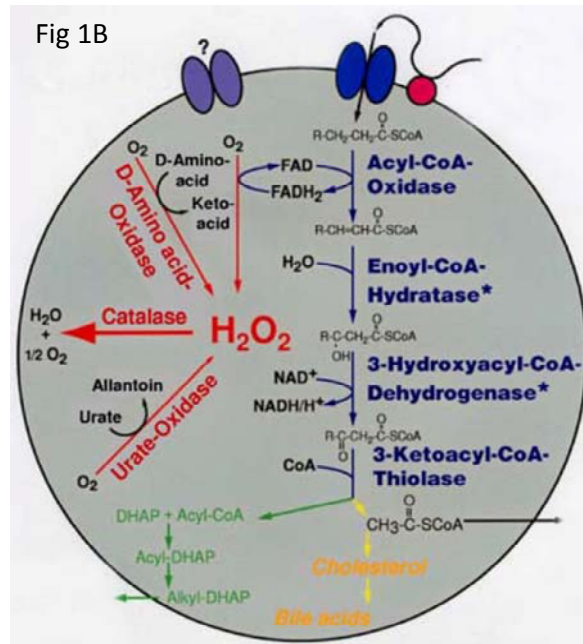


Fig. 1A) Summary of different functions of peroxisomes. 1B) Metabolic pathways of peroxisomes. This picture is provided by kind courtesy of Prof. Dr. Baumgart-Vogt.

Introduction

Details of peroxisomal functions are listed as follows:

1) Metabolism of ROS/RNS: Peroxisomal enzymes play an important role in the production and degradation of reactive oxygen and nitrogen species, such as H_2O_2 , $O_2^{\cdot-}$ and $\cdot NO$.

a) Various oxidases and nitric oxide synthase (see below list of oxidant enzymes), generating

H_2O_2 , $O_2^{\cdot-}$ or $\cdot NO$

b) Peroxisomal enzymes that degrade ROS

Fig. 2 A schematic overview of peroxisomal enzymes that produce or degrade ROS according to Scharder 2004. The oxidant enzymes present in peroxisomes are listed in table.1 and the antioxidant enzymes (also from other cell compartments) in table 2

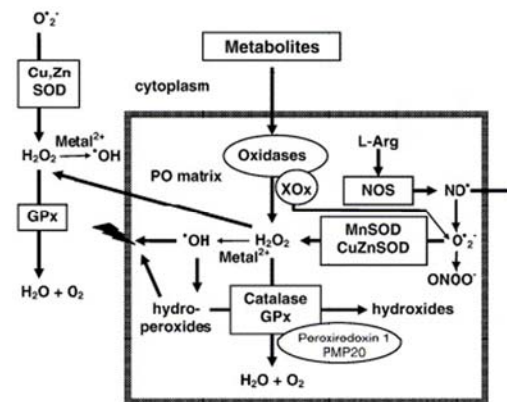


Table 1: Oxidant enzymes in peroxisomes

| Sr. No | Enzyme | Substrate | ROS |
|--------|------------------------------------|---|-----------------------------|
| 1 | Acyl-CoA oxidases | | |
| a) | Palmitoyl-CoA oxidase | Long chain fatty acids | H_2O_2 |
| b) | Pristanoyl-CoA oxidase | Methyl branched chain fatty acids | H_2O_2 |
| c) | Trihydroxycoprostanoyl-CoA oxidase | Bile acid intermediates | H_2O_2 |
| 2 | L-alpha-hydroxyacid oxidase | Glycolate, lactate | H_2O_2 |
| 3 | D-amino acid oxidase | D-Proline | H_2O_2 |
| 4 | D-aspartate oxidase | D-aspartate, <i>N</i> -methyl-D-aspartate | H_2O_2 |
| 5 | Nitric oxide synthase, inducible | L-Arginine | $\cdot NO$ |
| 6 | Pipecolic acid oxidase | L-pipecolic acid | H_2O_2 |
| 7 | Poly amine oxidase | <i>N</i> -Acetyl spermine/spermidine | H_2O_2 |
| 8 | Sarcosine oxidase | Sarcosine, pipecolate | H_2O_2 |
| 9 | Urate oxidase | Uric acid | H_2O_2 |
| 10 | Xanthine oxidase | Xanthine | H_2O_2 and $O_2^{\cdot-}$ |

Table 2: Antioxidant enzymes of various intracellular compartments

| Sr.No | Enzyme | Substrate | Enzyme is also present in |
|-------|------------------------|----------------|----------------------------------|
| 1 | Catalase | H_2O_2 | Cytoplasm and nucleus |
| 2 | Cu, Zn SOD | $O_2^{\cdot-}$ | Cytoplasm |
| 3 | Epoxide hydrolase | Epoxides | ER, cytoplasm and peroxisomes |
| 4 | Glutathione peroxidase | H_2O_2 | All cell compartments |
| 5 | Mn SOD | $O_2^{\cdot-}$ | Mitochondria |
| 6 | Peroxiredoxin 1 | H_2O_2 | Cytoplasm, nucleus, mitochondria |
| 7 | Peroxiredoxin 5 | H_2O_2 | Peroxisomes |

2) Lipid biosynthesis

- Synthesis of ether phospholipids /plasmalogens and glycerophospholipids via the DHAP-pathway (Hajra et al., 1979; Lee, 1998)
- synthesis of bile acids (Pedersen, 1993; Pedersen, 1987) (side chain oxidation of cholesterol via β -oxidation)
- synthesis of cholesterol and dolichol (Krisans, 1996; Olivier and Krisans, 2000)
- synthesis of retinoic acid (Fransen et al., 1999)
- fatty acid elongation (Horie et al., 1989) (via inversion of β -oxidation)

3) Fatty acid degradation

- A) Long/very-long fatty acid activation
- B) β -oxidation of VLCFA (very-long-chain fatty acids; >24, branched-chain-fatty acids) and LCFA (long-chain fatty acids; C14-C22) to a length of C12-C6 (Hashimoto, 2000; Lazarow and De Duve, 1976; Mannaerts et al., 2000). β -oxidation of dicarboxylic acids, branched chain fatty acids, unsaturated fatty acids, leukotrienes and metabolism of prostaglandins (=eicosanoids) (Schepers et al., 1988) and xenobiotic compounds (Mannaerts and Van Veldhoven, 1993)
- C) Fatty acid α -oxidation of phytanic acid (Croes et al., 1996; Mannaerts et al., 2000; Poulos et al., 1993)

4) Regulation of acyl-CoA/CoA ratio

5) Protein/amino acid metabolism

6) D-amino acid degradation (De Duve and Baudhuin, 1966)

7) Metabolism of aminoacid-transamination and degradation (Masters, 1997; Mihalik et al., 1991)

8) Degradation of polyamines (Van den Munckhof et al., 1995)

9) Catabolism of purines through xanthine oxidase (Angermüller et al., 1987) and urate oxidase (Völkl et al., 1998)

10) Glyoxylate and dicarboxylate metabolism (Poosch and Yamazaki, 1989)

11) Hexose monophosphate pathway (Antonenkov, 1989)

1.2.1 The peroxisomal β -oxidation system

Fatty acids undergo oxidation via different mechanisms, however, most fatty acid break-down is catalysed by peroxisomal β -oxidation. The peroxisomal β -oxidation system was first identified in

plants (Cooper and Beevers, 1969) and later in animals (Lazarow and De Duve, 1976). Peroxisomes possess a fatty acid β -oxidation machinery similar in many aspects to the one in mitochondria. In both organelles, the mechanism of β -oxidation involves a set of four consecutive reactions: 1) dehydrogenation 2) hydration of the double bond 3) a second dehydrogenation and 4) thiolitic cleavage (Lazarow, 1978). β -oxidation is a cyclic process by which fatty acids are degraded from their COOH-terminal end (Figure 1B). Each cycle of β -oxidation shortens the fatty acid carbon chain by two carbon atoms, releasing an acetyl-CoA unit, which further might be degraded in the citric acid cycle to produce CO₂ and H₂O. Even though the β -oxidation process is similar in mitochondria and peroxisomes, these systems have different functions as they catalyse the β -oxidation of different fatty acids and fatty acid derivatives. Mitochondria catalyse the β -oxidation of the bulk of fatty acids derived from the diet, such as palmitate, oleate, etc. for energy generation, whereas peroxisomes play an important role by oxidizing a variety of toxic and bioactive fatty acid derivatives. The contribution of peroxisomal β -oxidation to the oxidation of the LCFA, palmitic acid, was estimated to be only 5-20%. Under same conditions, however, peroxisomal β -oxidation might contribute to 70% of the overall β -oxidation (Mannaerts and Van Veldhoven, 1993). In contrast, longer chain fatty acids such VLCFA (>C22) are exclusively oxidized in peroxisomes in liver (Singh et al., 1984), brain (Singh and Singh, 1986) and skin fibroblasts (Singh et al., 1984). In addition to β -oxidation of saturated fatty acids, the peroxisomal β -oxidation has gained more importance by the recognition of its participation in the cleavage of the cholesterol side chain in the synthesis of bile acids (Pedersen and Gustafsson, 1980), and in the catabolism of dicarboxylic acids (Vamecq, 1987), prostaglandins (Diczfalusy and Alexson, 1988), unsaturated fatty acids (Hiltunen et al., 1986), pristanic acid (Singh et al., 1990), pipecolic acid (Chang, 1978) and glutaric acid (Vamecq et al., 1985). All these compounds possess long aliphatic carbon chains that are poorly soluble in water. Thus peroxisomal the β -oxidation process transforms nonpolar to polar metabolites, facilitating their elimination.

1.2.1.1 Peroxisomal β -oxidation enzymes

As mentioned above, the peroxisomal β -oxidation proceeds via four consecutive reactions that take place in the peroxisomal matrix. The first reaction in peroxisomal β -oxidation, an oxidation reaction in which acyl-CoA is desaturated to a 2-*trans*-enoyl-CoA, is catalysed by an acyl-CoA oxidase (ACOX), which is regarded as an important rate limiting enzyme in controlling the flux throughout the pathway. In mammals, there are three ACOX genes described until now (ACOX1:

Introduction

palmitoyl-CoA oxidase (Baumgart et al., 1996); ACOX2: pristanyol-CoA oxidase (Vanhooren et al., 1996); ACOX3: cholestanoyl-CoA oxidase (Baumgart et al., 1996). In rodent livers, peroxisomal proliferators induce ACOX1 that catalyses the oxidation of LCFA and MCFA (Vamecq, 1987). In human, the ACOX3 gene is not functional. Acox1p acts only on straight chain acyl-CoAs whereas Acox2p and Acox3p can desaturate straight and 2-methyl branched acyl-CoAs (Van Veldhoven et al., 2001; Wanders et al., 2001).

The second reaction in peroxisomal β -oxidation is a hydration reaction (see pictures below), which converts the unsaturated intermediate enoyl-CoA to L-3-hydroxyacyl-CoA catalyzed by the bifunctional enzyme. The next step, a second oxidation step which dehydrogenates the hydroxy

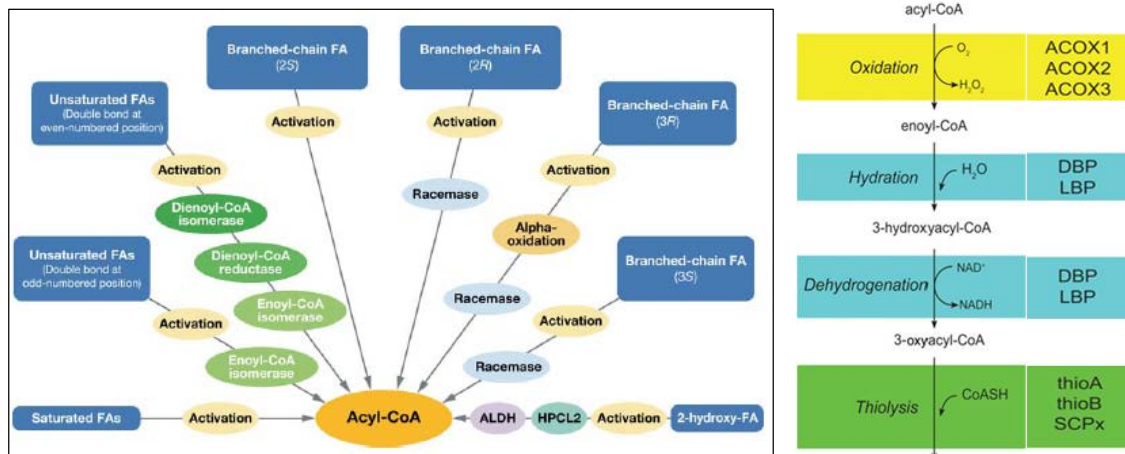


Fig. 3 According to Visser 2007, the generated acyl-CoA can be involved in different reactions

intermediate to a 3-ketoacyl-CoA is exerted by the same enzyme. Therefore, this enzyme had been attributed different names, such as D-bifunctional protein (DBP), D-peroxisomal bifunctional enzyme (D-PBE), multifunctional enzyme II (MFE-II), multifunctional protein 2 (MFP-2). The final step is the thiolytic cleavage (thiolysis), which releases acetyl-CoA and an acyl-CoA two carbon atoms shorter than the original molecule that can re-enter the next round for further β -oxidation. This final thiolytic cleavage step of the peroxisomal β -oxidation process is carried by two thiolases, which were first described in rat liver: pTH1 – thiolase A and pTH2 – thiolase B (Hijikata et al., 1990) and the sterol protein X (Seedorf et al., 1994). The 3-Ketoacyl-CoA thiolase acts on straight chain ketoacyl-CoAs and sterol carrier protein X catalyzes the cleavage of both straight chain and 2-methyl ketoacyl-CoAs (Antononkov et al., 1997). Though vast information is available on peroxisomal β -oxidation in the liver, until now nothing is known about these pathways in

different pulmonary cell types of mouse and human lung as well as peroxisome deficient mouse lungs.

1.2.2 Biosynthetic pathways of cholesterol and ether-phospholipids in peroxisomes

Cholesterol synthesis

Biosynthesis of cholesterol in the peroxisomal compartment was discovered by the localization of HMG-CoA reductase in the peroxisome in addition to the endoplasmic reticulum (Keller et al., 1985; Thompson and Krisans, 1990). HMG-CoA reductase is the rate limiting enzyme of the cholesterol synthesis and converts HMG-CoA to mevalonic acid. Three other enzymes localized in peroxisomes catalyze the reactions required to convert mevalonate into isopentyl diphosphate (IPP). These three enzymes are phosphomevalonate kinase (PMvK), mevalonate diphosphate decarboxylase (MPD) and isopentenyl diphosphate isomerase (IPP). Further, the farsenyl diphosphate synthase (FPP) catalyzes the conversion of IPP to FPP. Finally, the conversion of FPP to lanosterol is believed to occur in the ER (Kovacs et al., 2002). Interestingly, no differences of cholesterol biosynthesis rate were observed in PEX5 KO mouse fibroblasts cultures; however, PEX2 KO mice showed drastic alterations in the enzymes of cholesterol pathway.

Etherphospholipid synthesis

Biosynthesis of etherphospholipids starts in the peroxisome with the production of dihydroxyacetonephosphate (DHAP) to acyl-DHAP, catalyzed by the peroxisomal enzymes dihydroxyacetonephosphate-acyltransferase (DHAPAT = Gnpat) and alkyl-DHAP synthase. Further, the third step is processed in two different compartments, in the peroxisome and the endoplasmic reticulum (ER). This step is catalyzed by the enzyme alkyl/acyl-DHAP:NAD(P)H oxidoreductase. The product of this reaction alkylglycerol-3-phosphate (alkyl-G-3P) undergoes subsequent conversion into plasmalogens in the ER.

1.3 Biogenesis of peroxisomes

The half-life of peroxisomes is three days. In order to continue their function, peroxisomes are constantly formed or replaced by new peroxisomes. This process is termed “peroxisomal biogenesis” or assembly of peroxisomes. Biogenesis of peroxisomes includes mainly three steps: a) formation of the peroxisomal membrane, b) import of peroxisomal matrix proteins, c)

proliferation of peroxisomes. The biogenesis of peroxisomes, including the import of matrix proteins into the organelle, is mediated by a group of structurally diverse proteins called “peroxins” with the acronym of corresponding genes or proteins abbreviated as PEX or Pex..p and numbered according to their date of discovery (Distel et al., 1996). Distinct peroxin classes are conserved during evolution and demonstrate a broad level of similarity from yeast to man. Peroxisomes are probably derived from pre-existing organelles (Lazarow and Fujiki, 1985) by division of mature organelles. Peroxisomes enlarge by import of peroxisomal matrix and membrane proteins that are synthesized on free ribosomes and transported post-translationally into the organelle via one of either two pathways requiring peroxisomal targeting signal (PTS) sequences (Subramani, 1998; Terlecky and Fransen, 2000). The importance of peroxisomal biogenesis for human health was stressed by the identification of a new class of lethal human diseases in which no recognizable peroxisomes were present (Goldfischer et al., 1973). In addition, the interest in peroxisomal biogenesis was substantiated by the fact that treatment of rodents with various hypolipidemic agents or other xenobiotics called as peroxisome proliferators leads to a significant proliferation of peroxisomes in liver and other organs.

1.3.1 Peroxisomal targeting signals

PTS1

The peroxisomal targeting signal 1 is a major peroxisomal targeting signal sequence, consisting of a *carboxy-terminal* conserved tripeptide with conserved substitutions (PTS1- “**S**/A/C – **K**/R/H – **L**/M”) of the consensus sequence (Gould et al., 1989). PTS1 signal carrying proteins are recognized and bound by tetratricopeptide repeats (TPR) of the cytoplasmic receptor protein Pex5p. This TPR protein consists of six direct repeats of the degenerate 34 amino acid TPR motif.

PTS2

The peroxisomal targeting signal 2 is an amino-terminal nonapeptide with the conserved motif (**R**/K) - (**L**/I/V) - X₅ - (**H**/Q) - (**L**/A/F), found only in a few peroxisomal matrix proteins and first identified in peroxisomal thiolase (Rehling et al., 1996; Swinkels et al., 1991). The PTS2 is recognized by six tryptophan and aspartic acid repeats of approximately 40 amino acids long (WD40), of the cytoplasmic receptor Pex7p.

1.3.2 Docking of the cargo-receptor complex to the peroxisomal membrane

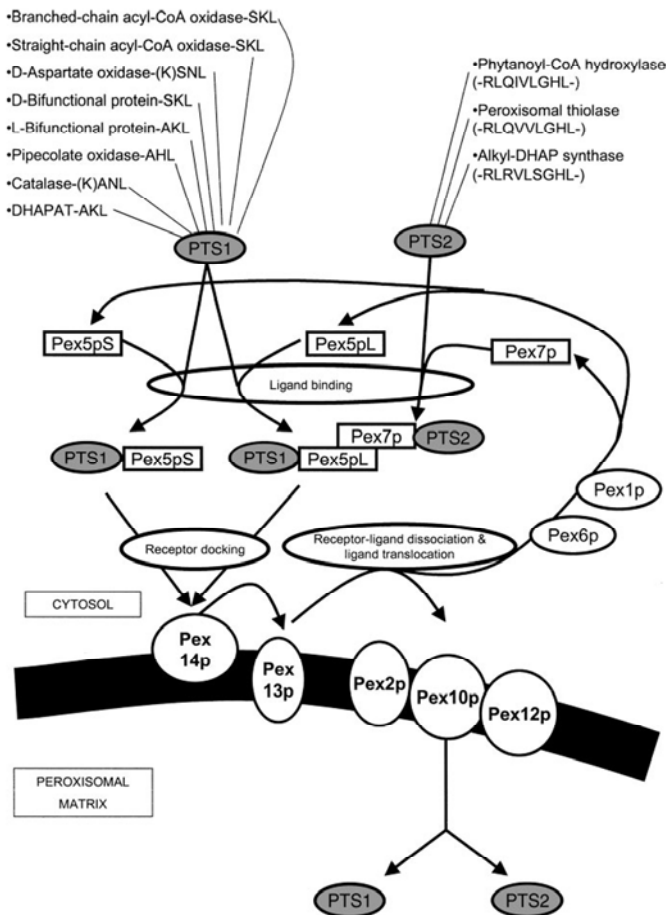


Fig. 4 Model of peroxisome biogenesis according to Wanders 2004. Diagrammatic representation of the peroxisomal targeting receptors, involved in the translocation of peroxisomal matrix proteins through the docking complex of the peroxisomal membrane (Wanders, 2004).

As mentioned above, Pex5p recognizes the PTS1 signal and Pex7p recognizes the PTS2 signal of peroxisomal matrix proteins. Upon binding, these receptors carry peroxisomal proteins to the translocation machinery of the docking complex on the peroxisomal membrane. The docking complex includes three

peroxins, Pex13p, Pex14p and the peripheral membrane protein Pex17p. Pex17p is believed to form a part of the docking complex by associating with Pex14p in a tight core complex (Agne et al., 2003; Huhse et al., 1998), however, its exact role is not yet known. Pex13p is an integral peroxisomal membrane protein that has both its amino and carboxy-termini extending into the cytoplasm. The N-terminal domain binds the PTS2 receptor (Pex7p) (Stein et al., 2002) and the carboxy-terminal region contains a Src-homology-3 (SH3) domain, which directly binds to the PTS1 receptor (Pex5p) as well as its partner docking protein, Pex14p (Albertini et al., 1997; Elgersma et al., 1996; Erdmann and Blobel, 1996; Gould et al., 1996; Pires et al., 2003). The proline-rich SH3-ligand motif in Pex14p is responsible for the binding to the SH3 domain of Pex13p (Girzalsky et al., 1999; Pires et al., 2003). Pex5p directly interacts with Pex13p and Pex14p (Barnett et al., 2000; Urquhart et al., 2000). The PTS2 receptor, Pex7p, also interacts directly with Pex14p but not with Pex13p (Stein et al., 2002). Two-hybrid analyses in mammalian cells and complementary *in vitro* binding assays have proven that the pentapeptide repeat motifs

(WXXXF/Y) in Pex5p bind to Pex14p with high affinity (Otera et al., 2002; Saidowsky et al., 2001). Pex14p provides the initial docking site for cargo-loaded Pex5p, which subsequently is expected to be transported to the other components of the import machinery (Eckert and Erdmann, 2003; Otera et al., 2000). However, the exact mechanism how the cargo-receptor complex is translocated across the peroxisomal membrane is still unknown.

1.3.3 Translocation, dissociation and receptor cycling

Translocation of the cargo-complex is achieved by docking the receptor-cargo complexes to the peroxisomal membrane. The receptors dissociate from the cargo either prior to the transport process or after translocation step in the peroxisomal lumen and recycle back into the cytosol to repeat the same process. Pex8p triggers the association of the docking and the RING-finger complex proteins, Pex2p, Pex10p and Pex12p. These second groups of membrane proteins are suggested to play a role in translocation as the putative peroxisomal import complex (importomer) (Chang et al., 1997; Erdmann et al., 1997; Hettema et al., 1999; Holroyd and Erdmann, 2001). They expose their RING-finger domains to the *cis*-side of the peroxisomal membrane and form a heteromeric complex. These proteins also might be involved in the ubiquitination of the import receptor Pex5p in an ATP dependent manner (Costa-Rodrigues et al., 2004; Gouveia et al., 2003)

1.3.4 Import and assembly of peroxisomal membrane proteins

To import proteins into the peroxisomal matrix, integral and peripheral peroxisomal membrane proteins (PMPs) must be present on the limiting membrane of the organelle. However, very little information is available concerning the targeting and import of PMPs in comparison to matrix proteins. In a similar fashion to matrix proteins, PMPs are also synthesized on free polyribosomes and are imported post-translationally from the cytoplasm into the organelle membrane. However, the mechanism of targeting and inserting PMPs is independent from the peroxisomal matrix protein import pathways. Peroxisomal membrane targeting signals (mPTS) were identified for several PMPs (Dyer et al., 1996; Honsho and Fujiki, 2001; Honsho et al., 2002; Pause et al., 2000). Three membrane proteins Pex3p, Pex16p, and Pex19p seem to play a role in the early steps of peroxisomal biogenesis and are involved in the membrane-assembly. In most studies on fibroblasts with mutations in peroxisomal genes significant disturbances in matrix protein import,

were observed. However, in these cell lines no differences in assembling of peroxisomal membrane proteins occurred (Pool et al., 1998; Santos et al., 1988). A number of hypotheses were proposed over the years for the biogenesis of peroxisomes. De Duve proposed a model based on their metabolic functions, peroxisomes should multiply as an autonomous organelle (Hoepfner et al., 2005; Lazarow and Fujiki, 1985; Li and Gould, 2002). In contrast, due to the catalase-negative membrane attachments to peroxisomes observed under proliferation conditions with electron microscopy, Novikoff and Shin defended the idea that peroxisomes bud of the endoplasmic reticulum (Novikoff, 1964). Indeed, more careful electron microscopical studies with cytochemical and immunocytochemical stainings by Baumgart and colleagues could prove that the membrane extensions described on peroxisomes were catalase-negative segments of the peroxisomal membrane and not attachments to the ER (Baumgart et al., 1989). Lazarow and Fujiki proposed the peroxisomal reticulum hypothesis, which suggests that peroxisomes are separate entities that fuse and bud and proliferate by division of pre-existing organelles (Lazarow and Fujiki, 1985). The involvement of the ER in the biogenesis of peroxisomes is discussed nowadays again for the biogenesis of the peroxisomal membrane (Hoepfner et al., 2005). In 1998, Titorenko and Rachubinski proposed again that the ER might play an essential role in the biogenesis of the peroxisomal membrane (Titorenko and Rachubinski, 1998). Recently, Hoepfner and colleagues found additional evidence that the ER contributes to the formation of peroxisomes (Hoepfner et al., 2005). The authors concluded that ER localized Pex3p recruits Pex19p and facilitates the insertion of PMPs, resulting in the capacity to import matrix proteins. Pex3p and Pex19p physically interact with each other and play an essential role in the biogenesis of peroxisomes. Finally, recent reports question the ER hypothesis again and the biogenesis of the peroxisomal membrane is still under debate.

1.3.5 Peroxisome growth and division

Generally accepted in the field of peroxisome biogenesis is the idea that peroxisomes are replicated by fission of pre-existing ones due to the involvement of Pex11p (Hoepfner et al., 2001) and VpS1p (South and Gould, 1999). PEX11 proteins are components of the peroxisomal membrane in a wide variety of species, including yeast, protozoan parasites and mammals (Li et al., 2002). Mammalian Pex11p contains three different isoforms, Pex11 α , Pex11 β , and Pex11 γ (Erdmann and Blobel, 1995). PEX11 deletion studies from yeast suggested a significant reduction in peroxisome numerical abundance and over expression of PEX11 cause a pronounced increase

in their abundance (Li and Gould, 2002). Similar results were also observed in peroxisome proliferation in man (Abe and Fujiki, 1998). Marshall and Schrader 1996 also observed a hyperproliferation of peroxisomes upon overexpression of Pex11p (Marshall et al., 1995a; Schrader et al., 1998). In 2002 Smith and colleagues identified Pex25p as a novel peroxin also involved in peroxisome proliferation in yeast (Smith et al., 2002). In addition, conflicting results exist on PEX11 function in the peroxisome field. To date, several groups proposed different hypothesis concerning the functions of PEX11 proteins. Some of the researchers believed that PEX11 proteins are involved in peroxisome division (Erdmann and Blobel, 1995; Gould and Valle, 2000; Marshall et al., 1995a; Marshall et al., 1995b). However, based on their results, other researchers suggested a direct role of PEX11 β in MCFA degradation, affecting peroxisome abundance indirectly (van Roermund et al., 2001; van Roermund et al., 2000). The importance and functions of PEX11 β were elucidated by the generation of PEX11 β deficient mice (Li et al., 2002). The authors reported that PEX11 β KO mice are not defective in two unrelated peroxisomal metabolic pathways, suggesting that PEX11 β plays a direct role in peroxisome biogenesis rather than in peroxisomal metabolism (Li and Gould, 2002). Indeed now, the role of PEX11 β in peroxisome biogenesis is clearer. Reports showed that peroxisome division involves the Pex11 proteins and dynamin-like protein DLP1, which performs an essential but transient role in peroxisome division. Li and colleagues reported that PEX11 promotes peroxisome division by recruiting DLP1 to the peroxisomal membrane through an indirect mechanism (Li et al., 2002). In contrast, the Schrader-group proposed that dynamin-like protein 1 (DLP1) plays a direct role in peroxisomal fission and in the maintenance of peroxisomal morphology in mammalian cells (Koch et al., 2003).

1.3.6 Peroxisomal diseases

The importance of peroxisomal metabolism for human health is most obvious in patients suffering from peroxisomal biogenesis disorders (PBDs), in which the all peroxisomal functions are defective due to mistargeting of peroxisomal proteins. PBDs are autosomal recessive diseases that arise from mutations in *PEX* genes that encode proteins, the so called peroxins (= Pex...p), required for the normal biogenesis of peroxisomes (Distel et al., 1996; Gould and Valle, 2000). The best-studied example for a PBD is the cerebro-hepato-renal syndrome of Zellweger, which is associated with extreme hypotonia, severe mental retardation, and early death of the children within the first year of life due to cardiac or respiratory problems (Goldfischer et al., 1973).

Mutations in peroxins either directly disrupt the apparatus required for posttranslational import of matrix proteins (containing peroxisomal targeting signals PTS 1 or PTS 2) into the peroxisomes or indirectly prevent matrix protein import by disrupting peroxisomal membrane formation (Purdue and Lazarow, 2001). The PBDs are thus characterized by the absence, or deficiency of normal peroxisomes and loss of the organelle's usual complement of proteins and metabolic pathways. Three different phenotypic variations of PBDs exist 1) Zellweger syndrome (ZS), 2) neonatal adrenoleukodystrophy (NALD), and 3) infantile Refsum's disease (IRD), which represents a clinical continuum, called the disorders of the Zellweger syndrome spectrum, with ZS being the most severe and IRD the mildest form of a similar spectrum. The second group of peroxisomal diseases (= single enzyme deficiencies) is characterized by deficiency of a single peroxisomal function, e.g in X-linked adrenoleukodystrophy (X-ALD), a disease caused by a defect in the ALD protein, an ABC transporter for VLCFA, now called ABCD1 (Moser, 1993).

1.4 Pathological consequences of PEX11 β deficiency

Li and Baumgart et al generated and bred PEX11 β knockout mice (Li et al., 2002). Even though these animals still have a reduced number of peroxisomes, they die immediately after birth and



Fig. 5 PEX11 β KO animals died after the birth and showed the features of Zellweger syndrome.

exhibit numerous pathological features of Zellweger syndrome, showing developmental delay, general hypotonia, neuronal migration defects as well as enhanced neuronal apoptosis. Even though deficiency of PEX11 β in mice led to severe pathological alterations in different organ systems, until now the role and functions of PEX11 β in lungs of these mice remain unknown.

In addition, the molecular pathogenesis of all described pathological alterations is unknown. However, yet unknown metabolic alterations in these mice might influence the activation or inactivation of multiple signalling pathways (for an overview see discussion of PPAR γ) (Karnati and Baumgart-Vogt, 2008).

1.5 Animals models for general peroxisomal biogenesis disorders (PEX5, PEX2 and PEX13 knockout mice)

The peroxisomal biogenesis diseases are characterized by the absence or dysfunction of peroxisomal matrix protein import, altering various peroxisomal metabolic pathways in different organ systems. Until now, this complex phenomenon has been investigated by using various peroxisomal gene mutations in yeast or animals. Animal models provided the most valuable tool for investigating the pathogenesis of the corresponding human diseases. Three mouse models for Zellweger Syndrome have been developed through targeted disruption of PEX2 (Faust and Hatten, 1997), PEX5 (Baes et al., 1997) or PEX13 (Maxwell et al., 2003). All of these three knockout animals exhibit many of the organ abnormalities, typical for Zellweger Syndrome of human patients. However, these animals die immediately after the birth. In addition, all of them showed similar or comparable biochemical parameters, typical for peroxisomal disorders, such as accumulation of VLCFA, deficient plasmalogens and hardly detectable peroxisomal β -oxidation. Further, abnormalities in neuronal migration were found in all three KO mice also described in Zellweger patients (Evrard et al., 1978). Furthermore, Zellweger patients showed the mitochondrial changes (Goldfischer et al., 1973) and in PEX5 KO animals also display disturbances in mitochondrial respiratory chain complexes (Baumgart et al., 2001). Also PEX2 KO animals showed alterations in mitochondrial cristal (Faust and Hatten, 1997). The exact cause of death of these knockouts is yet unknown. PEX5 and PEX2 KO animals showed no obvious functional alterations of heart and lung. However, PEX13 KO animals exhibited respiratory distress in rare cases. Taken together, various knockout mice serve as a good model system for understanding the pathogenesis of human peroxisomal biogenesis disorders.

1.6 Control of peroxisome abundance and composition by the action of nuclear receptors

Peroxisomal proliferator-activated receptors are ligand-activated transcription factors belonging to the nuclear hormone receptor family including also the retinoid, glucocorticoid and thyroid hormone receptors (Evans, 1988). PPARs consist of an amino-terminal region that allows ligand-independent activation of transcription, a DNA-binding domain and a carboxy-terminal ligand-dependent activation domain (Moras and Gronemeyer, 1998). To date, three different PPAR

subtypes have been identified: PPAR α , PPAR β (also known as PPAR δ) and PPAR γ . PPAR γ is expressed at least in 2 different isoforms γ 1 and γ 2. These isoforms differ only by the addition of 30 amino acids at the amino terminus of γ 2, however, they appear to be functionally equivalent. The term PPAR was derived from the fact that activation of PPAR α resulted in peroxisome proliferation in rodent hepatocytes (Issemann and Green, 1990). However, activation of PPAR β or PPAR γ does not show this response in other cell types.

1.6.1 Functions of PPAR γ in organ systems

PPAR γ plays a critical role in adipocyte differentiation (Spiegelman and Flier, 1996). Although most of the literature was published on the adipogenic role of PPAR γ , recent reports suggest more diverse functions of PPAR γ in the regulation of cellular differentiation, lung maturation and inflammation. PPAR γ influences organ development and controls tissue homeostasis. A novel function of PPAR γ is its involvement in establishing and maintaining of normal lung structure through regulation of epithelial cell differentiation or through the control of lung inflammation (Simon and Mariani, 2007). In addition, PPAR γ can promote the expression of terminal differentiation markers and inhibit surfactant proteins (Bren-Mattison et al., 2005; Chang and Szabo, 2000; Yang et al., 2003). Furthermore, PPAR γ regulates monocyte/macrophage differentiation and promotes cellular activation as measured by increased ROS levels in these cell types (Ricote et al., 1998). Recent reports indeed suggest that PPAR γ functions as an immunomodulator and has a potential anti-inflammatory role in asthma (Belvisi et al., 2006). Anti-inflammatory properties of PPAR γ ligands have been well described in atherosclerosis and diabetes type 2 (Belvisi et al., 2006; Rizzo and Fiorucci, 2006). Various studies demonstrated the anti-inflammatory role of PPAR γ ligands in different animal models, such as arthritis, ischaemia-reperfusion, and Alzheimers disease (Scher and Pillinger, 2005). In the lung, PPAR γ ligands inhibit allergic airway inflammation and hyperresponsiveness in a mouse model of asthma (Honda et al., 2004; Ward et al., 2006). PPAR γ ligands also inhibit the release of pro-inflammatory cytokines from activated macrophages (Jiang et al., 1998) and airway epithelial cells (Wang et al., 2001). In addition, PPAR γ ligands showed potential anti-fibrotic activity in vivo (Kawaguchi et al., 2004; Leclercq et al., 2006; Uto et al., 2005) and in vitro (Burgess et al., 2005). Airway epithelial cell-specific-PPAR γ deficient mice showed a defect in postnatal lung maturation (Simon et al., 2006b) and structural as well as functional abnormalities at maturity, including enlarged airspaces. Whole

lung genome-wide expression profiling suggests a general decrease in extra cellular matrix gene expression in the animals leading to the abnormal structure. In addition, airway specific PPAR γ deficiency disrupts epithelial mesenchymal interactions.

1.6.2 PPARs in the lung

The PPAR α protein was described in macrophages, neutrophils, lymphocytes (Reynders et al., 2006), eosinophils (Woerly et al., 2003), epithelial cells (Trifilieff et al., 2003) and airway smooth muscle cells (Patel et al., 2003). Furthermore, the PPAR β protein is also found in macrophages, neutrophils, lymphocytes (Reynders et al., 2006), mast cells (Sugiyama et al., 2000) and epithelial cells (Trifilieff et al., 2003). Also the PPAR γ protein was described in a variety of cell types in the lung such as the airway epithelium (Benayoun et al., 2001; Wang et al., 2001), bronchial smooth muscle cells (Benayoun et al., 2001; Patel et al., 2003), endothelial cells (Calnek et al., 2003), macrophages (Chinetti et al., 1998), fibroblasts (Huang et al., 2005) eosinophils (Woerly et al., 2003), AECII (Michael et al., 1997) and dendritic cells (Gosset et al., 2001). Spatial and temporally restricted pattern of PPAR γ expression was found in conducting airway epithelium of the normal mouse lungs (Simon et al., 2006b).

1.6.3 Molecular mechanisms of PPAR transcription

The molecular mechanism of gene regulation by PPARs is a complex process. The heterodimerization of PPARs with retinoid X receptor (RXR) is probably affected by competition between PPAR-isoforms and other nuclear receptors that are also RXR partners, such as retinoic acid, Vitamin D and thyroid hormone receptor.

Molecular gene regulation by transcription can occur in the following ways:

- 1) Transcriptional activation or suppression can occur following the recognition of PPAR response elements (PPRE) in promoters of target genes (Desvergne and Wahli, 1999).
- 2) PPAR can negatively regulate gene expression by antagonizing other signal dependent transcription factors such as NF κ B, CCAAT/-enhancer-binding proteins (C/EBPs), signal transducers and activators of transcription (STAT) or activator protein 1 (AP-1). This can occur via direct binding to cause transrepression (Straus et al., 2000).

3) PPAR γ ligands may also mediate responses via activation of mitogen associated protein kinase (MAPK) and phosphoinositide-3-kinase pathways (P13k) (Harris et al., 2002; Patel et al., 2005). PPAR γ and its ligands serve as negative regulators for SP-B gene expression in respiratory epithelial cells (Yang et al., 2003). PPAR γ and C/EBPs are involved in controlling the transcription of several lung-specific proteins (Barlier-Mur et al., 2003). C/EBPs and PPAR γ were induced during in vitro maturation of AECII and were enhanced by cAMP (Michael et al., 1997). Further, PPAR γ ligands in combination with retinoic acid activate Nrf2 and C/EBP β , both transcription factors essential for glutathione-S transferase A2 expression (Park et al., 2004). PPAR γ agonists directly inhibit the expression of iNOS (Crosby et al., 2005).

1.7 Research so far done on peroxisomes in mouse and human lungs

Despite the bulk of information on peroxisomes in liver and other organs, only scarce information is available on lung tissue, which mostly came from older, purely descriptive electron microscopic studies in rat, rabbit, cat, pig and monkey. Very little is known about peroxisomal metabolism in mouse lungs (Ossendorp et al., 1994) and no information is available on this topic for human lungs. Older studies on peroxisomes were performed only at the electron microscopic level by using the alkaline DAB-method for the localization of catalase activity under normal (Petrik, 1971; Schneeberger, 1972a) and experimental or pathological conditions (Eguchi et al., 1980; Hirai et al., 1983). In these studies, it was suggested that AECII and Clara cells were the only cell types containing a considerable amount of peroxisomes among the various different cell types identified in the rodent lung (Sorokin, 1988). In addition, in rats and man it was demonstrated with the same electron microscopic technique that peroxisomes disappear parallel to the differentiation of AECII into AECl (Moriguchi et al., 1984; Schneeberger, 1972b). Most AECl were devoid of peroxisomes in mouse lungs (Hirai et al., 1983) and no peroxisomes were found in fully differentiated human AECl (Moriguchi et al., 1984).

Hardly any thing is known about peroxisomes in AECl cells and no knowledge is available for this organelle in other cell types of the lung, such as alveolar macrophages. However, peroxisomes could play an important role in macrophages due to their intimate metabolism in ROS and lipids. Alveolar macrophages are the first line of defence against invading microorganisms and are capable of secreting various cytokines and lipid mediators like leukotrienes and eicosanoids. In

this respect, it is interesting that macrophages are activated by ROS that regulate the release tumor necrosis factor- α through the NF- κ B dependent pathway (Rose et al., 2000). Alveolar macrophages are the main important source of NO formation by iNOS in the lung (Fujii et al., 1998). Peroxisomal proteins mainly involved in the intracellular degradation of ROS are catalase, peroxiredoxin I and V (Immenschuh and Baumgart-Vogt, 2005). Moreover, the loss of peroxisomes in KO mice with Zellweger syndrome (PEX 5^{-/-} mouse) leads to drastic mitochondrial defects, most probably induced by generation of ROS in the defective mitochondrial respiratory chain in these animals (Baumgart et al., 2001). Although many peroxisomal proteins have been characterized at the tissue and cellular level in recent years in other organs, there are no reports on enzyme composition and localization of different peroxisomal proteins in mouse and human lungs and their functions are still not understood in the lung. Knowledge on the peroxisomal compartment in the lungs of man and mice, however, is of special importance to investigate the possible involvement of peroxisomal metabolism in human lung diseases and to study the molecular pathogenesis of these diseases in corresponding mouse models.

1.8 Peroxisomes in development and maturation of the lung

To study of peroxisomes in lung development and maturation is important, since it provides a better understanding of lung cell biology from a broader view from basic to clinical science. Lung development and maturation are a continuous series of processes requiring co-ordination of several significant pathways from the primitive foregut endoderm into the gas-exchange organ lung. In parallel the formation of airway and blood vessel branches and the development of more than 40 different cell types is needed (Sorokin, 1988). A better understanding of peroxisomal functions during the perinatal and postnatal development of mice will improve possible treatment strategies and/or might prevent a variety of neonatal and adult lung diseases. However, only one article in the literature described that in immunohistochemical preparations peroxisomal enzymes, such as catalase, ACOX and thiolase, were only weakly or hardly detectable in different cell types of the developing rat fetal lung (Nardacci et al., 2004). Until now, nothing is known about the role and functions of peroxisomal proteins in the postnatal development of the mouse lung.

1.9 Peroxisomal metabolic changes during transition of AECII to AECI

Many reports showed that different cell culture conditions have a significant effect on the transition of AECII to an AECl phenotype (Borok et al., 1995; Cheek et al., 1989; Danto et al., 1995; Dunsmore et al., 1996; Shannon et al., 1992; Sugahara et al., 1995). In this respect, the keratinocyte growth factor (KGF), an epithelial mitogen stimulates rat AECII proliferation both in vitro and in vivo (Panos et al., 1993; Ulich et al., 1994), suggesting a role for KGF in repairing the alveolar epithelium following lung injury (Mason et al., 1996; Panos et al., 1995). KGF increases surfactant apo-proteins such as SP-A and SP-B after its addition into the AECII culture (Sugahara et al., 1995). KGF also played an important role in clearing the alveolar fluid after lung injury by increasing the sodium channels and upregulating the transport of sodium across the alveolar epithelium (Borok et al., 1998a). Upon AECl cell damage by BHT treatment, AECII cells differentiate into AECl cells. Morphological peroxisomal changes were described under these conditions on the electron microscopic level in mice (Hirai et al., 1983). However, until now, the influence of KGF on the modulation of differentiation and alteration of the peroxisomal compartment is unknown. KGF has a protective role in the alveolar epithelium and also peroxisomes are essential in protecting the respiratory epithelium against ROS. Therefore KGF modulation of the transdifferentiation process might regulate also the peroxisomal compartment, possibly providing new insights on the role of these organelles for the treatment of lung injury.

1.10 Peroxisomes in human lung diseases

Due to its large surface area with exposure to high concentrations of oxygen, its extensive blood supply and surfactant lipid metabolism, the lung is very susceptible to oxidative injury by ROS and lipid peroxidation (Rahman and MacNee, 2000). Increase of ROS could result in tissue damage, associated with many chronic inflammatory diseases (Rahman and MacNee, 1996, 2000; Rahman et al., 1996; Rahman et al., 2006). Alterations in the lung antioxidant balance can lead to a variety of airway diseases such as asthma, chronic obstructive pulmonary disease (COPD) and idiopathic pulmonary fibrosis (IPF). Peroxisomes are organelles with extensive metabolism of reactive oxygen species and might therefore be affected by different lung diseases. However, there is only one article available in the literature, showing peroxisomal changes during the differentiation of AECII to AECl in pulmonary proteinosis (Moriguchi et al., 1984). Besides this, nothing is known about the role and functions of peroxisomes in different pulmonary diseases.

2 Aims of the study

Scientific basis for the goals of this study:

Most of the knowledge on peroxisomes was obtained from studies on major metabolic organs, such as liver or kidney. Only scarce information is available on the function of these organelles in mouse and human lungs. However, peroxisomal enzyme composition is extremely heterogenous in distinct cell types or organ systems. Since AECII synthesize and secrete pulmonary surfactant and the major part of surfactant is lipid, peroxisomes might be involved in regulation of surfactant homeostasis. Indeed, a higher number of peroxisomes were described in old electron microscopical studies only in AECII and Clara cells in lung tissue.

Furthermore, upon injury of AECI or under disease conditions AECII differentiate into AECI a process which is paralleled by the disappearance of peroxisomes in transdifferentiating cells. Peroxisomal number in AECII increases rapidly after the birth however, the role and functions of peroxisomes during postnatal development of mice remains unknown.

The constitutional control of peroxisomal number and the proliferation of peroxisomes are under normal conditions regulated by the Pex11 β protein, the importance of which is this protein is best studied in PEX11 β KO mice. To date, nothing is known on the role of PEX11 β and peroxisome proliferation in wild type mouse lungs and on the pathological consequences of PEX11 β deficiency in mouse lungs.

To date, hardly any information is available on the alterations of the peroxisomal compartment in human lung diseases, such as idiopathic pulmonary fibrosis (IPF). Since, peroxisomes contain a variety of antioxidative enzymes, the regular function of peroxisomal metabolism might be necessary to protect pulmonary epithelia against oxidative and nitrosative stress. Pathological alterations in peroxisomal antioxidative enzyme content could therefore lead to an aggregation of pulmonary diseases and vice versa. A stimulation of peroxisomal metabolism might improve the pathologies in human lung diseases.

Aims

The aims of this study were therefore:

- ❖ To localize and characterize peroxisomes in all cell types in the lung
- ❖ To reveal the differences and possible functional heterogeneity of peroxisomal metabolism in distinct pulmonary cell types of the adult mouse and human lung
- ❖ To characterize peroxisomal enzyme composition in freshly isolated and cultured mouse AECII
- ❖ To characterize the role of peroxisomes during the postnatal development of the lung
- ❖ To investigate the pathological alterations in the lungs of PEX11 β deficient mice and to characterize their molecular pathogenesis
- ❖ To start a first attempt for a comparative analysis of peroxisomes in lung tissue of human donors versus patients with idiopathic pulmonary fibrosis.

3 Materials & Methods

3.1 Experimental animals, instruments and materials

3.1.1 Experimental animals and patient characteristics

a) Mice

Specified Pathogen Free (SPF) C57Bl/6J wild type mice were purchased for experimental purposes from Charles River Laboratories, Sulzfeld, Germany. They were kept on a normal laboratory diet and water *ad libitum* and housed in cages under standardized environmental conditions (12 hours light/dark cycle, 23°C ± 1°C and 55 % ± 1 % relative humidity). The mice were transported to our institute two days prior to the experiments. All experiments with laboratory mice were approved by the German Government Commission of Animal Care. All litters of PEX11β knockout mice with C57Bl/6J background were bred under SPF conditions in the Central Animal Facility (ZTL = Zentrales Tierlabor) of the Justus Liebig University.

b) Human patient characteristics (adult human donor lung and idiopathic pulmonary fibrosis)

Human lung tissue, which was not or only partially used for transplantation was obtained from 3 donor lungs and 4 lungs with idiopathic pulmonary fibrosis from the tissue collection bank of the University of Giessen Lung Centre (UGLC). Characteristics of all patients are given in table 3. The study protocol for human tissue use was approved by the local internal review board of the Ethics

| Diagnosis | Age (yr) | Sex |
|-----------|----------|-----|
| Donor 1 | 56 | F |
| Donor 2 | 87 | M |
| Donor 3 | 53 | M |
| IPF 1 | 52 | M |
| IPF 2 | 54 | F |
| IPF 3 | 64 | M |
| IPF 4 | 62 | M |

Table 3. Human lung patient characteristics

Committee of the Faculty of Medicine (Justus Liebig University of Giessen) in accordance with national law and with the guidelines for "Good Clinical Practice/International Conference on Harmonisation". For protein extraction, lung tissue was snap-frozen directly after explantation. For morphological studies, lung tissue was immersion-fixed as described below (see in chapter 4.1) and embedded in paraffin.

3.2 Laboratory instruments, general materials, proteins and chemicals

All instruments used in the laboratory are listed alphabetically:

| Instruments | Company name |
|--|---|
| AGFA Horizon Ultra Colour Scanner | AGFA, Mortsels, Belgium |
| Biocell A10 water system | Milli Q-Millipore, Schwabach, Germany |
| Biofuge Fresco | Heraeus, Hanau, Germany |
| Biofuge Pico | Heraeus, Hanau, Germany |
| Bio-Rad electrophoresis apparatus | Bio-Rad, Heidelberg, Germany |
| Dish washing machine | Miele, Gütersloh, Germany |
| Cary 50 Bio-UV-visible spectrophotometer | Varian, Darmstadt, Germany |
| Gel-Doc 2000 gel documentation system | Bio-Rad, Heidelberg, Germany |
| Fraction collector Heidolph pump drive 5101 | Heidolph Instruments, Schwabach, Germany |
| Hera cell 240 incubator | Heraeus, Hanau, Germany |
| Hera safe, clean bench | Heraeus, Hanau, Germany |
| Ice machine, Scotsman AF-100 | Scotsman Ice Systems, Vernon Hills, IL, USA |
| iCycler PCR machine | Bio-Rad, Heidelberg, Germany |
| Leica DMRD fluorescence microscope | Leica, Bensheim, Germany |
| Leica DC 480 camera | Leica, Bensheim, Germany |
| Leica TP1020 embedding machine | Leica, Nussloch, Germany |
| Leica TCS SP2 confocal laser scanning microscope | Leica, Heidelberg, Germany |
| Leica SM 2000 R rotation microtome | Leica, Nussloch, Germany |
| Leica ultracut E ultramicrotome | Leica, Nussloch, Germany |
| Microwave oven | LG, Willich, Germany |
| Mini-Protean 3 cell gel chamber | Bio-Rad, Heidelberg, Germany |
| Microtome stretching water bath | Vieth Enno, Wiesmoor, Germany |
| Multifuge 3 SR centrifuge | Heraeus, Hanau, Germany |
| pH meter | IKA, Weilheim, Germany |
| Pipettes | Eppendorf, Hamburg, Germany |
| Potter-Elvehjem homogenizer | B.Braun, Melsungen, Germany |
| Power supply - 200, 300 and 3000 Xi | Bio-Rad, Heidelberg, Germany |
| Pressure/Vacuum Autoclave FVA/3 | Fedegari, Albuzzano, Italy |
| Sorvall Evolution RC centrifuge | Kendro, NC, USA |
| Smartspec™ 3000 spectrophotometer | Bio-Rad, Heidelberg, Germany |
| T25 basic homogenizer | IKA, Staufen, Germany |
| Thermo plate | Medax, Kiel, Germany |
| Thermo mixer HBT 130 | HLC, BioTech, Bovenden, Germany |
| Trans-Blot SD semidry transfer cell | Bio-Rad, Heidelberg, Germany |
| Trimmer TM60 | Reichert, Wolfratshausen, Germany |
| TRIO-thermoblock | Biometra, Göttingen, Germany |
| Ultra balance LA120 S | Sartorius, Göttingen, Germany |
| Ultra Turrax T25 basic homogenizer | Junke & Kunkel, Staufen, Germany |
| Vortex M10 | VWR International, Darmstadt, Germany |
| Water bath, shaker GFL 1083 | GFL, Burgwedel, Germany |
| General materials and culture media | Company name |
| Bronchial epithelial growth medium (BEGM) | Clonetics, MD, USA |

Materials & Methods

| | |
|--|--|
| Bronchial epithelial basal medium (BEBM) | Clonetics, MD, USA |
| BioMax MR-films | Kodak, Stuttgart, Germany |
| Cover slips | Menzel-Gläser, Braunschweig, Germany |
| Dulbecco's Modification of Eagle's Medium (DMEM) | Sigma, Steinheim, Germany |
| Filter tips and canules | Braun, Melsungen, Germany |
| Microtome blade A35 | Feather, Köln, Germany |
| Molecular weight markers (DNA, RNA) | Fermentas, St.Leon-Rot, Germany |
| Multi-well cell culture plates (12 wells) | BD Biosciences, Heidelberg, Germany |
| Nylon meshes (100, 20 and 10 µm) | Bückmann, Mönchengladbach, Germany |
| Oligo-dT primer | Invitrogen, Heidelberg, Germany |
| PAP pen | Polysciences, Eppelheim, Germany |
| Paraffin | Paraplast Plus, MO, USA |
| PVDF membranes | Millipore, Schwalbach, Germany |
| RT-PCR primers (various) (see table 5) | Operon, Cologne, Germany (see table 5) |
| Proteins and enzymes | Company name |
| Antibodies (various antigens) see table 4 | Various companies see table 4 |
| Bovine serum albumin (BSA) | Roth, Karlsruhe, Germany |
| Dispase | BD Biosciences, NJ, USA |
| DNase I | Sigma, Steinheim, Germany |
| Fetal calf serum | HyClone, UT, USA |
| Immunostar-alkaline phosphatase | Bio-Rad, Heidelberg, Germany |
| Keratinocyte growth factor from <i>H.sapiens</i> | Peptotech, NJ, USA |
| Matrigel | BD Biosciences, NJ, USA |
| Milk powder | Roth, Karlsruhe, Germany |
| Precision Plus protein standards, dual color | Bio-Rad, Heidelberg, Germany |
| Precision Plus protein standards, unstained | Bio-Rad, Heidelberg, Germany |
| Proteinase K | Sigma, Steinheim, Germany |
| SuperScript III reverse transcriptase | Invitrogen, Heidelberg, Germany |
| <i>Taq</i> DNA polymerase | Invitrogen, Heidelberg, Germany |
| Trypsin | Sigma, Steinheim, Germany |
| Chemicals | Company name |
| Acrylamide | Roth, Karlsruhe, Germany |
| Agarose LE | Roche, Grenzach-Wyhlen, Germany |
| BDMA | Plano, Wetzlar, Germany |
| Bradford reagent | Sigma, Steinheim, Germany |
| Bromophenol blue | Riedel-de-Haën, Seelze, Germany |
| Calcium chloride | Merck, Darmstadt, Germany |
| Citric acid | Merck, Darmstadt, Germany |
| 3,3'-Diaminobenzidine-tetrahydrochloride (DAB) | Sigma, Steinheim, Germany |
| Dodoceny succinic anhydride (DDSA) | Plano, Wetzlar, Germany |
| Epoxy Resin 812 | Agar, Essex, England |
| Ethanol | Riedel-de-Haën, Seelze, Germany |
| Ethidium bromide | Fluka, Neu-Ulm, Germany |
| Ethylene diamine tetraacetic acid (EDTA) | Fluka, Neu-Ulm, Germany |
| Formvar 1595 E | Serva, Heidelberg, Germany |
| Glutaraldehyde (GA) | Serva, Heidelberg, Germany |

Materials & Methods

| | |
|--|------------------------------------|
| Glycine | Roth, Karlsruhe, Germany |
| Glycerol | Sigma, Steinheim, Germany |
| HEPES/4-(2-hydroxyethyl)-1-piperazineethanesulfonic acid | Roth, Karlsruhe, Germany |
| Hydrogen peroxide (H ₂ O ₂) | Merck, Darmstadt, Germany |
| Ketavet | Bayer, Leverkusen, Germany |
| L-Glutamate | Cambrex BioScience, MD, USA |
| LR white medium grade | LR White Resin, Berkshire, England |
| Methanol | Merck, Darmstadt, Germany |
| Methylnadic anhydride (MNA) | Plano, Wetzlar, Germany |
| MOPS 3-[N-Morpholino]-propanesulfonic acid | Serva, Heidelberg, Germany |
| Mowiol 4-88 | Polysciences, Eppelheim, Germany |
| N-propyl-gallate | Sigma, Steinheim, Germany |
| Osmium tetroxide | Polysciences, Eppelheim, Germany |
| Paraformaldehyde (PFA) | Sigma, Steinheim, Germany |
| Penicillin/Streptomycin | PAN Biotech, Aidenbach, Germany |
| PIPES/1,4 Piperazine bis (2-ethanosulfonic acid) | Sigma, Steinheim, Germany |
| Ponceau S | Serva, Heidelberg, Germany |
| Potassiumhexacyanoferrate | Merck, Darmstadt, Germany |
| Rompun | Bayer, Leverkusen, Germany |
| Rotiphorese Gel 30 | Roth, Karlsruhe, Germany |
| RNaseZap | Sigma, Steinheim, Germany |
| Sodium carbonate | Merck, Darmstadt, Germany |
| Sodium chloride | Roth, Karlsruhe, Germany |
| Sodium hydrogen carbonate | Merck, Darmstadt, Germany |
| Sodium hydroxide | Merck, Darmstadt, Germany |
| Sucrose | Merck, Darmstadt, Germany |
| Sodium dodecyl sulphate | Sigma, Steinheim, Germany |
| Tetramethylethylenediamine (TEMED) | Roth, Karlsruhe, Germany |
| Tris (trishydroxymethylaminomethane) | Merck, Darmstadt, Germany |
| Triton X-100 | Sigma, Steinheim, Germany |
| Trypan blue | Sigma, Steinheim, Germany |
| Tween 20 | Fluka, Steinheim, Germany |
| Uranyl acetate | Merck, Darmstadt, Germany |
| Xylene | Merck, Darmstadt, Germany |

3.2.1 Kits

Alphabetical list of used kits

| Kits | Company name |
|---|--------------------------------------|
| Avidin/Biotin-blocking kit | Vector Laboratories, Burlingame, USA |
| Novared Peroxidase-Substrate kit | Vector Laboratories, Burlingame, USA |
| PCR kit | Qiagen, Hilden, Germany |
| Rabbit ExtrAvidin Peroxidase-Staining kit | Sigma, Steinheim, Germany |
| RNeasy kit | Qiagen, Hilden, Germany |
| RT-PCR kit | Invitrogen, Heidelberg, Germany |

3.2.2 Buffer solutions

| Buffer or Solution | Components |
|---|---|
| Solutions for Morphology | |
| A) Solutions for light and confocal microscopy | |
| Perfusion fixative solution (PFA) | 4% PFA in 1X PBS (150 mM NaCl, 13.1 mM K ₂ HPO ₄ , 5 mM KH ₂ PO ₄), pH 7.4 |
| 10 X PBS | 1.5 M NaCl, 131 mM K ₂ HPO ₄ , 50 mM KH ₂ PO ₄ , pH 7.4 |
| Trypsin (0.01%) | Fresh 0.01 g trypsin in 100 ml of 1X PBS buffer |
| H ₂ O ₂ (3%) | 10 ml of fresh H ₂ O ₂ (30%) + 90 ml of ddH ₂ O |
| Citrate buffer | Buffer A: 1 mM C ₆ H ₈ O ₇ ·H ₂ O; Buffer B: 50 mM C ₆ H ₅ Na ₃ O ₇ ·2H ₂ O Final concentration: 0.15 mM buffer A + 8.5 mM buffer B |
| Blocking buffer- 4% PBSA + 0,05% Tween 20 | To 8 g BSA add 200 ml of 1X PBS and 100 µl of Tween 20 |
| Dilution buffer- 1% PBSA + 0,05% Tween 20 | To 2 g BSA add 200 ml of 1X PBS and 100 µl of Tween 20 |
| Mowiol 4-88 solution | Overnight stirring of 16.7 % Mowiol 4-88 (w/v) + 80 ml of 1X PBS, add 40 ml of glycerol, stir again over night; centrifuge at 15000U/min for 1 hr and take off the supernatant and store at -20°C |
| Anti-fading agent (2.5%) | 2.5 g N-propyl-gallate in 50 ml of PBS and add 50 ml of glycerol |
| Mounting medium | 3 parts of Mowiol 4-88 + 1 part of anti-fading agent |
| B) Solutions for Electron Microscopy | |
| Perfusion fixative solution | 4% PFA (w/v) in cacodylate buffer + 2% sucrose (w/v) + 0.05% glutardialdehyde (w/v), pH 7.4 |
| Immersion fixation solution | 4% PFA (w/v) in cacodylate buffer + 2% sucrose (w/v), pH 7.4 |
| Teorell-Stenhagen buffer (TS) | 50 mM H ₃ PO ₄ , 75 mM boric acid, 35 mM citric acid, 345 mM NaOH, pH 10.5 |
| Na-Cacodylate buffer | 0.1 M sodium cacodylate, pH 7.4 |
| DAB | 0.2 % DAB (w/v), 0.01 M TS buffer 0.15 % H ₂ O ₂ , pH 10.5 |
| PIPES 1,4 Piperazine bis (2-ethanosulfonic acid) buffer | 0.1 M PIPES, pH 7.4 |
| Epon (50 ml) Epoxy resin Agar 812 | 24 g epoxy resin + 16 g DDSA + 10 g MNA stir together for at least 30 min and add drop by drop 1.5 g BDMA and stir at least for 30 min |
| Uranyl acetate | 1% uranyl acetate in ddH ₂ O. Centrifuge for 5 min before use |
| Lead citrate | 0.19 mM lead nitrate + 0.22 mM sodium citrate- shake for 30 min- crystal free solution-fill with ddH ₂ O to 25 ml, pH 10.0 |
| C) Solution for Biochemistry | |
| Homogenization buffer (HMB) | To 50 ml of 0.25 M sucrose and 5 mM MOPS (pH 7.4) add only before use 500 µl 100 mM EDTA + 50 µl 100% ethanol + 5 µl 2 M DTT + 50 µl 1 M aminocaproic acid and 100 µl cocktail of protease inhibitors |
| A) SDS-PAGE solutions | |

Materials & Methods

| | |
|---|--|
| Resolving gel buffer A | 1.5 M Tris-HCL pH 8.8 + 0.4% SDS |
| Stacking gel buffer B | 0.5 M Tris-HCL pH 6.8 + 0.4% SDS |
| 12 % Resolving gel (for 4 SDS-PAGE gels) | 8 ml of 30% acrylamide + 10 ml of buffer A + 2 ml of ddH ₂ O + 15 µl of TEMED + 130 µl of 10% APS |
| 12 % Stacking gel (for 4 SDS-PAGE gels) | 1.25 ml of 30% acrylamide + 5 ml of buffer B + 5 ml of DH ₂ O + 15 µl of TEMED + 130 µl of 10% APS |
| 10X Sample buffer | 3.55 ml ddH ₂ O + 1.25 ml 0.5 M Tris-HCl, pH 6.8 + 2.5 ml 50% (w/v) glycerol + 2.0 ml 10% (w/v) SDS + a pinch of 0.05% bromophenol blue. Before use add 50 ml β-mercaptoethanol |
| 10% Blocking buffer | 10 g fat free milk powder in 100 ml of ddH ₂ O |
| B) Western Blotting solutions | |
| 10X Electrophoresis buffer | 250 mM Tris + 2 M glycine + 1% SDS |
| 20X Transfer buffer | Bis-Tris-HCl buffered (pH 6.4) polyacrylamide gel; NuPAGE transfer buffer, Invitrogen, Heidelberg, Germany |
| 10X TBS | 0.1 M Tris + 0.15 M NaCl in 1000 ml of ddH ₂ O, adjust to pH 8.0 |
| 1X Washing buffer (TBST) | 10 mM Tris/HCl, 0.15 M NaCl, 0.05% Tween 20, pH 8.0 |
| Stripping buffer (500 ml) | 62.5 mM Tris, 0.2 % SDS, 500 ml ddH ₂ O – 42°C water bath for 40 min pH 6.8 |
| Ponceau S solution | 0.1 % (w/v) Ponceau S in 5 % (v/v) acetic acid |
| Solutions for Molecular Biology | |
| Transfer buffer 10X (TAE) | 40 mM Tris base + 20 mM acetic acid + 1 mM EDTA pH 7.6 |
| RNA-loading dye (10 ml) | 16 µl saturated aqueous bromophenol blue, 80 µl 500 mM EDTA, pH 8.0, 720 µl 37% formaldehyde, 4 ml 10X gel buffer fill upto 10 ml ddH ₂ O |
| 10X RNA transfer buffer | 200 mM MOPS, 50 mM sodium acetate, 10 mM EDTA, pH 7.0 |
| 1X Formaldehyde gel | 100 ml 10X RNA transfer buffer + 20 ml 37% formaldehyde + 880 ml ddH ₂ O |

3.2.3 Antibodies

Table 4 depicts the overview of primary antibodies against lung cell-type-specific antigens, peroxisomal, mitochondrial and cytoplasmic antigens as well as corresponding secondary antibodies, which were used for various morphological methods and for Western blots.

3.2.4 Primers

Table 5 depicts the list of primer pairs used in this study.

| Primary antibodies | | Cell type-specific antigens | | Species ab raised in (AB) | | Dilution (IHC) | Dilution (IF) | Immunogen EM | Dilution (WB) | Supplier |
|--|---------------------|------------------------------------|---------|----------------------------------|----------|--|----------------------|---------------------|--|-----------------|
| Clara Cell 10 (CC10), mouse | Rabbit, polyclonal | 1:2,000 | 1:2,000 | - | - | - | - | - | Santa Cruz Biotechnology Inc., Heidelberg, Germany, Cat. no: sc-9773 | |
| Clara Cell 10 (CC10), mouse | Goat, polyclonal | - | 1:50 | - | - | - | - | - | Santa Cruz Biotechnology Inc., Heidelberg, Germany, Cat. no: sc-25555 | |
| Mucin 5AC, human | Mouse, monoclonal | - | 1:500 | - | - | - | - | - | BIOTREND chemicals, Köln, Germany, Cat. no: 1695-0128 | |
| α -tubulin, sea urchin | Mouse, monoclonal | - | 1:500 | - | - | - | - | - | Sigma, Missouri, USA, Cat. no: T5168 | |
| Surfactant protein B (SP-B), sheep | Rabbit, polyclonal | - | 1:1,000 | - | - | - | - | - | Chemicon International, Temecula, Canada, Cat. no: ab3780 | |
| Pro surfactant protein C (pro-SP C), human | Rabbit, polyclonal | - | 1:2,000 | - | - | - | - | - | Chemicon International, Temecula, Canada, Cat. no: ab3786 | |
| Surfactant protein D (SP-D), mouse | Rabbit, polyclonal | - | 1:1,000 | - | - | - | - | - | Chemicon International, Temecula, Canada, Cat. no: ab3434 | |
| Podoplanin (Ti α), mouse | Hamster, monoclonal | - | 1:500 | - | - | - | - | - | Acris Antibodies GmbH, Hiddenhausen, Germany, Cat. no: dm3501 | |
| Aquaporin 5 (AQP5), rat | Rabbit, polyclonal | - | 1:1,000 | - | - | - | - | - | Chemicon International, Temecula, Canada, Cat. no: ab3069 | |
| von Willebrand Factor (vWF), mouse | Mouse, monoclonal | - | 1:500 | - | - | - | - | - | Santa Cruz, Cat. no: sc-59810 | |
| CD68, human | Mouse, monoclonal | 1:1,000 | 1:1,000 | - | - | - | - | - | Abcam, Cambridge, UK, Cat. no: ab955 | |
| Cluster of Differentiation 16/32 (CD16/32), mouse | Rat, monoclonal | AECL cell isolation – panning | - | - | - | - | - | - | BD Pharmingen, CA, USA, Cat. No: 553141 | |
| Cluster of Differentiation 45 (CD45), mouse | Rat, monoclonal | AECL cell isolation – panning | - | - | - | - | - | - | BD Pharmingen, CA, USA, Cat. No: 553076 | |
| Peroxisomal | | | | | | | | | | |
| "SKL", mouse peptide | Rabbit, polyclonal | - | - | - | - | 1:5,000 | - | - | Gift from Denis I. Crane, School of Biomol. Biophys. Sci., Griffith Univ., Nathan, Brisbane, Australia; see reference: (Maxwell et al. 2003) | |
| ABC-transporter D3 (ABCD3/PMP70), mouse | Sheep, polyclonal | - | 1:1,000 | - | - | 1:3,000 | - | - | Gift from Steve Gould, Johns Hopkins Univ., Dept. Biol. Chem., Baltimore, MD, USA; see reference: (Fang et al. 2004) | |
| ABC-transporter D3 (ABCD3/PMP70), mouse | Rabbit, polyclonal | - | 1:1,000 | - | - | - | - | - | Gift from Alfred Völk, Dept. of Anatomy and Cell Biology, Heidelberg, Germany; see reference: (Islinger et al. 2006) | |
| Peroxin 13 (Pex13p), mouse | Rabbit, polyclonal | - | 1:2,000 | - | - | 1:5,000 | - | - | Gift from Denis I. Crane (address see above); see reference: (Maxwell et al. 2003) | |
| Peroxin 14 (Pex14p), mouse | Rabbit, polyclonal | 1:2,000 | 1:2,000 | - | - | 1:30,000 | - | - | Gift from Denis I. Crane (address see above); see reference: (Maxwell et al. 2003) | |
| Catalase (CAT), mouse | Rabbit, polyclonal | 1:4,000 | 1:4,000 | 1:5,000 | - | 1:50,000 | - | - | Gift from Denis I. Crane (address see above); see reference: (Maxwell et al. 2003) | |
| Acyl-CoA oxidase 1 (ACOX1), mouse | Rabbit, polyclonal | - | 1:1,000 | - | - | 1:5,000 | - | - | Gift from Paul P. van Veldhoven, Dept. of Molecular Cell Biology, Pharmacology, Catholic University Leuven, Belgium; see reference: (Huyghe et al. 2001) | |
| Thiolase, mouse | Rabbit, polyclonal | - | 1:1,000 | - | - | 1:5,000 | - | - | Gift from Paul P. von Veldhoven (address see above); see reference: (Antonenkov et al. 1999) | |
| Peroxisedoxin V (Prx V), human | Goat, polyclonal | - | 1:200 | - | - | - | - | - | Santa Cruz, Cat. no: sc-23977 | |
| Mitochondrial | | | | | | | | | | |
| Oxidative phosphorylation complex III (OxPhosIII), human | Mouse, monoclonal | - | 1:1,000 | - | - | - | - | - | Molecular Probes/Invitrogen, Carlsbad, USA, Cat. no: A11143 | |
| Superoxide dismutase 2 (SOD2), rat | Rabbit, polyclonal | - | 1:1,000 | - | - | - | - | - | Research Diagnostics, Inc., NJ, USA, Cat. no: RDI-RTSODMabr | |
| Cytoplasm | | | | | | | | | | |
| Glutathione reductase (GR), human | Rabbit, polyclonal | - | 1:1,000 | - | - | - | - | - | Biozol, Eching, Germany, Cat. no: ab16801 | |
| Cytochrome P450 side chain cleavage enzyme (P450sc), rat | Rabbit, polyclonal | - | 1:1,000 | - | - | - | - | - | Abcam, Cat. no: ab13513 | |
| Inducible nitric oxide synthase (iNOS), mouse | Rabbit, monoclonal | - | 1:1,000 | - | - | - | - | - | Sigma, Steinheim, Germany, Cat. no: N7782 | |
| Secondary antibodies, extravidin and protein A | | | | | | | | | | |
| Secondary detection system used | | | | | | | | | | |
| Rabbit biotinylated IgG | Goat | IHC | IHC | Method | Dilution | Supplier | | | | |
| Extravidin | Rabbit | IHC | IHC | IHC | 1:250 | Rabbit Extravidin kit, Sigma, Steinheim, Germany, Cat. no: B6648 | | | | |
| anti-Rabbit-IgG AlexaFluor488 | Donkey | IF | IF | IF | 1:1,000 | Rabbit Extravidin kit, Sigma, Steinheim, Germany, Cat. no: E8386 | | | | |
| anti-Mouse-IgG AlexaFluor555 | Donkey | IF | IF | IF | 1:1,000 | Molecular Probes/Invitrogen, Cat. no: A21206 | | | | |
| anti-Goat-IgG AlexaFluor594 | Goat | IF | IF | IF | 1:1,000 | Molecular Probes/Invitrogen, Cat. no: A31570 | | | | |
| anti-Hamster-IgG AlexaFluor647 | Donkey | IF | IF | IF | 1:1,000 | Molecular Probes/Invitrogen, Cat. no: A11058 | | | | |
| anti-Sheep-IgG Rhodamine red-X | - | EM | EM | EM | 1:80 | Molecular Probes/Invitrogen, Cat. no: A21451 | | | | |
| Protein A-gold | Goat | WB | WB | WB | 1:20,000 | Dianova, Hamburg, Germany, Cat. no: 713-295-147 | | | | |
| anti-Rabbit IgG-alkaline phosphatase | Donkey | WB | WB | WB | 1:20,000 | See reference Slot and Geuze 1981 | | | | |
| anti-Sheep IgG-alkaline phosphatase | Donkey | WB | WB | WB | 1:20,000 | Sigma, Steinheim, Germany, Cat. no: A3687 | | | | |
| Counterstaining of nuclei for IF | | | | | | | | | | |
| Hoechst 33342 (1 μ g/ml) nucleic acid staining | - | - | - | - | - | Molecular Probes/Invitrogen, Cat. no: 33342 | | | | |
| TOTO-3 nucleic acid staining, 1:1,000 | - | - | - | - | - | Molecular Probes/Invitrogen, Cat. no: T-3604 | | | | |

Table 5. List of primers used in this study

| Gene target | Gene bank accession no. | Sense primer (5'-3') | Antisense primer (5'-3') | PCR product (bp) |
|---|-------------------------|---------------------------|----------------------------|------------------|
| Peroxisomal | | | | |
| PEX11 α | BC028786 | TCAGTGTCTGTGTTCTCAGTCCCT | GTACTTAGGAGGTCCTCCGGAGAGGA | 420 |
| PEX11 β | BC013812 | GTATGCTGTTCCTCTCTCG | CTCGGTTGAGGTGACTGACA | 215 |
| PEX11 γ | AK007582 | GACTCTGCTTGGTGGACACT | TGTCCTCCCACTCACCTTTAGGC | 682 |
| PEX5 | NM_008995 | GAGTGAAGAAGCAGTGGCTGCATAC | GGACAGAGACGCTCATCCCTACAA | 508 |
| PEX13 | BC023683 | GACCACGTAGTTCGAAGAGCAGAGT | CTGAGGCAGCTTGTTGTTCTACTG | 717 |
| PEX14 | BC028952 | CACTGCCCTGTCCAAGAGCTA | CTGACAGGGGAGATGTCACACTG | 978 |
| ABCD1 | BC011273 | GACGTCCTGTCTGGAGGTGAGAA | GGGATAAGGTCCCCAGTCAAAGT | 421 |
| ABCD3 | BC050102 | CTGGGGCTGAAATGACTAGATTGG | AGTGCACATTGTCCAAGTACTCC | 523 |
| ACOX1 | BC056448 | CTGAACAAGACAGAGTCCACGAA | TGTAAGGGCCACACACTCACATCT | 565 |
| MFP1 | NM_023737 | ATGGCCAGATTTCAAGAAATG | TGCCACTTTTGTGATTTGC | 211 |
| pTH1 | AY273811 | TCAGGTGAGTGATGGAGCAG | CACACGTAGACGGCCTGAC | 241 |
| ACOX2 | BC021339 | CTCTTGCACGTATGAGGTGAGAA | CTAGATTTGGCTGGGACTTCTG | 688 |
| ACOX3 | BC024609 | GCCAAAGCTGATGGTGAGCTCTAT | AGGGGTGGCATCTATGCTTTTCAG | 813 |
| MFP2 | NM_008292 | GAGCAGGATGGATTGGAAAA | TGACTGTFACGGTTTGGTGA | 223 |
| SCP2 | NM_011327 | GGCCTTCTTCAAGGGAAAC | ACCACGCCAAATTAGCAAC | 230 |
| GNPAT | BC025972 | TGAGGACGTGCAAGCCTTTG | TCCAGAAAGTACGGGTGAA | 759 |
| AGPS | NM_172666 | TTTTGGGAAACAAAAAGCTCAA | TTGGAGCAACACACTTCAGG | 250 |
| ID1L | BC004801 | TCTGTCTCGGCTTCAGACAGGATG | AGTACCTGGGAGTCCAGAGAAAGGTG | 480 |
| HMGCR | NM_008255 | CCACCGAGCAAACTTGTGTC | TGAGCCCACTGATCACCC | 741 |
| ROS metabolizing enzymes | | | | |
| a) peroxisomal | | | | |
| CAT | BC013447 | GGAGAGGAAACGCTGTGTGA | GTCAGGGTGGACGTCAGTGAAA | 103 |
| PRX1 | NM_011034 | TCCTTTTCAGGGGCTTTTT | CCAAAACACAGCTCAGACCA | 396 |
| PRX5 | BC008174 | AGATGCCAATCCCTCAGTGGAG | GGTGGGAGAGATGGGAGAGTCA | 791 |
| b) other | | | | |
| SOD1 | BC086886 | AGCGGTGAACCAAGTTGTGTTGT | CCACACAGGGAATGTTACTGCG | 405 |
| SOD2 | NM_013671 | AAGTAGGTAGGGCTGTCCGATG | CTAAGGGACCCAGACCCCAACAAG | 624 |
| SOD3 | BC010975 | GGAGAGCGAGTGCAGAACCACTT | TCAAAGTGTCTCACTGGGAAAGTC | 485 |
| GSTA1 | BC132572 | GCAGACCAGGCCATTCACACTAC | CTGCCAGGCTGTAGGAACCTTCTC | 408 |
| PRX6 | NM_007453 | TTGATGATAAGGGCAGGGAC | CTACCATCAGCTCTCTCCC | 260 |
| HMOX1 | NM_010442 | GCACTATGTAAGGCTCTCCACGAG | CCAGGCAAGATTCCTCTTACAGAG | 610 |
| GPX | BC086649 | GGGACTACCGAGATGAACGA | ACCATTCACTTCGCACCTTCTCA | 430 |
| Epithelial lineage differentiation markers and surfactant proteins | | | | |
| SP-A | NM_023134 | CCCTCTTCTTGACTGTTGTTGCTG | GAGTGGCTTCAATCACACCTA | 375 |
| SP-B | BC032785 | AATGACCTGTCCAAAGTGTGAG | GCCATTCTTCTATCAGAGGCTCCA | 673 |
| SP-C | BC061137 | CTGATGGAGAGTCCACCGGATAC | GAAGATCGACTCGGAACCAAGTA | 485 |
| SP-D | BC003705 | GGACTCCAGGACTTCCAGGTATT | TGGCAGCATCTCAGTAGCAGAAC | 583 |
| T1 α | BC026551 | GGAGGGACTATAGCGGTGAATG | GGGCAAGTTGGAAAGCTCTTTA | 405 |
| CC10 | NM_011681 | ACTGTGGTCATGCTGTCCATCT | GCAGTGACAAGGCTTTAGCAG | 318 |
| AQP5 | NM_009701 | GATCTACTCACCGGCTGTCC | TAGGGAGAGGTGCTCCAAACTC | 340 |
| CAV1 | BC038280 | GGAAITGGTTGCTGTCTCCTCACT | AGAGGTCTCACCCCAATTTGTCT | 430 |
| Signalling molecules | | | | |
| PPAR α | BC016892 | AGACCGTACGGAGCTCACA | GGCTGCCATCTCAGGAAAAG | 584 |
| PPAR β | BC070398 | CACCGAGTTCGCCAAGAACA | AGAGCCCGAGAATGGTGTCT | 363 |
| PPAR γ | BC021798 | TCCGTAGAAGCCGTGCAAGA | CACCTTGGCGAACAGCTGAG | 441 |
| WNT-5a | NM_009524 | GGACGCTAGAGAAAGGGAACGAAT | TCGGTCTGCACCTGTCTAAACTGG | 468 |
| Controls | | | | |
| GAPDH | BC092063 | CACCATGGAGAAAGCCGGGG | GACGGACACATTTGGGGTGTAG | 418 |
| 28S rRNA | NR_003279 | CCCTCGATGTCGGCTCTTCTAT | GGCGTTCAATGTCATAATCCACAG | 254 |

4 Methods

4.1 Techniques for light and fluorescence microscopy

4.1.1 Fixation of mouse lungs for light microscopy by tracheal instillation

a) Animals and anaesthesia

Newborn (P0), postnatal 15 (P15) and adult wild type C57Bl/6J mice (25–28 g, 12-15 weeks of age; Charles River, Sulzfeld, Germany) were anaesthetised intraperitoneally with a combination of rompun (13 µg/g b.w.) and ketavet (65 µg/g b.w.). For comparative experiments between WT and PEX11β KO animals E19 lungs were used, since PEX11β deficient mice die immediately after birth.

b) Fixation by tracheal instillation and immersion

The fur of the mouse was vertically incised from the pelvis to the mandibles and removed to both sides. The trachea was cannulated through a midline neck incision, the abdomen was opened and a bilateral pneumothorax was produced by puncturing the abdominal surface of the diaphragm. The sternum was cut in the middle and the thorax was opened with a thorax spanner. Thereafter, the mice were exsanguinated by cutting the inferior vena cava and the left renal artery. The right ventricle of the heart was punctured with a 24 size gauge needle and for removal of the blood 10-20 ml saline was flushed through the pulmonary circulation. Subsequently, for fixation 2 ml of 4% freshly depolymerized paraformaldehyde, containing 2% sucrose in PBS (pH 7.4), were injected into the trachea. The trachea was finally ligated, the lungs were removed and further fixed from the outside by overnight immersion fixation. The lung tissue was embedded into paraffin with a Leica TP1020 embedding machine (3 x 70%, 80%, 90% 100% alcohol-90 min each step; 2 x Xylene-90 min each step; 2 x Paraffin-120 min each step). Three µm sections were cut with a rotation microtome (Leica SM 2000 R) and mounted on Superfrost Plus(+) slides.

c) Perfusion fixation of E19 animals

For the perfusion of the newborn WT and PEX11β KO animals, the skin of the pups was opened, the right ventricle of the heart was punctured with a 18 size gauze needle. Thereafter the left atrium

was cut open and the animals were perfused via the right ventricle with 500 µl saline followed by perfusion with 10 ml 4% PFA fixative in PBS, pH 7.4.

4.1.2 Immersion fixation of human lungs

Human lung tissue was excised from non-transplanted healthy donor lungs or IPF and immediately placed in immersion fixative with 4% depolymerised PFA in PBS (pH 7.4) within 10 min after explantation. Lungs were fixed for 24 h at 4°C prior to paraffin embedding. For our experiments, paraffin embedded human donor lung samples were obtained from the central tissue bank of the University of Giessen Lung Center (UGLC).

4.1.3 Immunohistochemistry (IHC) with the ABC-peroxidase method

Paraffin embedded lung sections 2-3 µm were deparaffinized with xylene (3 x 5 min) followed by rehydration in a series of ethanol (2 x 99%, 96%, 80%, 70%, 50% ETOH, 1.5 min each step). For antigen retrieval and improved accessibility of epitopes, rehydrated sections were subjected to 0.01% trypsin digestion for 10 min at 37°C and additional irradiation for 3 x 5 min in a microwave oven (850 W, in citrate buffer, pH 6) with subsequent cooling for one hr to room temperature (RT). Blocking of endogenous peroxidase was done by incubating the sections for 5 min with 3% H₂O₂ (Merck, Darmstadt, Germany) in a moist chamber at RT. Non-specific protein binding sites and endogenous biotinylated proteins in lung sections were blocked for 2 hr with 4% BSA in PBST (PBS / 0.05% tween 20, pH 7.4) containing avidin (dilution 1:250) (Avidin/Biotin blocking kit, Vector, Burlingame, CA). Washing steps were performed between all following steps with PBST for 5 min. After washing, sections were incubated overnight with primary antibodies against different peroxisomal proteins (such as CAT or Pex14p) and other distinct markers of the pulmonary cell types (such as CC10), in PBST at 4°C, including free biotin (dilution 1:250) to saturate the bound avidin (Avidin/Biotin blocking kit). Details of all antibodies used in this study are listed in table 4. For detection of antigen-antibody complexes the sections were incubated with a biotinylated goat anti-rabbit secondary antibody (1:100) for 2 hr at room temperature. The bound secondary antibody was detected with peroxidase-coupled extravidin system (Rabbit Extravidin Kit) and visualized by histochemical staining of the peroxidase activity using Novared as substrate (4 min at RT). This reaction was stopped with H₂O and the sections were counterstained with hematoxylin for 10 min,

dehydrated in a series of ethanol and xylene and mounted with Depex. Negative controls were incubated in parallel without primary antibody. All sections were analyzed with a Leica DMRD microscope equipped with a Leica DC 480 camera.

4.1.4 Indirect immunofluorescence on paraffin sections of wildtype and PEX11 β ^{-/-} mouse and human lung tissues

Pretreatment and antigen-retrieval of paraffin sections of mouse, human and PEX11 β deficient mouse lung tissue were performed in the same way as for the ABC-peroxidase-stainings. Subsequently to blocking with 4% bovine serum albumin in PBST, sections were incubated with antibodies against cell type-specific marker proteins, peroxisomal and mitochondrial as well as pro- and anti-oxidant enzymes; for details on the antibodies see table 4. For staining of peroxisomes, several antibodies against a) peroxisomal membrane proteins, e.g. rabbit anti-biogenesis proteins Pex13p and Pex14p (Maxwell et al., 2003) and the ABC-transporter D3 (ABCD3) (Fang et al., 2004; Islinger et al., 2006) and b) peroxisomal matrix proteins, such as rabbit anti-catalase (Maxwell et al., 2003), acyl-CoA oxidase I (Huyghe et al., 2001) and peroxisomal 3-oxo-acyl-CoA thiolase (Antonenkov et al., 1999) were used. All antibodies against peroxisomal proteins were already tested for specificity in immunofluorescence preparations of paraffin sections of other tissues (brain: Ahlemeyer et al 2007 and testis: Nenicu et al 2008). The antibodies were kind gifts from Denis I. Crane (catalase, Pex13p and Pex14p: Griffith University, Brisbane, Australia), Steve J. Gould (ABCD3: Johns Hopkins University, Baltimore, USA), Paul P. Van Veldhoven (ACOX1 and thiolase: Catholic University, Leuven, Belgium), Alfred Völkl (ABCD3: University of Heidelberg, Heidelberg, Germany). The antigen-antibody complexes were visualized by commercially available fluorescently-labeled secondary antibodies: anti-rabbit IgG Alexa Fluor 488, anti-mouse IgG Alexa Fluor 555, anti-goat-IgG Alexa Fluor 594, anti-hamster IgG Alexa Fluor 647 and anti-sheep IgG Rhodamine red (see table 4). Except for Alexa Fluor 647 labeling sections were counterstained with TOTO-3 iodide for identification of nuclear morphology and mounted in Mowiol 4.88 with N-propylgallate in a ratio of 3:1. Optimal stainings of antibodies were tested out in dilution series in single labeling experiments. Thereafter, antibodies against cell-type specific markers and peroxisomal proteins were combined for double-labeling experiments. Double-immunofluorescence preparations were examined using a Leica TCS SP2 confocal microscope using a 63 x objective and “Airy 1” setting.

4.1.5 Indirect immunofluorescence on freshly isolated or cultured AECII

Immunofluorescence labeling was performed on freshly isolated cells as well as cultured AECII by fixing with 4% PFA / PBS (pH 7.4) for 20 min. Cells were permeabilized with Triton X-100 (10 min, 0.01%) followed by blocking of the aldehyde groups with 0.1% glycine for 5 min. Cells were washed during each step with PBST for 15 min. Thereafter, cells were incubated overnight with primary antibodies against AECII marker proteins, polyclonal rabbit pro SP-C and peroxisomal membrane and matrix proteins Pex13p, Pex14p and catalase and polyclonal sheep ABCD3. Subsequently, antigen-antibody complexes were visualized with Alexa Fluor 488-conjugated anti-rabbit IgG or Rhodamine red-labeled anti-sheep IgG for 2 h. For detailed description of the antibodies, see table 4. Counter staining of cell nuclei was performed using TOTO-3 iodide. All preparations were mounted in Mowiol 4.88 with N-propylgallate in ratio of 3:1 and analysed either with a regular fluorescence microscope or with a confocal laser scanning microscope. The purity of the isolated cell preparation was assessed by counting the number of total cells under phase contrast versus the number of pro-SP-C positive cells in the overlay by fluorescence microscopy.

4.2 Techniques for electron microscopy

4.2.1 Fixation and embedding for routine electron microscopy

For electron microscopy, lung perfusion of 3 adult mice was performed via the right ventricle with a mixture of 4% PFA and 0.05% glutaraldehyde in 0.1 M sodium cacodylate buffer with 2% sucrose, pH 7.4. Thereafter, the dissected lungs were immersed overnight in a fixative containing only 4% paraformaldehyde in 0.1 M sodium cacodylate buffer with 2% sucrose at 4°C. Thin razor blade sections were cut and lung slices were placed in a vacuum exsiccator for 1 hr in fixative solution at RT to remove the air, followed by an additional fixation step for 15 min in a fixative with 1% glutaraldehyde in 0.1 M cacodylate buffer, pH 7.4. For routine EM, sections were post-fixed with 1% reduced osmium overnight. Thereafter, the sections were dehydrated in a graded series of ethanol, and embedded in the epoxy resin 812. Embedded tissue blocks were trimmed with a Reichert TM 60 diamond trimmer. Semi thin sections were cut and selected regions were subjected to ultrathin sectioning (80 nm) with a Leica ultracut E ultramicrotome.

4.2.2 Cytochemical localization of the catalase activity with the alkaline DAB-method

To enhance the peroxidatic activity of catalase for cytochemical stainings, wet sections of lung tissue were additionally fixed for 15 min with 1 % glutaraldehyde in 0.1M cacodylate buffer. Sections were rinsed three times with 0.01 M Teorell-Stenhagen buffer, pH 10.5, and were transferred to the freshly prepared alkaline DAB medium (Angermuller and Fahimi, 1981), containing 0.2 % 3,3'-diaminobenzidine (DAB), 0.15 % H₂O₂, 0.01 M Teorell-Stenhagen buffer, pH 10.5. In contrast to Angermüller and Fahimi (1981), the DAB-incubation was done for 2 hr in a shaking water bath at 45°C to obtain an optimal catalase reaction in the lung. Thereafter, the sections were washed 3 times with 0.1 M cacodylate buffer, pH 7.4, at RT and post-fixed overnight with 1 % aqueous osmium tetroxide at 4°C. Osmicated sections were dehydrated in a graded series of ethanol and embedded in the epoxy resin 812. Embedded tissue blocks were trimmed with a diamond Reichert TM 60 trimmer. Semithin sections were cut and selected regions were subjected to ultrathin sectioning (80 nm) with a Leica ultracut E ultramicrotome. Ultrathin sections were collected on formvar-coated nickel grids and contrasted with uranyl acetate for 2 min and lead citrate for 45 s, followed by examination in a LEO 906 transmission electron microscope.

4.2.3 Post-embedding immunoelectron microscopy

After vacuum exsiccation for 1 hr in 4% PFA in cacodylate buffer pH 7.4, the second group of wet mouse lung sections was directly dehydrated after the 4 % PFA-fixation (see above) and embedded in LR white medium grade according to the protocol of Newman and colleagues (Newman et al., 1983). Ultrathin lung sections (80 nm) were collected on formvar-coated nickel grids and non-specific protein binding sites were blocked by placing the grids on 1% BSA in TBS, pH 7.4 for 30 min. Ultrathin lung sections were incubated overnight in a wet chamber with the rabbit anti-mouse catalase antibody (1:4,000 in 0.1% BSA in TBS (TBSA); see table 4). The next morning the sections were washed on a series of 12 TBSA drops. Subsequently, the grids were incubated for 60 min with the protein A-gold complex (PAG, gold particle size 15 nm) diluted 1:75 in TBSA (Slot and Geuze, 1981). Thereafter, the grids were washed shortly in a flow of distilled water and air dried. Incubated sections were contrasted with uranyl acetate for 2 min and lead citrate for 45 s. For negative controls, ultrathin sections were incubated in parallel with non-specific rabbit IgG, followed by the protein A-gold complex or with protein A-gold complex alone.

4.2.4 Illustrations

EM Gigabitfilm negative films were scanned with a AGFA-Horizon Ultra Colour Scanner and all digital pictures were processed with Adobe Photoshop (version 6) on a Microsoft windows computer.

4.3 Biochemical techniques

4.3.1 Isolation of enriched peroxisomal fractions from frozen lung and liver tissue by differential centrifugation

Since fresh human lung tissue for biochemical experiments could only be obtained as snap-frozen samples (see above), also mouse lungs and livers were processed in the same way. In contrast to frozen homogenates of mouse tissue, peroxisomal proteins could only be poorly detected in general homogenates of human lung tissue. Therefore, we used enrichment of peroxisomes in crude subcellular fractions by differential centrifugation after mild homogenization of the frozen samples. Two g of each tissue were homogenized with a Potter-Elvehjem homogenizer at 1000 rpm (1 stroke, 60 s) in 2 ml ice-cold homogenization buffer (HMB: 0.25 M sucrose and 5 mM MOPS, pH 7.4, 1 mM EDTA, 0.1 % ethanol, 0.2 mM DTT, 1 mM aminocaproic acid and 100 µl cocktail of SERVA protease inhibitors # 39102). The quality of the homogenization process was controlled by trypan blue staining of the lung homogenates with a light microscope. Clumps of connective tissue, nuclei and large mitochondria were sedimented by centrifugation of the homogenates at 2,500 × g for 20 min at 4°C. The supernatant was further processed by centrifugation at 50,000 × g for 20 min at 4°C to obtain enriched peroxisomal fractions. The resulting pellet consists of a mixture of peroxisomes, light mitochondria, lysosomes and few microsomes. These enriched peroxisomal fractions were used for further analysis. The protein concentrations of all fractions were assayed using a Bradford assay (Bradford, 1976) with Bio-Rad solutions according to the manufacturer's instructions.

4.3.2 Subcellular fractionation of primary AECII for enriched peroxisomal fractions

To determine the composition of AECII peroxisomes in comparison to the one in liver (mainly hepatocytes), freshly isolated AECII were used for isolating enriched peroxisomal fractions. ~3.5

Materials & Methods

$\times 10^8$ freshly isolated AECII were homogenized with a Potter-Elvehjem homogenizer at 1000 rpm (1 stroke, 60 s) in 100 μ l ice-cold homogenization buffer (see 4.3.1 for composition). The homogenization process was controlled by trypan blue staining of the AECII lysates. A mixed pellet with heavy mitochondria and nuclei was prepared by centrifugation of the homogenates at 2500 \times g for 20 min at 4°C (for detailed scheme of centrifugation see Fig. 14A). The supernatant was collected and the pellet resuspended in 50 μ l of HB. Both fractions were stored in liquid nitrogen. The post nuclear supernatant was further centrifuged at 50000 \times g for 20 min at 4°C to obtain an enriched peroxisomal fraction of AECII. The pellet consists the majority of peroxisomes and less amounts of other cell organelles, such as small mitochondria, lysosomes and microsomes. The collected supernatants and pellets were further subjected to protein determination and SDS-PAGE, followed by Western blotting (Fig. 14B).

4.3.3 Subcellular fractionation of adult mouse liver for enriched peroxisomal fractions

For isolation of enriched liver peroxisomes, adult male C57Bl/6J animals were used. Under anaesthesia the livers were perfused via the portal vein for a maximum of 1-2 min until all blood was washed out. Thereafter, the livers were excised and minced in chilled HB and cut into pieces with a small scissor. Three grams of liver pieces were homogenized with a Potter-Elvehjem homogenizer at 1000 rpm in 100 μ l of ice-cold HB, followed by collection of a heavy mitochondrial and enriched peroxisomal fraction by the identical differential centrifugation steps described in the Fig. 14A.

4.3.4 Western blotting

SDS-PAGE was performed using a Bio-Rad Trans-Blot SD electrophoresis apparatus. Enriched peroxisomal fractions (tissue: 50 μ g of human and mouse lung samples and 20 μ g of mouse liver; cells: 9 μ g and 4.8 μ g of freshly isolated AECII) from each sample were separated by SDS-PAGE on 12% or 15% resolving gels, depending on the proteins to be analysed. As molecular weight markers, 5 μ l of colour-stained and 5 μ l of biotinylated Precision markers from Bio-Rad were used. Protein transfer was done by semi-dry blotting onto polyvinylidene difluoride membranes (PVDF) with a semi-dry Trans-Blot SD apparatus. Non-specific protein binding sites on membranes were blocked overnight at 4°C in blocking solution, consisting of 10% fat-free milk powder in TBST. Primary

antibodies were diluted in 5% blocking solution and applied for 1 hr at room temperature on a rotor shaker at concentrations listed in table 4. After washing with TBST (3 × 10 min), blots were incubated for 1 hr with alkaline phosphatase conjugated anti-rabbit - / or anti-mouse - / or anti-sheep IgG antibodies. After a final washing step, immunoreactive bands were visualized with the Immunostar™ – AP detection kit (Bio-Rad) with a chemiluminescent substrate for alkaline phosphatase, followed by exposure of the membrane to BioMax MR-films (Kodak, Stuttgart, Germany). The biotinylated marker proteins on membranes were visualized by incubating with an alkaline phosphatase-labeled streptavidin conjugate (see table 4). Blots of different gels were stripped several times with 10 % SDS and 0.7% β-mercaptoethanol at 42°C for 45 min and reprobed with other primary antibodies. Blots were documented and densitometrically analyzed using the Gel doc 2000 digital gel documentation system.

4.3.5 Catalase activity assay

Frozen lung and liver homogenates from newborn, P15, adult lungs and adult liver samples were homogenized on ice with a Potter-Elvehjem homogenization buffer (HB). The homogenate was centrifuged for 10 min at 1000 rpm and the supernatant fraction was used for analysis of catalase enzyme activity. Protein concentrations were determined by using the Bradford assay. The supernatant fractions were used to determine catalase enzyme activity (EC 1.11.1.6) at 410 nm spectrophotometrically according to the method described by Baudhuin et al. (Baudhuin et al., 1964). Briefly, samples were incubated at 0°C with hydrogen peroxide as substrate. Hydrogen peroxide consumption was determined at 405 nm after addition of titanium oxysulfate, which forms a yellow complex with hydrogen peroxide. Results are shown as mU/μg protein. The specific activity values were calculated with respect to appropriate parallel negative controls (blanks).

4.4 Molecular biological techniques

4.4.1 RNA isolation

Total RNA was isolated from 1) AECII cell culture experiments [freshly isolated and cultured AECII that were treated with and without KGF for a period of seven days], 2) newborn, P15, adult lungs and adult liver as well as 3) snap frozen mouse lungs of different phenotypes: [PEX11β^{+/+}, PEX11β^{+/-} and PEX11β^{-/-}] using the RNeasy Mini Kit from Qiagen. Homogenization of the tissue or cells in RLT

buffer was performed with an Ultra Turrax T25 basic homogenizer for 30 sec. RNA extraction was carried out according to the manufacturer's protocol. The isolated RNA was redissolved in RNase free water and stored at -80°C. The quantity and integrity of the isolated RNA was assessed by optical density measurements, obtaining the ratio of absorbance values at 260 and 280 nm using a Bio-Rad spectrophotometer. The integrity of the RNA was determined by visualization of intact 28S, 18S and 5S ribosomal RNA bands on 1% denaturing formaldehyde agarose gels after electrophoresis. For the following RT-PCR experiments, we have used the RNA samples with best quality as confirmed by 1% denaturing formaldehyde agarose gel electrophoresis.

4.4.2 cDNA synthesis

4.4.2.1 DNase I digestion

Prior to reverse transcription, we have performed a DNase digestion to remove residual DNA in the RNA preparation. One µg of the RNA sample was added to the Dnase digestion mixture and incubated for 15 min at RT. The DNase I reaction was stopped by the addition of 1 µl of 25 mM EDTA solution to the reaction mixture and further incubation for 10 min at 65°C. Thereafter, the samples were stored at -80°C. Prior to the PCR experiments, complete removal of DNA was controlled by performing PCR reactions with gene-specific primers generally used for genotyping of animals on chromosomal DNA.

Preparation of RNA samples for DNase digestion prior to RT-PCR

| | |
|-------------------------------------|----------|
| RNA sample | 1 µg |
| 10X DNase I reaction buffer | 1 µl |
| DNase I, amplification grade, 1U/µl | 1 µl |
| RNase free water | to 10 µl |

4.4.2.2 Reverse Transcription

Total RNA (1 µg) was reverse-transcribed into cDNA using 0.5 µg oligo(dT) 12-18 primers and 10 mM dNTP mixture as described in the below protocol. The reaction was stopped by heating at 70°C for 15 min. After synthesis, single-stranded cDNA was directly used for PCR or stored at -20°C.

Reverse Transcriptase reaction mixture and protocol

| | |
|----------------------------|----------|
| Oligo(dT)12-18 (500 µg/ml) | 1 µl |
| RNA (1 µg) | ~ 4-8 µl |
| dNTP mixture (10 mM each) | 1 µl |
| Sterile distilled water | to 12 µl |

For denaturation the RNA mixture was heated to 65°C for 5 min and thereafter immediately chilled on ice. Promptly 4 µl of 5X first strand buffer was added to the reaction mixture.

| | |
|--------------------|------|
| 0.1 M DTT | 2 µl |
| RNaseOUT™ (40U/µl) | 1 µl |

The reaction mixture was mixed gently and incubated at 42°C for 2 min. Finally 1 µl of SuperScript™ II Reverse Transcriptase (200U) was added and the complete solution incubated at 42°C for 50 min for reverse transcription. The reaction was stopped by heating at 70°C for 15 min.

4.4.3 Primer design

4.4.3.1 Exon-specific primers

All primers used in this dissertation are described in table 5. Complete cDNA sequences of corresponding mRNAs to be analyzed were downloaded from the Nucleotide Database of the NCBI (<http://www.ncbi.nlm.nih.gov/sites/entrez?db=nucleotide>). For a standard PCR, 20-22 bp long primers were designed with the Primer3 online software (<http://frodo.wi.mit.edu>). The AT and GC content was checked and the difference in the melting temperature (T_m) between the forward and reverse primers was kept in a range of 2-4°C.

4.4.3.2 Intron-spanning primers

Intron-spanning primers were designed to prevent amplification of genomic DNA. As a control, the specificity of each primer was confirmed by BLAST searches against the EST and non-redundant mouse transcriptome database (<http://www.ncbi.nlm.nih.gov/blast/Blast.cgi>). Only primers were selected which gave in the BLAST search gave no matching results. Primers were ordered online from Operon (<https://www.operon.com>). All primers were tested and the PCR conditions optimized by using them in a gradient PCR from (55°C-70°C) on a BioRad iCycler prior to parallel analysis of cDNA samples from distinct positive control tissue or cell material.

4.4.4 Reverse transcription-polymerase chain reaction (RT-PCR)

RT-PCR was performed to analyze the abundance of specific mRNA molecules within a cell or tissue as a measure of gene expression. The polymerase chain reaction (PCR) was set up in a final volume of 25 μ l using 1 μ g of the transcribed cDNA preparation. The PCR was undertaken with a primer

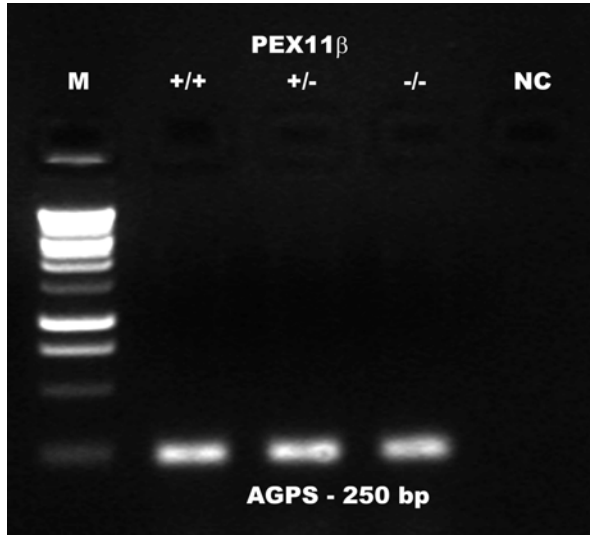


Fig. 6 An example of a PCR. Note that water is used instead of template in negative control samples.

concentration of 10 pmol/ μ l in a Bio-Rad iCycler and the following program: denaturation at 94°C for 4 min, and 35 cycles of 1) denaturation at 94°C for 30 s, 2) annealing at 55-68°C for 30 s, 3) extension at 72°C for 1min, and a final round of product elongation at 72°C for 5 min. The size of the PCR products was between 100 and 800 bp. 28S ribosomal RNA and GAPDH served as house keeping genes and internal controls to normalize expression levels for different mRNAs. “Water” negative controls were run in parallel without specific cDNA product (see left side). All RT-PCR

experiments were performed three times with RNA from three distinct isolation experiments.

Components of RT-PCR Master mix:

| | |
|-----------------------------------|-------------------|
| Nuclease-free water | 18,1-19,1 μ l |
| 10X PCR buffer | 1,0 μ l |
| 10 mM dNTPs | 2,5 μ l |
| Forward primer (10 pmol/ μ l) | 1,0 μ l |
| Reverse primer (10 pmol/ μ l) | 1,0 μ l |
| Taq DNA polymerase (5U/ μ l) | 0,2 μ l |
| Template (1 μ g) | 0,7-1,2 μ l |
| Total PCR volume | 25,0 μ l |

The reaction solution was mixed gently and microfuged briefly before inserting it into the PCR machine.

4.4.5 Gel electrophoresis

4.4.5.1 Formaldehyde agarose gel electrophoresis for analysis of RNA integrity

The integrity and size distribution of different samples of total RNA isolated with the RNeasy Kit, were checked by electrophoresis of 1% denaturing formaldehyde agarose gels. For denaturation of the RNA, the samples (4 µl of the RNA and 1 µl of RNA loading buffer) were incubated at 65°C for 4 min, thereafter immediately chilled on ice and loaded onto a 1% equilibrated formaldehyde gel. The gel was run in 1 X formaldehyde gel running buffer for 60 min at 60V.

4.4.5.2 Agarose gel electrophoresis for the analysis of RT-PCR products

For semi-quantitative analysis of the PCR products, 10 µl of each RT-PCR reaction was analyzed on 2% agarose gels in 1 X TAE buffer, containing 0,5 µg/ml ethidium bromide. Samples were prepared in 5x loading buffer (containing bromophenol blue dye). The agarose gel was run in 1 X TAE buffer for 60 min at 90 V. Depending on the fragment size either GeneRuler 100bp DNA Ladder (100 bp) or 1000 bp ladder (Fermentas) used. Bands were visualised under the UV-Transilluminator of the Gel Doc system from Bio-Rad. All PCR signals were normalized to the GAPDH or 28S rRNA signal of the corresponding RT products to get semi-quantitative estimates of the gene expression levels.

4.5 Cell culture methods

4.5.1 Isolation of AECII from adult mouse lungs

AECII were isolated from six-week-old female C57Bl/6J mice as described by Corti et al with the following modifications (Corti et al., 1996): Briefly, mice were anesthetized by intraperitoneal injection with a combination of rompun (13 µg/g b.w.) and ketavet (65 µg/g b.w.). The abdominal cavity was opened, and mice were exsanguinated by cutting the inferior vena cava and the left renal artery. The trachea was separated by dissection of the neck region for cannulation with a 20-gauge luer-stub adapter. The diaphragm was cut and the complete sternum and thymus were removed. To remove the blood, lungs were perfused via the right ventricle with 20 ml of 0.9 % saline with the use of a 21-gauge needle fitted on a 20 ml syringe. Thereafter, 2-3 ml of dispase was rapidly instilled through the cannula in the trachea followed by 0.5-1.0 ml of 1% low melting

agarose warmed to 45°C. Lungs were immediately covered with ice for 2 min to gel the agarose. After chilling, the lungs were removed from the animals. For additional external digestion, lungs were incubated in 1-1.5 ml of dispase for 45 min at RT. Lungs were subsequently transferred to a 60-mm culture dish containing 7 ml of HEPES-buffered DMEM and 100 U/ml DNase I, and lung tissue was gently teased from the bronchi. The cell suspension was filtered through nylon meshes with 100, 20 and 10 µm pore size. Cells were collected by centrifugation at 130 g for 8 min (4°C) and placed on 100-mm tissue culture plates that had been coated for 24–36 h at 4°C with 21 µg of CD45 and 10 µg of CD32 antibodies in PBS to bind monocytes, granulocytes, macrophages and fibroblasts. After 2 hrs of incubation at 37°C AECII were washed gently from the plate and collected by centrifugation at 130 g for 8 min. The yield of AECII was in the range of 3.5 to 4 × 10⁶ per mice and the viability was greater than 97% as determined by trypan blue exclusion. The purity of AECII preparation was typically > 95%, as assessed by immunofluorescence staining with an anti-rabbit pro SP-C antibody (see Fig. 13 A-C).

4.5.2 Primary Culture of AECII

Purified AECII were either immediately used for RNA or protein extraction (thereafter designated as freshly isolated AECII) subjected for isolation of peroxisomes or seeded directly on cell culture plates that were pre-coated with matrigel. To prepare the petridishes the matrigel was thawed overnight on ice in a refrigerator. Pipette, cell culture plates and cover slips were pre-cooled at 20°C prior to use. Multi-well culture plates (12 wells) were coated with 50-100 µl of matrigel per well. The hardening of the matrigel was performed at 37°C in an incubator for 1 h. Thereafter, the matrigel coated plates were equilibrated with cell culture medium for 1 h in a 37°C incubator prior to culturing of the AECII. AECII were plated on the matrix-coated cover slips at a density of 1.2 × 10⁶ cells / ml. Cells were grown in BEBM culture medium, supplemented with 5% CS-FBS with or without 10 ng / ml KGF (BEGM with 5 % CS-FBS + 10 ng / ml KGF), at 37°C and a 5% CO₂ atmosphere for 7 days. The culture medium was changed at day 1 and every day thereafter. Cell viability was determined using trypan blue exclusion and was consistently >90%.

5 Results

For easier reading all genuine results are written in normal format and all explanatory or introductory parts in italic letter format.

5.1 Characterization of peroxisomes in mouse and human lung tissue with various morphological techniques

We started our investigations on peroxisomes in human and mouse lungs with the establishment of an optimal immunohistochemical technique to visualize different proteins in the peroxisomal compartment. This is especially important since catalase might be present also in the cytoplasm in aging mice (Terlecky et al., 2006) and all peroxisomal matrix proteins could be mislocalized into the cytoplasm in conditions of defective peroxisomal import, such as in patients or knockout mice with peroxisomal biogenesis disorders (Baumgart et al., 2003). In addition, catalase might be genuinely present in multiple compartments (peroxisomes, cytoplasm and nucleus) in other animal species, such as guinea pig and sheep, whereas other peroxisomal enzymes are still solely localized in peroxisomes in these species (Bulitta et al., 1996; Holmes and Masters, 1972; Roels, 1976; Roels et al., 1982; Yamamoto et al., 1988)

5.1.1 Catalase- and Pex14p are detectable in individual peroxisomes of various cell types in mouse and human lungs by immunohistochemistry with the ABC-peroxidase technique

We were only able to visualize peroxisomes in a punctuate staining pattern in different lung cell types, when optimal antigen-retrieval (trypsin digestion and microwaving) in combination with the sensitive ABC-peroxidase method and Novared as substrate was used. Due to the heterogeneity of peroxisomal enzyme content in distinct cell types in complex tissues, we processed paraffin sections of lung with several different antibodies against peroxisomal marker proteins. Only with the antibodies against catalase and Pex14p a positive specific staining was obtained in paraffin sections of mouse and human lungs (Fig.7). By comparing the staining patterns between labeled tissue sections for catalase and Pex14p, we were able to detect significant differences in the

Results

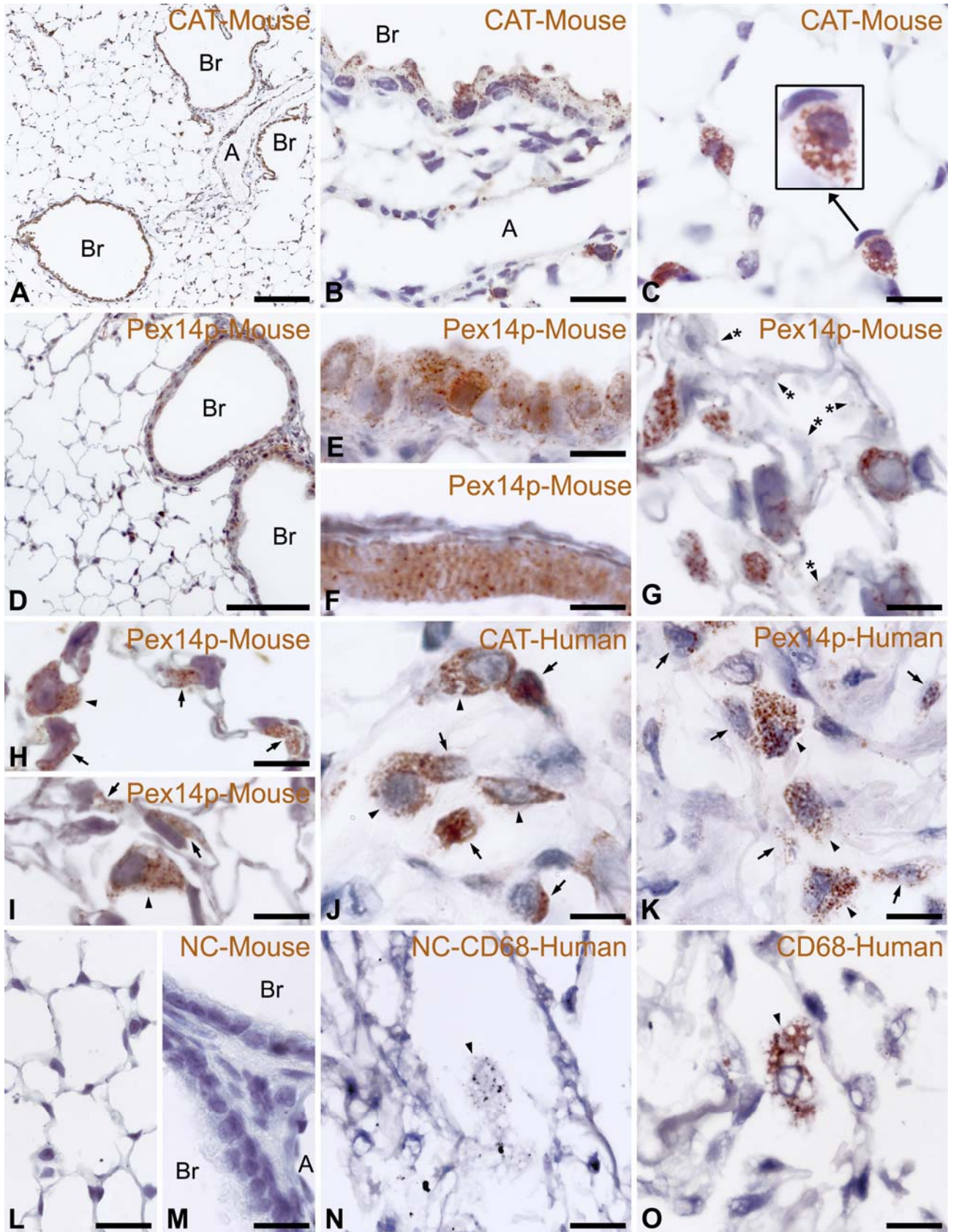


Figure 7. For figure legend see page 45

Results

Fig. 7 Localization of catalase and Pex14 in mouse and human lung with the ABC peroxidase method. Staining for catalase (CAT) (A-C, J) and Pex14p (D-I, K) in mouse (A-I) and human (J, K) lung. (A) Low magnification view of catalase labelling showing positive staining mainly in bronchioles and in larger cells in alveoli in mouse lungs. B, C) Higher magnification of the specific punctuate staining pattern for the peroxisomal subcompartment in Clara cells (B) and AECII (C). D-I) Labelling for Pex14p in different cell types. In addition to Clara cells of bronchioles (D, E) and to AECII (D, G-I), Pex14p-positive peroxisomes are present in striated cardiac muscle cells of large pulmonary veins (F), macrophages (H, I) and very faint, small particles also in AECl (G; see tangential region of AECl). J) Localization of catalase in an adult human donor lung shows the presence of this enzyme in AECII and large macrophages. K) Pex14p-positive peroxisomes in human tissue were mainly seen in AECII and large alveolar macrophages (K) as well as in Clara cells (not shown). All corresponding negative controls for mouse (L, M) and human (N) lung tissue were devoid of reaction product. Positive staining for CD68 showed the high specificity of the ABC-peroxidase method used. A: artery; arrowheads: macrophages; arrowhead with asterisk: AECl cells; arrows: AECII cells; Br: bronchiole. Bars represent: A, D: 100 μ m; B, C, E: 25 μ m; F-O: 10 μ m.

distribution and abundance of these peroxisomal proteins in various lung cell types already at the light microscopical level in mouse and human samples. Catalase, the generally used marker protein for peroxisomes, was highly abundant in Clara cells, AECII and macrophages (Fig.7A-C, J) in both species, whereas other cell types were only weakly stained in the cytoplasm or remained negative. In optimally processed mouse samples with short staining times (only 4 min peroxidase reaction), peroxisomes could be visualized on the subcellular level in a punctuate staining pattern with hardly any diffuse cytoplasmic background reaction (Fig.7B and C). In contrast, in human lung samples, the peroxidase reaction times had to be prolonged to visualize catalase and the individual peroxisomes were less well resolved, with the smaller sized AECII showing a stronger and more diffuse reaction product than the macrophages (Fig.7J). *These interspecies differences can be explained by the lower catalase levels in individual human donor lung peroxisomes, as shown later in Western blot experiments.* Peroxisomes in human donor lung samples were best visualized with the antibody against Pex14p. Highest staining intensity and peroxisome abundance were found in macrophages in comparison to less numerous and weaker stained peroxisomes of human AECII (Fig.7K). Excellent staining of peroxisomes was obtained with this antibody also in optimally processed mouse samples, in which these organelles could be visualized in all pulmonary cell types, however with distinct abundance and size (Fig.7D-I). Similar to human lung samples, a high numerical abundance of peroxisomes was observed in Clara cells, AECII and macrophages in mouse lungs. In addition, peroxisomes were also present in high numbers in striated cardiac muscle cells of large pulmonary veins (Fig.7F). Furthermore, small and less numerous peroxisomes could be visualized in AECl, especially obvious in regions with tangentially sectioned epithelium (Fig.7G). Parallel sections of corresponding negative controls were devoid of reaction product (Fig.7L-N). Positive controls with

an anti-CD68 antibody showed specific staining for human macrophages (plasma membrane/endosomal and lysosomal compartment; Fig.7O), even in human samples with collapsed alveoli and less well conserved morphology.

5.1.2 Double-immunofluorescence labelling reactions confirm the presence of peroxisomes in all pulmonary cell types and reveal the heterogeneity in peroxisomal protein content

Immunofluorescence analysis of paraffin sections of the adult mouse lung incubated with specific antibodies against different lung cell types like 1) α -tubulin for ciliated cells 2) CC10 for nonciliated Clara cells, 3) pro surfactant protein C (pro-SP C) for AECII, 4) podoplanin/T1 α for AECl, and 5) von Willebrand-factor (vWF) for endothelial cells (Figs. 8A-F, 8H-J) showed strong specific staining of each individual cell type with no cross-reactivities to other cell types. The high specificities of these labellings enabled us to identify peroxisomes with certainty in the distinct pulmonary cell types. As revealed by double-stainings for cell markers and Pex14p, peroxisomes are present in all lung cell types, although with distinct numerical abundance. The highest peroxisome number was observed in AECII, in which they appeared clustered and elongated and the individual organelles could hardly be separated from each other. High numerical abundance of larger peroxisomes was also noted in nonciliated Clara cells, in which individual organelles were readily detectable (Fig. 8D, 8E) in comparison to the smaller and less numerous peroxisomes in ciliated cells of the bronchiolar epithelium (Fig. 8D). The fluorescence intensity of the Pex14p labelling was comparable on all peroxisomes, suggestive for the presences of similar Pex14p-protein levels on individual peroxisomes in different lung types. Therefore, with this marker, peroxisomes could also be visualized effectively in AECl (Fig. 8H, I) and endothelial cells (Fig. 8J).

In contrast to the ABC-peroxidase method, with immunofluorescence we were able to stain peroxisomes of different lung cell types with antibodies against other marker proteins, such as ABCD3 (Fig. 8F) – an ABC-transporter involved in lipid transport over the peroxisomal membrane. In double-labelling experiments of peroxisomes for ABCD3 and Pex14p, we were indeed able to identify both proteins within the same intracellular compartment (yellow colour in overlay of the 3 CLSM channels in Fig. 8G). In contrast, peroxisomes were clearly distinguished from other organellar compartments in double-labelling experiments with pro-SP C (Fig. 8F: secretory vesicles

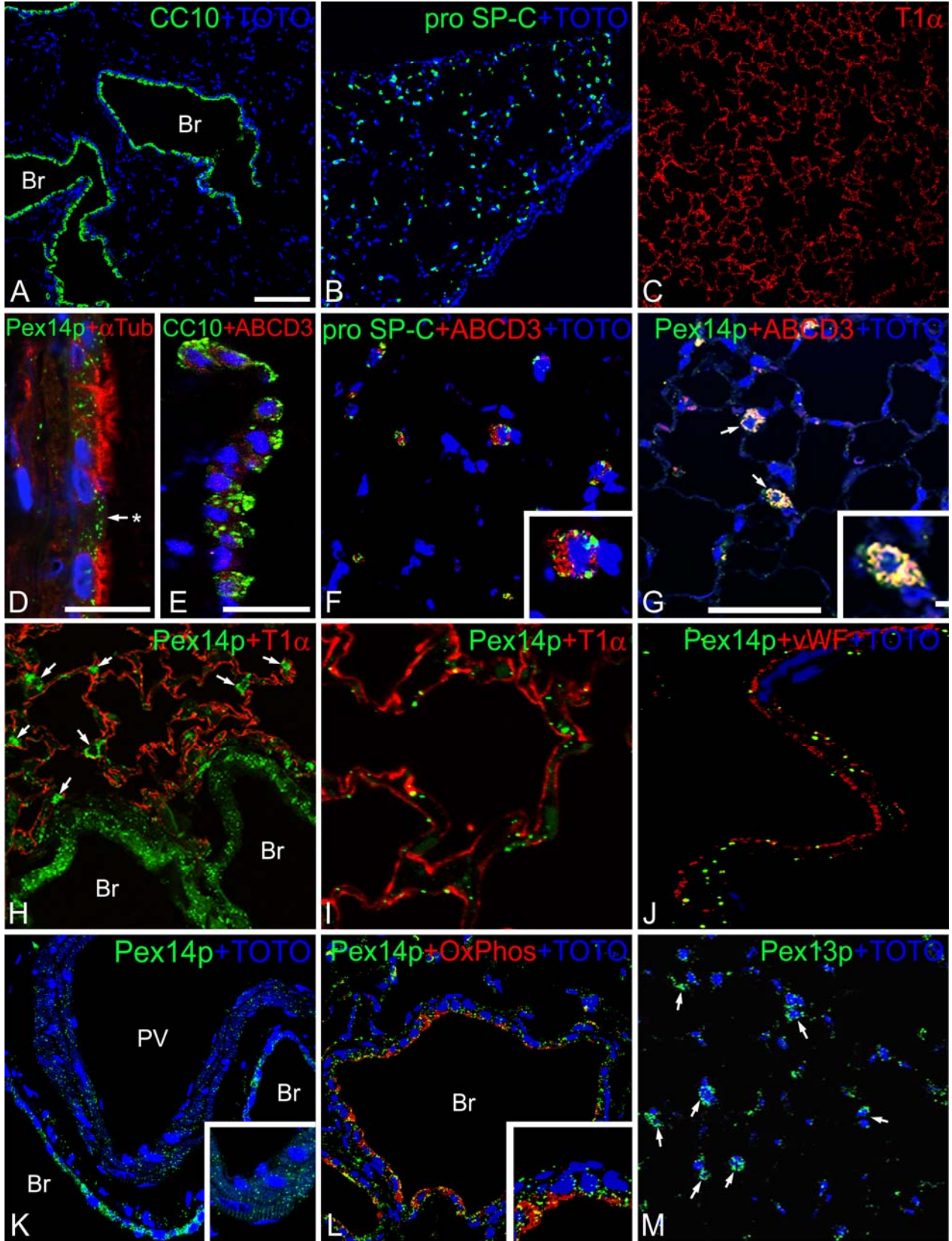


Figure 8. For figure legend see page 48.

Results

Fig. 8 Detection of peroxisomes in distinct pulmonary cell types of the mouse lung by immunofluorescence-labelling for peroxisomal membrane proteins. Overviews of preparations with antibodies against marker proteins for specific pulmonary cell types, such as CC10 for Clara cells (A), pro-SP C for AECII (B) T1 α / podoplanin for AECl (C), α -tubulin for ciliated cells of bronchioles (D) showing the high specificity of our immunofluorescence protocol. Double-immunofluorescence for ABCD3 together with CC10 (E) or pro-SP C (F) or Pex14p (G) depict peroxisomes in Clara cells and show tubular peroxisomes in AECII (F, G). Peroxisomes in all cell types could be visualized with the anti-Pex14p antibody (D, G-L). Double-immunofluorescence preparations for Pex14p and T1 α / podoplanin (H, I) or “von Willebrand” factor (vWF) (J) revealed peroxisomes in addition to AECII (arrows) and Clara cells of a small bronchiole (Br) (H) also clearly and specifically in AECl (H, I) or endothelial cells (J). K) Peroxisomes in striated cardiac muscle cells of a large pulmonary vein of the mouse lung. L) Double-immunostainings for Pex14p and complex III of the respiratory chain showed intensive labelling for both proteins in bronchioli, however, in distinct subcellular compartments – peroxisomes (green) and mitochondria (red). M) Ubiquitous staining of peroxisomes for Pex13p. Nuclear counter staining was done with TOTO. Arrows: AECII cells; arrow with asterisk: Clara cell; Br: bronchiole; PV: pulmonary vein. Bars represent: A-C: 100 μ m; D: 25 μ m; E-H, K-M: 50 μ m; I, J: 10 μ m.

in green versus ABCD3-stained peroxisomes in red) or with CC10 (Fig. 8E: secretory vesicles in green versus ABCD3-stained peroxisomes in red). The highest level of the ABCD3 protein was found in AECII on elongated or tubular peroxisomes (Fig. 8G), followed by Clara cells (Fig. 8E), in which clusters of peroxisomes were often located beneath the CC10-positive secretory granules at the apical pole. In contrast to peroxisomes, mitochondria were most prominently stained for complex III of the mitochondrial respiratory chain in the bronchiolar epithelium and were less strongly stained in AECII (Fig. 8L: mitochondria in red versus Pex14p-stained peroxisomes in green). Stainings were clearly indicative for the localization of mitochondrial complex III of the respiratory chain in a different subcellular compartment in comparison to peroxisomes. Finally, staining of mouse lung samples for Pex13p was generally much weaker than for Pex14p, but showed a similar ubiquitous distribution (Fig. 8M).

5.1.3 Peroxisomes in AECl contain lower levels of catalase, but high levels of β -oxidation enzymes and the lipid transporter ABCD3

As mentioned above, double-immunofluorescence analysis of paraffin-embedded mouse lung sections incubated with Pex14p revealed strong labeling of the peroxisomes in flat AECl co-localized with T1 α (Fig. 8H, I). In addition, peroxisomes in AECl were also labeled for marker enzymes of the β -oxidation pathway 1 and the lipid transporter ABCD3 (Fig. 9E-I). Acyl-CoA oxidase 1 (ACOX1) seemed to be expressed at comparable levels in individual peroxisomes in distinct lung cell types (Fig. 9E-G). Peroxisomal 3-oxo-acyl-CoA thiolase was also present at comparable levels in most cell types of the lung, including ciliated cells of the bronchiolar epithelium, AECl, endothelial cells,

Results

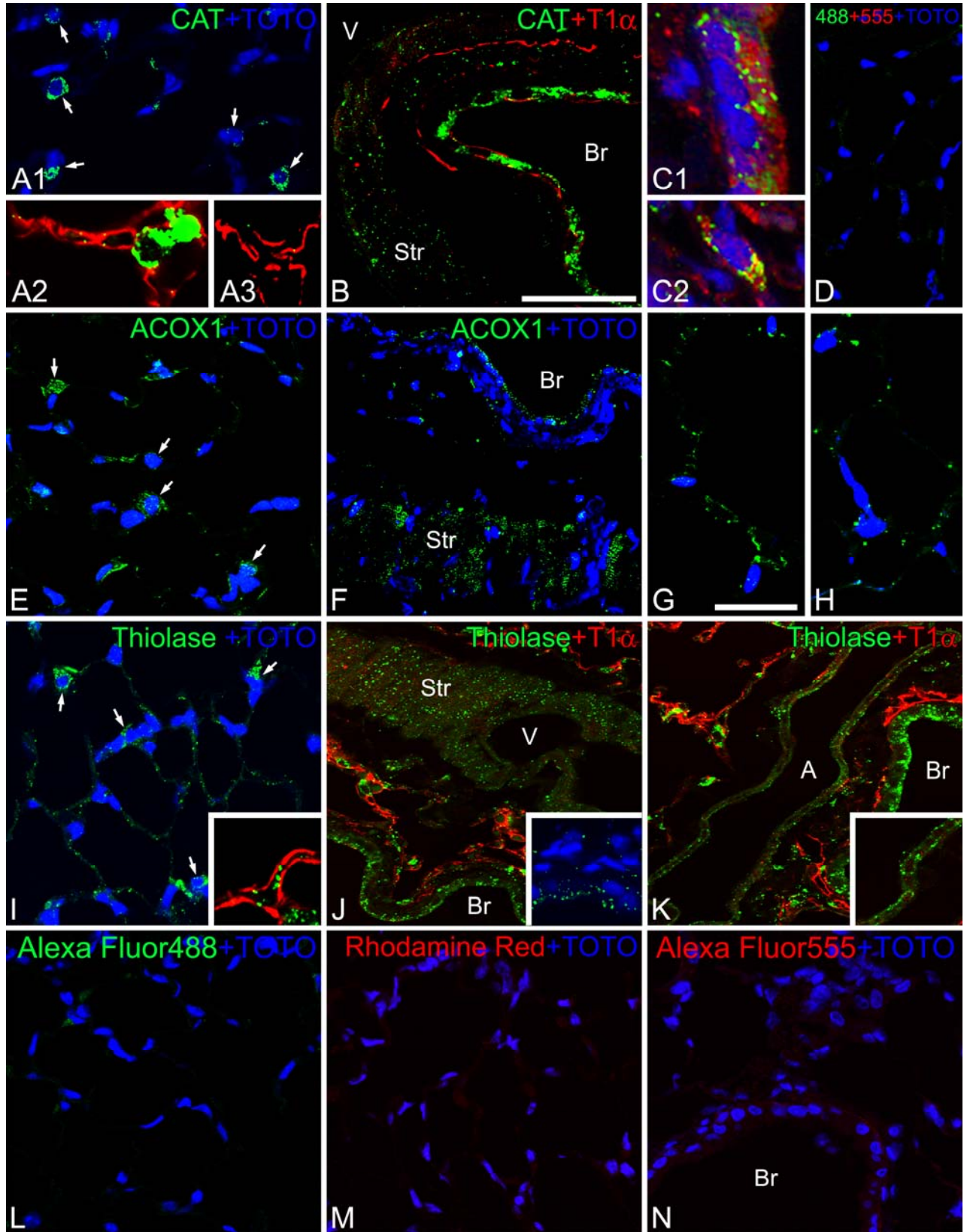


Figure 9. For figure legends see page 50.

Results

Fig. 9 Localization of different peroxisomal matrix enzymes in distinct pulmonary cell types of mouse lung. Stainings for catalase (CAT) (A-C) and the β -oxidation enzymes acyl-CoA oxidase 1 (ACOX1) (E-G) and 3-oxo-acyl-CoA thiolase (thiolase) (I-K). The anti-catalase antibody stained AECII (A1, C2) and Clara cells (B, C1) with high intensity also in immunofluorescence preparations. A2, A3) Double-labelling for CAT and T1 α ; images taken with prolonged CLSM-exposure time, revealing peroxisomes also in AECI. B) Catalase in peroxisomes of Clara cells and of striated cardiac muscle cells of a pulmonary vein. C1, C2). Double-labelling for peroxisomal catalase and mitochondrial complex III of the respiratory chain in Clara cells (C1) or AECII (C2). ACOX1 (E-G) and thiolase (I-K) are present in a more ubiquitous way in distinct pulmonary cell types (E-K). ACOX1-positive AECII and AECI are depicted in (E), Clara cells and striated muscle cells in (F) and a higher magnification of AECI in (G). H) ABCD3-positive AECI cells. Thiolase-positive AECII and AECI are depicted in (I; inset with double IF for thiolase and T1 α), Clara cells and striated cardiac muscle cells of a pulmonary vein in (J; inset with fibroblast peroxisomes above Clara cells) and various cells types, including smooth muscle cells in (K). Negative controls: D) Negative control of secondary antibodies used for stainings in (A-C) with anti-rabbit Alexa488 and anti-mouse Alexa555. L-N) Negative control for anti-rabbit Alexa488 (L), anti-sheep Rhodamine red (M) and anti-mouse Alexa555 (N). Nuclei were counterstained with TOTO except for T1 α preparations. A: artery; arrows: AECII cells; Br: bronchiole; Str: striated cardiac muscle cells; V: vein. Bars represent: A1, B, E, F, I-N: 50 μ m; G, H: 20 μ m; D: 50 μ m.

smooth muscle cells of lung arteries and striated cardiac muscle cells of a large pulmonary vein (Fig. 9I-K). However, in contrast to ACOX1, the first and rate-limiting enzyme of the peroxisomal β -oxidation pathway 1, peroxisomal thiolase, the third enzyme of this pathway, was slightly more prominent in AECII (arrows in Fig. 9I) and Clara cells (see Fig. 9K in the epithelium of the small bronchiole - Br). Similar to the results obtained with the ABC-peroxidase method, catalase staining in immunofluorescence preparations was highly abundant in AECII and Clara cells with “regular” exposure times in which peroxisomes in these cell types were optimally resolved (Fig. 9A1, B). Hardly any catalase labelling was visualized in AECI peroxisomes under these conditions. However, peroxisomes with low levels of catalase were detected in AECI cells after alteration of the CLSM-setting conditions and long-term exposure, by which AECII were completely overexposed and individual peroxisomes could no longer be distinguished from each other in this cell type (Fig. 9A2, A3). Our results with different marker proteins suggest a distinct relative enzyme composition in peroxisomes of AECI and AECII.

5.1.4 Peroxisomes in mouse AECII are often tubular, larger in size than in other cell types and show a close association with lamellar bodies

Localization of peroxisomes at the electron microscopic level in good quality in samples of human donor lungs was not possible since only frozen tissue samples from the tissue bank of the University of Giessen Lung Center were available. Therefore, we only analyzed wet sections of perfusion-fixed adult mouse lungs for distribution, size and structure of peroxisomes in different lung cell types at

the electron microscopic level with the alkaline DAB method. Small peroxisomes (“microperoxisomes”) in mouse lung sections were optimally revealed at the electron microscopic level by incubation for 2 h at 45°C in the alkaline DAB-solution to obtain optimal precipitation of sufficient electron-dense reaction product to reveal small organelles. With the help of this technique, small peroxisomes could be readily visualized in all cell types in the lung. These organelles are bounded by a single unit membrane and contain a finely granular matrix, in which the electron-dense DAB reaction product was precipitated (Fig. 10A-M, P, Q). Peroxisomes were more abundant, larger in size and more intensely stained with DAB in a) nonciliated Clara cells in comparison to ciliated cells of the bronchiolar epithelium (Fig. 10A-D) and b) AECII in comparison to AECI, endothelial cells or mouse alveolar macrophages of the alveolar region (Fig. 10E-M, P, Q). The largest spherical peroxisomes were observed in nonciliated Clara cells of the bronchiolar epithelium (Fig. 10C). In ciliated cells these organelles were in many cases tubular and more pleomorphic than in other cell types, ranging from spherical to rod-shaped or tubular. Interestingly, very elongated peroxisomes were mostly observed in AECII compared to other cell types of the alveolus (see Fig. 10J, L, M). In some AECII cells with a high number of lamellar bodies, tubular peroxisomes often covered the surface of these lamellar bodies, or were in close vicinity to segments of the smooth endoplasmic reticulum and in close neighbourhood to mitochondria (Fig. 10J-M). Very frequently peroxisomes also formed clusters of organelles.

5.1.5 Post-embedding protein A-gold immunocytochemistry for catalase localization revealed exclusive labelling of peroxisomes

In addition to the localization of the catalase activity at the electron microscopic level, we investigated the localization of the catalase protein by post-embedding immunocytochemistry with the protein A-gold method. As shown in Fig. 10N and 7O, gold particles are confined exclusively to the matrix region of peroxisomes in AECII cells (Fig. 10G), depicting the high specificity of the antibody. Elongated peroxisomes were also visualized by this technique with usually 4-6 gold particles (Fig. 10O inset). In optimal preparations, mitochondria and other cell organelles were always negative. In addition, the close relationship of peroxisomes with lamellar bodies was also clearly visible in these preparations (Fig. 10N, O).

Results

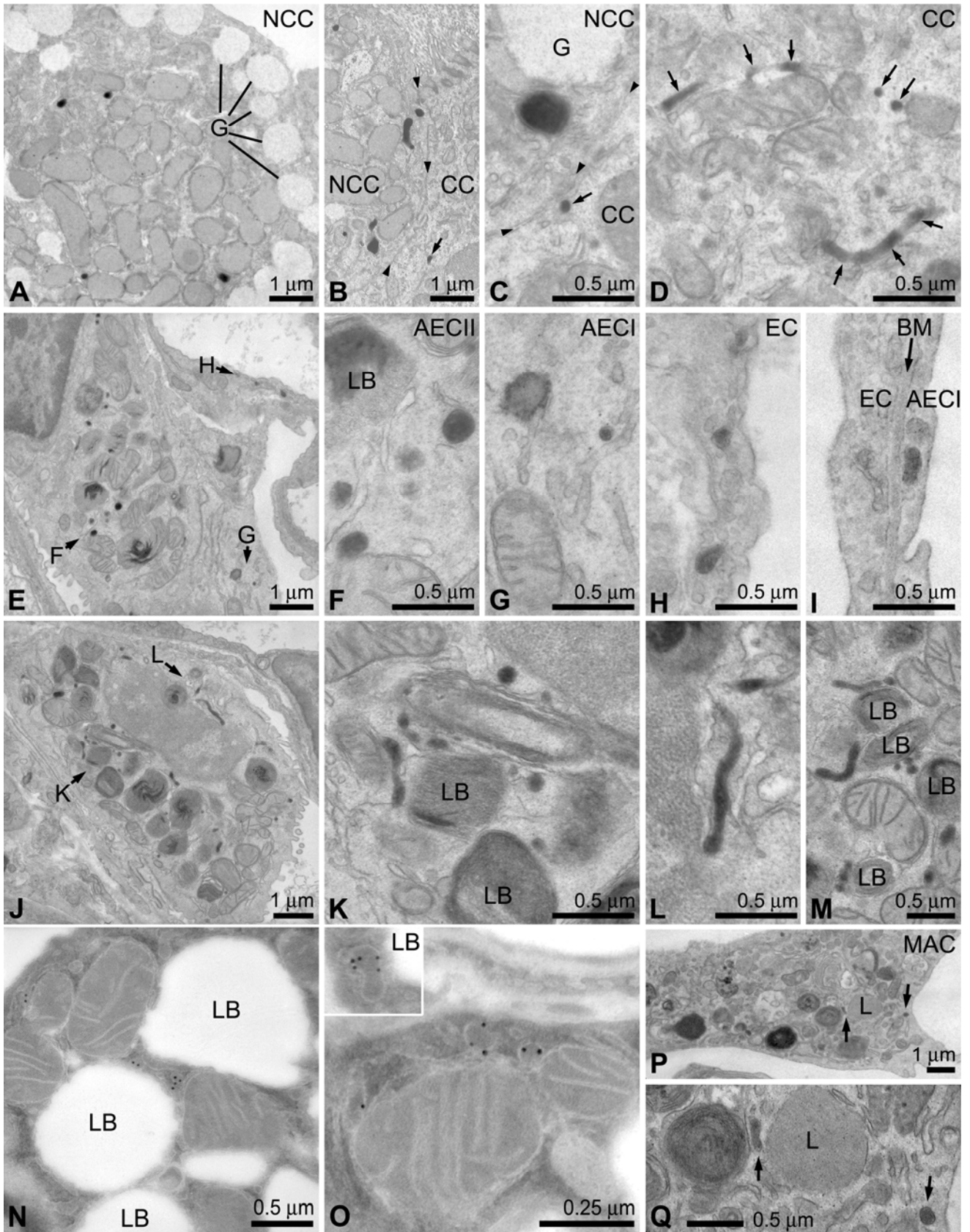


Figure 10. For figure legends see page 53.

Results

Fig. 10 Ultrastructural localization of catalase activity and protein in different cell types of the mouse lung. Cytochemical staining of catalase activity with the modified alkaline DAB method (A-M, P, Q) and immunocytochemical localization of the catalase protein with the post-embedding protein A-gold technique (N, O). A) Lower magnification view of nonciliated Clara cells of a small bronchiole containing many mitochondria and four peroxisomes in the apical cell pole underneath of the secretory granules (G). B) Lower magnification view of neighbouring nonciliated (NCC) and ciliated cells (CC) showing the size difference of peroxisomes in these cell types. C) Higher magnification view of both cell types with a large peroxisome in a nonciliated Clara cell and a very small peroxisome in the neighbouring ciliated cell. Note the clear difference in DAB staining intensity of both peroxisomes. D) An example of different cross – and longitudinal sections through tubular peroxisomes of a ciliated cell (arrows). E) Lower magnification view of a region with peroxisomes in AECII, AECl and endoelial cells. F-I) Higher magnification of selected peroxisomes from (E) in AECII (F), AECl (G) and in an endothelial cell (H). Note the difference in the size of cross-sectioned peroxisomes in AECII with larger particles (ca. 200-250 nm) in comparison to AECl, in which the cross-section of the peroxisome has the same diameter as the neighboring smooth endoplasmic reticulum (ca. 85-90 nm). I) Region of the blood-air barrier with a small rod-shaped peroxisome in an AECl. J) Low magnification view of an AECII exhibiting many elongated peroxisomes in the vicinity of lamellar bodies. K) Higher magnification view of (J) depicting a tangentially sectioned region of lamellar bodies, showing several peroxisomal profiles in their vicinity. L) A long tubular peroxisome of the AECII in (J). M) A different AECII with tubular peroxisomes or groups of small cross-sectioned peroxisomes in the vicinity of lamellar bodies. The close vicinity of peroxisomes and lamellar bodies was also seen frequently in stainings for the catalase protein with the post-embedding protein A-gold technique (N, O inset). Peroxisomes were also often found closely associated with the smooth endoplasmic reticulum and mitochondria (O). P, Q) Peroxisomes in an alveolar macrophage in low (P) and higher (Q) magnifications. Arrows in B-D, P and Q depict peroxisomes; arrowheads in B and C mark cell borders. G: secretory granules; NCC: nonciliated cell; CC: ciliated cell; LB: lamellar bodies. The size of magnification bars are indicated in the figure 10.

5.1.6 Peroxisomes are present in all cell types of human donor lungs, are most abundant in AECII and macrophages and show heterogeneity of their enzyme content

Unfortunately, many of the monoclonal antibodies against cellular marker proteins did not stain their corresponding counterparts in samples of human donor lungs. Only staining of secretory vesicles for pro-SP C in AECII and CC10 in nonciliated Clara cells worked properly in human, since this was done with polyclonal antibodies from rabbit or goat. Staining for pro-SP C was exclusively found in AECII, revealing the distribution of AECII in human lung sections (Fig. 11B). Similarly to antibodies against some cellular marker proteins, also our antibody against the peroxisomal ABCD3-protein raised in sheep was not functional on human samples (data not shown). However, by comparing parallel sections to each other - either labeled for pro-SP C or for different peroxisomal proteins - peroxisomes in AECII and macrophages could be easily distinguished. In addition, we used a mouse anti-human CD68 antibody for this purpose, a specific marker only for human macrophages. Double-immunofluorescence preparations with rabbit anti-pro SP C and mouse anti-CD68 showed specific positive labeling for each individual cell type (Fig. 11C). This marker was also used in double-labeling experiments to depict macrophages in staining reactions for different peroxisomal proteins (Fig. 11C, G, and H).

Results

The overall distribution and abundance of peroxisomal proteins was similar between mouse and human lung samples. Similar to mouse lungs, catalase was localized in high abundance in peroxisomes of AECII (Fig. 11A and inset) and alveolar macrophages (Fig. 11A). AECII and alveolar macrophages were also readily detected with antibodies against Pex14p, ABCD3 and ACOX1 (Fig. 11E, G, I, J). However, similar as in mouse lung samples, these proteins generally showed a more ubiquitous expression pattern also in other cell types. Only thiolase showed a weaker labelling intensity compared to mouse samples, with only low levels of this protein revealed in AECII and very weak or no staining in alveolar macrophages (Fig. 11H). The best staining reaction of peroxisomes in different cell types of human donor lungs was observed with the antibody against Pex14p (Fig. 11J-M) with highest numerical abundance and labeling intensity of peroxisomes in macrophages (Fig. 11J right inset). With this marker protein, peroxisomes could be nicely visualized also in the distinct cell types of the epithelia in the conducting airways (bronchioli or bronchi) (Fig. 11L, M). In ciliated cells clusters of peroxisomes were readily observed in the apical region of the cells directly underneath of the cilia. In double-immunofluorescence preparations of bronchioles Pex14p staining was clearly confined to a different subcellular compartment as the one for CC10, the marker protein for secretory granules of nonciliated Clara cells (see inset in Fig. 11L). Peroxisomes were often located in near neighbourhood to the secretory granules. A similar close relationship was seen between MUC5-positive secretory granules and peroxisomes in goblet cells in the human bronchial epithelium (Fig. 11M). In goblet cells, peroxisomes were less abundant and smaller than in Clara cells or ciliated cells (Fig. 11M inset). Appropriate parallel controls without primary antibodies were always negative (Fig. 11D, N).

5.1.7 The difference in the distribution and expression of distinct peroxisomal proteins in samples of human and mouse lungs are also revealed in Western blotting experiments

Western blots made from complete homogenates of human donor lungs, mouse lungs and mouse livers (used as a positive control due to high expression levels of most peroxisomal proteins in hepatocytes) produced specific bands revealing distinct peroxisomal proteins only after long-term exposure (ca. 20 min), which also led to the production of several non-specific protein bands on the blots especially in human samples (not shown). Therefore, all frozen homogenates from lungs of human donors, mouse lungs and mouse livers were subjected directly after thawing to subcellular

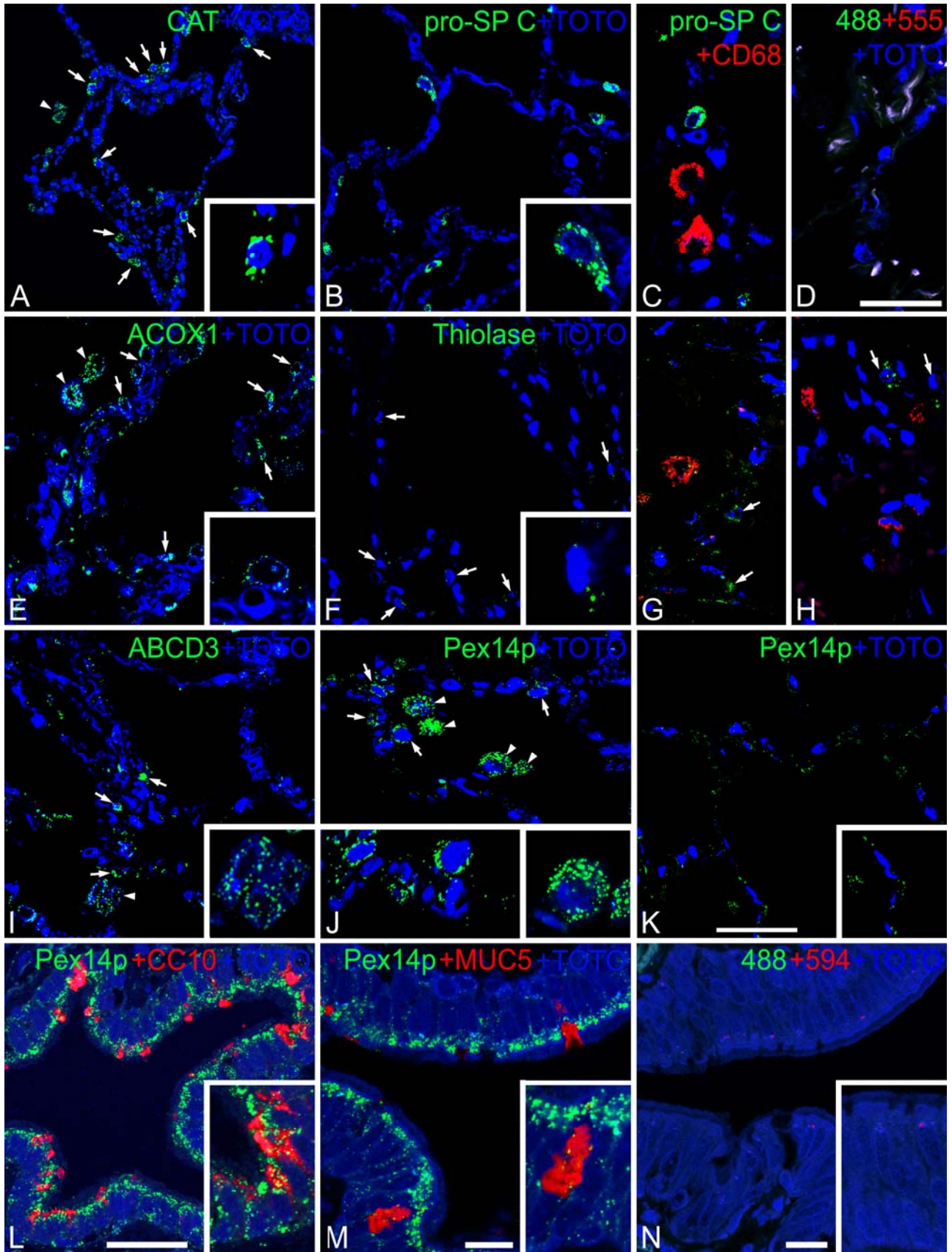
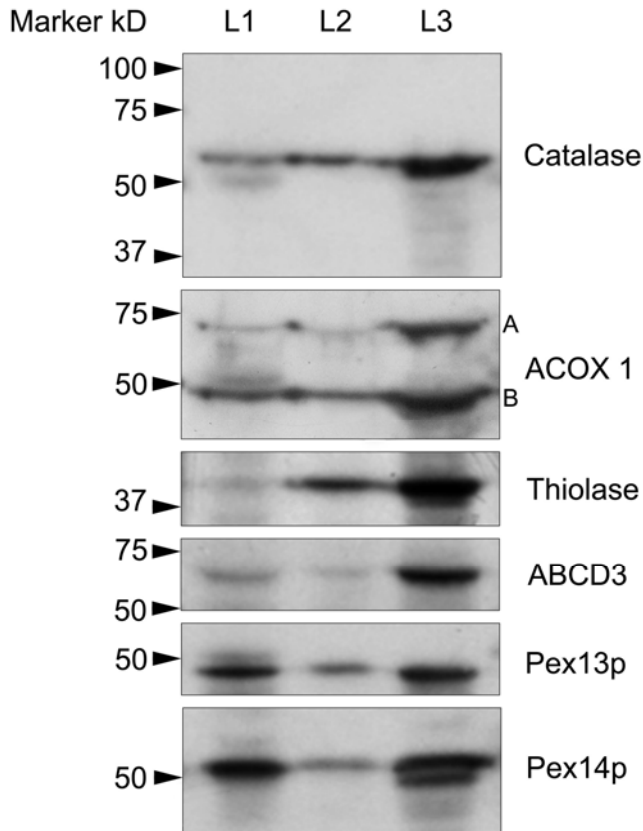


Figure 11. For figure legends see page 56.

Results

Fig. 11 Localization of peroxisomal proteins in human lung. Staining for peroxisomal proteins (A: catalase; E, G: ACOX1; F, H: thiolase; I: ABCD3; J-M: Pex14p) and cell-type specific markers (B, C: pro-SP C for AECII; C, G, H: CD68 for macrophages; L: CC10 for Clara cells; M: MUC5 for goblet cells) in paraffin sections of human lung. A) Catalase (CAT) is present in human AECII and alveolar macrophages (inset: peroxisomes in AECII). B) pro-SP C staining for AECII (inset: secretory vesicles in AECII). C) Double-staining for pro-SP C in AECII and CD68 in macrophages, depicting the specific labelling of the correct cell types. E) Labelling for ACOX1 is present in all cell types, with macrophages and AECII showing higher numerical densities of peroxisomes (inset: AECII). F) Thiolase labelling was very weak, revealing peroxisomes only in AECII (inset). G) Double-labelling of ACOX1 and CD68. H) Double-labelling of thiolase and CD68. I) Alveolar region depicting peroxisomes labeled for ABCD3 (inset: ABCD3-positive peroxisomes in macrophages). J) Alveolar region stained for Pex14p, depicting peroxisomes in several AECII cells and macrophages (left inset: peroxisomes in AECII and AECI; right inset: peroxisomes in macrophages). K) Peroxisomes in human AECI, labeled for Pex14p (inset: higher magnification of AECI peroxisomes). L) Double immunofluorescence preparations of Pex14p and CC10 (L) or Pex14p and MUC5 (M) depicting peroxisomes in ciliated cell (L, M) and nonciliated Clara cells (L) or goblet cells (M). Negative controls are shown in (D) with anti-rabbit IgG-Alexa488 and anti-mouse IgG-Alexa555 or in (N) with anti-rabbit IgG-Alexa488 and anti-mouse IgG-Alexa594. Nuclei were counterstained with TOTO. Arrows: AECII cells; arrowheads: macrophages. Bars represent: A, B, E, F, I-K: 50 μ m; L: 50 μ m; C, D, G, H: 25 μ m; M, N: 25 μ m.

fraction by differential centrifugation, for relative enrichment of the organelle mixtures with



peroxisomes. These fractions were used for a second round of Western blotting experiments, in which all antibodies (against catalase, ACOX1, thiolase, ABCD3, Pex13p and Pex14p) recognized specific polypeptide bands at the expected molecular size in all different tissues (Fig. 12). The relative amount of most peroxisomal proteins in enriched peroxisomal fractions was much lower in lung compared to liver. The relative amount of Pex13p and Pex14p was higher in enriched fractions of human donor lungs than in mouse lungs. Similar to morphological results, catalase and thiolase were more enriched in adult mouse lungs than in human lungs. Thiolase was barely detectable in the adult human donor lungs.

Fig. 12 Comparative Western blot analysis of enriched peroxisomal fractions isolated from human donor lungs, adult mouse lungs and livers. Loading of gels: 50 μ g of proteins of enriched peroxisomal fractions from human lung (L1), mouse lung (L2) and 20 μ g from mouse liver (L3). The size of markers are indicated on the left and names of peroxisomal proteins on the right.

5.2 Characterization of peroxisomes in highly purified freshly isolated or cultured mouse AECII

Previous chapters describe the characterization of various peroxisomal proteins in distinct pulmonary cell types of mouse and human lung tissues. As mentioned, AECII and Clara cells contain the highest amount of peroxisomes. Except for the described morphological data, nothing is known about the exact role and the characterization of peroxisomal proteins in AECII. Thus, we characterized the peroxisomal compartment in highly purified, freshly isolated or cultured AECII with various cell biological techniques.

5.2.1 Immunofluorescence analysis revealed the high purity of the isolated AECII preparations

At first, the immunofluorescence (IF) technique was adapted to cytospin preparations of AECII. IF analysis of freshly isolated AECII, incubated with the AECII marker antibody anti-pro SP-C, revealed the high purity and good quality of the AECII preparation (Fig. 13A-C). As assessed by trypan blue exclusion, the viability of the cells was >95%. Isolated AECII were incubated with antibodies against peroxisomal matrix or membrane proteins, such as anti-catalase (Fig. 13D), anti-Pex14p (Fig. 13E) and anti-Pex13p (Fig. 13F). The stainings revealed a selective punctuate pattern of peroxisomal labelling in these cells. The intensity of the immunofluorescence staining in AECII was highest for Pex14p, followed by catalase and was lowest for Pex13p (Fig. 13D-F). In addition, co-localization of pro SP-C with ABCD3 in double-IF, revealed labeling of distinct particles, corresponding to the localization of these proteins in different subcellular organelles (Fig. 13G-J). Double localization of ABCD3 with peroxisomal markers (such as catalase, Pex14p or Pex13p) showed a complete co-localization of both markers in the peroxisomal compartment for ABCD3 and Pex14p double-labellings (see Fig. 13J). *Taken together, these results suggest that, Pex14p is the best marker protein for identification of all peroxisomes in cultured AECII. These results completely corroborate the results obtained in tissue sections of adult mouse lungs.*

5.2.2 Subcellular fractionation of primary AECII revealed a high enrichment of AECII peroxisomes with ACOX1

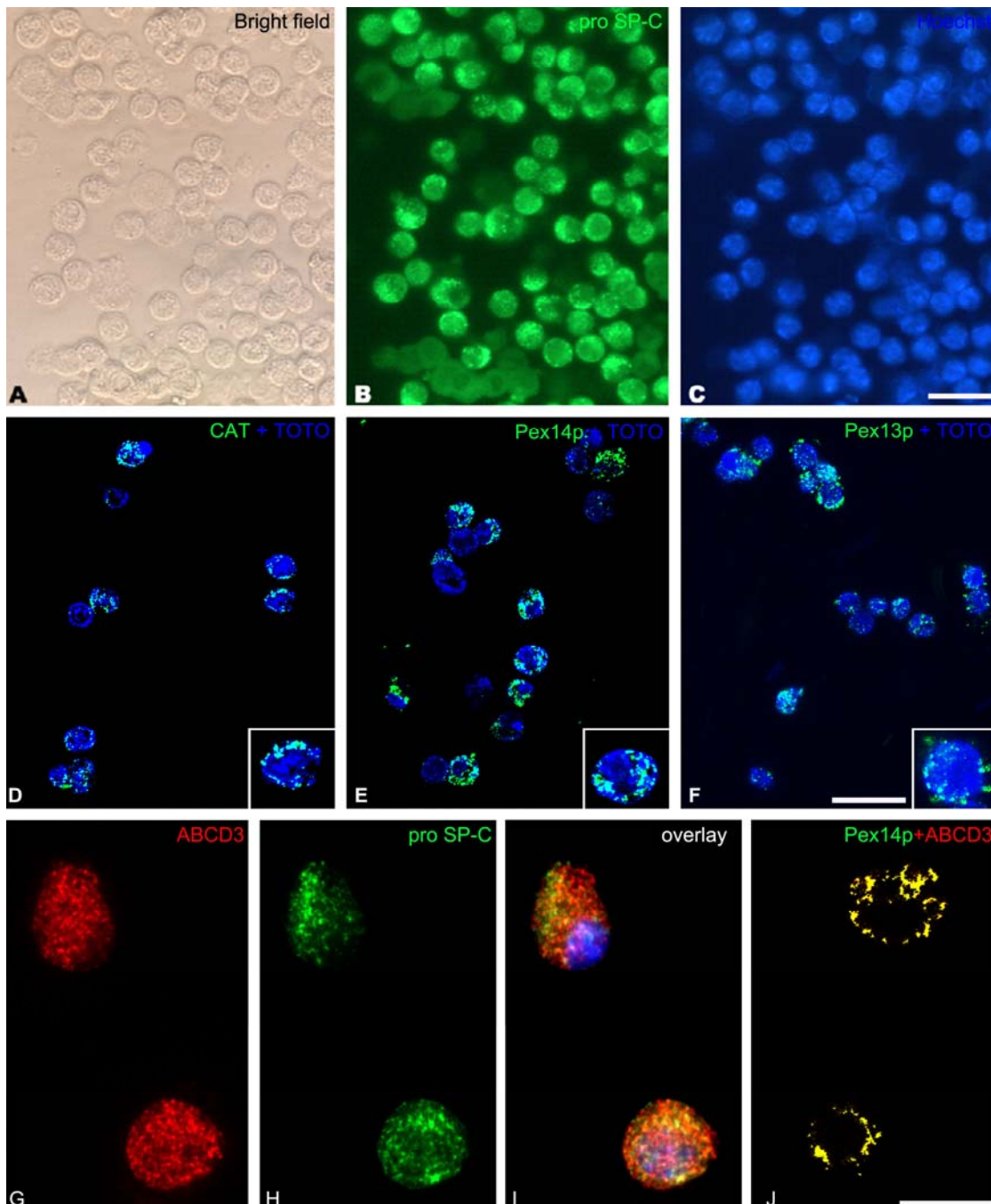
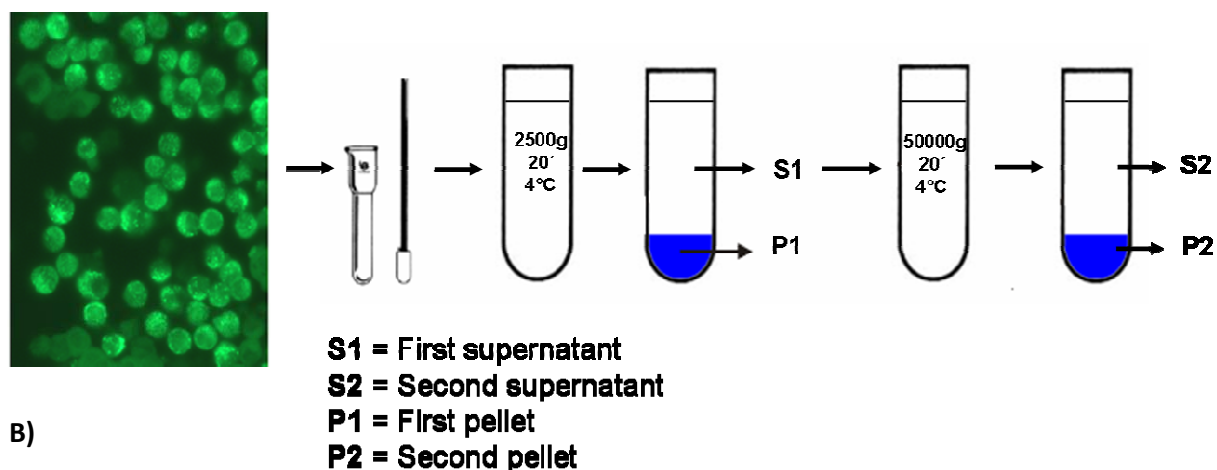


Fig. 13 Characterization of peroxisomes in freshly isolated highly purified AECII. Freshly isolated AECII were fixed, stained by IF for pro SP-C followed by nuclear staining with Hoechst 33258. A: AECII under phase contrast. B: Expression of pro SP-C in the preparation demonstrating the high purity of the AECII. C: AECII nuclei stained with Hoechst 33258. Further, fixed cells were stained for peroxisomal proteins such as anti-catalase (D), anti-Pex13p (E) and anti-Pex14p (F). Double IF of the peroxisomal lipid transporter ABCD3 and pro SP-C as AECII marker. G: ABCD3 staining in AECII. H: Distribution of pro SP-C in the same AECII. I: Overlay picture of all layers. J: Double IF of the peroxisomal lipid transporter ABCD3 and Pex14p showing a clear co-localization of the same compartment. Bars represent A-C, D-F: 20 μ m; G-J: 15 μ m.

Results

Figure 14A) Scheme for isolation of enriched peroxisomes from isolated AECII



B)

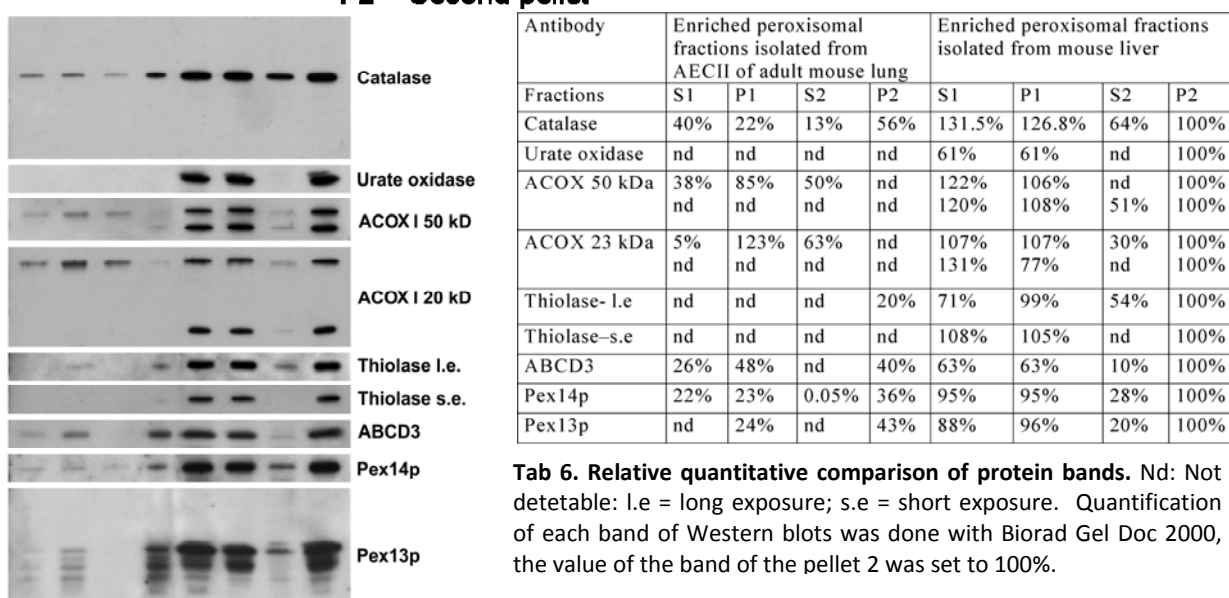


Figure 14B) Western blot analysis of enriched peroxisomal fractions isolated from AECII and liver homogenate. 20 μ l of S1, P1, S2 and P2 dissolved in 50 μ l and 10 μ l of homogenizing buffer 1) Followed by protein determination using Bradford method 2) 9 μ g and 4.8 μ g of protein was loaded in each lane subjected for Western blotting 3) The two Western blots were stripped and reprobed for 5 times. For detailed description of the antibodies, see table 4.

The peroxisomal compartment of AECII was characterized by using subcellular fractionation and subsequent Western blot analysis of enriched main fractions of in comparison to liver protein fractions. Fig. 14A and 14B illustrate the steps involved in this subcellular fractionation process and depict the peroxisomal protein distribution in distinct fractions. The P1 pellet consists in addition to large peroxisomes mainly of heavy mitochondria and nuclei, whereas the P2 fraction contains light mitochondria, lysosomes and many regular sized peroxisomes. As can be seen in the immunoblot pictures below, most peroxisomal enzymes are enriched in the light mitochondrial P2 fraction, whereas only few micro peroxisomes are found in S2, a fraction mainly containing microsomes and

cytoplasmic proteins. The comparative Western blot analysis and quantitative assessment of bands revealed a relatively lower abundance of peroxisomal proteins in AECII in comparison to liver, which corresponds to the lower numerical abundance of peroxisomes in AECII. In addition, a distinct relative composition of peroxisomal proteins in AECII in comparison to liver was noted, with a selective enrichment of peroxisomes in catalase and ABCD3 in comparison to Pex14p and Pex13p in AECII. Surprisingly, most of the Acyl-CoA oxidase I was not cleaved into its subunits B and C. Only the full length protein (A) was revealed with both antibodies against either the large B subunit (50 kD) or the small C subunit (20kD). In addition, the relative intensity of the band pattern of Pex13p was shifted to smaller bands in comparison to the liver samples. Finally, urate oxidase, the protein of the crystalline cores in peroxisomes is not present in AECII peroxisomes, which is in agreement with the absence of cores in peroxisomes of AECII.

5.2.3 Downregulation of peroxisomal enzymes during transition of AECII to AECI

Freshly isolated mouse AECII were grown under optimized culture conditions as previously described (Rice et al., 2002). They were seeded on matrigel and cultured in bronchial epithelial growth medium for 1, 3 and 7 days in the presence and absence of 10 ng/ml KGF. Immunofluorescence preparations with specific antibodies against peroxisomal proteins and RT-PCR of corresponding mRNAs were used to determine whether growth medium supplemented with or without KGF could alter the peroxisomal compartment during cultivation of AECII. The analysis revealed that KGF treatment led to maintenance of AECII in a differentiated state with high peroxisome content. In contrast, in vitro experiments with AECII cultures without KGF over a period of seven days led to the transdifferentiation of AECII into AECI like cells. This transdifferentiation process was accompanied by a downregulation of pro SP-C (Fig. 15D-F) and in parallel a drastic reduction of catalase (Fig. 15J-L). Furthermore, an increase of the AECI cell marker caveolin 1 was observed (Fig. 17). In contrast, in KGF-treated cells the mRNAs for SP-B and pro SP-C were still highly expressed after 7 days of culture. Interestingly, catalase- and Gnpat- mRNAs were induced by KGF treatment and were highest at day 3 in the cultures. Even after 7 days their expression was slightly higher in comparison to control levels at day 1. In addition, cultured AECII, stained for Pex14p, were filled up with many peroxisomes, which showed the typical punctuate cluster pattern in the KGF treated group over the whole treatment period (Fig. 13A-C). In contrast, in the absence of KGF this cluster pattern was only seen at day 1 and lost thereafter, suggesting the induction of peroxisomal KGF-

Results

mediated metabolism by treatment with this growth factor. This increase was also much pronounced for Pex14p and ACOX1, two proteins abundant nearly at similar levels in individual

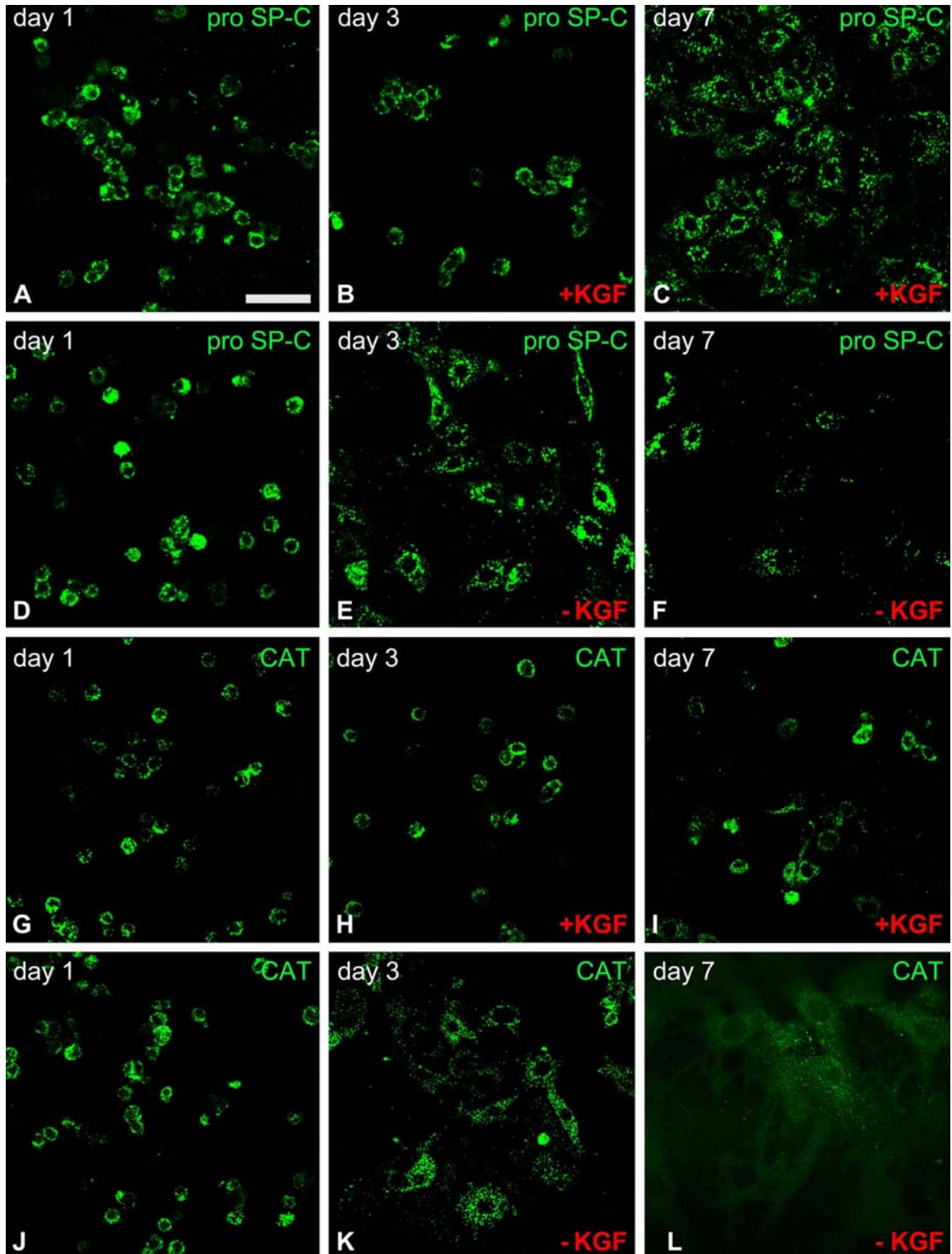


Fig. 15 Disappearance of peroxisomal markers during differentiation of AECII to AECI. Primary AECII cells were cultured with KGF and without KGF for a period of seven days, and IF was performed with anti-pro SP-C (A-F) and anti-catalase (G-L) on days 1, 3, and 7. Bar represents: 80 μ m.

Results

peroxisomes in AECI in comparison to AECII, which remained almost constant until day 7 also in groups without KGF treatment. After 3-7 days only individual and less numerous peroxisomes were observed in the culture (Fig. 16E-G). At day 3, the cells without KGF-treatment already showed the typical AECI “large and flat” epithelial cell pattern. Interestingly, tubular peroxisomes of different size (Fig. 16F with inset) were observed after 3 days in culture with the anti PEX14p antibody as marker. The tubular peroxisomes in the KGF (-) group were intermediate structures, which disappeared again until the seventh culture day at which only spherical peroxisomes were observed, suggesting the fission of the tubular organelles into spherical ones. Interestingly, tubular peroxisomes seemed to partition into small spherical particles at the exact time point at which drastical size and area increases of the transdifferentiating cells occurred. Similar to the immunofluorescence results, an intermediate transitional state of the peroxisomal compartment between day 3 and 7 of the AECII culture was noted on the mRNA level. During this time-period, the reaction of each peroxisomal enzyme to KGF-treatment was distinct from each other. On the one hand the mRNA levels for PEX14p and ACOX1 showed almost constant levels also without KGF-

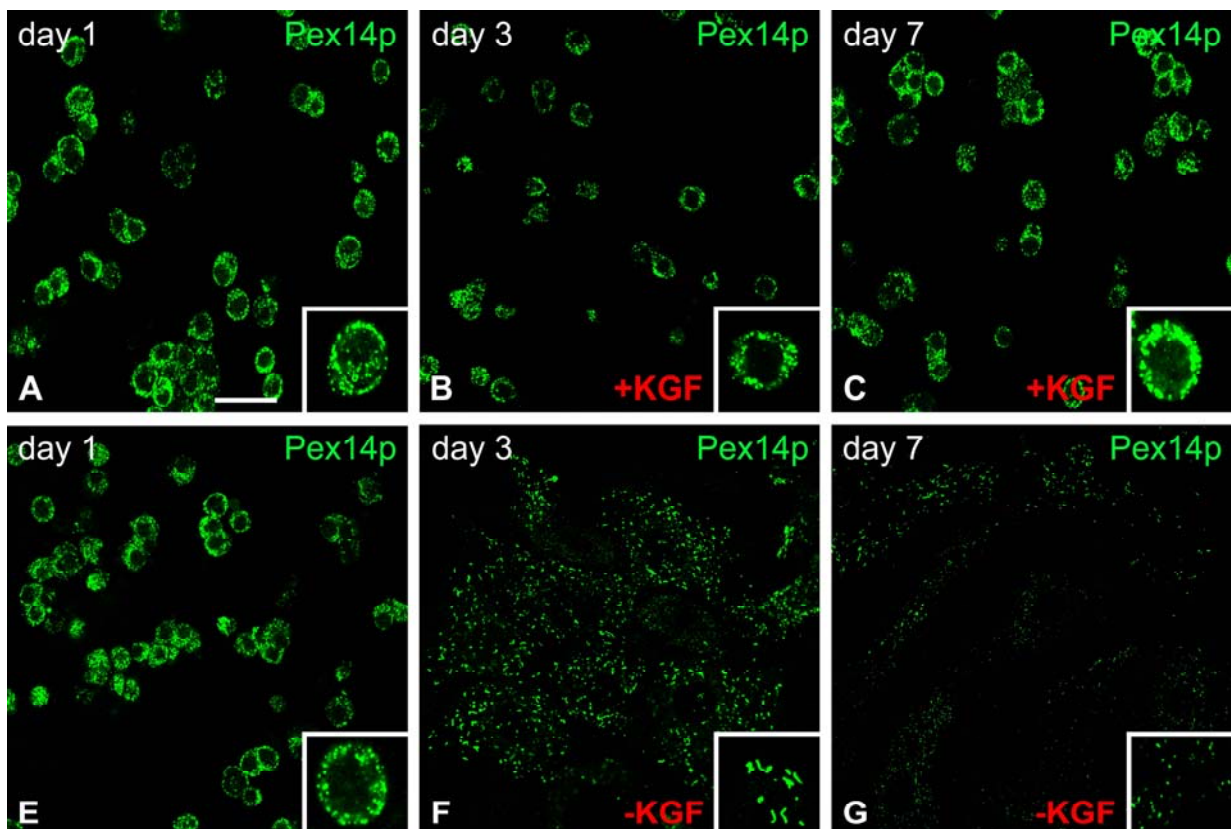


Fig. 16 IF analysis for the peroxisomal biogenesis protein Pex14p on cultured AECII with and without KGF for a period of seven days. Bar represents: 80 μ m.

Results

treatment after 7 days. On the other hand, the mRNA levels for catalase and Gnpat were drastically downregulated in the group without KGF treatment, whereas the ones in the KGF supplemented group showed high expression levels. Indeed, also by immunofluorescence analysis, a high level of catalase staining was noted in the highly differentiated AECII in cultures after 7 days of treatment with KGF, whereas only very few peroxisomes with catalase could be visualized in 7 day old culture without KGF. In addition, also Pex14p staining revealed a drastic downregulation of peroxisomal numerical density in 7 day cultures without supplemented with KGF.

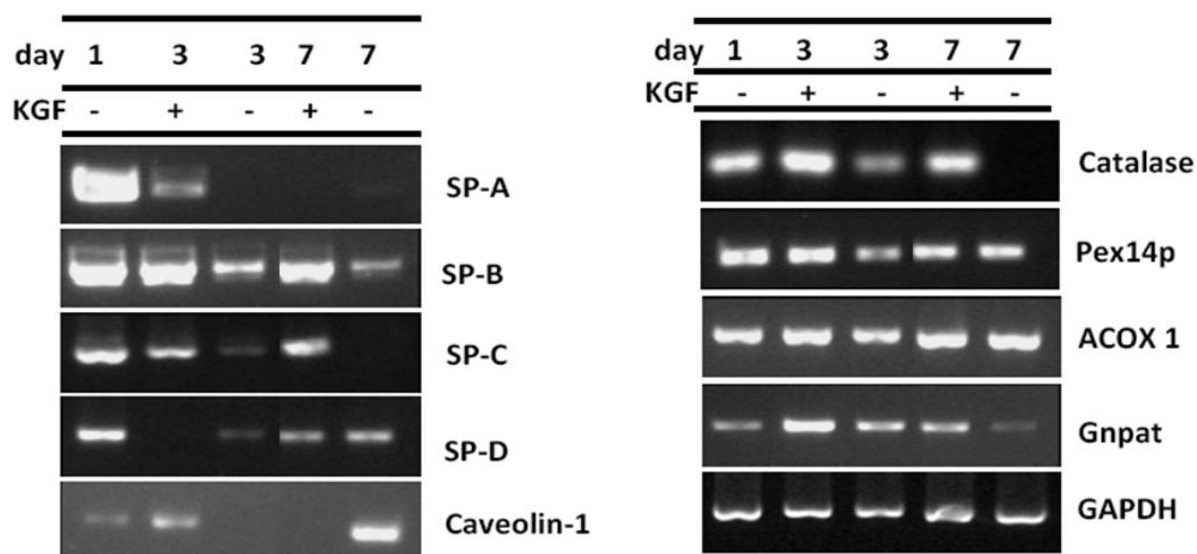


Fig. 17 Gene expression profiling of cultured AECII, depending on KGF supplementation. Primary AECII were cultured with KGF and without KGF for seven days and total RNA isolated from cultured primary AECII subsequently on days 1, 3 and 7. RT-PCR was performed to analyze specific gene expression. GAPDH served as an internal control to normalize the expression levels. For a list of primer pairs and size of PCR product see table 5.

5.3 Characterization of peroxisomal proteins during the neonatal development of the lung

Since animals are weaned with fat-containing milk in the early postnatal period, peroxisomes might play an important role for the postnatal development and final differentiation of organ systems. This notion is supported by the fact that many peroxisomal KO animals with single enzyme deficiencies die during the weaning period (Li et al., 2002). In addition, in this period alveolarization proceeds in the lung and a huge amount of surfactant is needed to reduce the alveolar surface tension. However, until now nothing is known about the role and functions of peroxisomes during the postnatal development of the lung. Thus, we characterized the peroxisomal compartment using biochemical and molecular biological methods in the different stages of the postnatal development. We have compared multiple mRNAs encoding for various peroxisomal biogenesis and metabolic proteins, ROS metabolizing enzymes of different subcellular compartments, epithelial lineage markers and surfactant proteins in the tissues of newborn lung (P0.5), lungs from P15, and adult animals and adult liver homogenates.

5.3.1 The mRNA expression levels of peroxisomal docking complex proteins decrease during the postnatal development of the lung

RT-PCR analysis revealed that the mRNA levels for peroxisomal proteins, involved in matrix protein import (such as PEX5, PEX13 and PEX14 - mRNAs) were decreased in their expression levels during the postnatal development of the lung (Fig. 18B). The PEX5 mRNA was reduced more strongly than those for PEX13 or PEX14.

5.3.2 The mRNA level of the peroxisomal lipid transporter, ABCD3 exhibited the biggest differences in expression levels during the postnatal development

A heterogeneous regulation of individual mRNA expression patterns for various peroxisomal enzymes involved in catabolic lipid metabolic pathways and their regulatory nuclear receptors (PPARs) were noted during postnatal development of the lung. The highest mRNA levels at birth for peroxisomal proteins involved in fatty acid degradation was noted for ABCD3, one of the lipid transporters on the peroxisomal membrane, followed by ACOX1, the regulatory enzyme of the β -oxidation pathway 1. In addition, both mRNAs were significantly downregulated during postnatal development. Similar alterations of the expression patterns were also observed for the Scp2-mRNA

Results

regulation (Fig. 18C). In contrast, the mRNA levels for MFP2 and thiolase were hardly affected in their expression levels during postnatal development.

Interestingly, the mRNA levels of the two other acyl-CoA oxidase (ACOX2, ACOX3), involved in the degradation of distinct lipid substrates from ACOX1, were regulated in a completely different way. Whereas the ACOX2 mRNA levels were high at birth, decreased at P15 and were upregulated in lungs of adult animals, the one of ACOX3 were hardly detectable at birth, increased strongly at P15 and were slightly downregulated again in the adult lung. Similar patterns was observed for the MFP1 mRNA levels, which were also low at birth, increased strongly at P15 and were downregulated in adult animals again to a higher level in comparison to newborn animals. In contrast, the expression level of the mRNA encoding ABCD1 was low at birth and it was not significantly altered during postnatal development. The mRNAs encoding for the Gnpat and Agps, involved in the synthesis of ether lipids, did not show any alterations during postnatal development of the lung. In addition, the mRNAs encoding for peroxisomal cholesterol synthesizing enzymes, such as IDI1 and HMGCR, which is a bicompartamentally localized enzyme (ER and peroxisome), also did not show any alterations during postnatal development of the lung (Fig. 18E). Similarly to the individual regulation of mRNA expression patterns of distinct β -oxidation enzymes and lipid transporters, the expression patterns for the mRNAs of the three different members of the PPAR-family varied significantly to each other. Whereas the PPAR α mRNA was expressed at low level at birth and increased until adulthood, the one for PPAR β was present at higher levels at birth but was not altered during postnatal development. In addition, the one for PPAR γ was expressed at an intermediate level at birth and decreased during development. Finally, a drastic downregulation from very high to an almost undetectable level was noted for the Wnt5a-mRNA, encoding a protein involved in the transcriptional regulation of genes involved in the process of distal morphogenesis (Fig. 18J).

5.3.3 The mRNA levels for peroxisomal peroxiredoxins are lower expressed in newborn mouse lungs compared to adult animals

RT-PCR analysis of mRNA levels for other peroxisomal ROS metabolizing enzymes such as peroxiredoxin I and V revealed an increase in their expression levels during the postnatal development of the lung. In contrast, the one for peroxiredoxin VI and catalase did not change significantly.

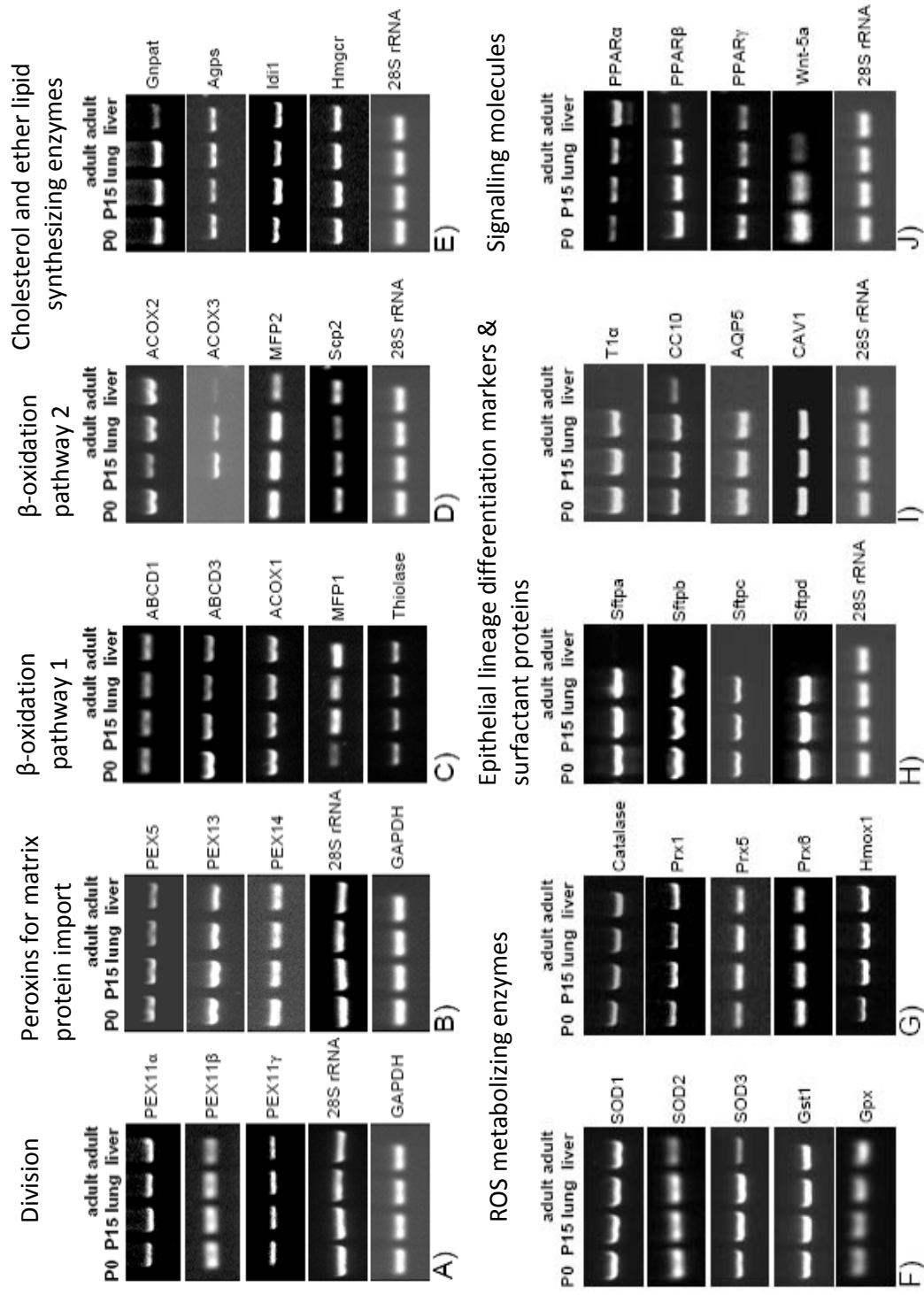


Fig 18A-J) RT PCR analysis of various mRNAs from newborn, P15, and adult lungs and adult liver. All mRNAs were depicted in the columns according to the function of their proteins. GAPDH and 28S rRNA served as internal control (n = 3 animals).

5.3.4 Differential mRNA expression levels of ROS metabolizing enzymes of different subcellular compartments

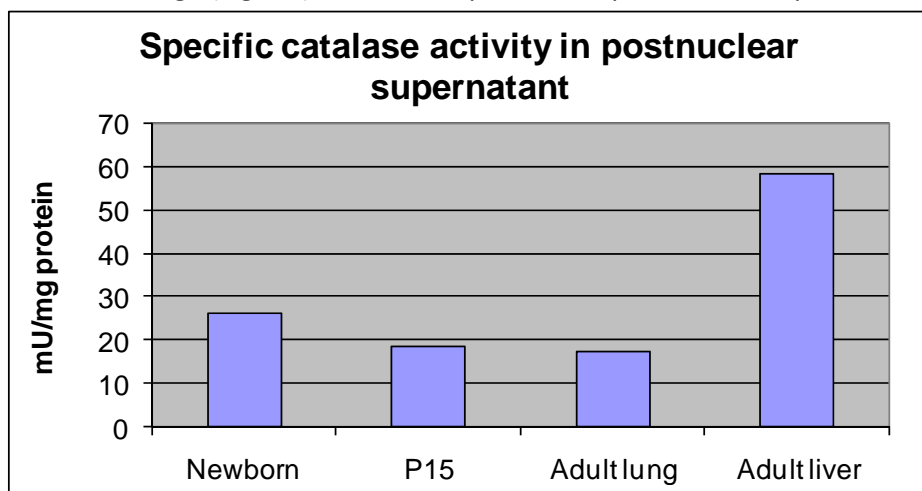
The mRNA levels for the mitochondrial antioxidative enzyme, SOD2 did not show any changes during the postnatal development of the lung. On the other hand, the mRNA levels for antioxidative enzymes of other subcellular compartments such as, glutathione S-transferase 1 (cytoplasm), glutathione peroxidase (cytoplasm and peroxisome) and hemoxygenase (endoplasmic reticulum) were upregulated during the postnatal development of the lung (Fig. 18F, G).

5.3.5 No changes in the mRNA levels of cell-type-specific differentiation markers and of surfactant proteins were noted

We did not find any specific differences in the mRNA expression levels of surfactant proteins such as surfactant protein A, B, C and D during the postnatal development of the lung (Fig. 18H). In addition, the mRNAs encoding for cell-type specific proteins such as T1 α (podoplanin), CC10 and AQP5 did not show any alterations in their expression levels during the postnatal development of the lung (Fig. 18I).

5.3.6 Downregulation of catalase activity during the postnatal development of the lung

Analysis of postnuclear supernatants (= enriched peroxisomal fractions) of different lung stages for catalase activity suggests a higher catalase activity in the newborn lungs in comparison to P15 and adult lungs (Fig. 19). In these experiments, postnuclear supernatants from adult liver were



used as a positive control, which showed higher specific catalase activity than all lung samples.

Fig. 19 Catalase activity is high in the newborn lungs compared to P15 and adult lungs. Catalase activity was measured in post nuclear supernatants. Data were expressed as mU/mg protein.

5.4 Pathological consequences of peroxisome-dysfunction in the lung. A study with PEX11 β KO mice

Peroxisomes vary in number and enzyme composition in distinct organs. Peroxisomal abundance is controlled by metabolic factors and by Pex11 proteins, peroxins regulating peroxisomal division. In the lung peroxisomes are most abundant in AECII and Clara cells, both secreting components of the lung surfactant. However, to date, only basic information is available about the functions of these organelles in AECII or Clara cells and nothing is known about the pathological consequences of PEX11 β deficiency in the lung. Even though peroxisomes are present in all tissues and cell types of PEX11 β -deficient mice, these animals display several pathologic features, shared by knockout mouse models of the Zellweger syndrome, in which peroxisomes are absent. In this study, we used the PEX11 β -knockout mouse model to analyse the alterations of lung structure, function and molecular mRNA and protein expression patterns due to a peroxisome proliferation defect. In our previous study, we clearly showed that especially Clara cells and AECII possess a high numerical density of peroxisomes (Karnati and Baumgart-Vogt, 2008). Wherefore, in this investigation, the main emphasis was laid on the alterations and pathological consequences of PEX11 β deficiency in Clara cells. In addition, alterations of typical marker proteins of other pulmonary cell types were analysed.

5.4.1 Upregulation of peroxisomal biogenesis proteins in PEX11 β deficient mouse lungs

Results from in situ-hybridization studies with PEX11 β cRNA probes suggested that the PEX11 β -mRNA is strongly expressed in the distal epithelium of bronchioles in the lungs of new born mice (Karnati and Baumgart-Vogt, 2009). *In distal bronchiolar epithelia of mice mainly Clara cells are present, whereas ciliated cells are less frequent in number. As shown by IF analysis of paraffin sections of the E19 wild type mouse lungs, antibodies against the peroxisomal biogenesis proteins Pex13p and Pex14p showed specific positive labelling of large peroxisomes mainly in the apical part of Clara cells and the labelling intensity was slightly increased (especially the one for Pex13p) in PEX11 β KO animals (Fig. 20B, D, F, H, J, L). In addition, formation of numerous thick clusters of peroxisomes was observed with both antibodies in the KO lungs (Fig. 20D, H, J, L).*

Results

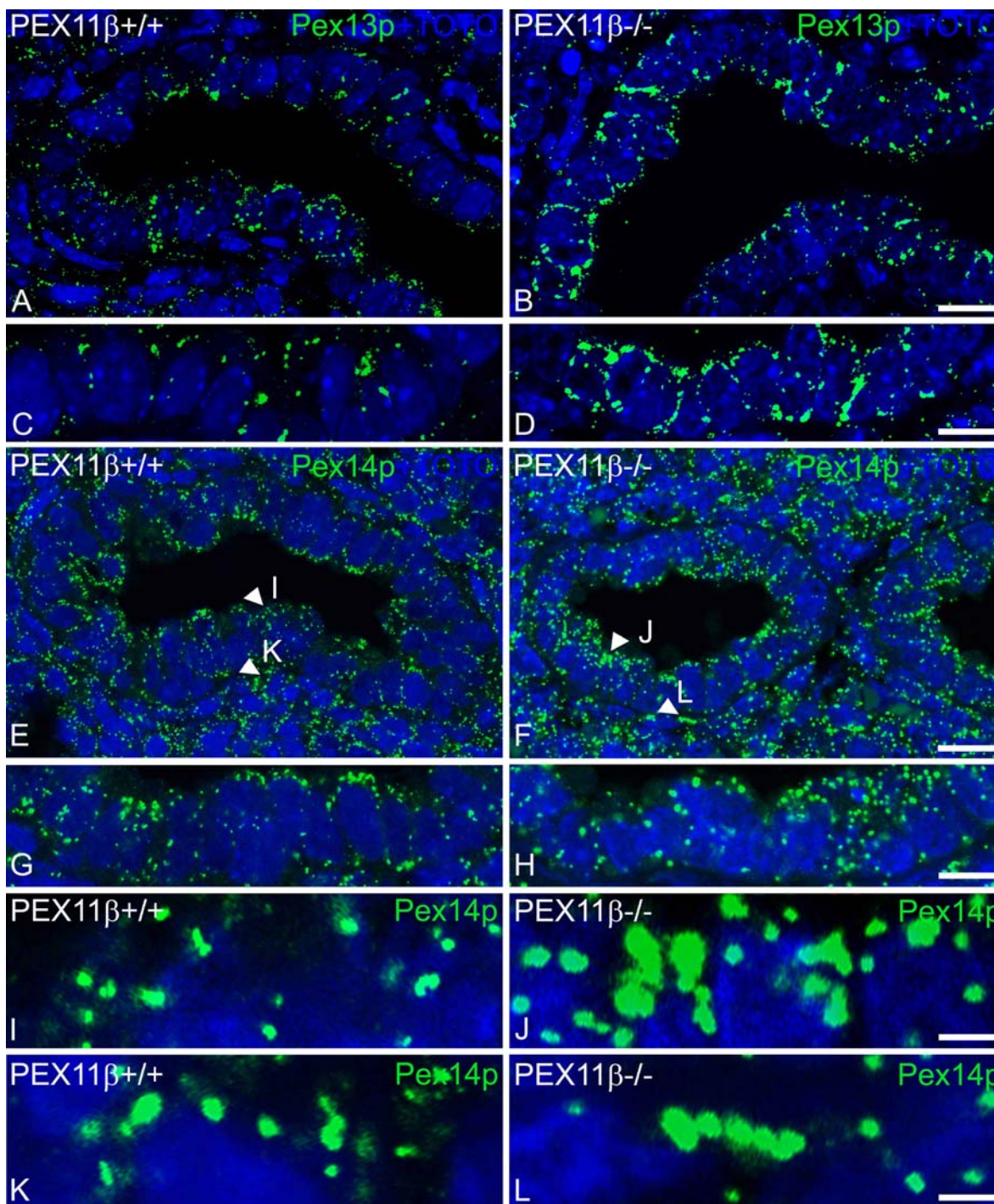


Fig 20. IF detection of Pex13p and Pex14p in perfusion-fixed and paraffin-embedded lung sections of E19 WT versus PEX11 β KO mice. Representative lower (A, B, E, F) and higher magnifications (C, D, G, H, I, J, K, L) of cross sections of small bronchioles in the mouse lung are depicted, stained for the localization of Pex13p and Pex14p. Mainly Clara cells are present in this type of epithelium, which contain a high number of intensively labelled peroxisomes. Note that in PEX11 β -knockout animals these organelles appear to be increased in size and are often interconnected with each other (I-L). Bars represent A, B, E, F: 20 μ m; C, D, G, H: 10 μ m; I, J, K, L: 5 μ m.

5.4.2 Increased mRNA and protein levels of peroxisomal lipid transporter and β -oxidation enzymes of pathway 1

IF analysis of the E19 wild type and PEX11 β KO mouse lungs with antibodies against the peroxisomal lipid transporter ABCD3 revealed a strong upregulation of this protein in Clara cells (Fig. 21A-D). Furthermore, antibodies against peroxisomal β -oxidation enzymes of pathway 1 such as acyl-CoA oxidase 1 (ACOX1) (Fig. 21E-H) and 3-ketoacyl-CoA-thiolase (thiolase) (Fig. 21I-L) showed increased protein levels in Clara cells of PEX11 β KO lungs, with the increase being more pronounced in preparations stained for thiolase.

5.4.3 Imbalance of peroxisomal antioxidative enzymes in PEX11 β deficient lungs

In addition, to the increased levels of peroxisomal biogenesis proteins, and proteins involved in lipid degradation, an imbalance of antioxidative enzymes was noted in PEX11 β deficient mouse lungs. IF analysis for the peroxisomal marker enzyme catalase (CAT) showed a decrease in the catalase protein, resulting in “smaller-appearing” peroxisomes in Clara cells of PEX11 β KO lung (Fig. 22H). In addition, the peroxisomal located antioxidative enzyme peroxiredoxin V (Prx V), *whose function is to catalyze the degradation of lipidhydroperoxides and hydrogen peroxide*, was drastically downregulated in Clara cells of PEX11 β KO mouse lungs (Fig. 22I-L).

5.4.4 Alterations of antioxidant enzymes in other subcellular compartments

The manganese superoxide dismutase 2 (MnSOD or SOD2), is considered to be one of the most important antioxidant enzymes in mitochondria. In contrast to the peroxisomal catalase and Prx V, this mitochondrial antioxidant enzyme was significantly upregulated in Clara cells of PEX11 β KO animals (Fig. 23A-D). Contrarily to mitochondrial SOD2 and similarly to the peroxisomal antioxidative enzymes, our results show a dramatic decrease in cytoplasmic glutathione reductase (GR) in Clara cells of PEX11 β KO animals, *the enzyme catalyzing the reduction of glutathione disulphide (GSSG) to glutathione (GSH)* (Fig. 23E-H). Thus, deficiency of PEX11 β might lead to an imbalance of the expression of antioxidative enzymes in different subcellular compartments, leading to oxidative stress and altering ROS metabolism and the maintenance of the cellular redox system in the lung.

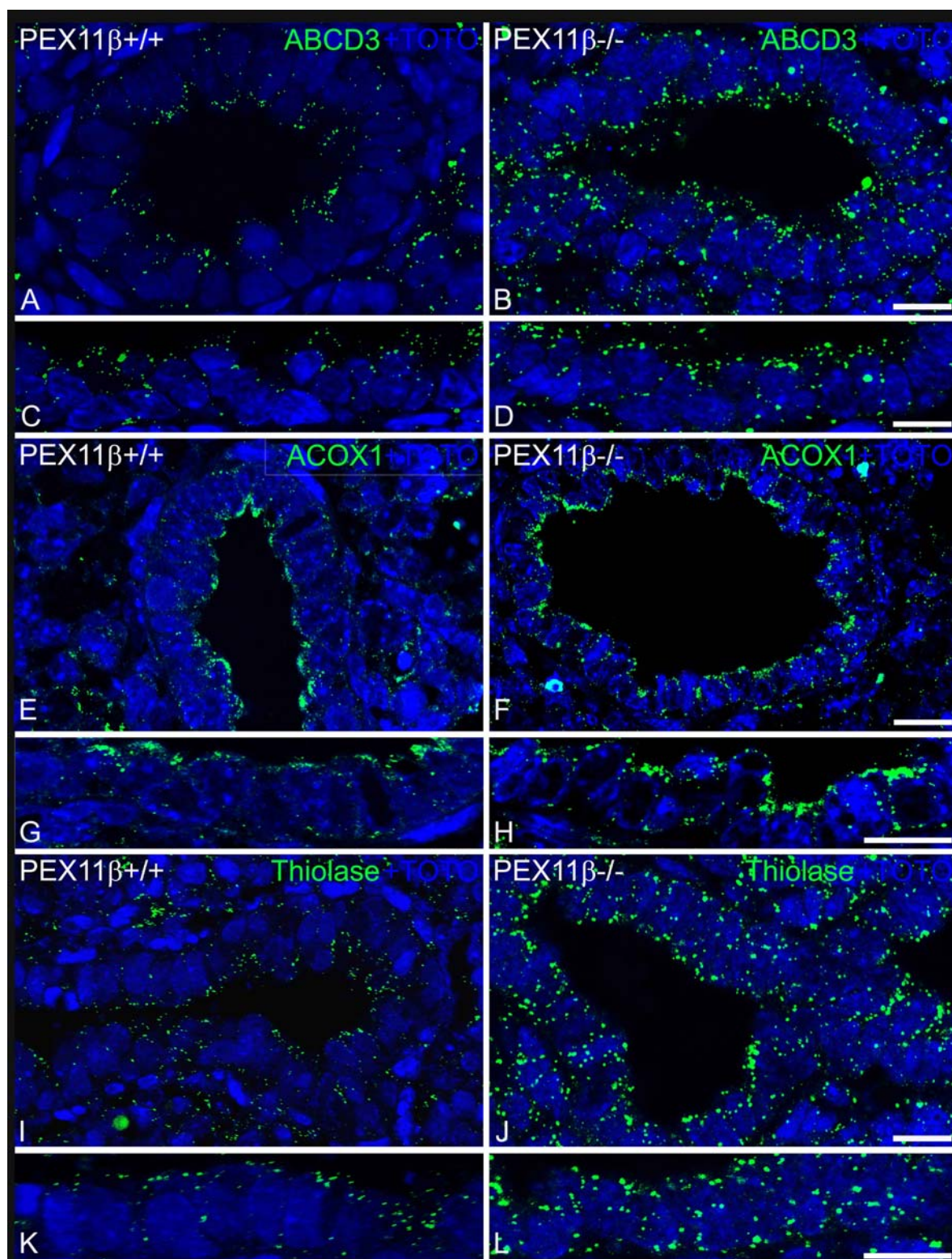


Fig 21. IF detection of ABCD3, ACOX1 and thiolase in perfusion-fixed and paraffin-embedded tissue sections of E19 WT versus PEX11 β KO mice. Representative lower (A, B, E, F, I, J) and higher magnifications (C, D, G, H, K, L) of cross sections of small bronchioles in the mouse lung are depicted, stained for the localization of ABCD3 and acyl-CoA oxidase I (ACOX1) as well as thiolase. Upregulations of ABCD3, ACOX1 and thiolase were observed in the Clara cells of PEX11 β KO mouse lungs. Bars represent: A, B: 20 μ m; E, F, I, J: 15 μ m; C, D, G, H, K, L: 10 μ m.

Results

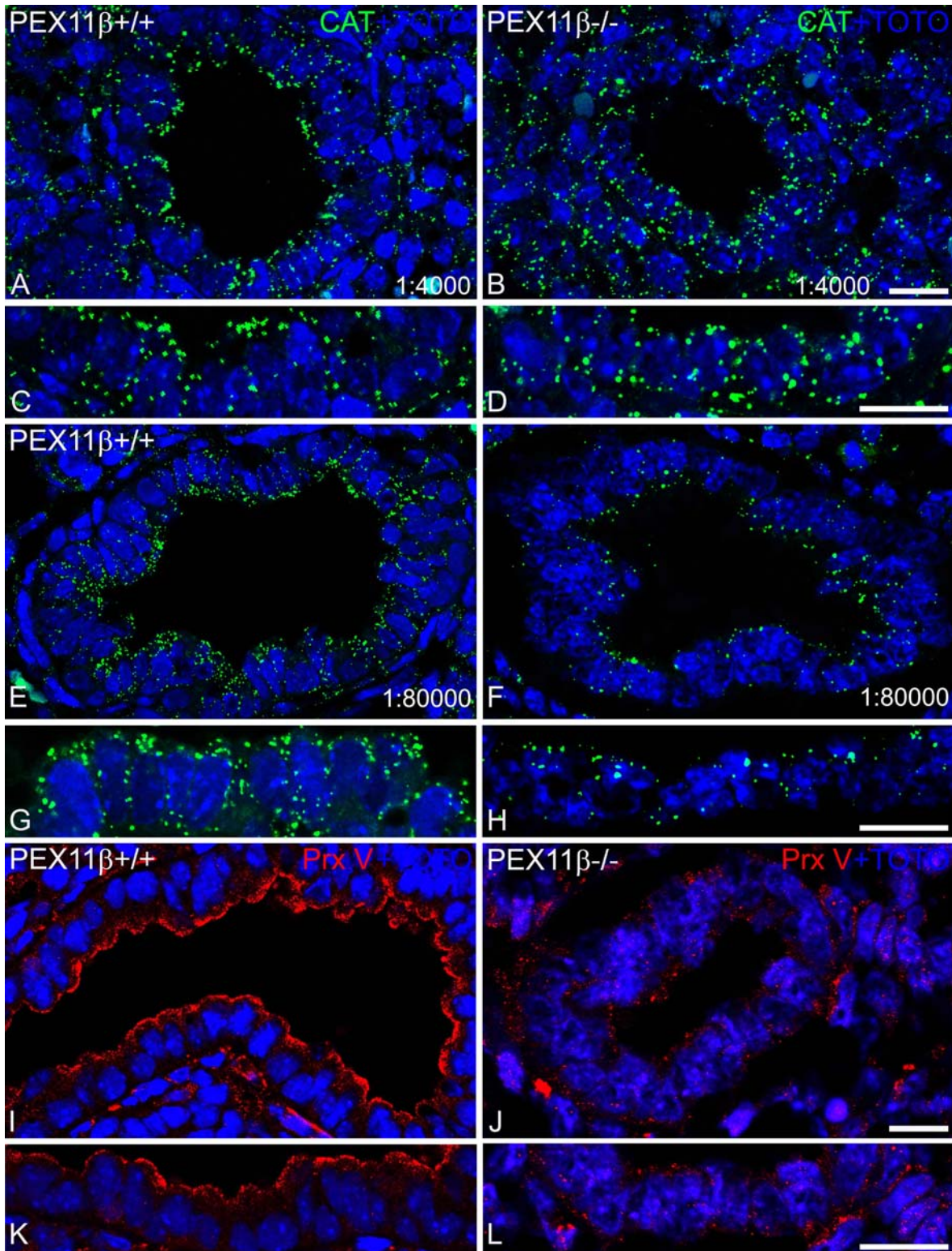


Fig 22. IF detection of catalase and peroxiredoxin V in perfusion-fixed and paraffin-embedded tissue sections of E19 WT versus PEX11 β KO mice. Representative lower (A, B, E, F, I, J) and higher magnifications (C, D, G, H, K, L) of bronchioles in the mouse lung, showing the localization of the peroxisomal antioxidative enzymes, catalase and peroxiredoxin V. Note that, with the regular dilution of 1:4000 of the catalase antibodies, no significant alterations in the Clara cells of wild type and PEX11 β KO mouse lungs were found. However with a dilution of 1:80,000 of the catalase antibody, a clear downregulation of catalase was observed in these lungs. In addition, peroxiredoxin V was also strongly downregulated in these lungs. Bars represent: A, B: 25 μ m; E, F, I, J: 20 μ m; C, D, G, H, K, L: 10 μ m.

Results

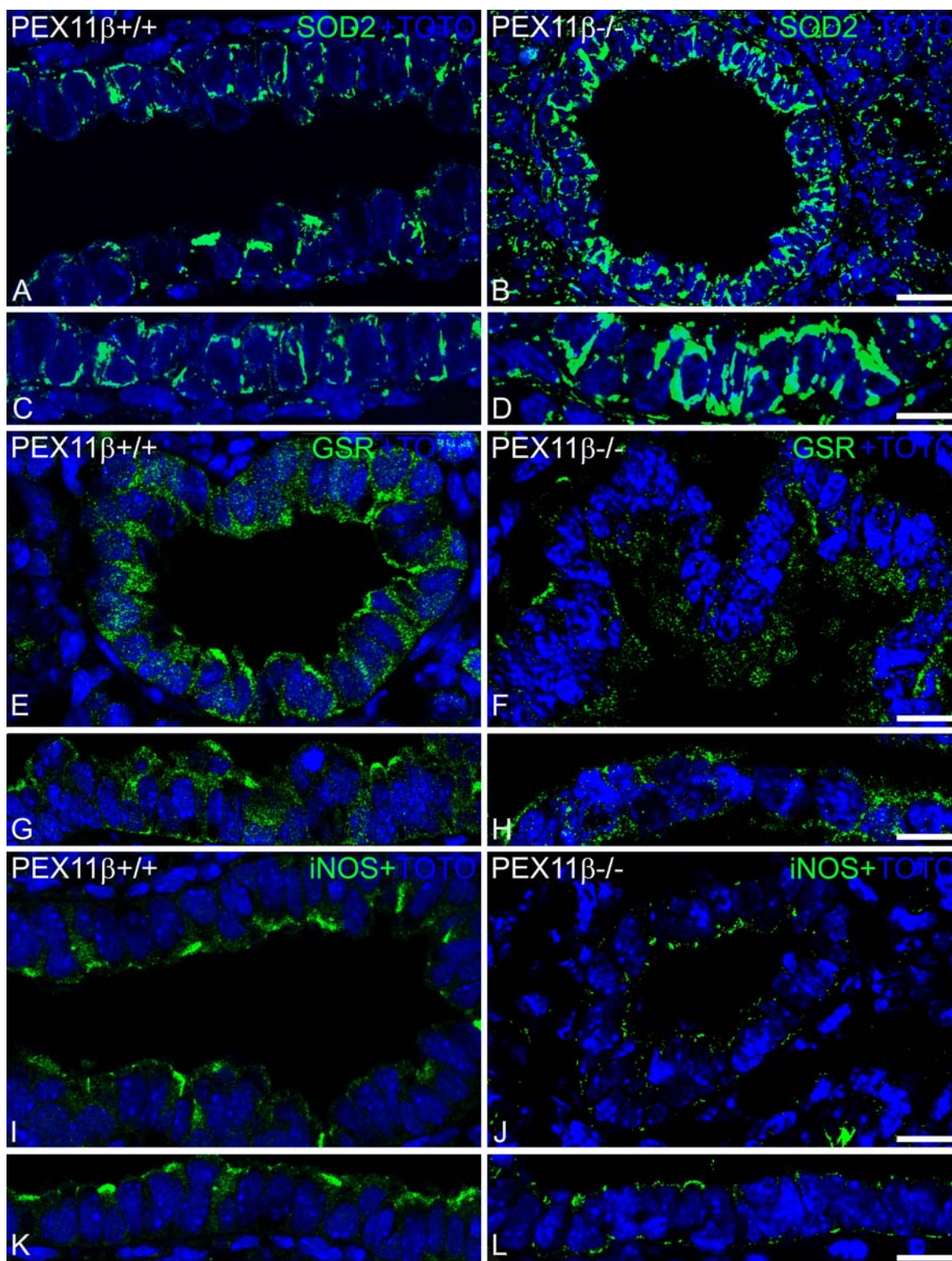


Fig 23. IF detection of manganese superoxide dismutase 2, glutathione reductase and inducible nitric oxide synthase in perfusion-fixed and paraffin-embedded tissue sections of E19 WT versus PEX11 β KO mice. Representative lower (A, B, E, F, I, J) and higher magnifications (C, D, G, H, K, L) of bronchioles in the mouse lung showing the localization for antioxidative enzymes of distinct subcellular compartments such as SOD2 (mitochondrial), GSR (cytoplasmic) and iNOS (cytoplasm and peroxisomes). A downregulation of glutathione reductase (E-H) and iNOS (I-L) was observed in PEX11 β KO mouse lungs. However, a significant upregulation of mitochondrial SOD2 was noted in these lungs (A-D). Bars represent: A, B, E, F, I, J: 25 μ m; C, D, G, H, K, L: 10 μ m.

Results

Cytoplasmic inducible nitric oxide synthase (iNOS) has an important function in pro-inflammatory signalling in airway inflammation and it has been closely correlated with the pathophysiology in a variety of diseases and inflammation. In addition to macrophages and AECII, Clara cells are one of the major cell types expressing iNOS in the lung. As shown by IF, iNOS was mainly localized in the apical part of Clara cells (Fig. 23I-L). PEX11 β deficiency leads to a drastic downregulation of iNOS in Clara cells of PEX11 β KO mice (Fig. 23I-L). A more punctate staining pattern was observed in PEX11 β KO animals, suggestive for a possible shift of iNOS into peroxisomes as it is known from the literature (Loughran et al., 2005).

5.4.5 Alterations of cell type-specific marker proteins in the PEX11 β KO lungs

5.4.5.1 A severe downregulation of the Clara cell protein CC10 occurred in the lung of PEX11 β deficient animals

One of the vital functions of CC10 is to inhibit the phospholipase A2 activity, a potent regulator of the lung inflammatory response. Deficiency of CC10 protein may therefore be associated with more alterations in lung homeostasis with direct or indirect effects on the immunoregulation of the lung. Alterations in the CC10 protein are associated with a variety of pulmonary diseases in humans.

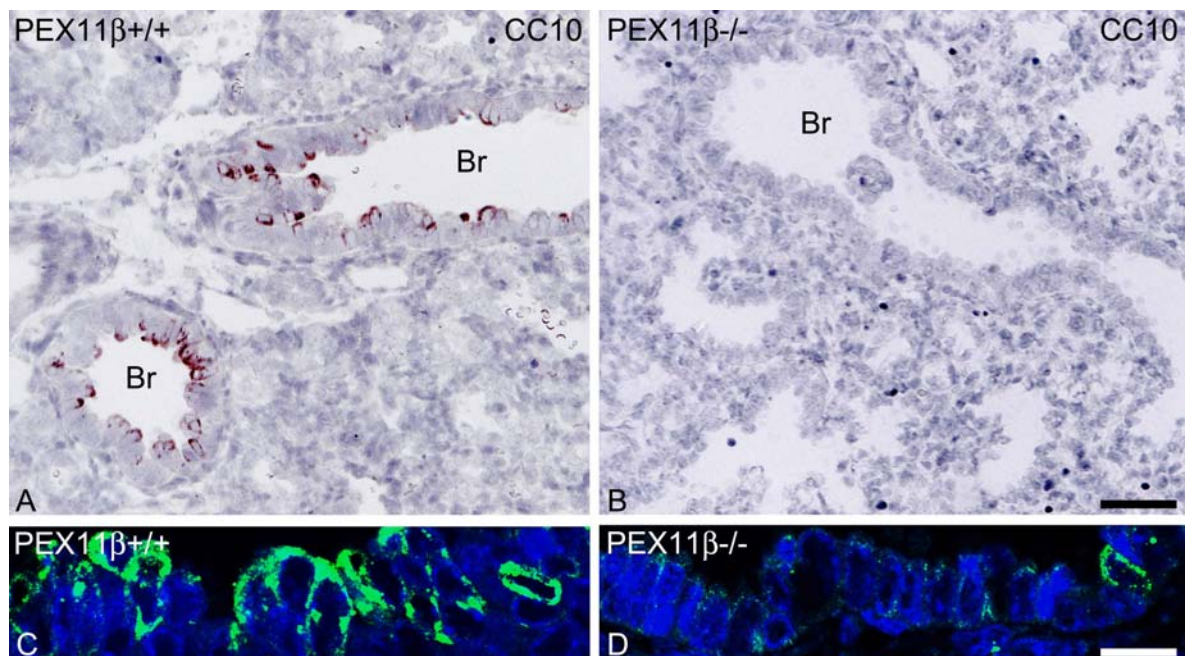


Figure 24. For figure legend see page 75.

Results

Fig 24. Immunohistochemistry and IF for the localization of CC10 in Clara cells in paraffin-embedded lung sections of a E19 wild type and PEX11 β KO mice. Already the IHC-staining revealed a significant downregulation in PEX11 β deficient mouse lungs (A-B). Lower panel C and D are higher magnifications, depicting the CC10 staining in Clara cells with immunofluorescence. Note that, with immunohistochemistry, all bronchioles were negative for CC10 in PEX11 β KO mouse lungs (B), however, with IF a very weak staining for CC10 was observed (D). For overviews of IF preparations for CC10 see also Fig. 25A-D, I-L. Bars represent: A, B; 50 μ m; C, D: 10 μ m.

In the present study, the CC10 protein was clearly detectable in secretory granules at the apical pole of the Clara cells in WT animals (Fig. 24A, C). However, a marked reduction or the complete absence of the CC10 protein was observed in PEX11 β deficient mouse lungs. *This result was already observed with the less sensitive ABC-peroxidase staining method and was confirmed by using the more sensitive immunofluorescence method (25A-D).*

5.4.5.2 Distinct alterations of surfactant proteins due to PEX11 β deficiency

We analysed if a deficiency of PEX11 β could alter the expression of surfactant proteins. The SP-A protein is exclusively expressed only in AECII in E19 lungs. Therefore, in the PEX11 β KO mouse model we could not be able to stain the SP-A protein in Clara cells. SP-B is synthesized and produced in Clara cells and AECII. Expression of SP-B in the cells of the terminal airways or alveolar junctions suggests that Clara cells may contribute to the formation of the surfactant film in the terminal bronchioles, however, the exact functions of Clara cells SP-B are unclear. SP-B facilitates lamellar body formation in AECII and phospholipid spreading during the respiratory cycles. SP-C is not expressed in Clara cells. In contrast, Clara cell SP-D plays an important role in host defence against lung inflammation. The results of the present study showed a drastic downregulation of SP-B in Clara cells of PEX11 β deficient mouse lungs (Fig. 25E-H). In contrast, double IF for SP-D and CC10 proteins showed an upregulation of SP-D and the already described decrease of CC10 in Clara cells of the PEX11 β KO mouse lung (Fig. 25I-L).

5.4.5.3 Alterations of the type I cell marker T1 α /podoplanin

The podoplanin gene (T1 α) is highly expressed by AECI cells, lining most of the gas exchange surface of the lung. T1 α is localized in the apical plasma membrane of AECI cells. T1 α gene expression is also developmentally regulated however, the exact functions of this protein remains unclear. Loss of podoplanin alters the proliferation rate of distal lung cells and might lead to disruption of epithelial-mesenchymal signalling (Ramirez et al., 2003). In PEX11 β deficient mouse model, we observed a downregulation of the AECI cell marker T1 α (Fig. 26E, F).

Results

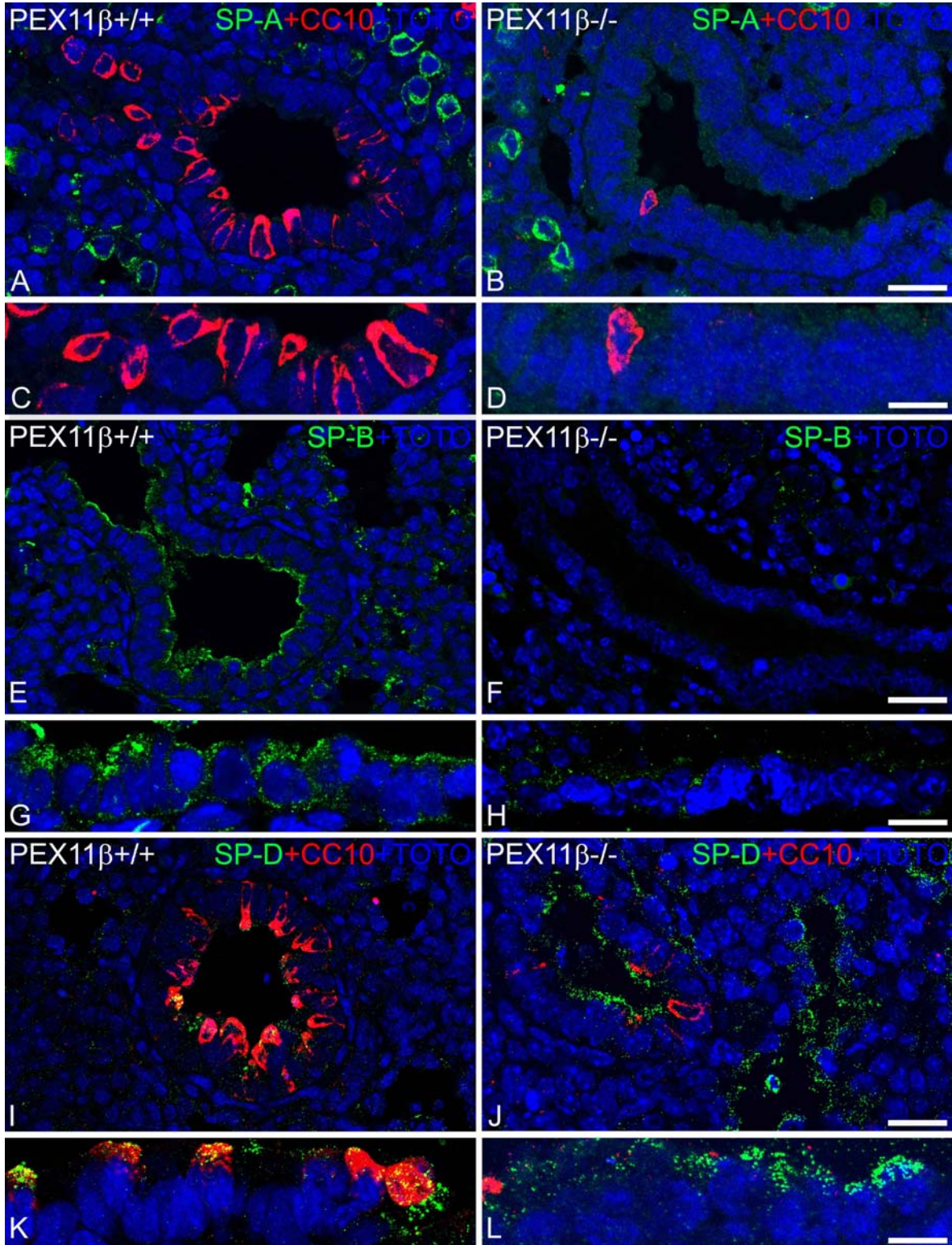


Fig 25. IF detection of surfactant proteins (SP-A, SP-B and SP-D) in perfusion-fixed and paraffin-embedded tissue sections of E19 WT versus PEX11 β KO mice. Representative lower (A, B, E, F, I, J) and higher magnifications (C, D, G, H, K, L) of bronchioles in the mouse lung, showing the localization for various surfactant proteins. A downregulation of the SP-B protein was observed in the Clara cells of PEX11 β KO lungs (E-H). The double-labelling for CC10 and SP-D revealed elevated levels of SP-D in Clara cells of the KO animals (I-K). Note that, the antibody against an SP-A protein did not stain Clara cells however, it strongly labelled AECII in WT and PEX11 β KO animals. Bars represent: A, B, E, F, I, J: 25 μ m; C, D, G, H, K, L: 10 μ m.

Results

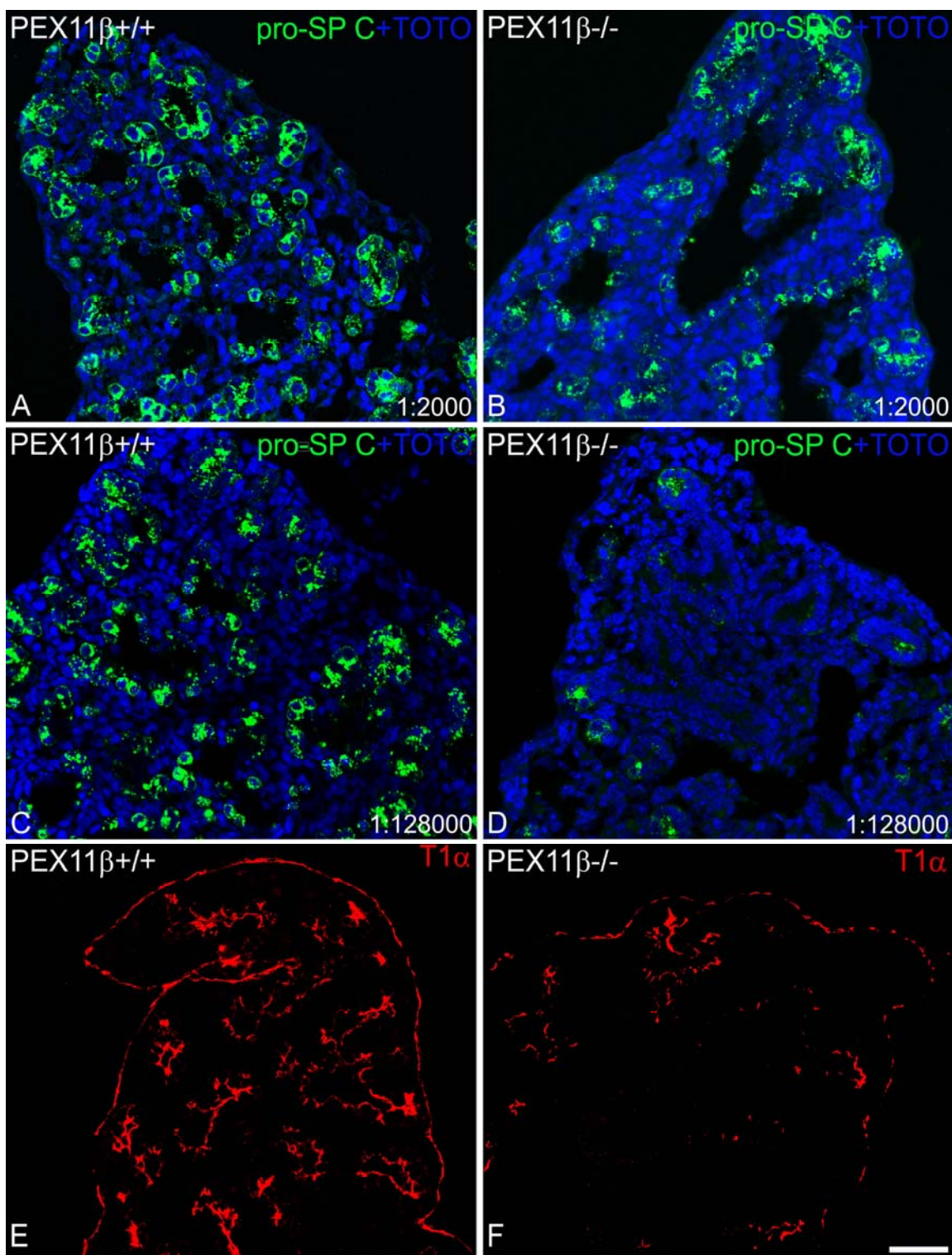


Fig 26. IF detection of pro SP-C and T1 α in perfusion-fixed and paraffin-embedded tissue sections of E19 WT versus PEX11 β KO mice. pro SP-C staining in AECII (A-D). Note that with a regular 1:2,000 dilution of the anti pro SP-C antibody no differences in AECII of PEX11 β KO mouse lungs were observed. However, at a 1:128,000 dilution, a clear decrease of the AECII marker protein pro SP-C could be demonstrated in PEX11 β KO mouse lungs. In addition, the AECI cell marker protein, T1 α /podoplanin was also downregulated in the KO mouse lungs. Bars represent A-F: 20 μ m.

5.4.6 Semi-quantitative RT-PCR analysis of WT, PEX11 β HZ and KO lungs

5.4.6.1 Severe alterations of expression levels of multiple mRNAs encoding for peroxisomal biogenesis, and lipid metabolic proteins in PEX11 β KO mouse lungs

In comparison to wild type (WT) animals only a slight reduction of the PEX11 β mRNA was noted in heterozygous animals (HZ), whereas the PEX11 β mRNA was completely absent in the PEX11 β KO animals reflecting the PEX11 β gene deletion. Quantitative analysis of RT-PCR bands for PEX11 α revealed a strong decrease in the expression level in PEX11 β KO mouse lungs, whereas the one for PEX11 γ was only slightly downregulated (Fig. 27A). In addition, the mRNAs for the peroxisomal C-terminal targeting signal import receptor PEX5 was also downregulated in PEX11 β KO mouse lungs. In contrast, the ones for PEX13 and PEX14 encoding the biogenesis proteins of the docking complex in the peroxisomal membrane involved in matrix protein import were slightly upregulated (Fig. 27B). Furthermore, the mRNAs for two enzymes of the peroxisomal β -oxidation pathway 1, (ACOX1, thiolase) as well as ABCD1 and 3, the lipid transporters were upregulated (Fig. 27C). In addition, also the mRNAs for ACOX2 and 3 of the peroxisomal β -oxidation pathway 2 were upregulated in PEX11 β KO mouse lungs (Fig. 27D). In contrast, the expression levels of the mRNAs of the multifunctional proteins (MFP1 and MFP2) of both β -oxidation pathways and of SCP2/ScPX were decreased. In addition, the mRNA IDI1, for the peroxisomal enzyme involved in the synthesis of cholesterol, was strongly downregulated, whereas *the one for Hmgcr was not altered. The Hmgcr protein is localized in two compartments: the endoplasmic reticulum and the peroxisomes and it still remains obscure, how this protein is targeted into peroxisomes (Krisans, 1992).* The mRNAs encoding for enzymes involved in the peroxisomal ether lipid synthesis Gnat and Agps were hardly affected (Fig. 27E).

5.4.6.2 Imbalance of mRNA levels for ROS metabolizing enzymes of distinct subcellular compartments

RT-PCR analysis of mRNA levels for peroxisomal ROS metabolizing enzymes such as catalase and peroxiredoxin 1 (Prx 1) did not reveal any alterations, however, the one for peroxiredoxin V (Prx V) was strongly downregulated (Fig. 27G). In contrast, the mRNA for the mitochondrial antioxidative enzyme manganese-superoxide dismutase 2 (SOD2) was upregulated in PEX11 β KO

mouse lungs (Fig. 27F). Furthermore, the mRNA levels for additional antioxidative enzymes of several other subcellular compartments, such as glutathione S-transferase 1 (Gst1), glutathione peroxidase (Gpx), and hemoxygenase 1 (hmox1) were downregulated in PEX11 β -deficient mouse lungs, suggestive for an imbalance of reactive oxygen species metabolism in the KO mouse lungs (Fig. 27F, G).

5.4.6.3 Alterations of expression levels of the mRNAs encoding for peroxisomal proliferator activated receptors in PEX11 β KO mouse lungs

PPARs are transcription factors with key regulatory functions on genes encoding proteins involved in peroxisomal β -oxidation and lipid cellular homeostasis. Significant upregulations of PPAR β and PPAR γ were noted in PEX11 β KO lungs (Fig. 27J). Whereas the expression level for the PPAR α mRNA was unaltered.

5.4.6.4 Regulation of Wnt5a in PEX11 β KO mouse lungs

Interestingly, also the mRNA for Wnt5a, encoding a protein involved in the distal morphogenesis of lung, was drastically downregulated in PEX11 β -deficient mouse lungs, corresponding to the lower maturation and differentiation of the alveolar region (Fig. 27J).

5.4.6.5 Alterations of mRNA levels for cell type-specific marker proteins and targeting signalling molecules in PEX11 β deficient mouse lungs

The mRNAs for the cell type-specific marker proteins CC10 and T1 α /podoplanin were decreased in PEX11 β deficient mouse lungs (Fig. 27I), whereas the mRNA levels for all surfactant proteins were unaffected. *This difference in protein and corresponding mRNA levels of surfactant proteins observed between immunofluorescence and RT-PCR results suggest a translation or post-translational modification of the half-life of surfactant proteins in PEX11 β KO animals.*

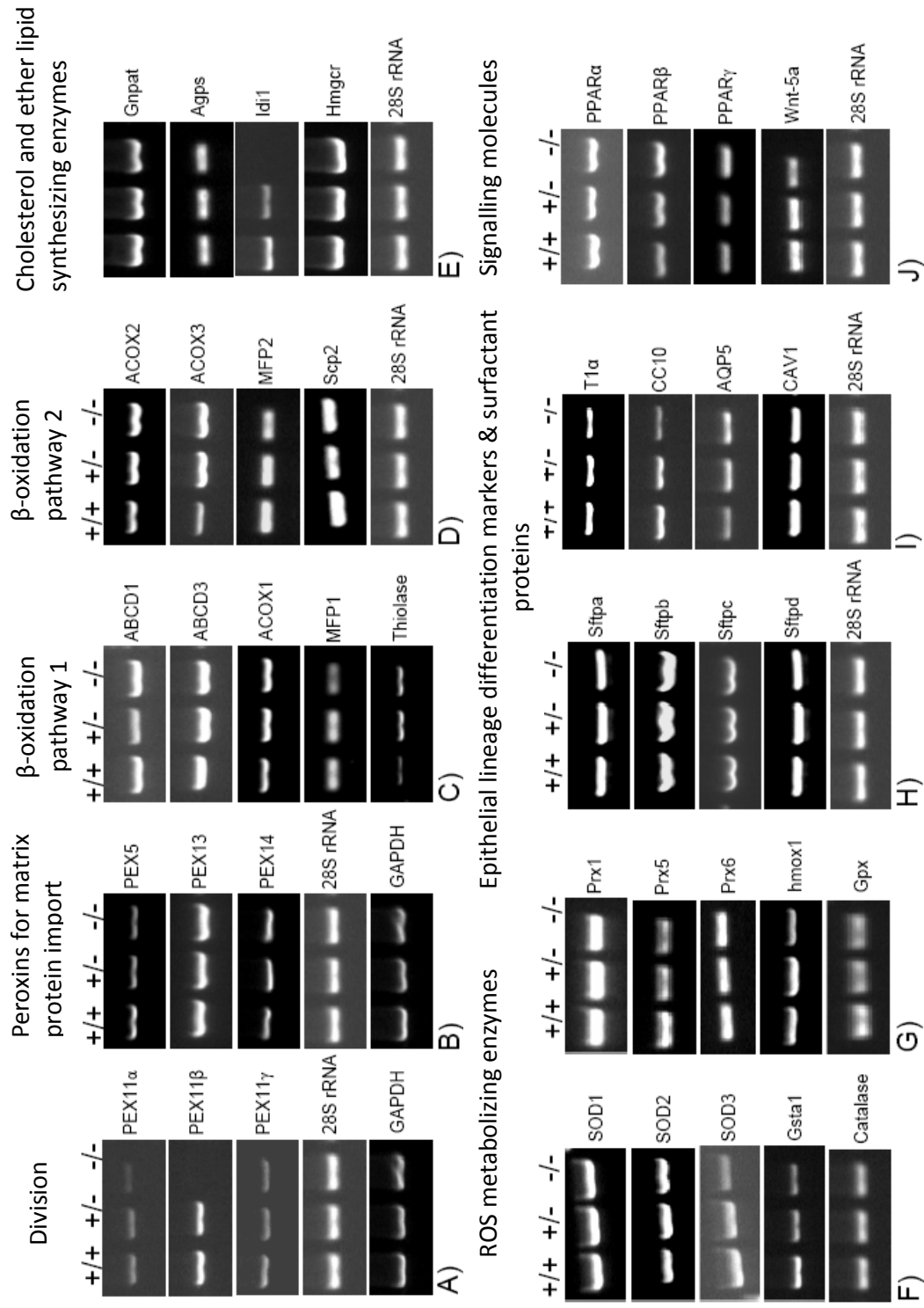


Fig 27A-J). RT PCR results from WT, HZ and PEX11 β KO lung homogenates. RT-PCR analysis revealed the absence of PEX11 β -mRNA in lung homogenates (A). Elevated expression levels of ACOX1, 2 and 3 were observed (C). The downregulations of Gnpat and Idi1 mRNAs occurred (E). Upregulations of SOD1 and SOD2 and downregulation of SOD3 were observed (F). Downregulations of Hmox, Prx5, Gpx indicate alterations in ROS metabolism. Downregulations of T1 α , CC10 were noted (I). Strong upregulation of PPAR γ and downregulation of Wnt-5a were observed (J) (n = 3). GAPDH and 28S rRNA were used as internal controls.

5.5 Upregulation of peroxisomal proteins (catalase and Pex14p) in alveolar epithelial cells in lung tissue of patients with idiopathic pulmonary fibrosis.

Samples of patients with idiopathic pulmonary fibrosis (IPF) were processed and analyzed to reveal if the peroxisomal compartment was altered in lung diseases.

As already described previously in the alveolar region of human donor lungs (see Fig.7, page number 44 and 45), only alveolar macrophages and AECII contain detectable amounts of catalase and Pex14p in human donor lung samples. Peroxisomes could be clearly identified in alveolar macrophages and AECII with both antibodies (Fig. 28A, C). The highest intensity of staining and best visualization of peroxisomes was achieved with the antibody against Pex14p in macrophages.

The IPF samples were characterized by irregular expanding and massive fibrosis in between interconnecting air spaces with thickened alveolar walls (see lower magnification views in Fig. 28B, D). Interestingly, catalase (Fig. 28B) and Pex14p (Fig. 28D) were increased in transitional epithelial cells of thickened alveolar walls. In higher magnification views, it is obvious that catalase (Fig. 28G) and Pex14p (Fig. 28H) protein levels are strongly expressed in the single-layered flattened epithelial cells of thickened fibrotic alveoli and in alveolar macrophages of IPF patients. *These preliminary data show that the peroxisomal compartment is indeed altered in lung diseases. Future studies taking IPF as an example, will clarify the influence of the peroxisomal metabolism in the pathogenesis of these lung diseases.*

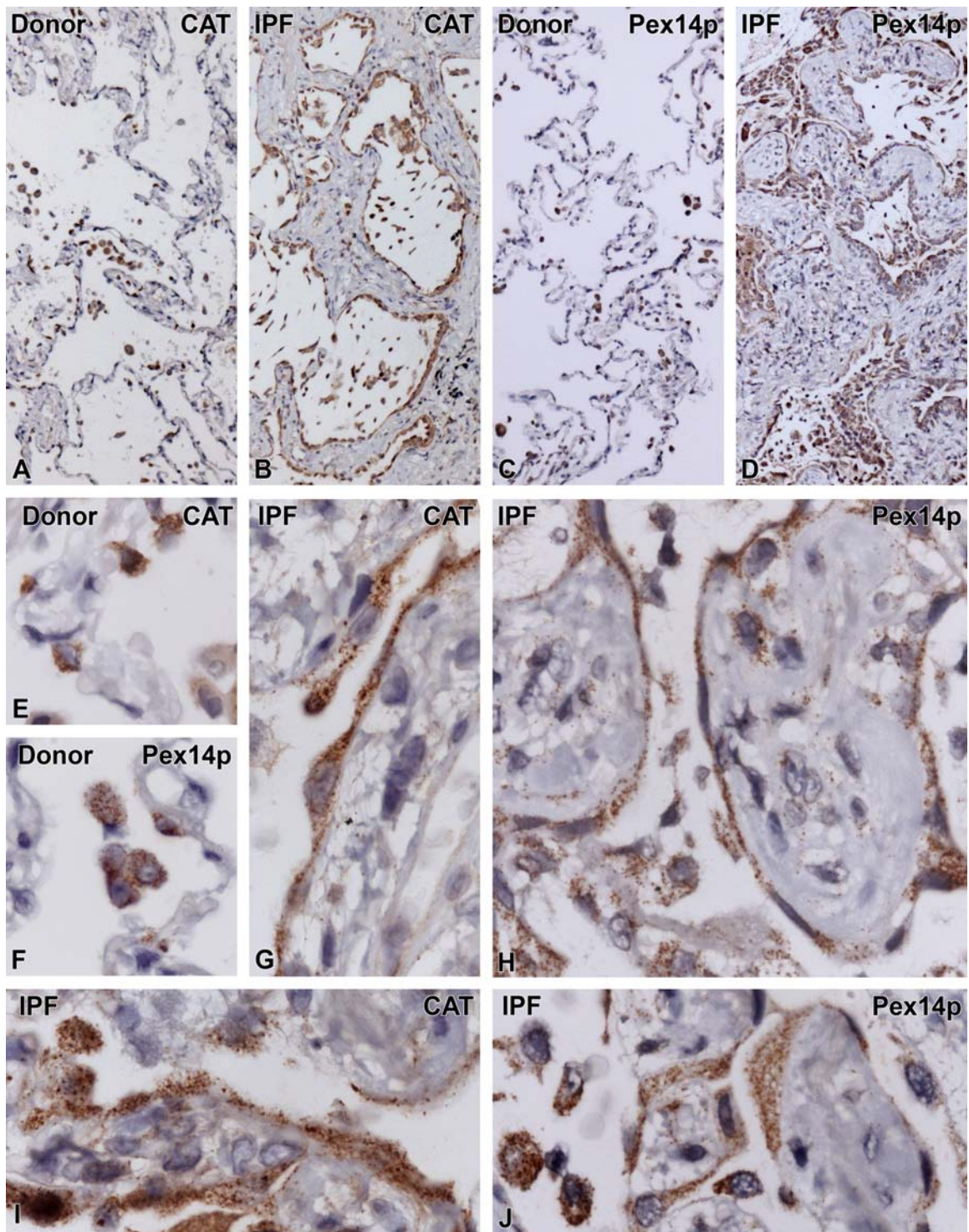


Fig. 28 Localization of catalase and Pex14p in donor and IPF lungs with immunohistochemistry ABC peroxidase method. Low magnification view of preparations stained for catalase (A) and Pex14p (C), showing positive labelling mainly in alveolar macrophages and AECII of the human donor lungs. Low magnification view of catalase (B) and Pex14p (D) showing the labelling at the lining of the alveolar epithelium of the IPF lung. Higher magnification of the specific punctuate staining pattern for the peroxisomal subcompartment in AECII and macrophages of the donor with catalase (E) and Pex14p (F). Higher magnification of the staining for catalase (G) and Pex14p (H) in the lining of the alveolar epithelium. Note the upregulation of catalase (I) and Pex14p (J) in the alveolar epithelium of the IPF lung. All corresponding negative controls were devoid of reaction product (not shown here. For a control on the method, see Fig. 7).

6 DISCUSSION

In the present study, the peroxisomal compartment in human and murine lungs was analysed with sensitive morphological, biochemical as well as molecular biological methods and a variety of peroxisomal markers to achieve insights on their possible metabolic roles in distinct pulmonary cell types. Peroxisomes were found in all lung cell types of adult human and murine lungs, however, with cell-type specific numerical abundance and distinct protein composition, suggestive of specific functional differences, depending on metabolic needs of the corresponding cell types. Furthermore, the effect of KGF on the peroxisomal compartment, an important growth factor, involved in the proliferation of AECII and in the regulation of the alveolar epithelium was analysed. In addition, the alterations of peroxisomal metabolism during AECII to AECl transdifferentiation were examined. Moreover, partial functions of peroxisomes were described in bronchiolar epithelial cells, e.g. Clara cells of distal pulmonary airways. Studies using PEX11 β knockout animals with dysfunctions of peroxisomal proliferation revealed that peroxisomes play an important role in the defence mechanisms of the bronchiolar epithelium against oxidative stress. In addition, first preliminary results revealed that the peroxisomal compartment is altered in AECII and macrophages in lung tissue of patients with idiopathic pulmonary fibrosis. Further investigations are needed to reveal the exact role of this organelle in airway cell biology and pathology.

6.1 Catalase as marker for peroxisomes in different pulmonary cell types

Peroxisomes were described already in the early 1970-80 by cytochemical localization of catalase activity with DAB at the electron microscopic level in the lung of a variety of species, such as mouse, rat, hamster, guinea pig, rabbit, cat, pig, monkey and man (Eguchi et al., 1980; Goldenberg et al., 1978; Moriguchi et al., 1984; Petrik, 1971; Schneeberger, 1972a; Van Meir and Scheuermann, 1988). In all of these studies peroxisomes were mainly found in bronchiolar Clara cells and AECII, the latter of which exhibited significant species-specific differences in size and structure (Schneeberger, 1972a). Only in extremely rare cases peroxisomes or only “remnants” of peroxisomes were observed in AECl of mice (Hirai et al., 1983; Schneeberger, 1972a) and none

Discussion

were described in cat or human lungs in fully differentiated AECI (Mercurio and Rhodin, 1976; Moriguchi et al., 1984). In addition, in other pulmonary cell types, such as macrophages or endothelial cells, no peroxisomes were found in different species (Schneeberger, 1972a) and no reports are available in the literature on peroxisomes in ciliated or goblet cells of conducting airways. In our study, we used a modified protocol of the alkaline DAB-method from Angemüller and Fahimi (1981), which had been developed by our group to demonstrate “catalase-less” peroxisomes in germ cells at the electron microscopic level (Nenicu et al., 2007). This technique allowed us to detect peroxisomes in all cell types in the lung, combined with good ultrastructural morphology. Indeed, peroxisomes of ciliated cells of the epithelia of conducting airways or AECI of the alveolar region contain only low levels of catalase and exhibit a diameter similar to the endoplasmic reticulum (see Fig. 10). Therefore, these organelles most probably have been overlooked in the past. Due to application of a higher incubation temperature of 45°C and a prolonged incubation time of 2 hr in our study, the precipitated oxidized DAB product was sufficient for visualization of peroxisomes in these cell types.

Due to the high abundance of catalase in peroxisomes of AECII Farioli-Vecchioli and colleagues were able to use a catalase antibody in combination with ABC-peroxidase immunohistochemistry for automatic detection of AECII at the light-microscopic level (Farioli-Vecchioli et al., 2001). However, in their study no correct subcellular staining pattern was achieved to unequivocally localize catalase inside of peroxisomes, instead the employed technique only led to a massive staining of the cytoplasm of AECII (Farioli-Vecchioli et al., 2001). Due to the facts that a) in some animal species catalase may be a genuine multi-compartmental enzyme (for a review see: Fahimi et al., 1996) and b) in aging as well as under pathological conditions catalase import into peroxisomes is impaired in mice with mislocalization of the enzyme to the cytoplasm (for reviews see: Baumgart et al. 2003; Terlecky et al. 2006) optimal and sensitive methods for the appropriate subcellular localization of the enzymes are essential. In a previous study by our group, we noticed that only with the best pre-treatment conditions, small peroxisomes – formerly called microperoxisomes – could be visualized as individual organelles in paraffin sections (Grabenbauer et al., 2001). By using an adapted version of this protocol for lung tissue we were able to achieve optimal staining for catalase with the ABC-peroxidase method in a punctuate staining pattern in AECII and Clara cells in mouse lungs, indicative for peroxisomes. The higher diffusion-reaction of the Novared substrate in the cytoplasm of human samples labeled for

catalase might be related to the facts that a) longer staining times had to be applied for the peroxidase-reactions and b) the tissue was obtained from non-transplanted parts of organs which had remained several hours in the “conservation buffer solution” prior to immersion fixation. Indeed, cytoplasmic diffusion of catalase due to destruction of the peroxisomal membrane was described on the ultrastructural level even in glutaraldehyde-fixed tissue samples after storage for several hours in buffer solutions (Fahimi, 1974). The peroxisomal membrane alterations in these preparations were most probably induced by the action of 15-lipoxygenase, since destruction of the peroxisomal membrane was prevented by addition of corresponding enzyme inhibitors (Yokota et al., 2001). In our study, the ‘cytoplasmic diffusion’ problems as observed in light microscopic immunohistochemistry could be circumvented by subjecting paraffin sections of human lung tissue to an immunofluorescence technique for catalase localization, suggesting that the longer incubation time for the localization of catalase in the peroxidase-based immunohistochemical reaction was the main reason for the cytoplasmic diffusion artifacts. In addition, with the immunofluorescence technique higher sensitivity was observed to reveal smaller particles, enabling visualization of peroxisomes with lower levels of catalase also in ciliated and goblet cells of the conducting airway epithelia as well as alveolar macrophages, AECI cells and endothelial cells or fibroblasts in the alveolar region corroborating our ultrastructural results in mouse lung.

6.2 Peroxisomes can be best visualized in mouse or human lungs at the light-microscopical level with Pex14p as marker

The best marker for peroxisomes at the light microscopic level was Pex14p, which stained peroxisomes in a uniform and ubiquitous way in all cell types of mouse and human lung samples. Comparable results with this peroxisomal marker protein have been obtained in other tissues, in which catalase-less peroxisomes are present, such as many neurons in the central nervous system and germ cells in the testis (Ahlemeyer et al., 2007; Nenicu et al., 2007). The ubiquitous expression of Pex14p is logical, since this protein is located in the docking complex for peroxisomal matrix protein import, which should be present in all functional peroxisomes (Eckert and Erdmann, 2003). In addition to their well-known localization in AECII and Clara cells, stainings for Pex14p in the present study revealed the relative richness of alveolar macrophages with peroxisomes. Peroxisomal ROS and lipid-metabolism could play an important role in

macrophages, since this cell type is activated by ROS and they secrete lipid mediators, such as leukotrienes and prostaglandins. In addition, alveolar macrophages are the major source of NO formation by iNOS in the lung. In this context it is of interest that iNOS was localized recently to peroxisomes (at least in hepatocytes) (Loughran et al., 2005; Stolz et al., 2002). The exact role of peroxisomal iNOS is not understood, but it was shown that NO has an effect on the regulation of peroxisomal enzymes (Kremser et al., 1995).

Double immunofluorescence stainings for Pex14p and ABCD3 revealed that peroxisomes in mouse AECII cells are densely packed, tubular organelles, forming network-like arrangements. Complete tubular organelles (sometimes up to 8 μm in length) are much less frequently found due to statistical reasons within the plane of an 80 nm-thick ultrathin section in comparison to 3-5 μm thick paraffin section. Therefore, peroxisomes appear at the ultrastructural level in mouse AECII mostly as multiple segments with varying shape (round, oval to rod-shaped) cut through the same or neighbouring organelles. The large aggregates in fluorescence micrographs of AECII of human lungs can be explained by the occurrence of groups of clustered peroxisomes in human AECII (see Fig. 1a in Moriguchi et al. 1984).

6.3 Peroxisomal β -oxidation enzymes are ubiquitously expressed in distinct cell types of mouse and human lungs

Peroxisomal β -oxidation enzymes in the lung have not yet been characterized. In an older study with pig lungs Goldenberg and colleagues were not able to show functional β -oxidation by biochemical activity measurements (Goldenberg et al., 1978). In contrast, in our study acyl-CoA oxidase 1 (ACOX1) as well as 3-keto-oxo-acyl-CoA thiolase (thiolase), the first and the third enzymes of the β -oxidation pathway 1, could be identified in Western blots by their specific protein bands in the correct molecular weight range in enriched peroxisomal fractions of mouse and human lungs. These biochemical data were corroborated by the ubiquitous labelling of peroxisomes in all pulmonary cell types with the specific antibodies against both enzymes in immunofluorescence preparations. Whereas ACOX1 was more homogeneously expressed in peroxisomes of all pulmonary cell types in murine and human lungs, the peroxisomal thiolase was slightly enriched in peroxisomes of AECII. The weak labelling of the thiolase on human paraffin sections was corroborated by the low protein content in enriched peroxisomal fractions in

Western blot analysis of lung tissue of the same donor. In addition, these results are supported by the 2.2-fold lower number of “expressed sequence target” sequences (ESTs) of the peroxisomal thiolase obtained by data base mining at <http://www.ncbi.nlm.nih.gov/UniGene> with the “EST Profile Viewer” of the UniGene program. We found 251/1x10⁶ ESTs for peroxisomal thiolase in mouse versus 115/ 1x10⁶ in human lung cDNA libraries. In contrast for ACOX1 this value was 100/1x10⁶ ESTs in mouse versus 121/1x10⁶ ESTs in human cDNA libraries and in our study this enzyme could also be adequately stained in the human lung. With the help of the “EST Viewer program” also EST-sequences for all enzymes of the second β -oxidation pathway (ACOX2 and 3, MFP2 and the SCPX-thiolase) were found in mouse and human lung, suggesting also the presence of the complete pathway 2 in peroxisomes of the lung. Additional evidence from our study for active lipid metabolism in lung peroxisomes was obtained by the localization of ABCD3 (formerly called PMP70) in these organelles, which is an ABC-transporter involved in the transport of lipid substrates across the peroxisomal membrane (Visser et al., 2007). In addition, high levels of the non-specific lipid-transfer protein/sterol carrier protein 2 (SCP2) were described in the matrix of lung peroxisomes (Ossendorp et al., 1994). The SCP2 protein is involved in the shuttle of lipid intermediates within the multi-enzyme complex of the peroxisomal β -oxidation system (Wouters et al., 1998).

6.4 Possible functions of peroxisomal β -oxidation in the lung - Connection to PPAR regulation

Peroxisomal β -oxidation has much broader substrate specificity than mitochondrial β -oxidation and is able to degrade a variety of insoluble, toxic and bioactive lipids, regulating inflammatory processes (prostaglandins and leukotrienes), signalling from the plasma membrane (e.g. arachidonic acid) or acting as lipid ligands for nuclear receptors (Mannaerts and Van Veldhoven, 1993). Therefore, peroxisomal β -oxidation in the lung might be integrated in a variety of metabolic processes and regulatory circuits.

The transcriptional activation of the genes of the peroxisomal β -oxidation enzymes of pathway 1 is activated by PPAR/RXR heterodimers (Dreyer et al., 1992; Krey et al., 1995) and LXR alpha (Hu et al., 2005). These receptors are activated by eicosanoid derivatives or fatty acids, retinoids or pristanic acid and oxysterol derivatives, which are all metabolized by peroxisomal β -oxidation

enzymes. Therefore, the induction of the peroxisomal β -oxidation enzymes by distinct nuclear receptors might work as a feed-back loop in the control of the homeostasis of nuclear receptor ligands for prevention of lipid toxicity in pulmonary cell types. Especially ACOX1 seems to be an important enzyme in this feed-back loop, since it conducts the rate-limiting step of the β -oxidation chain and its absence leads to steatohepatitis and tumorigenesis in the liver (Fan et al., 1998). Interestingly, both PPAR α and PPAR γ were described in the lung (Braissant and Wahli, 1998). Activation of either one of the two receptors in the lung seems to protect lung tissue against pathologic inflammatory and fibrotic processes (Lakatos et al., 2007). In addition, an involvement of PPAR γ in normal lung maturation has been described recently in a study with pulmonary airway epithelium-specific PPAR γ -knockout mice (Simon et al., 2006a).

6.5 Peroxisomal β -oxidation may provide acetyl-CoA units for biosynthetic pathways in peroxisomes, such as PUFA-, plasmalogen- and cholesterol synthesis

In addition to the regulation of lipid ligands for nuclear receptors, the β -oxidation enzymes in peroxisomes of AECII, AECl and alveolar macrophages are certainly involved in the modification and recycling of surfactant lipids. This is probably not only exerted by the simple β -oxidation and degradation of “used and non-functional” surfactant lipid components. Peroxisomal β -oxidation enzymes can also be used for the modification and synthesis of polyunsaturated fatty acids (Hiltunen et al., 1996), which are important components of surfactant and protect against oxygen toxicity (Sosenko et al., 1991; Zoeller et al., 1999).

In addition, peroxisomal β -oxidation is also capable of providing acetyl-CoA units for the synthesis of plasmalogens or cholesterol in these organelles (Hayashi and Takahata, 1991). Interestingly, the enzymes for different steps of these biosynthetic pathways are localized in distinct subcellular compartments: the endoplasmic reticulum, mitochondria and peroxisomes. This might explain the close ultrastructural association of peroxisomes with these organelles or with the surface of lamellar bodies, observed in AECII for facilitating the modification and shuttle of lipid intermediates between the different subcellular compartments. High activity of the dihydroxyacetone phosphate acyl-transferase (DHAPAT now named Gnpat), the first enzyme in

peroxisomal ether lipid synthesis has been described in lung homogenates with values even higher than in liver (Van Veldhoven and Mannaerts, 1985). In addition to ether lipid synthesis, the peroxisomal enzymes of this pathway might in addition also contribute up to 40-50 % to the synthesis of other glycerolipids via the acyl-DHAP pathway, also components of surfactant lipids. Plasmalogens and cholesterol are important minor lipid components of surfactant, regulating its viscosity and function on surface tension (Rüdiger et al., 1998; Tölle et al., 2002) but are also involved intracellularly in important signal transduction pathways and vesicle fusion (for a review, see (Brites et al., 2004)). Plasmalogens and cholesterol serve different functions in surfactant. Plasmalogens promote the formation of hexagonal lipid structures and are able to regulate the movement of lipids during the breathing cycle into and out of the surface layer of surfactant, whereas non-bilayer structures formed by cholesterol stabilize the surface layer of surfactant and interact with the surfactant protein B (SP-B) for fine tuning of lipid-mediated surface properties (Tölle et al., 2002). Interestingly, PPAR γ regulates SP-B synthesis (Yang et al., 2003). Peroxisomal β -oxidation might therefore interfere in two different ways in the synthesis, modification and recycling of surfactant lipids: a) by its coupling to the “biosynthetic pathways” in peroxisomes and b) by regulating of PPAR-ligands. Indeed, it is known from the literature that alterations of the peroxisomal compartment by treatment with hypolipidemic agents such as clofibrate or nafenopin, which both inhibit HMG-CoA reductase for cholesterol synthesis and activate PPAR α , exert significant alterations in lamellar bodies of AECII and in surfactant morphology and amount in the alveoli as well as induce “foamy” macrophages (Fringes et al., 1988; Fringes and Reith, 1988). In this respect, it is interesting to note that in our study we have found that especially alveolar macrophages in human lung tissue contained a high number of peroxisomes, which were strongly labeled for Pex14p and contained similar high levels of ACOX1 and ABCD3 as AECII.

6.6 Coupling of lipid and ROS metabolism

In our study we found that peroxisomes in Clara cells and AECII of mouse lungs contained the highest levels of catalase and peroxisomal thiolase. The significance of catalase in the protection of the normal function of peroxisomal β -oxidation was noted in studies from Hashimoto and Hayashi, who demonstrated the inhibition of peroxisomal thiolase by high H₂O₂ levels and showed that NADH can be directly oxidized by acetoacetyl-CoA and H₂O₂ (Hashimoto and Hayashi, 1987, 1990). Therefore, the function of peroxisomal β -oxidation is directly coupled to the function

of antioxidative enzymes. Contrarily, it has been shown that the well-known PPAR γ -activator 15-d-PGJ₂, a prostaglandin derivative degraded in peroxisomes, directly interferes with redox-sensitive transcription factor pathways independently of the action of PPAR γ (Kim and Surh, 2006). Interestingly, peroxisomes harbour a variety of antioxidative and pro-oxidative enzymes (Schrader and Fahimi, 2004) and contain a compartment-specific management of H₂O₂ (Fritz et al., 2007), which might lead to “metabolic signalling” from this organelles under metabolic stress conditions as suggested already earlier by Masters (Masters, 1996) and shown in plants (Nyathi and Baker, 2006).

6.7 Alterations of the peroxisomal compartment during transdifferentiation of AECII into AECl – Effects of the keratinocyte growth factor (KGF) on this process

The physiological maintenance of the lung alveolar epithelium is ensured by the stem cells of the alveolus, the cuboidal corner cells, also called great alveolar cells or AECII. AECII are surrounded by AECl cells, which are derived from the AECII stem cells (Adamson and Bowden, 1974; Evans et al., 1975; Evans et al., 1976; Hirai et al., 1983; Hirai et al., 1977). Maintenance and differentiation of AECII is affected by different soluble and insoluble macromolecules present in the extracellular matrix, such as growth factors that are released in the course of the injury of the alveolar epithelium and the exposure of the underlying connective tissue (Boudreau and Bissell, 1998; Lukashev and Werb, 1998; Lwebuga-Mukasa, 1991; Rannels and Rannels, 1989). Growth factors as well as other components of the extracellular matrix tend to change in response to injury and are required for cell growth and differentiation as well induce cell division, migration and re-epithelization during repair of the injured lung (Roman, 1996; Yano et al., 1996). Released KGF acts as a potential mitogen for AECII and has been shown to maintain AECII in culture in a differentiated phenotype (Abraham et al., 1999; Borok et al., 1998b; Rice et al., 2002). In addition, this growth factor promotes AECII proliferation in vitro (Panos et al., 1993) and in vivo (Ulich et al., 1994).

In the present study, the alterations of the peroxisomal compartment during the transdifferentiation of AECII into AECl over a period of seven days were investigated in primary cell cultures and the effects of KGF on peroxisomes and dependent gene expression were studied

in comparison to the AECII/AECI phenotypes. The AECII to AECI transition was verified by RT-PCR analyses of specific expressions of mRNAs for AECII and AECI marker proteins and by IF with an antibody against pro SP-C, a selective AECII marker protein. Indeed, in primary AECII cultures KGF administration over a period of seven days maintained the AECII phenotype (as shown by strong IF staining for pro SP-C, see Fig. 13) and conserved the typical structural pattern and high numerical abundance of peroxisomes with high catalase protein content (as shown by IF for catalase, see Fig. 13) and strong expression of “peroxisomal mRNAs”. In contrast, in AECII cultures without KGF-supplementation the peroxisomal compartment underwent significant alterations during AECII to AECI transition. A severe downregulation of mRNAs for catalase and peroxisomal enzymes for ether lipid synthesis occurred during parallel to the AECII to AECI transdifferentiation process. In parallel, a loss of the mRNA for pro SP-C and an increase for the one for caveolin 1 was noted, which was suggested to be a robust indicator of a “real” transdifferentiation of AECII into AECI (Fuchs et al., 2003; Qiao et al., 2003). In seven day old cultures without KGF-supplementation the transdifferentiated AECI contained much lower numerical peroxisome abundance with low catalase protein levels. They exhibited downregulated mRNAs for catalase and Gnpat but showed still high expression levels of mRNAs for peroxisomal β -oxidation enzymes (ACOX1) and of the peroxisomal biogenesis protein Pex14p, a typical feature of AECI in situ in the mature mouse lung (Karnati and Baumgart-Vogt, 2008).

The only experimental evidence in the literature for alterations of the peroxisomal compartment during AECII to AECI transdifferentiation was provided in an ultrastructural study by Hirai and colleagues (1983) in rats after lung injury with butylated hydroxytoluene (BHT). They observed a lower numerical abundance of peroxisomes with lower catalase content in regenerating alveolar cells 7 days after BHT treatment (Hirai et al., 1983). The results of this dissertation are in complete agreement with their speculation that the peroxisomal compartment is downregulated during AECII to AECI transition.

6.8 Which signalling mechanisms could be triggered by KGF administration?

KGF initiates a cascade of signalling pathways upon administration to AECII cultures and various other experimental model systems (Qiao et al., 2008). Previous reports suggest that KGF interacts

with a specific receptor, the FGF receptor IIIb (FGFIIIb) a tyrosine kinase receptor (RTK) to initiate the cascade of signalling events. KGF signalling induces rapid changes in the phosphorylation state of secondary signalling proteins and activates a variety of transcriptional factors (Nrf2; SREBP1C; C/EBP), regulating antioxidative and lipogenic enzymes in the lung (Braun et al., 2002; Chang et al., 2005; Portnoy et al., 2004).

6.9 KGF and Nrf2-signalling in the protection against ROS-mediated oxidative lung injury

Exogenous application of recombinant KGF protects the lung from various forms of injury, including acid instillation (Yano et al., 1996), α -naphthylthiourea (Mason et al., 1996), hyperoxia (Guo et al., 1998), bleomycin (Deterding et al., 1997; Yi et al., 1998; Yi et al., 1996) and γ -irradiation (Yi et al., 1996). In all of these models, increased ROS levels are inducing AECI damage and lung injury. In addition to exogenous noxes, many pulmonary diseases are associated with increased oxidative stress. Crucial cellular components such as DNA, lipids and proteins are greatly affected by ROS. ROS induced lung injury leads to DNA strand breaks, lipid peroxidation and oxidative modification of proteins. KGF might protect the alveolar epithelium against oxidative injury by several different mechanisms: a) KGF may exert its protective effect by proliferation of AECII that could maintain an intact epithelial surface (Panos et al., 1995; Panos et al., 1993); b) KGF augments the expression of surfactant apoproteins in AECII that regulate surfactant functions (Sugahara et al., 1995); c) KGF may limit oxidant induced increases in lung epithelial cell permeability by protein kinase C (PKC) dependent mechanism (Waters et al., 1997); d) KGF reduces oxidant-induced DNA damage by promoting DNA repair (Takeoka et al., 1997); e) KGF reduces the oxidative injury by triggering the transcription of the Nrf2 gene, encoding a transcription factor, regulating genes of antioxidative enzymes (Braun et al., 2002).

Nrf2 is a member of the cap 'n' collar family of transcription factors (Moi et al., 1994) and binds to cis-acting elements (antioxidant response elements ARE) of the promoter region of target genes (Rushmore et al., 1991). These target genes encode a series of antioxidative proteins, such as glutathione S-transferase (Rushmore et al., 1990), hemoxygenase 1 (Prester et al., 1995). In addition, the catalase and superoxide dismutase 1 genes are regulated by Nrf2, both encoding peroxisomal enzymes (Chan and Kan, 1999). The results of this dissertation suggest that KGF-

mediated signal transduction may be protective against ROS-mediated lung injury by stimulating - in addition to the strong AECII proliferation- the induction of higher levels of peroxisomal catalase and enzymes of ether lipid synthesis (see Fig. 17, p. 63). Indeed, catalase is “the” enzyme with the highest capacity to degrade H₂O₂. In addition, plasmalogens as well as poly-unsaturated fatty acids (PUFAs), both synthesized in peroxisomes, are important antioxidant lipids, trapping various ROS species. Furthermore, the increased catalase might also protect the peroxisomal β -oxidation system against ROS-mediated inhibition of the 3-keto-acyl-CoA thiolase (Hayashi and Takahata, 1991). A possible explanation for the downregulation of catalase and ether lipid synthesizing enzymes during the transdifferentiation in the absence of KGF could be due to a downregulation of Nrf2. However, the underlying mechanism has to be proven in future studies.

6.10 Interference of KGF-mediated signalling with pulmonary lipid metabolism

As mentioned above (chapter 6.8), KGF induces activation of several transcription factors involved in the regulation of lipogenesis. Two classes of transcriptional factors mainly regulate lipogenesis in AECII: a) sterol response element binding protein (SREBP) family members, b) CCAAT/enhancer binding protein (C/EBP) family members and c) PPAR γ (Fajas et al., 1998; Rosen et al., 2000). Lipogenesis is a very important process for the synthesis of pulmonary surfactant, which has two important functions: a) it reduces the surface tension at the air-liquid interface of the lung and b) it plays a role in host defense against infection and inflammation. Pulmonary surfactant is composed of 90% lipids and 10% surfactant proteins. About 80 to 90% of surfactant lipid is represented by phospholipids. Cholesterol is one of the major neutral lipids in surfactant. Indeed, cholesterol is considered to be an important lipid for surfactant function, especially after compression.

Interestingly, AECII peroxisomes contain high amounts of sterol carrier protein-2 (SCP2) that stimulates the biosynthesis of both dolichol and cholesterol (Ossendorp et al., 1994). In vitro studies also confirmed the involvement of the SCP2 in cholesterol synthesis (Kesav et al., 1992; Ossendorp and Wirtz, 1993). SCP2 in AECII is thought to transfer surfactant lipids between the endoplasmic reticulum and lamellar bodies. In peroxisomes, SCP2 might be involved in the transfer of lipid intermediates between the different β -oxidation enzymes. In addition to SCP2, all

Discussion

enzymes synthesizing isoprenoids, which are cholesterol precursors from acetoacetyl-CoA to farnesyl pyrophosphate, are located in peroxisomes (Kovacs et al., 2007; Krisans, 1996). These enzymes are: HMG-CoA synthase, HMG-CoA reductase, mevalonate kinase, phosphomevalonate kinase, mevalonate diphosphate decarboxylase, isopentyl pyrophosphate isomerase and farnesyl pyrophosphate synthase (Kovacs et al., 2004; Kovacs et al., 2007; Krisans, 1996). In a recent study with ChIP-Chip technology, Reed and colleagues showed that the promoters of the corresponding genes of all of these peroxisomal proteins bind SREBP-1 transcription factors (Reed et al., 2008).

Sterol regulatory element-binding proteins (SREBPs) are a family of transcription factors consisting of SREBP1a, SREBP1c, and SREBP2 responsible for the activation of more than 30 genes involved in the synthesis and metabolism of cholesterol, fatty acids, triglyceride metabolism and phospholipids (Horton et al., 2002a, b; Reed et al., 2008). SREBP1 and SREBP2 have overlapping binding properties to sterol responsive elements or regular E-boxes in the promoters of dependent genes. SREBP2 regulates mainly genes of cholesterol metabolism whereas, SREBP-1C mainly activates genes involved in fatty acid and triglyceride metabolism (Shimano, 2009). KGF stimulates SREBP1c, which is a key transcriptional factor for regulation of fatty acid and phospholipid synthesis in AECII (Chang et al., 2006; Chelly et al., 1999).

Peroxisomes harbour the necessary enzymes for the DHAP-pathway in glycerophospholipids and ether-phospholipids (plasmalogen) synthesis. Glycerophospholipids are major components of the surfactant, whereas plasmalogens are less abundant but are functionally very important (see discussion p. 88). Peroxisomal glycerolipid synthesis may contribute up to 40% of the total glycerolipids (Hajra et al., 1979; Hajra et al., 2000). In this dissertation, we noted that KGF indeed increased the mRNA level of Gnpat, an important enzyme in peroxisomal glycerolipid and ether lipid synthesis. AECII convert fatty acids into phospholipids through C/EBP α -and SREBP-mediated pathways, which are both induced by KGF-treatment. Gene profiling studies with microarray technology suggest that, the PPAR γ mRNA is not altered by KGF-treatment, in basal medium in rat AECII cultures. These results corroborate the unaltered mRNA expression for ACOXI, an enzyme involved in peroxisomal β -oxidation, the genes of which are generally regulated by PPAR family members.

6.11 Role of KGF and PPARs in lung maturation (differentiation)

Interactions between mesenchymal and epithelial components are essential for regulating regular organ morphogenesis and differentiation in the lung (Chelly et al., 1999). Several growth factors and intracellular signalling molecules work together in an orchestrated action in lung development. Whereas aFGF and FGF-10 seem to play an important role in early branching morphogenesis, KGF and PPAR γ are both stimulators of final differentiation of epithelial cell types, such as AECII or bronchiolar epithelial cells (Chelly et al., 1999; Michael et al., 1997; Simon et al., 2006b). Interestingly, the mesenchymal components aFGF, FGF-10 and KGF bind to the same receptor on the alveolar cells, the KGF-receptor or FGF-R2IIIb, but apparently signal at different time points during lung development. In the late fetal period, KGF secretion by pulmonary fibroblasts leads to a strong signal in AECII, promoting the synthesis of important surfactant components (surfactant proteins as well as phospholipid components) at the time of surfactant accumulation in AECII shortly before birth (Chelly et al., 1999). Furthermore, KGF seems to exert a more sustained action at the same molar concentrations on the alveolar epithelial cells than EGF, another factor influencing AECII development, wherefore it is thought to control AECII differentiation rather than lung morphogenesis. Increased mRNA levels of KGF and the KGF-R (FGF-R2IIIb) were noted in the perinatal period (Dekowski and Snyder, 1995; Shiratori et al., 1996). Interestingly, also in this period the mRNAs for various peroxisomal enzymes that are involved in the synthesis of surfactant lipids (GNPAT, AGPS), involved in the biogenesis and proliferation of peroxisomes (PEX5, PEX13, PEX14 and PEX11 β) and lipid transporters (ABCD3, Scp2/ScpX) as well as β -oxidation enzymes (ACOX1 and MFP2) are already highly expressed in the newborn lungs. Since total RNA from lung homogenates has been used in this study, future in situ hybridization or specific microdissection experiments are necessary to clarify in which cell types these mRNAs are expressed (e.g. AECII versus Clara cells).

In addition to KGF signalling, signal transduction via PPAR γ 1, a nuclear receptor present in high amounts in Clara cells and AECII (Simon et al 2006) might control epithelial differentiation and lipid metabolism in response to cAMP stimulation (Michael et al., 1997). Michael and colleagues suggested that PPAR γ 1, an important transcription factor for adipocyte differentiation, could have similar effects in AECII. In addition, PPAR γ 1 responds to insulin-signalling, cAMP and fatty acids, promoting adipogenesis (triglyceride storage) (Michael et al., 1997). Even though, PPAR γ 1

mRNA expression was detectable in isolated fetal AECII (human and rabbit), the PPAR γ protein could only be visualized in paraffin sections of newborn lungs with weak immunoreactivity in conducting airway epithelia (Simon et al 2006). Interestingly, also the PEX11 β mRNA showed the strongest expression in distal airway epithelia in newborn mouse lungs (Karnati and Baumgart-Vogt 2009). Peroxisomes were more generally abundant in different cell types of the distal airways and in the undifferentiated alveolar regions as compared with adult lungs (Karnati and Baumgart-Vogt 2009). In addition, peroxisomes in most cells of the yet undifferentiated alveolar region showed strong staining for catalase, most probably labelling AECII in the early phase in the process of their transdifferentiation into AECI. In contrast to E18.5 lungs, peroxisomes were mainly present in high abundance in Clara cells and AECII in the adult mouse lungs and were more prominently stained for catalase than any other cell type (Karnati and Baumgart-Vogt, 2008, 2009). This pattern is completely in accordance with the PPAR γ distribution in the adult lung (Simon et al 2006) with highest staining of PPAR γ in Clara cells and AECII. In addition, Simon and colleagues revealed that airway-specific PPAR γ knockout mice exhibited a significant enlargement of the smaller airways and lower expression of mRNAs for elastic and collagen fiber components, suggesting the importance of PPAR γ signalling in mesenchymal-derived cell types, such as fibroblasts (Simon et al 2006). The microarray analysis with total lung RNA of the Clara cell-specific PPAR γ knockout animals suggested that PPAR γ is an important regulator of the differentiation of airway epithelia and Clara cell lipid metabolism. Interestingly, in the absence of PPAR γ the PEX7 mRNA is strongly upregulated, a gene encoding for the cytoplasmic PTS2-receptor protein, involved in PTS-2 dependent peroxisomal matrix protein import.

6.12 Technical pitfalls influencing the comparative analysis of lung tissue immunofluorescence preparations of wild type and PEX11 β KO mice.

If the antibodies are used in higher concentrations (saturated range) for detection of a certain antigens, slight differences in antigen abundance between wild type and knockout animals might be overlooked due to saturation of the fluorescent intensity and “equalization” of signals in morphological specimens. Careful comparative examinations revealed that both antibody concentrations and CLSM settings for image acquisition influenced the comparison of relative alterations of marker proteins between wild type and knockout animals. E.g. at standard concentrations (1:1000) no differences in the abundance of pro SP-C were noted due to over-

saturation of the antibody staining. However, serial dilutions (up to 1:128.000) revealed significant differences in the protein amounts of pro SP-C between wild type and PEX11 β KO animals. Similar problems were observed by using CLSM-settings leading to “oversaturation of images only when” the correct CLSM settings were used, differences between the experimental groups were obvious. Therefore, for each antibody ad IF-preparation, correct Ab-dilutions and CLSM settings were carefully selected to prevent false-negative interpretation of the data.

6.13 Pathological consequences of PEX11 β deficiency in the lung with special emphasis on alterations in Clara cells

The half life of peroxisomes is only 3 days, wherefore these organelles are constantly formed or replaced by newly built peroxisomes, a process which is termed “peroxisomal biogenesis”. Peroxisomes are replicated by fission of preexisting ones, regulated by proteins of the Pex11 family and DLP1/VpS1p (Delille et al., 2009). Most information provided for PEX11 β in the international literature concerns its involvement in the steady state regulation of peroxisomal numerical abundance, however, until now no knowledge is available on the molecular consequences of a PEX11 β deficiency in the lung. Our own studies on the localization of the PEX11 β mRNA in the newborn, using nonradioactive cRNA-hybridization, revealed that the PEX11 β mRNA is expressed in the lung at higher levels than in the liver. In the newborn lung the strongest expression of the PEX11 β mRNA was observed in the distal epithelium of the conducting airways (Karnati and Baumgart-Vogt 2009). Similarly to the distribution of the PEX11 β mRNA, peroxisomes were highly abundant in Clara cells in immunohistochemical preparations using distinct marker antibodies. Clara cell peroxisomes contain high levels of catalase, β -oxidation enzymes and metabolic transporters wherefore we first mainly focused on the alterations of this cell type to understand the pathological consequences induced by the PEX11 β deficiency and therewith the role of peroxisomes in Clara cells.

6.13.1 Significant alterations of secretory proteins in Clara cells of PEX11 β KO animals

Based upon morphology and histochemistry, Clara cells, the nonciliated cells of bronchioli, were first described by Kölliker (Kölliker, 1881) and characterized comprehensively by Clara (Clara, 1937). Clara cells are nonmucous, nonserous, nonciliated, and columnar to cuboidal secretory

Discussion

cells with a club-shaped cytoplasmic projection. Appearance and distribution of Clara cells along the airways is different among various distinct species. They are generally observed in the lining of the bronchiolar epithelium of pulmonary airways and make up ca. 80% of the bronchiolar epithelium in mice (Plopper et al., 1983). Clara cells secrete mainly the Clara cell 10 KDa (CC10) protein and three members of the surfactant protein family, namely SP-(A, B, D). Eventhough, extensive morphological and transgenic studies on Clara cells were performed in previous years, to date their functional role is still not completely understood. On the one hand, cell culture studies with isolated Clara cells showed that implantation of these cells in the denuded trachea restored the alveolar epithelium, which led to the suggestion that Clara cells may serve as progenitor cells for the respiratory epithelium in injured lungs (Brody et al., 1987). On the other hand, Khoor and coworkers revealed an important role of Clara cells in the development and maturation of the airway epithelium (Khour et al., 1996).

During the last 15 years several studies were performed to discover the functions of the major secretion product CC10. Interestingly, lipids such as phosphatidylcholine and phosphatidylinositol were described in fractions of purified human CC10 protein, prepared for X-ray diffraction studies (Umland et al., 1994). Indeed, CC10 binds phosphatidylcholine and thus reduces the activity of phospholipase A2 by binding to this substrate. In addition, observations from Mantile and colleagues suggested a functional role of CC10 in the modulation of inflammatory reactions (Mantile et al., 1993). Indeed, Clara cell alterations are associated with a variety of human chronic lung diseases, such as asthma and chronic obstructive pulmonary disease (COPD) (Bernard et al., 1992; Jorens et al., 1995; Shijubo et al., 1999; Van Vyve et al., 1995). Interestingly, tobacco smoke induces decreased levels of CC10 in serum as well as a decrease of the CC10 protein also in Clara cells, suggesting that the level of the CC10 protein could act as a biomarker for Clara cell damage (Hermans et al., 1999). Furthermore, adult CC10 knockout mice showed an altered pulmonary response after exposure to hyperoxia and are very susceptible to hyperoxic lung injury (Johnston et al., 1997). In addition, experiments with CC10 knockout mice suggested that the CC10 deficiency resulted in alterations in the composition of the epithelial airway lining fluid (Stripp et al., 2002). Taken together, many published studies suggest that, CC10 is a biomarker of airway injury. In this dissertation, a significant decrease of the CC10 protein was observed in the lungs of PEX11 β knockout animals, which suggests that Clara cell functions might be strongly altered in PEX11 β deficient mice. The CC10 reduction might in consequence play an indirect role in the

Discussion

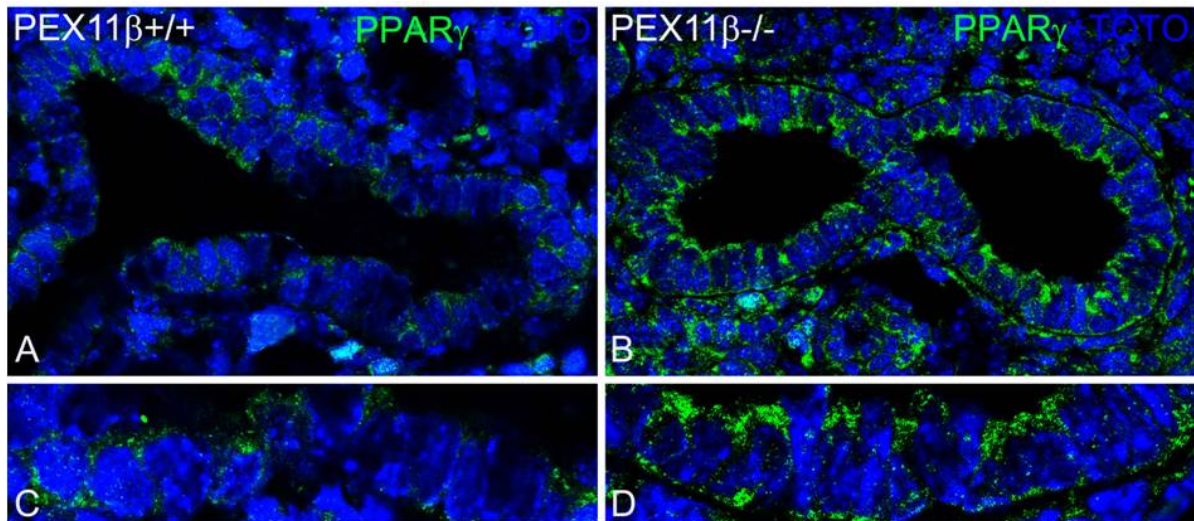
contribution to the molecular pathogenesis of lung alterations in mice with peroxisomal deficiency.

Similarly to the strong downregulation of CC10 in PEX11 β deficient mouse lungs, the Clara cell surfactant protein B (SP-B) was also drastically downregulated. Clara cell SP-B, an 8 kDa hydrophobic protein, is involved in enhancing the adsorption, spreading and stabilizing of phospholipids and the phospholipid monolayer on the bronchiolar epithelium (Cochrane and Revak, 1991; Possmayer, 1990). In addition, SP-B is also involved in alveolar maturation and facilitates the formation of lamellar bodies. In this respect, it is noteworthy that the alveolar maturation was delayed and AECII contained less well developed lamellar bodies in the lungs of PEX11 β animals (EM data from Prof. Baumgart-Vogt already obtained prior to this dissertation).

Despite the strong downregulation of CC10 and SP-B proteins, the Clara cells in PEX11 β knockout mice exhibit the classical club shaped projection and show the typical mature characteristics for this cell type. It is very unlikely that the developmental delay of the PEX11 β KO mice alone should produce alterations only in a subset of Clara cell secretory proteins. If this was the case, immature Clara cells in PEX11 β KO mice should in contrast not be able to produce any of their secretory proteins. However, opposit to CC10 and SP-B, SP-D was upregulated in Clara cells (see Results section, Fig. 25, P 76), suggesting that the observed alterations are not induced by a delay or general growth retardation phenomenon in PEX11 β KO animals. In contrast, this observation suggests that the secretory pathway in Clara cell is functional, but rather the production of some secretory proteins is negatively transcriptionally influenced. Since SP-D is functionally mainly involved in host defence and also mediates effects on the immune response in airways of the lung in an allergic asthma mouse model of ovalbumin-induced allergic airway inflammation (Hohlfeld et al., 2002; Kasper et al., 2002), the higher SP-D production in the Clara cells could contribute to an induction of inflammation in distal pulmonary airways in PEX11 β KO mice (Fig. 25I-L, P. 76). However, due to the short life span of PEX11 β animals (they die only a few hours after birth), long term studies could not be performed to investigate this hypothesis.

6.13.2 PPAR-mediated signalling in the Clara cells of PEX11 β KO animals

Interestingly, the SP-B gene expression and homeostasis are regulated by neutral lipid metabolites and nuclear receptors of the PPARs-family in the lung. Yang and colleagues reported that PPAR γ and its ligands (15d-PGJ2) inhibit also the transcription of the SP-B gene in cell lines and whole lung explants (Yang et al., 2003). In addition, treatment of cultures of non-small lung cancer cells with the PPAR γ ligand 15d-PGJ2 induced a downregulation of the Clara cell lineage marker CC10, suggesting that PPAR γ also modulates the expression of the CC10 gene (Chang and Szabo, 2000). Indeed, the majority of Clara cells show a prominent immunostaining for PPAR γ in the mouse lung (Simon et al., 2006a). To evaluate the pathophysiological alterations in the airway epithelium due to PPAR γ deficiency, RNA of the lung of a Clara cell-specific PPAR γ KO

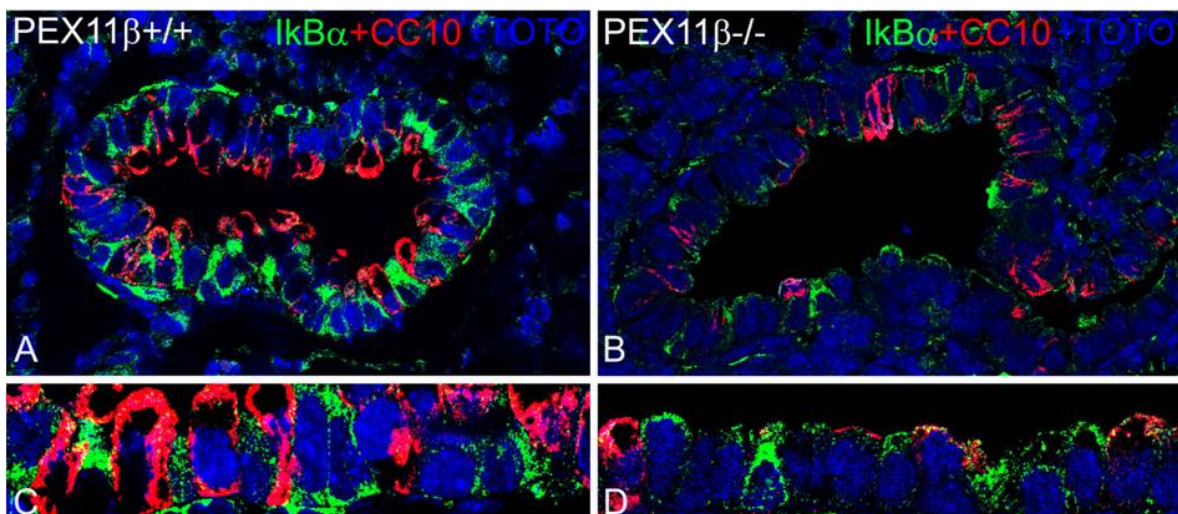


mouse was subjected to gene microarray analyses. Surprisingly, the PEX7 mRNA, encoding the peroxisomal targeting signal 2 (PTS2) receptor protein was drastically upregulated in PPAR γ KO mice. In the present study, PPAR γ was strongly upregulated (see above figure) and SP-B as well as CC10 was decreased, suggesting that the lack of peroxisome proliferation due to PEX11 β deficiency leads to a PPAR-mediated repression of the SP-B and CC10 genes. Furthermore, the broad functions of nuclear receptors of the PPAR family in the lung were further substantiated in a recent article, showing a novel transcriptional regulatory mechanism of the Wnt/ β -catenin pathway by cytoplasmic phospholipase A2 and PPAR β (Han et al., 2008). In PEX11 β deficient mouse lungs a severe upregulation of PPAR γ and PPAR β and a drastic downregulation of Wnt5a were observed. Since Wnt5a is involved in the distal morphogenesis of the lung epithelium, a direct link between the increased levels of PPARs and the downregulation of this Wnt-family

member in PEX11 β KO mouse lungs might exist. The strong downregulation of Wnt5a in PEX11 β animal might explain the strong delay in basal alveolarization observed in the lungs of PEX11 β KO animals.

6.13.3 Oxidant and antioxidant imbalance in the Clara cells of PEX11 β deficient mouse lungs

In addition to alterations of Clara cell secretory proteins, significant changes of pro- and antioxidant enzymes and an imbalance in ROS metabolism was observed in PEX11 β KO mouse lungs. A strong and reproducible increase of mitochondrial SOD2 expression in AECII and Clara cells in PEX11 β KO lungs was observed, suggesting an increase in oxidative stress. An increase in mitochondrial SOD2 was also described in other tissues in a knockout mouse model with defective peroxisome biogenesis (PEX5 knockout mice) (Baumgart et al., 2001). In these knockout animals, a defect in mitochondrial respiration has been demonstrated. Indeed, in many cases of mitochondrial respiratory complex defects (e.g. I + III), the loose coupling of the mitochondrial respiratory chain leads to significantly more superoxide radical release by mitochondria. In consequence, the SOD2 is upregulated to convert this radical into less toxic H₂O₂, which might be decomposed further by the mitochondrial glutathione peroxidase or peroxiredoxin I. Interestingly, SOD2 is upregulated by NF- κ B signalling (Rahman and MacNee, 1998). Indeed, the latest experiments during the writing of this thesis revealed a drastic downregulation of I κ B α in the Clara cells of the PEX11 β animals (see figure below). In wild type animals, I κ B α degradation leads to NF- κ B translocation into the nucleus and the activation of the transcription of antioxidant



(e.g. SOD2) and pro-inflammatory signalling (e.g. interleukins) genes. The strong downregulation of I κ B α in PEX11 β KO animals would suggest that, NF- κ B signalling might be chronically activated in PEX11 β animals. Future experiments should reveal the relevance of NF- κ B signalling and its cross-talk with PPAR regulatory pathways for the molecular pathogenesis of organ defects in PEX11 β deficiency and in peroxisomal diseases.

In contrast to mitochondrial SOD2, many other antioxidative enzymes of distinct subcellular compartments are downregulated in PEX11 β deficiency, such as SOD1, catalase and Prx 5, wherefore cytoplasmic H₂O₂ might accumulate and activate the NF- κ B signalling cascade. Proteins of the peroxiredoxin family degrade a variety of lipid hydroperoxides and H₂O₂ (Chae et al., 1994). In addition to the protective effect of the lung by their antioxidative properties, peroxiredoxins are also involved in the activation of signalling cascades and the transcription of various genes involved in the intracellular homeostasis (Kropotov et al., 2004). As shown in this thesis (see Fig. 22, P. 72), bronchiolar epithelial cells, AECII and macrophages express high amounts of peroxiredoxin V. The significant downregulation of most antioxidant enzymes (except for SOD2) in the cell types in PEX11 β deficient mouse lungs suggests an imbalance in antioxidative mechanisms, leading to oxidative injury of pulmonary epithelia. Furthermore, under normal conditions, H₂O₂ accumulation or treatment of different cell types with H₂O₂ also induces different peroxisomal biogenesis (PEX) genes in wild type cells. Instead, in PEX11 β animals, the mRNA for PEX11 α and PEX5 were downregulated and the one for PEX11 γ , PEX13 or PEX14 were not altered, suggesting that the nuclear transcriptional antioxidative response in PEX11 β knockout animals is disturbed.

In addition to antioxidant enzymes, the ratio of GSSH:GSH is important in cellular antioxidant defence and is a good indicator of the cellular redox state (Park et al., 1998). Glutathione peroxidase converts glutathione to its oxidized form during metabolization of H₂O₂ into H₂O. The reduction of the oxidized (disulphide) form of glutathione (GSSH) is catalyzed by glutathione reductase, which is a very important enzyme in the maintenance of GSH in its active reduced form. In the literature it has been reported that glutathione peroxidase plays an important role in the protection against lung oxidative injury. Interestingly, hyperoxia or pro-inflammatory mediators such as TNF α or LPS alter the cellular GSSH/GSH levels, leading to modulation and induction of various antioxidative enzymes, such as glutathione peroxidase and SOD2 (Cotgreave

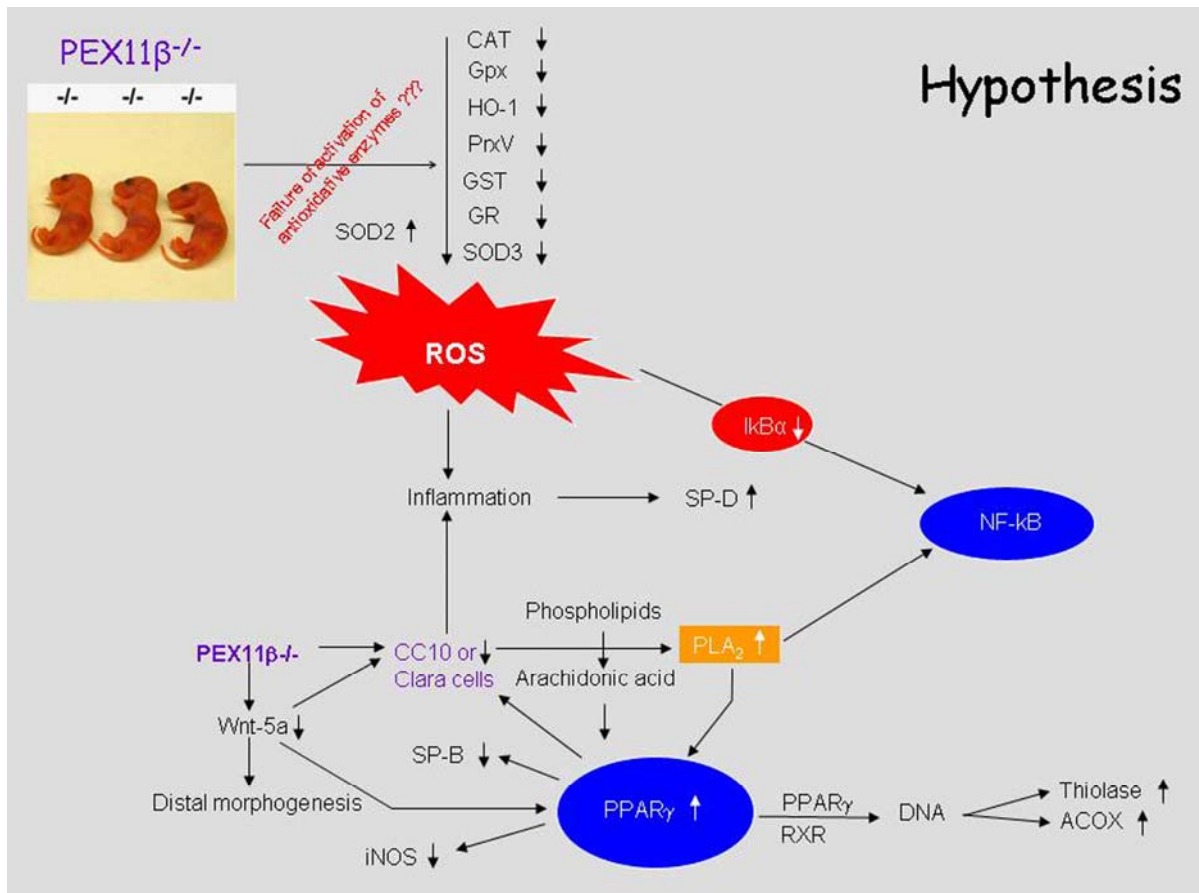
and Gerdes, 1998; Das et al., 2001). In the PEX11 β KO model, both glutathione peroxidase (at mRNA level) and glutathione reductase (at protein level) were drastically downregulated in Clara cells, possibly interfering with GSSG:GSH levels. Future experiments have to reveal if the redox state in Clara cells is altered in PEX11 β KO animals. Taken together, this study with PEX11 β KO animals revealed that normal peroxisomal functions are essential for ROS homeostasis and the antioxidant protection of the pulmonary airways.

6.13.4 Failure of iNOS regulation in the Clara cells of PEX11 β deficient mouse lungs

In wild type animals, ROS production, I κ B α degradation and NF- κ B signalling leads to the activation of iNOS (besides the increase of SOD2). The induction of this proinflammatory gene is one of the early reactions to inflammatory stimuli. Interestingly, the iNOS-upregulation seems to be compromised in PEX11 β KO animals by the strong increase of PPAR γ (see page 100 of discussion). Indeed, PPAR γ directly downregulates iNOS expression by binding to a PPAR responsive element in the iNOS promoter (Crosby et al., 2005). Experimental studies on the iNOS gene promoter showed that C/EBP β and NF- κ B modulates its transcription (Sakitani et al., 1998). The intensive cross-talk between these signalling pathways have to be elucidated in future studies with PEX11 β KO animals.

6.14 Hypothesis for the molecular pathogenesis of the pathological alterations due to PEX11 β deficiency

The results of this dissertation suggest that a drastic dysregulation of lipid signalling, antioxidative and proinflammatory pathways occur under conditions of pathologically reduced peroxisomal proliferation, such as in PEX11 β deficiency. Flooding of the limited number of peroxisomes with signalling lipids and an increased mitochondrial ROS production will lead to peroxidation products of poly-unsaturated fatty acids or eicosanoids, both strong inducers of PPAR γ . Due to the insufficient or missing peroxisomal feed-back-loop for the degradation PPAR γ -specific ligands, the strong and chronic PPAR γ -activation will interfere with the normal intracellular antioxidative and proinflammatory response by overriding the necessary NF- κ B activation in the promoters of corresponding genes, such as iNOS and HO-1, which might be necessary to activate the regular antioxidative response against inflammation.



The SP-B and CC10 gene repression by over activation of PPAR γ will lead to the further release of poly-unsaturated phospholipids via the activation of PLA $_2$, an enzyme that is generally inhibited by normal CC10 levels. In consequence, a vicious cycle will be induced, since the missing antioxidative response, resulting in higher ROS production will lead to further peroxidation of accumulating poly-unsaturated fatty acids or eicosanoids due to the missing peroxisomal proliferation response in the feed-back-loop in PEX11 β deficient animals. This will in consequence lead to more accumulation of PPAR γ ligands and the deeper entry into vicious cycle of dysregulated PPAR γ and NF- κ B pathways.

We therefore think that, peroxisomes are essential organelles in controlling the levels of metabolic signals in feed back loops between PPAR γ and NF- κ B pathways, involved in the activation of the antioxidative response and resolution of proinflammatory response. The results obtained in this study are the first description of the molecular consequences of a peroxisomal deficiency on the mouse lung. Future reporter gene studies investigating the biological involvement of PEX11 β deficient peroxisomes in arachidonic acid and eicosanoid metabolism as

well as PPAR activation in bronchiolar epithelial cells may provide new important information, concerning regulatory pathways in the pathogenesis of airway diseases. Taken together, our results suggest that PEX11 β and peroxisomes might indeed play an important role in airway homeostasis and eventually also in the molecular pathogenesis of chronic pulmonary lung diseases such as COPD or IPF in man. Future experiments have to prove the relevance of peroxisomal ROS metabolism in the protection against lung injury and chronic-inflammatory lung diseases.

6.15 Preliminary data on the alterations of peroxisomes in the alveolar epithelium in patients with idiopathic pulmonary fibrosis

Damage to the alveolar epithelium is thought to initiate fibrotic responses, however, the source of the initial epithelial injury is unknown. Since peroxisomes play an important role in protecting the lung epithelium against ROS and are involved in lipid and PPAR-ligand homeostasis, the characterization of the alterations of the peroxisomal compartment in IPF patients is necessary. After injury of the alveolar epithelium (AECI), growth factors (such as KGF) are released, that stimulate AECII to proliferate and to transdifferentiate into AECI. Alveolar lining cells in IPF indeed show an intermediate phenotype between AECII and AECI and contain an altered composition of intermediate filaments (Kasper and Haroske, 1996). As found in this study, peroxisomes in the alveolar lining epithelium in IPF patients are proliferated (see Pex14p staining, Fig. 28, p. 82) and contain a high amount of catalase. This effect might be mediated by the KGF release in the injured lung, which in turn leads to upregulation of catalase (see Fig. 28, p. 82).

Future analyses of IPF samples with antibody concentrations at unsaturated levels and double-IF analyses are necessary to reveal, whether macrophages and fibroblasts in IPF patients contain altered levels of peroxisomal enzymes. In addition, the exact characterization of the levels of β -oxidation enzymes (degrading eicosanoids) is necessary, since it is well known that LPS-treatment with subsequent TNF α -secretion from activated macrophages in the liver downregulates PPARs and the peroxisomal β -oxidation enzymes of pathway one. Since β -oxidation in AECII is coupled to glycerophospholipid, etherphospholipid and cholesterol synthesis, downregulated peroxisomal β -oxidation might influence the function of the AECII plasma membranes as well as functional properties of the surfactant film. Due to such lipid alterations, the alveolar lining cells could be

injured. Indeed, several studies indicate that induction of PPAR γ , a nuclear receptor regulating peroxisomal lipid metabolism is protective in IPF (Lakatos et al., 2007). In IPF patients TNF α is not only secreted from activated and proliferated macrophages, but also from AECII. Wherefore paracrine stimulated fibroblasts in underlying fibrotic areas might downregulate their peroxisomal compartment and might be activated to proliferate due to higher ROS production in their cytoplasm. This hypothesis might be tested easily in future experiments with isolated fibroblasts from IPF-patients. Those studies are already on the way in our department and are conducted by a master student under our (my and Prof. Baumgart-Vogt) supervision in the moment.

6.16 Conclusions and future perspectives

The results of this thesis are indicative for important protective functions of peroxisomes in lung epithelia (both bronchiolar and alveolar). Peroxisomes play a vital role in the regulation of the epithelial ROS levels and the intracellular lipid homeostasis. Thereby the variety of peroxisomal antioxidative enzymes and peroxisomal plasmalogens protect against oxidative stress in pulmonary epithelia. Peroxisomal β -oxidation might regulate the levels of eicosanoids, leukotrienes or prostaglandins, generally acting as signalling molecules of inflammation in various pulmonary disease models. Therefore, increased oxidative stress and accumulation of bioactive inflammatory lipid mediators due to a downregulation of peroxisomal β -oxidation may contribute to the pathogenesis of lung diseases, such as asthma, chronic obstructive pulmonary disease and idiopathic pulmonary fibrosis. Stimulation of peroxisomes and the use of drugs with positive influence on the peroxisomal metabolism are suggested as a new possibility for the development of treatment strategies in these diseases.

7 Summary

Only sparse information is available from the literature on the molecular consequences and pathological alterations of the peroxisomal compartment and its enzyme composition in mouse and human lungs. Neither were any studies performed on the molecular consequences of peroxisome deficiency on the lung in knockout mouse models nor on the alterations of the peroxisomal compartment in human lung diseases. Therefore, in this dissertation the peroxisomal compartment and its related gene expression were characterized in different cell types of mouse (C57Bl/6J) and human lungs, using a variety of light-, fluorescence- and electron microscopic as well as biochemical and molecular biological techniques. Furthermore, the molecular consequences and pathological alterations in the lung of PEX11 β knockout mice with deficient peroxisome proliferation were characterized and the changes of the peroxisomal compartment in epithelial cells in the lung of IPF patients described. In contrast to the literature, the results obtained in this dissertation reveal for the first time the presence of peroxisomes in all distinct cell types in the lung and describe significant differences in their cell type-specific numerical abundance, structure and enzyme composition. In this respect, Pex14p proved to be the marker of choice for identification of the whole peroxisomal population, independent of the specific cell type. In contrast, catalase, an enzyme used in many morphological studies to identify these organelles, was only present in high amounts in AECII and Clara cells. Furthermore, peroxisomes of the alveolar and bronchiolar epithelium, as well as alveolar macrophages were rich in the lipid transporter ABCD3 and β -oxidation enzymes, suggesting their involvement in the modification and recycling of surfactant lipids and in the control of pro-inflammatory lipid mediators and ligands for nuclear receptors of the PPAR family.

Prior to this dissertation, no information was available on the peroxisomal compartment during the transdifferentiation process of alveolar epithelial cells (AECII to AECl) and the effect of KGF on peroxisomal markers in this process. The results in this dissertation revealed that some peroxisomal proteins and corresponding mRNAs were tremendously downregulated during AECII transition in the absence of KGF, whereas KGF application conserved the AECII phenotype and led to an increase of catalase and ether lipid synthesizing enzymes. These results correspond to the significant differences observed in the peroxisomal compartment between AECII and AECl in situ

Summary

in lung sections. The results suggest that KGF might influence differentiation pathways in AECII, regulating peroxisome abundance and corresponding gene transcription. Additional results show that the peroxisomal numerical abundance is extremely high in AECII at birth, suggestive for a pivotal role of peroxisomal lipid metabolism during this period. Thereafter, with the concomitant increase of AECI number during alveolarization, the peroxisomal compartment is downregulated and is only prominent in AECII and alveolar macrophages in the mature adult lung.

Furthermore, the molecular consequences of peroxisomal deficiency for regular lung structure and function were analyzed by the use of a knockout mouse model with a peroxisomal biogenesis defect, in which peroxisomal proliferation is disrupted ($PEX11\beta^{-/-}$). These mice showed severe alterations in the abundance of ROS metabolizing enzymes and significant differences in cell type-specific markers, involved in different maturation or signal transduction pathways in the lung. With the help of $PEX11\beta^{-/-}$ mice, we could demonstrate that peroxisome deficiency influences lung morphogenesis and maturation, as indicated by severe alterations of the alveolarization process and the differences in the expression levels of mRNAs for components of signal transduction pathways, involved in distal morphogenesis (*Wnt5a*) and differentiation of individual lung cell types (PPARs). The severe alterations of antioxidant enzymes and pro-inflammatory proteins in $PEX11\beta^{-/-}$ lungs are suggestive for disturbed antioxidant and pro-inflammatory response in $PEX11\beta^{-/-}$ animals and suggest an essential role for peroxisomal metabolism in maintaining regular airway homeostasis.

Finally, preliminary results reveal alterations of the peroxisomal compartment in the lung tissue of patients with idiopathic pulmonary fibrosis (IPF), a devastating human lung disease. The exact role and the molecular consequences of these peroxisomal alterations in IPF, however, have to be investigated in future studies.

Taken together, the results of this dissertation suggest an important role of peroxisomes for regular lung development and adult lung homeostasis functions and indicate that this intracellular organelle compartment might be influenced as well in human lung diseases.

8 Zusammenfassung

Zu Beginn dieser Dissertation waren kaum Informationen zu Peroxisomen in der Lunge und deren Enzymzusammensetzung in der Literatur vorhanden. Weiterhin waren keinerlei Studien mit Knockoutmausmodellen zu den molekularen Auswirkungen einer Peroxisomedefizienz in der Lunge oder zu Veränderungen des peroxisomalen Kompartiments bei Lungenerkrankungen des Menschen ausgeführt worden. Deshalb wurden in dieser Dissertation das peroxisomale Kompartiment und die Expression dessen zugehöriger Gene in verschiedenen Zelltypen der Mauslunge (C57Bl/6J) und der humanen Lunge mit unterschiedlichen Licht-, Fluoreszenz- und elektronenmikroskopischen Techniken, sowie biochemischen und molekularbiologischen Methoden charakterisiert. Weiterhin wurden die durch Peroxisomenproliferationsdefekt ausgelösten pathologischen Veränderungen im Lungengewebe bei PEX11 β ^{-/-} Knockoutmäusen charakterisiert und erste Veränderungen des peroxisomalen Kompartiments bei Patienten mit IPF beschrieben.

Im Gegensatz zu früheren Arbeiten zeigen die Resultate dieser Dissertation zum ersten Mal, dass Peroxisomen in allen verschiedenen Zell-typen der Lunge vorkommen und beschreiben eindeutige Unterschiede in der zelltypspezifischen Organellenanzahl, deren Struktur und Enzymzusammensetzung. In diesem Zusammenhang erwies sich Pex14p als bester Marker zum Nachweis aller Peroxisomen, unabhängig des entsprechenden Zelltyps. Im Gegensatz hierzu war Katalase, ein Enzym, das in den meisten Publikationen als Standard-Marker für Peroxisomen eingesetzt wird, nur in hoher Menge in AECII- und Clara-Zellen vorhanden. Weiterhin waren Peroxisomen des Alveolar- und Bronchialepithels und der Alveolarmakrophagen reich an ABCD3-Lipidtransporter und β -Oxidationsenzymen, was ihre Funktion in der Modifizierung und Wiederverwertung des Lipidanteils von Surfactant und in der Kontrolle von pro-inflammatorischen Lipidmediatoren und Liganden für nukleäre Rezeptoren der PPAR Familie nahe legt.

Zusätzlich Resultate erbrachten, dass die Peroxisomendichte und deren Enzymgehalt bereits bei der Geburt extrem hoch war, was eine wichtige Rolle des peroxisomalen Lipidstoffwechsels in der Lunge gerade in der perinatalen Periode vermuten lässt. Während der postnatalen Lungenentwicklung, mit gleichzeitiger Vermehrung von AECI in Rahmen des Alveolarisierungsprozesses wurde das peroxisomale Kompartiment herunterreguliert und blieb

Zusammenfassung

nur in AECII und Makrophagen der Alveolarregion der matura adulten Lunge in starker Ausprägung vorhanden.

Weiterhin zeigten die Resultate dieser Dissertation aus Zellkulturversuchen mit AECII, dass das peroxisomale Kompartiment und entsprechende mRNAs während der AECII-AECI-Umdifferenzierung drastisch herunterreguliert wird, während die Zugabe von KGF ins Kulturmedium den AECII-Phänotyp der Zellen erhält und sogar eine Induktion von Katalase und den peroxisomalen Enzymen der Etherlipidsynthese bewirkt. Diese Resultate spiegeln exakt die starken Unterschiede in der Ausprägung des peroxisomalen Kompartiments zwischen AECII und AECI in licht- und elektronmikroskopischen Präparaten des adulten Lungengewebes wider und legen nahe, dass KGF Differenzierungssignale des peroxisomalen Kompartiments in AECII beeinflusst, die die Ausprägung und die Transkription zugehöriger Gene induzieren.

Weiterhin wurden in dieser Dissertation die molekularen Auswirkungen einer Peroxisomendefizienz auf die Lungenentwicklung in einem Knockoutmausmodell mit peroxisomalem Biogenesedefekt untersucht, durch den die Proliferation der Peroxisomen gestört ist (PEX11 β ^{-/-}). Knockoutmäuse mit PEX11 β -Defekt zeigten schwere Veränderungen des pulmonalen ROS- und Lipidstoffwechsels und wiesen eindeutige Unterschiede in der Expression zelltypspezifischer Marker auf. Mit Hilfe der PEX11 β ^{-/-} Mäuse konnte gezeigt werden, dass der Verlust peroxisomaler Funktionen zu Veränderungen der Alveolarisierung und der Expression von Wnt5a- oder PPAR-mRNAs führt, beides Faktoren, die in die distale Morphogenese (Wnt5a) oder die Ausdifferenzierung von Epithelzellen (PPARs) eingeschaltet sind. Schließlich konnten erste Resultate zu Veränderungen der Peroxisomen und deren Enzymzusammensetzung in Lungengewebe von Patienten mit idiopathischer Lungenfibrose (IPF), einer tödlichen Lungenerkrankung, erhoben werden. Die genaue Rolle der Veränderungen des peroxisomalen Stoffwechsels in der Lunge von IPF-Patienten muss jedoch in zukünftige Studien aufgeklärt werden.

Zusammenfassend legen die Resultate der Dissertation nahe, dass das peroxisomale Kompartiment und dessen Stoffwechselfunktionen eine wichtige Rolle in der Ausdifferenzierung bei der Lungenentwicklung spielen und für die reguläre Funktion und den Homöostaseerhalt im adulten Lungengewebe notwendig sind, sowie bei Lungenerkrankungen verändert werden können.

9 References

- Abe I, Fujiki Y (1998) cDNA cloning and characterization of a constitutively expressed isoform of the human peroxin Pex11p. *Biochem Biophys Res Commun* 252:529-533
- Abraham V, Chou ML, DeBolt KM, Koval M (1999) Phenotypic control of gap junctional communication by cultured alveolar epithelial cells. *Am J Physiol* 276:L825-834
- Adamson IY, Bowden DH (1974) The type 2 cell as progenitor of alveolar epithelial regeneration. A cytodynamic study in mice after exposure to oxygen. *Lab Invest* 30:35-42
- Agne B, Meindl NM, Niederhoff K, Einwachter H, Rehling P, Sickmann A, Meyer HE, Girzalsky W, Kunau WH (2003) Pex8p: an intraperoxisomal organizer of the peroxisomal import machinery. *Mol Cell* 11:635-646
- Ahlemeyer B, Neubert I, Kovacs WJ, Baumgart-Vogt E (2007) Differential expression of peroxisomal matrix and membrane proteins during postnatal development of mouse brain. *J Comp Neurol* 505:1-17
- Albertini M, Rehling P, Erdmann R, Girzalsky W, Kiel JA, Veenhuis M, Kunau WH (1997) Pex14p, a peroxisomal membrane protein binding both receptors of the two PTS-dependent import pathways. *Cell* 89:83-92
- Angermüller S, Bruder G, Volkl A, Wesch H, Fahimi HD (1987) Localization of xanthine oxidase in crystalline cores of peroxisomes. A cytochemical and biochemical study. *Eur J Cell Biol* 45:137-144
- Angermüller S, Fahimi HD (1981) Selective cytochemical localization of peroxidase, cytochrome oxidase and catalase in rat liver with 3,3'-diaminobenzidine. *Histochemistry* 71:33-44
- Antonenkov VD (1989) Dehydrogenases of the pentose phosphate pathway in rat liver peroxisomes. *Eur J Biochem* 183:75-82
- Antonenkov VD, Van Veldhoven PP, Waelkens E, Mannaerts GP (1997) Substrate specificities of 3-oxoacyl-CoA thiolase A and sterol carrier protein 2/3-oxoacyl-CoA thiolase purified from normal rat liver peroxisomes. Sterol carrier protein 2/3-oxoacyl-CoA thiolase is involved in the metabolism of 2-methyl-branched fatty acids and bile acid intermediates. *J Biol Chem* 272:26023-26031
- Antonenkov VD, Van Veldhoven PP, Waelkens E, Mannaerts GP (1999) Comparison of the stability and substrate specificity of purified peroxisomal 3-oxoacyl-CoA thiolases A and B from rat liver. *Biochim Biophys Acta* 1437:136-141
- Baes M, Gressens P, Baumgart E, Carmeliet P, Casteels M, Fransen M, Evrard P, Fahimi D, Declercq PE, Collen D, van Veldhoven PP, Mannaerts GP (1997) A mouse model for Zellweger syndrome. *Nat Genet* 17:49-57
- Barlier-Mur AM, Chailley-Heu B, Pinteur C, Henrion-Caude A, Delacourt C, Bourbon JR (2003) Maturation factors modulate transcription factors CCAAT/enhancer-binding proteins alpha, beta, delta, and peroxisome proliferator-activated receptor-gamma in fetal rat lung epithelial cells. *Am J Respir Cell Mol Biol* 29:620-626
- Barnett P, Bottger G, Klein AT, Tabak HF, Distel B (2000) The peroxisomal membrane protein Pex13p shows a novel mode of SH3 interaction. *EMBO J* 19:6382-6391
- Baudhuin P, Beaufay H, Rahman-Li Y, Sellinger OZ, Wattiaux R, Jacques P, De Duve C (1964) Tissue fractionation studies. 17. Intracellular distribution of monoamine oxidase, aspartate aminotransferase, alanine aminotransferase, D-amino acid oxidase and catalase in rat-liver tissue. *Biochem J* 92:179-184
- Baumgart E, Fahimi HD, Steininger H, Grabenbauer M (2003) A review of morphological techniques for detection of peroxisomal (and mitochondrial) proteins and their corresponding mRNAs during ontogenesis in mice: application to the PEX5-knockout mouse with Zellweger syndrome. *Microsc Res Tech* 61:121-138
- Baumgart E, Vanhooren JC, Fransen M, Marynen P, Puype M, Vandekerckhove J, Leunissen JA, Fahimi HD, Mannaerts GP, van Veldhoven PP (1996) Molecular characterization of the human peroxisomal branched-chain acyl-CoA oxidase: cDNA cloning, chromosomal assignment, tissue distribution, and evidence for the absence of the protein in Zellweger syndrome. *Proc Natl Acad Sci U S A* 93:13748-13753
- Baumgart E, Vanhorebeek I, Grabenbauer M, Borgers M, Declercq PE, Fahimi HD, Baes M (2001) Mitochondrial alterations caused by defective peroxisomal biogenesis in a mouse model for Zellweger syndrome (PEX5 knockout mouse). *Am J Pathol* 159:1477-1494
- Baumgart E, Volkl A, Hashimoto T, Fahimi HD (1989) Biogenesis of peroxisomes: immunocytochemical investigation of peroxisomal membrane proteins in proliferating rat liver peroxisomes and in catalase-negative membrane loops. *J Cell Biol* 108:2221-2231
- Belvisi MG, Hele DJ, Birrell MA (2006) Peroxisome proliferator-activated receptor gamma agonists as therapy for chronic airway inflammation. *Eur J Pharmacol* 533:101-109
- Benayoun L, Letuve S, Druilhe A, Boczkowski J, Dombret MC, Mechighel P, Megret J, Leseche G, Aubier M, Pretolani M (2001) Regulation of peroxisome proliferator-activated receptor gamma expression in human asthmatic airways: relationship with proliferation, apoptosis, and airway remodeling. *Am J Respir Crit Care Med* 164:1487-1494

References

- Bernard A, Marchandise FX, Depelchin S, Lauwerys R, Sibille Y (1992) Clara cell protein in serum and bronchoalveolar lavage. *Eur Respir J* 5:1231-1238
- Bernhard W, Rouiller C (1956) Microbodies and the problem of mitochondrial regeneration in liver cells. *J Biophys Biochem Cytol* 2:355-360
- Borok Z, Danto SI, Dimen LL, Zhang XL, Lubman RL (1998a) Na(+)-K(+)-ATPase expression in alveolar epithelial cells: upregulation of active ion transport by KGF. *Am J Physiol* 274:L149-158
- Borok Z, Hami A, Danto SI, Zabski SM, Crandall ED (1995) Rat serum inhibits progression of alveolar epithelial cells toward the type I cell phenotype in vitro. *Am J Respir Cell Mol Biol* 12:50-55
- Borok Z, Lubman RL, Danto SI, Zhang XL, Zabski SM, King LS, Lee DM, Agre P, Crandall ED (1998b) Keratinocyte growth factor modulates alveolar epithelial cell phenotype in vitro: expression of aquaporin 5. *Am J Respir Cell Mol Biol* 18:554-561
- Boudreau N, Bissell MJ (1998) Extracellular matrix signaling: integration of form and function in normal and malignant cells. *Curr Opin Cell Biol* 10:640-646
- Bradford MM (1976) A rapid and sensitive method for the quantitation of microgram quantities of protein utilizing the principle of protein-dye binding. *Anal Biochem* 72:248-254
- Braissant O, Wahli W (1998) Differential expression of peroxisome proliferator-activated receptor-alpha, -beta, and -gamma during rat embryonic development. *Endocrinology* 139:2748-2754
- Braun S, Hanselmann C, Gassmann MG, auf dem Keller U, Born-Berclaz C, Chan K, Kan YW, Werner S (2002) Nrf2 transcription factor, a novel target of keratinocyte growth factor action which regulates gene expression and inflammation in the healing skin wound. *Mol Cell Biol* 22:5492-5505
- Bren-Mattison Y, Van Putten V, Chan D, Winn R, Geraci MW, Nemenoff RA (2005) Peroxisome proliferator-activated receptor-gamma (PPAR(gamma)) inhibits tumorigenesis by reversing the undifferentiated phenotype of metastatic non-small-cell lung cancer cells (NSCLC). *Oncogene* 24:1412-1422
- Brites P, Waterham HR, Wanders RJ (2004) Functions and biosynthesis of plasmalogens in health and disease. *Biochim Biophys Acta* 1636:219-231
- Brody AR, Hook GE, Cameron GS, Jetten AM, Butterick CJ, Nettesheim P (1987) The differentiation capacity of Clara cells isolated from the lungs of rabbits. *Lab Invest* 57:219-229
- Bulitta C, Ganea C, Fahimi HD, Völkl A (1996) Cytoplasmic and peroxisomal catalases of the guinea pig liver: evidence for two distinct proteins. *Biochim Biophys Acta* 1293:55-62
- Burgess HA, Daugherty LE, Thatcher TH, Lakatos HF, Ray DM, Redonnet M, Phipps RP, Sime PJ (2005) PPARgamma agonists inhibit TGF-beta induced pulmonary myofibroblast differentiation and collagen production: implications for therapy of lung fibrosis. *Am J Physiol Lung Cell Mol Physiol* 288:L1146-1153
- Calnek DS, Mazzella L, Roser S, Roman J, Hart CM (2003) Peroxisome proliferator-activated receptor gamma ligands increase release of nitric oxide from endothelial cells. *Arterioscler Thromb Vasc Biol* 23:52-57
- Chae HZ, Robison K, Poole LB, Church G, Storz G, Rhee SG (1994) Cloning and sequencing of thiol-specific antioxidant from mammalian brain: alkyl hydroperoxide reductase and thiol-specific antioxidant define a large family of antioxidant enzymes. *Proc Natl Acad Sci U S A* 91:7017-7021
- Chan K, Kan YW (1999) Nrf2 is essential for protection against acute pulmonary injury in mice. *Proc Natl Acad Sci U S A* 96:12731-12736
- Chang CC, Lee WH, Moser H, Valle D, Gould SJ (1997) Isolation of the human PEX12 gene, mutated in group 3 of the peroxisome biogenesis disorders. *Nat Genet* 15:385-388
- Chang TH, Szabo E (2000) Induction of differentiation and apoptosis by ligands of peroxisome proliferator-activated receptor gamma in non-small cell lung cancer. *Cancer Res* 60:1129-1138
- Chang Y, Edeen K, Lu X, De Leon M, Mason RJ (2006) Keratinocyte growth factor induces lipogenesis in alveolar type II cells through a sterol regulatory element binding protein-1c-dependent pathway. *Am J Respir Cell Mol Biol* 35:268-274
- Chang Y, Wang J, Lu X, Thewke DP, Mason RJ (2005) KGF induces lipogenic genes through a PI3K and JNK/SREBP-1 pathway in H292 cells. *J Lipid Res* 46:2624-2635
- Chang YF (1978) Lysine metabolism in the rat brain: blood-brain barrier transport, formation of pipecolic acid and human hyperpipecolatermia. *J Neurochem* 30:355-360
- Cheek JM, Evans MJ, Crandall ED (1989) Type I cell-like morphology in tight alveolar epithelial monolayers. *Exp Cell Res* 184:375-387
- Chelly N, Mouhieddine-Gueddiche OB, Barlier-Mur AM, Chailley-Heu B, Bourbon JR (1999) Keratinocyte growth factor enhances maturation of fetal rat lung type II cells. *Am J Respir Cell Mol Biol* 20:423-432
- Chinetti G, Griglio S, Antonucci M, Torra IP, Delerive P, Majd Z, Fruchart JC, Chapman J, Najib J, Staels B (1998) Activation of proliferator-activated receptors alpha and gamma induces apoptosis of human monocyte-derived macrophages. *J Biol Chem* 273:25573-25580

References

- Clara M (1937) Zur Histobiologie des Bronchiaepithels. *Z Mikrosk Anat Forsch* 41:321-347
- Cochrane CG, Revak SD (1991) Pulmonary surfactant protein B (SP-B): structure-function relationships. *Science* 254:566-568
- Cooper TG, Beevers H (1969) Beta oxidation in glyoxysomes from castor bean endosperm. *J Biol Chem* 244:3514-3520
- Corti M, Brody AR, Harrison JH (1996) Isolation and primary culture of murine alveolar type II cells. *Am J Respir Cell Mol Biol* 14:309-315
- Costa-Rodrigues J, Carvalho AF, Gouveia AM, Fransen M, Sa-Miranda C, Azevedo JE (2004) The N terminus of the peroxisomal cycling receptor, Pex5p, is required for redirecting the peroxisome-associated peroxin back to the cytosol. *J Biol Chem* 279:46573-46579
- Cotgreave IA, Gerdes RG (1998) Recent trends in glutathione biochemistry--glutathione-protein interactions: a molecular link between oxidative stress and cell proliferation? *Biochem Biophys Res Commun* 242:1-9
- Croes K, Casteels M, De Hoffmann E, Mannaerts GP, Van Veldhoven PP (1996) alpha-Oxidation of 3-methyl-substituted fatty acids in rat liver. Production of formic acid instead of CO₂, cofactor requirements, subcellular localization and formation of a 2-hydroxy-3-methylacyl-CoA intermediate. *Eur J Biochem* 240:674-683
- Crosby MB, Svenson J, Gilkeson GS, Nowling TK (2005) A novel PPAR response element in the murine iNOS promoter. *Mol Immunol* 42:1303-1310
- Danto SI, Shannon JM, Borok Z, Zabski SM, Crandall ED (1995) Reversible transdifferentiation of alveolar epithelial cells. *Am J Respir Cell Mol Biol* 12:497-502
- Das KC, Pahl PM, Guo XL, White CW (2001) Induction of peroxiredoxin gene expression by oxygen in lungs of newborn primates. *Am J Respir Cell Mol Biol* 25:226-232
- De Duve C, Baudhuin P (1966) Peroxisomes (microbodies and related particles). *Physiol Rev* 46:323-357
- Dekowski SA, Snyder JM (1995) The combined effects of insulin and cortisol on surfactant protein mRNA levels. *Pediatr Res* 38:513-521
- Delille HK, Alves R, Schrader M (2009) Biogenesis of peroxisomes and mitochondria: linked by division. *Histochem Cell Biol* 131:441-446
- Desvergne B, Wahli W (1999) Peroxisome proliferator-activated receptors: nuclear control of metabolism. *Endocr Rev* 20:649-688
- Deterding RR, Havill AM, Yano T, Middleton SC, Jacoby CR, Shannon JM, Simonet WS, Mason RJ (1997) Prevention of bleomycin-induced lung injury in rats by keratinocyte growth factor. *Proc Assoc Am Physicians* 109:254-268
- Diczfalusy U, Alexson SE (1988) Peroxisomal chain-shortening of prostaglandin F₂ alpha. *J Lipid Res* 29:1629-1636
- Distel B, Erdmann R, Gould SJ, Blobel G, Crane DJ, Cregg JM, Dodt G, Fujiki Y, Goodman JM, Just WW, Kiel JA, Kunau WH, Lazarow PB, Mannaerts GP, Moser HW, Osumi T, Rachubinski RA, Roscher A, Subramani S, Tabak HF, Tsukamoto T, Valle D, van der Klei I, van Veldhoven PP, Veenhuis M (1996) A unified nomenclature for peroxisome biogenesis factors. *J Cell Biol* 135:1-3
- Dreyer C, Krey G, Keller H, Givel F, Helftenbein G, Wahli W (1992) Control of the peroxisomal beta-oxidation pathway by a novel family of nuclear hormone receptors. *Cell* 68:879-887
- Dunsmore SE, Lee YC, Martinez-Williams C, Rannels DE (1996) Synthesis of fibronectin and laminin by type II pulmonary epithelial cells. *Am J Physiol* 270:L215-223
- Dyer JM, McNew JA, Goodman JM (1996) The sorting sequence of the peroxisomal integral membrane protein PMP47 is contained within a short hydrophilic loop. *J Cell Biol* 133:269-280
- Eckert JH, Erdmann R (2003) Peroxisome biogenesis. *Rev Physiol Biochem Pharmacol* 147:75-121
- Eguchi M, Spicer SS, Mochizuki I (1980) Cytochemistry of type II pneumocytes in Chediak-Higashi syndrome of mice. *Exp Mol Pathol* 32:290-306
- Elgersma Y, Kwast L, Klein A, Voorn-Brouwer T, van den Berg M, Metzger B, America T, Tabak HF, Distel B (1996) The SH3 domain of the *Saccharomyces cerevisiae* peroxisomal membrane protein Pex13p functions as a docking site for Pex5p, a mobile receptor for the import PTS1-containing proteins. *J Cell Biol* 135:97-109
- Erdmann R, Blobel G (1995) Giant peroxisomes in oleic acid-induced *Saccharomyces cerevisiae* lacking the peroxisomal membrane protein Pmp27p. *J Cell Biol* 128:509-523
- Erdmann R, Blobel G (1996) Identification of Pex13p a peroxisomal membrane receptor for the PTS1 recognition factor. *J Cell Biol* 135:111-121
- Erdmann R, Veenhuis M, Kunau WH (1997) Peroxisomes: Organelles at the crossroads. *Trends Cell Biol* 7:400-407
- Evans MJ, Cabral LJ, Stephens RJ, Freeman G (1975) Transformation of alveolar type 2 cells to type 1 cells following exposure to NO₂. *Exp Mol Pathol* 22:142-150
- Evans MJ, Johnson LV, Stephens RJ, Freeman G (1976) Cell renewal in the lungs of rats exposed to low levels of ozone. *Exp Mol Pathol* 24:70-83
- Evans RM (1988) The steroid and thyroid hormone receptor superfamily. *Science* 240:889-895

References

- Evrard P, Caviness VS, Jr., Prats-Vinas J, Lyon G (1978) The mechanism of arrest of neuronal migration in the Zellweger malformation: an hypothesis based upon cytoarchitectonic analysis. *Acta Neuropathol* 41:109-117
- Fahimi HD (1968) Cytochemical localization of peroxidase activity in rat hepatic microbodies (peroxisomes). *J Histochem Cytochem* 16:547-550
- Fahimi HD (1969) Cytochemical localization of peroxidase activity of catalase in rat hepatic microbodies (peroxisomes). *J Cell Biol* 43:275-288
- Fahimi HD (1974) Effect of buffer storage on fine structure and catalase cytochemistry of peroxisomes. *J Cell Biol* 63:675-683
- Fahimi HD, Reich D, Völkl A, Baumgart E (1996) Contributions of the immunogold technique to investigation of the biology of peroxisomes. *Histochem Cell Biol* 106:105-114
- Fajas L, Fruchart JC, Auwerx J (1998) Transcriptional control of adipogenesis. *Curr Opin Cell Biol* 10:165-173
- Fan CY, Pan J, Usuda N, Yeldandi AV, Rao MS, Reddy JK (1998) Steatohepatitis, spontaneous peroxisome proliferation and liver tumors in mice lacking peroxisomal fatty acyl-CoA oxidase. Implications for peroxisome proliferator-activated receptor alpha natural ligand metabolism. *J Biol Chem* 273:15639-15645
- Fang Y, Morrell JC, Jones JM, Gould SJ (2004) PEX3 functions as a PEX19 docking factor in the import of class I peroxisomal membrane proteins. *J Cell Biol* 164:863-875
- Farioli-Vecchioli S, Nardacci R, Falciatori I, Stefanini S (2001) Catalase immunocytochemistry allows automatic detection of lung type II alveolar cells. *Histochem Cell Biol* 115:333-339
- Faust PL, Hatten ME (1997) Targeted deletion of the PEX2 peroxisome assembly gene in mice provides a model for Zellweger syndrome, a human neuronal migration disorder. *J Cell Biol* 139:1293-1305
- Fransen M, Van Veldhoven PP, Subramani S (1999) Identification of peroxisomal proteins by using M13 phage protein VI phage display: molecular evidence that mammalian peroxisomes contain a 2,4-dienoyl-CoA reductase. *Biochem J* 340 (Pt 2):561-568
- Fringes B, Gorgas K, Reith A (1988) Clofibrate increases the number of peroxisomes and of lamellar bodies in alveolar cells type II of the rat lung. *Eur J Cell Biol* 46:136-143
- Fringes B, Reith A (1988) Two hypolipidemic peroxisome proliferators increase the number of lamellar bodies in alveolar cells type II of the rat lung. *Exp Mol Pathol* 48:262-271
- Fritz R, Bol J, Hebling U, Angermüller S, Völkl A, Fahimi HD, Mueller S (2007) Compartment-dependent management of H₂O₂ by peroxisomes. *Free Radic Biol Med* 42:1119-1129
- Fuchs S, Hollins AJ, Laue M, Schaefer UF, Roemer K, Gumbleton M, Lehr CM (2003) Differentiation of human alveolar epithelial cells in primary culture: morphological characterization and synthesis of caveolin-1 and surfactant protein-C. *Cell Tissue Res* 311:31-45
- Fujii Y, Goldberg P, Hussain SN (1998) Contribution of macrophages to pulmonary nitric oxide production in septic shock. *Am J Respir Crit Care Med* 157:1645-1651
- Girzalsky W, Rehling P, Stein K, Kipper J, Blank L, Kunau WH, Erdmann R (1999) Involvement of Pex13p in Pex14p localization and peroxisomal targeting signal 2-dependent protein import into peroxisomes. *J Cell Biol* 144:1151-1162
- Goldenberg H, Hüttinger M, Kollner U, Kramar R, Pavelka M (1978) Catalase positive particles from pig lung. Biochemical preparations and morphological studies. *Histochemistry* 56:253-264
- Goldfischer S, Moore CL, Johnson AB, Spiro AJ, Valsamis MP, Wisniewski HK, Ritch RH, Norton WT, Rapin I, Gartner LM (1973) Peroxisomal and mitochondrial defects in the cerebro-hepato-renal syndrome. *Science* 182:62-64
- Gosset P, Charbonnier AS, Delerive P, Fontaine J, Staels B, Pestel J, Tonnel AB, Trottein F (2001) Peroxisome proliferator-activated receptor gamma activators affect the maturation of human monocyte-derived dendritic cells. *Eur J Immunol* 31:2857-2865
- Gould SJ, Kalish JE, Morrell JC, Bjorkman J, Urquhart AJ, Crane DI (1996) Pex13p is an SH3 protein of the peroxisome membrane and a docking factor for the predominantly cytoplasmic PTs1 receptor. *J Cell Biol* 135:85-95
- Gould SJ, Keller GA, Hosken N, Wilkinson J, Subramani S (1989) A conserved tripeptide sorts proteins to peroxisomes. *J Cell Biol* 108:1657-1664
- Gould SJ, Valle D (2000) Peroxisome biogenesis disorders: genetics and cell biology. *Trends Genet* 16:340-345
- Gouveia AM, Guimaraes CP, Oliveira ME, Reguenga C, Sa-Miranda C, Azevedo JE (2003) Characterization of the peroxisomal cycling receptor Pex5p import pathway. *Adv Exp Med Biol* 544:219-220
- Grabenbauer M, Fahimi HD, Baumgart E (2001) Detection of peroxisomal proteins and their mRNAs in serial sections of fetal and newborn mouse organs. *J Histochem Cytochem* 49:155-164
- Guo J, Yi ES, Havill AM, Sarosi I, Whitcomb L, Yin S, Middleton SC, Piguat P, Ulich TR (1998) Intravenous keratinocyte growth factor protects against experimental pulmonary injury. *Am J Physiol* 275:L800-805
- Hajra AK, Burke CL, Jones CL (1979) Subcellular localization of acyl coenzyme A: dihydroxyacetone phosphate acyltransferase in rat liver peroxisomes (microbodies). *J Biol Chem* 254:10896-10900

References

- Hajra AK, Larkins LK, Das AK, Hemati N, Erickson RL, MacDougald OA (2000) Induction of the peroxisomal glycerolipid-synthesizing enzymes during differentiation of 3T3-L1 adipocytes. Role in triacylglycerol synthesis. *J Biol Chem* 275:9441-9446
- Han C, Lim K, Xu L, Li G, Wu T (2008) Regulation of Wnt/beta-catenin pathway by cPLA2alpha and PPARdelta. *J Cell Biochem* 105:534-545
- Harris SG, Smith RS, Phipps RP (2002) 15-deoxy-Delta 12,14-PGJ2 induces IL-8 production in human T cells by a mitogen-activated protein kinase pathway. *J Immunol* 168:1372-1379
- Hashimoto F, Hayashi H (1987) Significance of catalase in peroxisomal fatty acyl-CoA beta-oxidation. *Biochim Biophys Acta* 921:142-150
- Hashimoto F, Hayashi H (1990) Significance of catalase in peroxisomal fatty acyl-CoA beta-oxidation: NADH oxidation by acetoacetyl-CoA and H₂O₂. *J Biochem* 108:426-431
- Hashimoto T (2000) Peroxisomal beta-oxidation enzymes. *Cell Biochem Biophys* 32 Spring:63-72
- Hayashi H, Takahata S (1991) Role of peroxisomal fatty acyl-CoA beta-oxidation in phospholipid biosynthesis. *Arch Biochem Biophys* 284:326-331
- Heijnen HF, van Donselaar E, Slot JW, Fries DM, Blachard-Fillion B, Hodara R, Lightfoot R, Polydoro M, Spielberg D, Thomson L, Regan EA, Crapo J, Ischiropoulos H (2006) Subcellular localization of tyrosine-nitrated proteins is dictated by reactive oxygen species generating enzymes and by proximity to nitric oxide synthase. *Free Radic Biol Med* 40:1903-1913
- Hermans C, Knoops B, Wiedig M, Arsalane K, Toubeau G, Falmagne P, Bernard A (1999) Clara cell protein as a marker of Clara cell damage and bronchoalveolar blood barrier permeability. *Eur Respir J* 13:1014-1021
- Hettema EH, Distel B, Tabak HF (1999) Import of proteins into peroxisomes. *Biochim Biophys Acta* 1451:17-34
- Hijikata M, Wen JK, Osumi T, Hashimoto T (1990) Rat peroxisomal 3-ketoacyl-CoA thiolase gene. Occurrence of two closely related but differentially regulated genes. *J Biol Chem* 265:4600-4606
- Hiltunen JK, Filppula SA, Koivuranta KT, Siivari K, Qin YM, Hayrinen HM (1996) Peroxisomal beta-oxidation and polyunsaturated fatty acids. *Ann N Y Acad Sci* 804:116-128
- Hiltunen JK, Karki T, Hassinen IE, Osmundsen H (1986) beta-Oxidation of polyunsaturated fatty acids by rat liver peroxisomes. A role for 2,4-dienoyl-coenzyme A reductase in peroxisomal beta-oxidation. *J Biol Chem* 261:16484-16493
- Hirai K, Yamauchi M, Witschi H, Cote MG (1983) Disintegration of lung peroxisomes during differentiation of type II cells to type I cells in butylated hydroxytoluene-administered mice. *Exp Mol Pathol* 39:129-138
- Hirai KI, Witschi H, Cote MG (1977) Electron microscopy of butylated hydroxytoluene-induced lung damage in mice. *Exp Mol Pathol* 27:295-308
- Hoepfner D, Schildknecht D, Braakman I, Philippson P, Tabak HF (2005) Contribution of the endoplasmic reticulum to peroxisome formation. *Cell* 122:85-95
- Hoepfner D, van den Berg M, Philippson P, Tabak HF, Hettema EH (2001) A role for Vps1p, actin, and the Myo2p motor in peroxisome abundance and inheritance in *Saccharomyces cerevisiae*. *J Cell Biol* 155:979-990
- Hohlfeld JM, Erpenbeck VJ, Krug N (2002) Surfactant proteins SP-A and SP-D as modulators of the allergic inflammation in asthma. *Pathobiology* 70:287-292
- Holmes RS, Masters CJ (1972) Species specific features of the distribution and multiplicity of mammalian liver catalase. *Arch Biochem Biophys* 148:217-223
- Holroyd C, Erdmann R (2001) Protein translocation machineries of peroxisomes. *FEBS Lett* 501:6-10
- Honda K, Marquillies P, Capron M, Dombrowicz D (2004) Peroxisome proliferator-activated receptor gamma is expressed in airways and inhibits features of airway remodeling in a mouse asthma model. *J Allergy Clin Immunol* 113:882-888
- Honsho M, Fujiki Y (2001) Topogenesis of peroxisomal membrane protein requires a short, positively charged intervening-loop sequence and flanking hydrophobic segments. study using human membrane protein PMP34. *J Biol Chem* 276:9375-9382
- Honsho M, Hiroshige T, Fujiki Y (2002) The membrane biogenesis peroxin Pex16p. Topogenesis and functional roles in peroxisomal membrane assembly. *J Biol Chem* 277:44513-44524
- Horie S, Suzuki T, Suga T (1989) Existence of acetyl-CoA-dependent chain elongation system in hepatic peroxisomes of rat: effects of clofibrate and di-(2-ethylhexyl)phthalate on the activity. *Arch Biochem Biophys* 274:64-73
- Horton JD, Goldstein JL, Brown MS (2002a) SREBPs: activators of the complete program of cholesterol and fatty acid synthesis in the liver. *J Clin Invest* 109:1125-1131
- Horton JD, Goldstein JL, Brown MS (2002b) SREBPs: transcriptional mediators of lipid homeostasis. *Cold Spring Harb Symp Quant Biol* 67:491-498
- Hu T, Foxworthy P, Siesky A, Ficorilli JV, Gao H, Li S, Christe M, Ryan T, Cao G, Eacho P, Michael MD, Michael LF (2005) Hepatic peroxisomal fatty acid beta-oxidation is regulated by liver X receptor alpha. *Endocrinology* 146:5380-5387

References

- Huang TH, Razmovski-Naumovski V, Kota BP, Lin DS, Roufogalis BD (2005) The pathophysiological function of peroxisome proliferator-activated receptor-gamma in lung-related diseases. *Respir Res* 6:102
- Huhse B, Rehling P, Albertini M, Blank L, Meller K, Kunau WH (1998) Pex17p of *Saccharomyces cerevisiae* is a novel peroxin and component of the peroxisomal protein translocation machinery. *J Cell Biol* 140:49-60
- Huyghe S, Casteels M, Janssen A, Meulders L, Mannaerts GP, Declercq PE, Van Veldhoven PP, Baes M (2001) Prenatal and postnatal development of peroxisomal lipid-metabolizing pathways in the mouse. *Biochem J* 353:673-680
- Immenschuh S, Baumgart-Vogt E (2005) Peroxiredoxins, oxidative stress, and cell proliferation. *Antioxid Redox Signal* 7:768-777
- Islinger M, Luers GH, Zischka H, Ueffing M, Volkl A (2006) Insights into the membrane proteome of rat liver peroxisomes: microsomal glutathione-S-transferase is shared by both subcellular compartments. *Proteomics* 6:804-816
- Issemann I, Green S (1990) Activation of a member of the steroid hormone receptor superfamily by peroxisome proliferators. *Nature* 347:645-650
- Jiang C, Ting AT, Seed B (1998) PPAR-gamma agonists inhibit production of monocyte inflammatory cytokines. *Nature* 391:82-86
- Johnston CJ, Mango GW, Finkelstein JN, Stripp BR (1997) Altered pulmonary response to hyperoxia in Clara cell secretory protein deficient mice. *Am J Respir Cell Mol Biol* 17:147-155
- Jorens PG, Sibille Y, Goulding NJ, van Overveld FJ, Herman AG, Bossaert L, De Backer WA, Lauwerys R, Flower RJ, Bernard A (1995) Potential role of Clara cell protein, an endogenous phospholipase A2 inhibitor, in acute lung injury. *Eur Respir J* 8:1647-1653
- Karnati S, Baumgart-Vogt E (2008) Peroxisomes in mouse and human lung: their involvement in pulmonary lipid metabolism. *Histochem Cell Biol* 130:719-740
- Karnati S, Baumgart-Vogt E (2009) Peroxisomes in airway epithelia and future prospects of these organelles for pulmonary cell biology. *Histochem Cell Biol* 131:447-454
- Kasper M, Haroske G (1996) Alterations in the alveolar epithelium after injury leading to pulmonary fibrosis. *Histol Histopathol* 11:463-483
- Kasper M, Sims G, Koslowski R, Kuss H, Thuemmler M, Fehrenbach H, Auten RL (2002) Increased surfactant protein D in rat airway goblet and Clara cells during ovalbumin-induced allergic airway inflammation. *Clin Exp Allergy* 32:1251-1258
- Kawaguchi K, Sakaida I, Tsuchiya M, Omori K, Takami T, Okita K (2004) Pioglitazone prevents hepatic steatosis, fibrosis, and enzyme-altered lesions in rat liver cirrhosis induced by a choline-deficient L-amino acid-defined diet. *Biochem Biophys Res Commun* 315:187-195
- Keller GA, Barton MC, Shapiro DJ, Singer SJ (1985) 3-Hydroxy-3-methylglutaryl-coenzyme A reductase is present in peroxisomes in normal rat liver cells. *Proc Natl Acad Sci U S A* 82:770-774
- Kesav S, McLaughlin J, Scallen TJ (1992) Participation of sterol carrier protein-2 in cholesterol metabolism. *Biochem Soc Trans* 20:818-824
- Khoor A, Gray ME, Singh G, Stahlman MT (1996) Ontogeny of Clara cell-specific protein and its mRNA: their association with neuroepithelial bodies in human fetal lung and in bronchopulmonary dysplasia. *J Histochem Cytochem* 44:1429-1438
- Kim EH, Surh YJ (2006) 15-deoxy-Delta12,14-prostaglandin J2 as a potential endogenous regulator of redox-sensitive transcription factors. *Biochem Pharmacol* 72:1516-1528
- Koch A, Thiemann M, Grabenbauer M, Yoon Y, McNiven MA, Schrader M (2003) Dynamin-like protein 1 is involved in peroxisomal fission. *J Biol Chem* 278:8597-8605
- Kölliker A (1881) Zurkeniniss des Baues der Lunge des Menschen. *Verh Phys Med Ges* 16: 1–24.
- Kovacs WJ, Olivier LM, Krisans SK (2002) Central role of peroxisomes in isoprenoid biosynthesis. *Prog Lipid Res* 41:369-391
- Kovacs WJ, Shackelford JE, Tape KN, Richards MJ, Faust PL, Fliesler SJ, Krisans SK (2004) Disturbed cholesterol homeostasis in a peroxisome-deficient PEX2 knockout mouse model. *Mol Cell Biol* 24:1-13
- Kovacs WJ, Tape KN, Shackelford JE, Duan X, Kasumov T, Kelleher JK, Brunengraber H, Krisans SK (2007) Localization of the pre-squalene segment of the isoprenoid biosynthetic pathway in mammalian peroxisomes. *Histochem Cell Biol* 127:273-290
- Kremser K, Stangl H, Pahan K, Singh I (1995) Nitric oxide regulates peroxisomal enzyme activities. *Eur J Clin Chem Clin Biochem* 33:763-774
- Krey G, Mahfoudi A, Wahli W (1995) Functional interactions of peroxisome proliferator-activated receptor, retinoid-X receptor, and Sp1 in the transcriptional regulation of the acyl-coenzyme-A oxidase promoter. *Mol Endocrinol* 9:219-231
- Krisans SK (1992) The role of peroxisomes in cholesterol metabolism. *Am J Respir Cell Mol Biol* 7:358-364

References

- Krisans SK (1996) Cell compartmentalization of cholesterol biosynthesis. *Ann N Y Acad Sci* 804:142-164
- Kropotov AV, Grudinkin PS, Pleskach NM, Gavrilov BA, Tomilin NV, Zhivotovsky B (2004) Downregulation of peroxiredoxin V stimulates formation of etoposide-induced double-strand DNA breaks. *FEBS Lett* 572:75-79
- Lakatos HF, Thatcher TH, Kottmann RM, Garcia TM, Phipps RP, Sime PJ (2007) The Role of PPARs in Lung Fibrosis. *PPAR Res* 2007:71323
- Lazarow PB (1977) Three hypolipidemic drugs increase hepatic palmitoyl-coenzyme A oxidation in the rat. *Science* 197:580-581
- Lazarow PB (1978) Rat liver peroxisomes catalyze the beta oxidation of fatty acids. *J Biol Chem* 253:1522-1528
- Lazarow PB, De Duve C (1976) A fatty acyl-CoA oxidizing system in rat liver peroxisomes; enhancement by clofibrate, a hypolipidemic drug. *Proc Natl Acad Sci U S A* 73:2043-2046
- Lazarow PB, Fujiki Y (1985) Biogenesis of peroxisomes. *Annu Rev Cell Biol* 1:489-530
- Leclercq IA, Sempoux C, Starkel P, Horsmans Y (2006) Limited therapeutic efficacy of pioglitazone on progression of hepatic fibrosis in rats. *Gut* 55:1020-1029
- Lee TC (1998) Biosynthesis and possible biological functions of plasmalogens. *Biochim Biophys Acta* 1394:129-145
- Li X, Baumgart E, Morrell JC, Jimenez-Sanchez G, Valle D, Gould SJ (2002) PEX11 beta deficiency is lethal and impairs neuronal migration but does not abrogate peroxisome function. *Mol Cell Biol* 22:4358-4365
- Li X, Gould SJ (2002) PEX11 promotes peroxisome division independently of peroxisome metabolism. *J Cell Biol* 156:643-651
- Loughran PA, Stolz DB, Vodovotz Y, Watkins SC, Simmons RL, Billiar TR (2005) Monomeric inducible nitric oxide synthase localizes to peroxisomes in hepatocytes. *Proc Natl Acad Sci U S A* 102:13837-13842
- Lukashev ME, Werb Z (1998) ECM signalling: orchestrating cell behaviour and misbehaviour. *Trends Cell Biol* 8:437-441
- Lwebuga-Mukasa JS (1991) Matrix-driven pneumocyte differentiation. *Am Rev Respir Dis* 144:452-457
- Mannaerts GP, Van Veldhoven PP (1993) Metabolic pathways in mammalian peroxisomes. *Biochimie* 75:147-158
- Mannaerts GP, Van Veldhoven PP, Casteels M (2000) Peroxisomal lipid degradation via beta- and alpha-oxidation in mammals. *Cell Biochem Biophys* 32 Spring:73-87
- Mantile G, Miele L, Cordella-Miele E, Singh G, Katyal SL, Mukherjee AB (1993) Human Clara cell 10-kDa protein is the counterpart of rabbit uteroglobin. *J Biol Chem* 268:20343-20351
- Marshall ES, Raichlen JS, Kim SM, Intenzo CM, Sawyer DT, Brody EA, Tighe DA, Park CH (1995a) Prognostic significance of ST-segment depression during adenosine perfusion imaging. *Am Heart J* 130:58-66
- Marshall PA, Krimkevich YI, Lark RH, Dyer JM, Veenhuis M, Goodman JM (1995b) Pmp27 promotes peroxisomal proliferation. *J Cell Biol* 129:345-355
- Mason CM, Guery BP, Summer WR, Nelson S (1996) Keratinocyte growth factor attenuates lung leak induced by alpha-naphthylthiourea in rats. *Crit Care Med* 24:925-931
- Masters C (1997) Gluconeogenesis and the peroxisome. *Mol Cell Biochem* 166:159-168
- Masters CJ (1996) Cellular signalling: the role of the peroxisome. *Cell Signal* 8:197-208
- Maxwell M, Bjorkman J, Nguyen T, Sharp P, Finnie J, Paterson C, Tonks I, Paton BC, Kay GF, Crane DI (2003) Pex13 inactivation in the mouse disrupts peroxisome biogenesis and leads to a Zellweger syndrome phenotype. *Mol Cell Biol* 23:5947-5957
- Mercurio AR, Rhodin JA (1976) An electron microscopic study on the type I pneumocyte in the cat: differentiation. *Am J Anat* 146:255-271
- Michael LF, Lazar MA, Mendelson CR (1997) Peroxisome proliferator-activated receptor gamma1 expression is induced during cyclic adenosine monophosphate-stimulated differentiation of alveolar type II pneumocytes. *Endocrinology* 138:3695-3703
- Mihalik SJ, McGuinness M, Watkins PA (1991) Purification and characterization of peroxisomal L-pipecolic acid oxidase from monkey liver. *J Biol Chem* 266:4822-4830
- Moi P, Chan K, Asunis I, Cao A, Kan YW (1994) Isolation of NF-E2-related factor 2 (Nrf2), a NF-E2-like basic leucine zipper transcriptional activator that binds to the tandem NF-E2/AP1 repeat of the beta-globin locus control region. *Proc Natl Acad Sci U S A* 91:9926-9930
- Moras D, Gronemeyer H (1998) The nuclear receptor ligand-binding domain: structure and function. *Curr Opin Cell Biol* 10:384-391
- Moriguchi K, Higashi N, Kitagawa S, Takase K, Ohya N, Uyeda T, Hirai K (1984) Differentiation of human pulmonary alveolar epithelial cells revealed by peroxisome changes in pulmonary proteinosis. *Exp Mol Pathol* 40:262-270
- Moser HW (1993) Peroxisomal diseases. *Adv Hum Genet* 21:1-106, 443-151
- Nardacci R, Falciatori I, Moreno S, Stefanini S (2004) Immunohistochemical localization of peroxisomal enzymes during rat embryonic development. *J Histochem Cytochem* 52:423-436

References

- Nenicu A, Lüers GH, Kovacs W, Otte D, Zimmer A, Bergmann M, Baumgart-Vogt E (2007) Peroxisomes in human and mouse testis: differential expression of peroxisomal proteins in germ cells and distinct somatic cell types of the testis. *Biol Reprod* 77:1060-1072
- Newman GR, Jasani B, Williams ED (1983) A simple post-embedding system for the rapid demonstration of tissue antigens under the electron microscope. *Histochem J* 15:543-555
- Novikoff AB, and Shin, W.Y (1964) The endoplasmic reticulum in the Golgi zone and its relations to microbodies, Golgi apparatus and autophagic vacuoles in rat liver cells *J Microsc (Paris)* 3:187-206
- Novikoff AB, Goldfischer S (1969) Visualization of peroxisomes (microbodies) and mitochondria with diaminobenzidine. *J Histochem Cytochem* 17:675-680
- Nyathi Y, Baker A (2006) Plant peroxisomes as a source of signalling molecules. *Biochim Biophys Acta* 1763:1478-1495
- Olivier LM, Krisans SK (2000) Peroxisomal protein targeting and identification of peroxisomal targeting signals in cholesterol biosynthetic enzymes. *Biochim Biophys Acta* 1529:89-102
- Ossendorp BC, Voorhout WF, van Golde LM, Wirtz KW, Batenburg JJ (1994) Identification of the non-specific lipid-transfer protein (sterol carrier protein 2) in peroxisomes of lung type II cells. *Biochem Biophys Res Commun* 205:1581-1588
- Ossendorp BC, Wirtz KW (1993) The non-specific lipid-transfer protein (sterol carrier protein 2) and its relationship to peroxisomes. *Biochimie* 75:191-200
- Otera H, Harano T, Honsho M, Ghaedi K, Mukai S, Tanaka A, Kawai A, Shimizu N, Fujiki Y (2000) The mammalian peroxin Pex5pL, the longer isoform of the mobile peroxisome targeting signal (PTS) type 1 transporter, translocates the Pex7p.PTS2 protein complex into peroxisomes via its initial docking site, Pex14p. *J Biol Chem* 275:21703-21714
- Otera H, Setoguchi K, Hamasaki M, Kumashiro T, Shimizu N, Fujiki Y (2002) Peroxisomal targeting signal receptor Pex5p interacts with cargoes and import machinery components in a spatiotemporally differentiated manner: conserved Pex5p WXXXF/Y motifs are critical for matrix protein import. *Mol Cell Biol* 22:1639-1655
- Panos RJ, Bak PM, Simonet WS, Rubin JS, Smith LJ (1995) Intratracheal instillation of keratinocyte growth factor decreases hyperoxia-induced mortality in rats. *J Clin Invest* 96:2026-2033
- Panos RJ, Rubin JS, Csaky KG, Aaronson SA, Mason RJ (1993) Keratinocyte growth factor and hepatocyte growth factor/scatter factor are heparin-binding growth factors for alveolar type II cells in fibroblast-conditioned medium. *J Clin Invest* 92:969-977
- Park EM, Park YM, Gwak YS (1998) Oxidative damage in tissues of rats exposed to cigarette smoke. *Free Radic Biol Med* 25:79-86
- Park EY, Cho IJ, Kim SG (2004) Transactivation of the PPAR-responsive enhancer module in chemopreventive glutathione S-transferase gene by the peroxisome proliferator-activated receptor-gamma and retinoid X receptor heterodimer. *Cancer Res* 64:3701-3713
- Patel HJ, Belvisi MG, Bishop-Bailey D, Yacoub MH, Mitchell JA (2003) Activation of peroxisome proliferator-activated receptors in human airway smooth muscle cells has a superior anti-inflammatory profile to corticosteroids: relevance for chronic obstructive pulmonary disease therapy. *J Immunol* 170:2663-2669
- Patel KM, Wright KL, Whittaker P, Chakravarty P, Watson ML, Ward SG (2005) Differential modulation of COX-2 expression in A549 airway epithelial cells by structurally distinct PPAR(gamma) agonists: evidence for disparate functional effects which are independent of NF-(kappa)B and PPAR(gamma). *Cell Signal* 17:1098-1110
- Pause B, Saffrich R, Hunziker A, Ansorge W, Just WW (2000) Targeting of the 22 kDa integral peroxisomal membrane protein. *FEBS Lett* 471:23-28
- Pedersen JI (1993) Peroxisomal oxidation of the steroid side chain in bile acid formation. *Biochimie* 75:159-165
- Pedersen JI, Gustafsson J (1980) Conversion of 3 alpha, 7 alpha, 12 alpha-trihydroxy-5 beta-cholestanoic acid into cholic acid by rat liver peroxisomes. *FEBS Lett* 121:345-348
- Pedersen JI, Kase, B. F, Prydz, K, Βφορκεμ, I (1987) Liver peroxisomes and bile acid formation. In: Fahimi HD and Sies H (Eds) *Peroxisomes in Biology and Medicine* Springer Verlag, Heidelberg S.67-77
- Petrik P (1971) Fine structural identification of peroxisomes in mouse and rat bronchiolar and alveolar epithelium. *J Histochem Cytochem* 19:339-348
- Pires JR, Hong X, Brockmann C, Volkmer-Engert R, Schneider-Mergener J, Oschkinat H, Erdmann R (2003) The ScPex13p SH3 domain exposes two distinct binding sites for Pex5p and Pex14p. *J Mol Biol* 326:1427-1435
- Plopper CG, Mariassy AT, Wilson DW, Alley JL, Nishio SJ, Nettesheim P (1983) Comparison of nonciliated tracheal epithelial cells in six mammalian species: ultrastructure and population densities. *Exp Lung Res* 5:281-294
- Pool MR, Lopez-Huertas E, Baker A (1998) Characterization of intermediates in the process of plant peroxisomal protein import. *EMBO J* 17:6854-6862
- Poosch MS, Yamazaki RK (1989) The oxidation of dicarboxylic acid CoA esters via peroxisomal fatty acyl-CoA oxidase. *Biochim Biophys Acta* 1006:291-298

References

- Portnoy J, Curran-Everett D, Mason RJ (2004) Keratinocyte growth factor stimulates alveolar type II cell proliferation through the extracellular signal-regulated kinase and phosphatidylinositol 3-OH kinase pathways. *Am J Respir Cell Mol Biol* 30:901-907
- Possmayer F (1990) The role of surfactant-associated proteins. *Am Rev Respir Dis* 142:749-752
- Poulos A, Sharp P, Singh H, Johnson DW, Carey WF, Easton C (1993) Formic acid is a product of the alpha-oxidation of fatty acids by human skin fibroblasts: deficiency of formic acid production in peroxisome-deficient fibroblasts. *Biochem J* 292 (Pt 2):457-461
- Prester T, Talalay P, Alam J, Ahn YI, Lee PJ, Choi AM (1995) Parallel induction of heme oxygenase-1 and chemoprotective phase 2 enzymes by electrophiles and antioxidants: regulation by upstream antioxidant-responsive elements (ARE). *Mol Med* 1:827-837
- Purdue PE, Lazarow PB (2001) Peroxisome biogenesis. *Annu Rev Cell Dev Biol* 17:701-752
- Qiao R, Yan W, Clavijo C, Mehrian-Shai R, Zhong Q, Kim KJ, Ann D, Crandall ED, Borok Z (2008) Effects of KGF on alveolar epithelial cell transdifferentiation are mediated by JNK signaling. *Am J Respir Cell Mol Biol* 38:239-246
- Qiao R, Zhou B, Liebler JM, Li X, Crandall ED, Borok Z (2003) Identification of three genes of known function expressed by alveolar epithelial type I cells. *Am J Respir Cell Mol Biol* 29:98-105
- Rahman I, MacNee W (1996) Role of oxidants/antioxidants in smoking-induced lung diseases. *Free Radic Biol Med* 21:669-681
- Rahman I, MacNee W (1998) Role of transcription factors in inflammatory lung diseases. *Thorax* 53:601-612
- Rahman I, MacNee W (2000) Oxidative stress and regulation of glutathione in lung inflammation. *Eur Respir J* 16:534-554
- Rahman I, Morrison D, Donaldson K, MacNee W (1996) Systemic oxidative stress in asthma, COPD, and smokers. *Am J Respir Crit Care Med* 154:1055-1060
- Rahman I, Yang SR, Biswas SK (2006) Current concepts of redox signaling in the lungs. *Antioxid Redox Signal* 8:681-689
- Ramirez MI, Millien G, Hinds A, Cao Y, Seldin DC, Williams MC (2003) T1alpha, a lung type I cell differentiation gene, is required for normal lung cell proliferation and alveolus formation at birth. *Dev Biol* 256:61-72
- Rannels DE, Rannels SR (1989) Influence of the extracellular matrix on type 2 cell differentiation. *Chest* 96:165-173
- Reed BD, Charos AE, Szekely AM, Weissman SM, Snyder M (2008) Genome-wide occupancy of SREBP1 and its partners NFY and SP1 reveals novel functional roles and combinatorial regulation of distinct classes of genes. *PLoS Genet* 4:e1000133
- Rehling P, Marzioch M, Niesen F, Wittke E, Veenhuis M, Kunau WH (1996) The import receptor for the peroxisomal targeting signal 2 (PTS2) in *Saccharomyces cerevisiae* is encoded by the PAS7 gene. *EMBO J* 15:2901-2913
- Reynders V, Loitsch S, Steinhauer C, Wagner T, Steinhilber D, Bargon J (2006) Peroxisome proliferator-activated receptor alpha (PPAR alpha) down-regulation in cystic fibrosis lymphocytes. *Respir Res* 7:104
- Rhodin J (1954) Correlation of ultrastructural organization and function in normal and experimentally changed proximal convoluted tubule cells in the mouse kidney. PhD thesis Karolinska Institute, Stockholm, Aktiebolaget Godvil
- Rice WR, Conkright JJ, Na CL, Ikegami M, Shannon JM, Weaver TE (2002) Maintenance of the mouse type II cell phenotype in vitro. *Am J Physiol Lung Cell Mol Physiol* 283:L256-264
- Ricote M, Li AC, Willson TM, Kelly CJ, Glass CK (1998) The peroxisome proliferator-activated receptor-gamma is a negative regulator of macrophage activation. *Nature* 391:79-82
- Rizzo G, Fiorucci S (2006) PPARs and other nuclear receptors in inflammation. *Curr Opin Pharmacol* 6:421-427
- Roels F (1976) Cytochemical demonstration of extraperoxisomal catalase. I. Sheep liver. *J Histochem Cytochem* 24:713-724
- Roels F, Geerts A, De Coster W, Goldfischer S (1982) Cytoplasmic catalase: cytochemistry and physiology. *Ann N Y Acad Sci* 386:534-536
- Roman J (1996) Extracellular matrix and lung inflammation. *Immunol Res* 15:163-178
- Rose ML, Rusyn I, Bojes HK, Belyea J, Cattley RC, Thurman RG (2000) Role of Kupffer cells and oxidants in signaling peroxisome proliferator-induced hepatocyte proliferation. *Mutat Res* 448:179-192
- Rosen ED, Walkey CJ, Puigserver P, Spiegelman BM (2000) Transcriptional regulation of adipogenesis. *Genes Dev* 14:1293-1307
- Rüdiger M, Kolleck I, Putz G, Wauer RR, Stevens P, Rüstow B (1998) Plasmalogens effectively reduce the surface tension of surfactant-like phospholipid mixtures. *Am J Physiol* 274:L143-148
- Rushmore TH, King RG, Paulson KE, Pickett CB (1990) Regulation of glutathione S-transferase Ya subunit gene expression: identification of a unique xenobiotic-responsive element controlling inducible expression by planar aromatic compounds. *Proc Natl Acad Sci U S A* 87:3826-3830
- Rushmore TH, Morton MR, Pickett CB (1991) The antioxidant responsive element. Activation by oxidative stress and identification of the DNA consensus sequence required for functional activity. *J Biol Chem* 266:11632-11639

References

- Saidowsky J, Dodt G, Kirchberg K, Wegner A, Nastainczyk W, Kunau WH, Schliebs W (2001) The di-aromatic pentapeptide repeats of the human peroxisome import receptor PEX5 are separate high affinity binding sites for the peroxisomal membrane protein PEX14. *J Biol Chem* 276:34524-34529
- Sakitani K, Nishizawa M, Inoue K, Masu Y, Okumura T, Ito S (1998) Synergistic regulation of inducible nitric oxide synthase gene by CCAAT/enhancer-binding protein beta and nuclear factor-kappaB in hepatocytes. *Genes Cells* 3:321-330
- Santos MJ, Imanaka T, Shio H, Small GM, Lazarow PB (1988) Peroxisomal membrane ghosts in Zellweger syndrome--aberrant organelle assembly. *Science* 239:1536-1538
- Schepers L, Casteels M, Vamecq J, Parmentier G, Van Veldhoven PP, Mannaerts GP (1988) Beta-oxidation of the carboxyl side chain of prostaglandin E2 in rat liver peroxisomes and mitochondria. *J Biol Chem* 263:2724-2731
- Scher JU, Pillinger MH (2005) 15d-PGJ2: the anti-inflammatory prostaglandin? *Clin Immunol* 114:100-109
- Schneeberger EE (1972a) A comparative cytochemical study of microbodies (peroxisomes) in great alveolar cells of rodents, rabbit and monkey. *J Histochem Cytochem* 20:180-191
- Schneeberger EE (1972b) Development of peroxisomes in granular pneumocytes during pre- and postnatal growth. *Lab Invest* 27:581-589
- Schrader M, Fahimi HD (2004) Mammalian peroxisomes and reactive oxygen species. *Histochem Cell Biol* 122:383-393
- Schrader M, Reuber BE, Morrell JC, Jimenez-Sanchez G, Obie C, Stroh TA, Valle D, Schroer TA, Gould SJ (1998) Expression of PEX11beta mediates peroxisome proliferation in the absence of extracellular stimuli. *J Biol Chem* 273:29607-29614
- Seedorf U, Brysch P, Engel T, Schrage K, Assmann G (1994) Sterol carrier protein X is peroxisomal 3-oxoacyl coenzyme A thiolase with intrinsic sterol carrier and lipid transfer activity. *J Biol Chem* 269:21277-21283
- Shannon JM, Jennings SD, Nielsen LD (1992) Modulation of alveolar type II cell differentiated function in vitro. *Am J Physiol* 262:L427-436
- Shijubo N, Itoh Y, Yamaguchi T, Sugaya F, Hirasawa M, Yamada T, Kawai T, Abe S (1999) Serum levels of Clara cell 10-kDa protein are decreased in patients with asthma. *Lung* 177:45-52
- Shimano H (2009) SREBPs: physiology and pathophysiology of the SREBP family. *FEBS J* 276:616-621
- Shiratori M, Oshika E, Ung LP, Singh G, Shinozuka H, Warburton D, Michalopoulos G, Katyal SL (1996) Keratinocyte growth factor and embryonic rat lung morphogenesis. *Am J Respir Cell Mol Biol* 15:328-338
- Simon DM, Arikan MC, Srisuma S, Bhattacharya S, Andalicio T, Shapiro SD, Mariani TJ (2006a) Epithelial cell PPARgamma is an endogenous regulator of normal lung maturation and maintenance. *Proc Am Thorac Soc* 3:510-511
- Simon DM, Arikan MC, Srisuma S, Bhattacharya S, Tsai LW, Ingenito EP, Gonzalez F, Shapiro SD, Mariani TJ (2006b) Epithelial cell PPAR[gamma] contributes to normal lung maturation. *FASEB J* 20:1507-1509
- Simon DM, Mariani TJ (2007) Role of PPARs and Retinoid X Receptors in the Regulation of Lung Maturation and Development. *PPAR Res* 2007:91240
- Singh H, Usher S, Johnson D, Poulos A (1990) A comparative study of straight chain and branched chain fatty acid oxidation in skin fibroblasts from patients with peroxisomal disorders. *J Lipid Res* 31:217-225
- Singh I, Moser AE, Goldfischer S, Moser HW (1984) Lignoceric acid is oxidized in the peroxisome: implications for the Zellweger cerebro-hepato-renal syndrome and adrenoleukodystrophy. *Proc Natl Acad Sci U S A* 81:4203-4207
- Singh RP, Singh I (1986) Peroxisomal oxidation of lignoceric acid in rat brain. *Neurochem Res* 11:281-289
- Slot JW, Geuze HJ (1981) Sizing of protein A-colloidal gold probes for immunoelectron microscopy. *J Cell Biol* 90:533-536
- Smith JJ, Marelli M, Christmas RH, Vizeacoumar FJ, Dilworth DJ, Ideker T, Galitski T, Dimitrov K, Rachubinski RA, Aitchison JD (2002) Transcriptome profiling to identify genes involved in peroxisome assembly and function. *J Cell Biol* 158:259-271
- Sorokin SP (1988) The Respiratory System: Cell and Tissue Biology. In: Weiss L (ed): Chapter 25, Sixth edn, Urban and Schwarzenberg, Munich:751-814, ISBN: 753-541-72176-72176
- Sosenko IR, Innis SM, Frank L (1991) Intralipid increases lung polyunsaturated fatty acids and protects newborn rats from oxygen toxicity. *Pediatr Res* 30:413-417
- South ST, Gould SJ (1999) Peroxisome synthesis in the absence of preexisting peroxisomes. *J Cell Biol* 144:255-266
- Spiegelman BM, Flier JS (1996) Adipogenesis and obesity: rounding out the big picture. *Cell* 87:377-389
- Stein K, Schell-Steven A, Erdmann R, Rottensteiner H (2002) Interactions of Pex7p and Pex18p/Pex21p with the peroxisomal docking machinery: implications for the first steps in PTS2 protein import. *Mol Cell Biol* 22:6056-6069
- Stolz DB, Zamora R, Vodovotz Y, Loughran PA, Billiar TR, Kim YM, Simmons RL, Watkins SC (2002) Peroxisomal localization of inducible nitric oxide synthase in hepatocytes. *Hepatology* 36:81-93

References

- Straus DS, Pascual G, Li M, Welch JS, Ricote M, Hsiang CH, Sengchanthalangsy LL, Ghosh G, Glass CK (2000) 15-deoxy-delta 12,14-prostaglandin J2 inhibits multiple steps in the NF-kappa B signaling pathway. *Proc Natl Acad Sci U S A* 97:4844-4849
- Stripp BR, Reynolds SD, Boe IM, Lund J, Power JH, Coppens JT, Wong V, Reynolds PR, Plopper CG (2002) Clara cell secretory protein deficiency alters clara cell secretory apparatus and the protein composition of airway lining fluid. *Am J Respir Cell Mol Biol* 27:170-178
- Subramani S (1998) Components involved in peroxisome import, biogenesis, proliferation, turnover, and movement. *Physiol Rev* 78:171-188
- Subramani S, Koller A, Snyder WB (2000) Import of peroxisomal matrix and membrane proteins. *Annu Rev Biochem* 69:399-418
- Sugahara K, Rubin JS, Mason RJ, Aronsen EL, Shannon JM (1995) Keratinocyte growth factor increases mRNAs for SP-A and SP-B in adult rat alveolar type II cells in culture. *Am J Physiol* 269:L344-350
- Sugiyama H, Nonaka T, Kishimoto T, Komoriya K, Tsuji K, Nakahata T (2000) Peroxisome proliferator-activated receptors are expressed in human cultured mast cells: a possible role of these receptors in negative regulation of mast cell activation. *Eur J Immunol* 30:3363-3370
- Swinkels BW, Gould SJ, Bodnar AG, Rachubinski RA, Subramani S (1991) A novel, cleavable peroxisomal targeting signal at the amino-terminus of the rat 3-ketoacyl-CoA thiolase. *EMBO J* 10:3255-3262
- Takeoka M, Ward WF, Pollack H, Kamp DW, Panos RJ (1997) KGF facilitates repair of radiation-induced DNA damage in alveolar epithelial cells. *Am J Physiol* 272:L1174-1180
- Terlecky SR, Fransen M (2000) How peroxisomes arise. *Traffic* 1:465-473
- Terlecky SR, Koepke JI, Walton PA (2006) Peroxisomes and aging. *Biochim Biophys Acta* 1763:1749-1754
- Thompson SL, Krisans SK (1990) Rat liver peroxisomes catalyze the initial step in cholesterol synthesis. The condensation of acetyl-CoA units into acetoacetyl-CoA. *J Biol Chem* 265:5731-5735
- Titorenko VI, Rachubinski RA (1998) The endoplasmic reticulum plays an essential role in peroxisome biogenesis. *Trends Biochem Sci* 23:231-233
- Tölle A, Meier W, Rüdiger M, Hofmann KP, Rüstow B (2002) Effect of cholesterol and surfactant protein B on the viscosity of phospholipid mixtures. *Chem Phys Lipids* 114:159-168
- Trifilieff A, Bench A, Hanley M, Bayley D, Campbell E, Whittaker P (2003) PPAR-alpha and -gamma but not -delta agonists inhibit airway inflammation in a murine model of asthma: in vitro evidence for an NF-kappaB-independent effect. *Br J Pharmacol* 139:163-171
- Ulich TR, Yi ES, Longmuir K, Yin S, Biltz R, Morris CF, Housley RM, Pierce GF (1994) Keratinocyte growth factor is a growth factor for type II pneumocytes in vivo. *J Clin Invest* 93:1298-1306
- Umland TC, Swaminathan S, Singh G, Warty V, Furey W, Pletcher J, Sax M (1994) Structure of a human Clara cell phospholipid-binding protein-ligand complex at 1.9 Å resolution. *Nat Struct Biol* 1:538-545
- Urquhart AJ, Kennedy D, Gould SJ, Crane DI (2000) Interaction of Pex5p, the type 1 peroxisome targeting signal receptor, with the peroxisomal membrane proteins Pex14p and Pex13p. *J Biol Chem* 275:4127-4136
- Uto H, Nakanishi C, Ido A, Hasuike S, Kusumoto K, Abe H, Numata M, Nagata K, Hayashi K, Tsubouchi H (2005) The peroxisome proliferator-activated receptor-gamma agonist, pioglitazone, inhibits fat accumulation and fibrosis in the livers of rats fed a choline-deficient, l-amino acid-defined diet. *Hepato Res* 32:235-242
- Vamecq J (1987) Liver peroxisomal oxidizing activities in physiological and pathological conditions. In: HD Fahimi and H Sies (eds) *Peroxisomes in Biology and Medicine* Springer-Verlag, Berlin, Heidelberg:364-373
- Vamecq J, de Hoffmann E, Van Hoof F (1985) Mitochondrial and peroxisomal metabolism of glutaryl-CoA. *Eur J Biochem* 146:663-669
- Van den Munckhof RJ, Denyn M, Tigchelaar-Gutter W, Schipper RG, Verhofstad AA, Van Noorden CJ, Frederiks WM (1995) In situ substrate specificity and ultrastructural localization of polyamine oxidase activity in unfixed rat tissues. *J Histochem Cytochem* 43:1155-1162
- Van Meir F, Scheuermann DW (1988) Microperoxisomes in type II pneumocytes and interstitial cells of postnatal rat lungs. *Cell Biol Int Rep* 12:579-586
- van Roermund CW, Drissen R, van Den Berg M, Ijlst L, Hettema EH, Tabak HF, Waterham HR, Wanders RJ (2001) Identification of a peroxisomal ATP carrier required for medium-chain fatty acid beta-oxidation and normal peroxisome proliferation in *Saccharomyces cerevisiae*. *Mol Cell Biol* 21:4321-4329
- van Roermund CW, Tabak HF, van Den Berg M, Wanders RJ, Hettema EH (2000) Pex11p plays a primary role in medium-chain fatty acid oxidation, a process that affects peroxisome number and size in *Saccharomyces cerevisiae*. *J Cell Biol* 150:489-498
- Van Veldhoven P, Mannaerts GP (1985) Comparison of the activities of some peroxisomal and extraperoxisomal lipid-metabolizing enzymes in liver and extrahepatic tissues of the rat. *Biochem J* 227:737-741

References

- Van Veldhoven PP, Casteels M, Mannaerts GP, Baes M (2001) Further insights into peroxisomal lipid breakdown via alpha- and beta-oxidation. *Biochem Soc Trans* 29:292-298
- Van Vyve T, Chanez P, Bernard A, Bousquet J, Godard P, Lauwerijs R, Sibille Y (1995) Protein content in bronchoalveolar lavage fluid of patients with asthma and control subjects. *J Allergy Clin Immunol* 95:60-68
- Vanhooren JC, Baumgart E, Fransen M, Mannaerts GP, Van Veldhoven PP (1996) Mammalian peroxisomal acyl-CoA oxidases. I. Molecular characterization of rat pristanoyl-CoA oxidase. *Ann N Y Acad Sci* 804:674-675
- Visser WF, van Roermund CW, Ijlst L, Waterham HR, Wanders RJ (2007) Metabolite transport across the peroxisomal membrane. *Biochem J* 401:365-375
- Vökl A, Mohr H, Weber G, Fahimi HD (1998) Isolation of peroxisome subpopulations from rat liver by means of immune free-flow electrophoresis. *Electrophoresis* 19:1140-1144
- Wanders RJ (2004) Metabolic and molecular basis of peroxisomal disorders: a review. *Am J Med Genet A* 126A:355-375
- Wanders RJ, Vreken P, Ferdinandusse S, Jansen GA, Waterham HR, van Roermund CW, Van Grunsven EG (2001) Peroxisomal fatty acid alpha- and beta-oxidation in humans: enzymology, peroxisomal metabolite transporters and peroxisomal diseases. *Biochem Soc Trans* 29:250-267
- Wang AC, Dai X, Luu B, Conrad DJ (2001) Peroxisome proliferator-activated receptor-gamma regulates airway epithelial cell activation. *Am J Respir Cell Mol Biol* 24:688-693
- Ward JE, Fernandes DJ, Taylor CC, Bonacci JV, Quan L, Stewart AG (2006) The PPARgamma ligand, rosiglitazone, reduces airways hyperresponsiveness in a murine model of allergen-induced inflammation. *Pulm Pharmacol Ther* 19:39-46
- Waters CM, Savla U, Panos RJ (1997) KGF prevents hydrogen peroxide-induced increases in airway epithelial cell permeability. *Am J Physiol* 272:L681-689
- Wiese S, Gronemeyer T, Ofman R, Kunze M, Grou CP, Almeida JA, Eisenacher M, Stephan C, Hayen H, Schollenberger L, Korosec T, Waterham HR, Schliebs W, Erdmann R, Berger J, Meyer HE, Just W, Azevedo JE, Wanders RJ, Warscheid B (2007) Proteomics characterization of mouse kidney peroxisomes by tandem mass spectrometry and protein correlation profiling. *Mol Cell Proteomics* 6:2045-2057
- Woerly G, Honda K, Loyens M, Papin JP, Auwerx J, Staels B, Capron M, Dombrowicz D (2003) Peroxisome proliferator-activated receptors alpha and gamma down-regulate allergic inflammation and eosinophil activation. *J Exp Med* 198:411-421
- Wouters FS, Bastiaens PI, Wirtz KW, Jovin TM (1998) FRET microscopy demonstrates molecular association of non-specific lipid transfer protein (nsL-TP) with fatty acid oxidation enzymes in peroxisomes. *EMBO J* 17:7179-7189
- Yamamoto K, Vökl A, Hashimoto T, Fahimi HD (1988) Catalase in guinea pig hepatocytes is localized in cytoplasm, nuclear matrix and peroxisomes. *Eur J Cell Biol* 46:129-135
- Yang L, Yan D, Yan C, Du H (2003) Peroxisome proliferator-activated receptor gamma and ligands inhibit surfactant protein B gene expression in the lung. *J Biol Chem* 278:36841-36847
- Yano T, Deterding RR, Simonet WS, Shannon JM, Mason RJ (1996) Keratinocyte growth factor reduces lung damage due to acid instillation in rats. *Am J Respir Cell Mol Biol* 15:433-442
- Yi ES, Salgado M, Williams S, Kim SJ, Masliah E, Yin S, Ulich TR (1998) Keratinocyte growth factor decreases pulmonary edema, transforming growth factor-beta and platelet-derived growth factor-BB expression, and alveolar type II cell loss in bleomycin-induced lung injury. *Inflammation* 22:315-325
- Yi ES, Williams ST, Lee H, Malicki DM, Chin EM, Yin S, Tarpley J, Ulich TR (1996) Keratinocyte growth factor ameliorates radiation- and bleomycin-induced lung injury and mortality. *Am J Pathol* 149:1963-1970
- Yokota S, Oda T, Fahimi HD (2001) The role of 15-lipoxygenase in disruption of the peroxisomal membrane and in programmed degradation of peroxisomes in normal rat liver. *J Histochem Cytochem* 49:613-622
- Zoeller RA, Lake AC, Nagan N, Gaposchkin DP, Legner MA, Lieberthal W (1999) Plasmalogens as endogenous antioxidants: somatic cell mutants reveal the importance of the vinyl ether. *Biochem J* 338 (Pt 3):769-776

10 Index of abbreviations

For abbreviations of enzyme names see table 4, page 28

| | |
|----------------------------------|---|
| APS | Ammonium persulfate |
| BLAST | Basic Local Alignment Search Tool |
| BSA | Bovine serum albumin |
| cDNA | Complementary deoxyribonucleic acid |
| °C | Degree celcius |
| DNA | Deoxyribonucleic acid |
| Na ₂ HPO ₄ | Disodium hydrogen phosphate |
| DTT | 1,4-dithio-DL-threitol |
| EDTA | Ethylene-diamine tetraacetate |
| h | Hour(s) |
| IgG | Immunoglobulin G |
| KH ₂ PO ₄ | Potassium dihydrogen phosphate |
| min | Minute(s) |
| M | Molar |
| mg | Milligram |
| ml | Millilitre |
| µg | Micrograms |
| µl | Microliter |
| µm | Micrometer |
| NCBI | National Centre for Biotechnology Information |
| ng | Nanograms |
| % | Percentage |
| PBD | Peroxisome biogenesis disorder |
| PBS | Phosphate-buffered saline |
| PBST | Phosphate-buffered saline with Tween |
| PCR | Polymerase chain reaction |
| PEX | Gene encoding a peroxin (peroxisome biogenesis protein) |
| PFA | Paraformaldehyde |
| PMP | Peroxisomal membrane protein |
| PPAR | Peroxisomal proliferators activated receptors |
| PTS | Peroxisomal targeting signal |
| RNA | Ribonucleic acid |
| RT | Room temperature |
| s | Second(s) |
| SDS-PAGE | Sodium dodecyl sulfate polyacrylamide gel electrophoresis |
| NaOH | Sodium hydroxide |
| TAE | Tris acetate EDTA buffer |
| TEMED | N, N, N, N-tetramethylethylenediamine |
| Tris | Tris (hydroxymethyl) aminomethane |
| v/v | Volume/volume |
| w/v | Weight/volume |

11 Acknowledgments

At the outset, I wish to express my profound heart felt thanks to my supervisor Prof. Baumgart-Vogt for giving me an opportunity to conduct research work. She has been a great support for me throughout my research work. Her observations and critical suggestions have intensified my thinking into finding new ways to deal with the research. Discussions with her always used to give good clues thwarting away the crisis periods and gave me a focus and vision of my scientific journey, I appreciate her keen interest and time in my scientific career and her attitude of helping in crucial times. She encouraged and facilitated my attendance to several national and international conferences, which exposed me to various scientists in my field and gave me an opportunity to feel and understand the science. She made my career not only in terms of scientific research oriented career but also taught how to be a good social, moral and honest human being. Without her motivation, encouragement and continuous support, I would not have considered a successful scientific career in pulmonary cell biology. The journey of my PhD research work under her guidance and supervision, I developed a new part of life that consists of a "FOCUS – VISION – POSITIVE ATTITUDE". At this stage, about my carrer and life all I can feel is **"THANK YOU MAM – YOU ARE MY BEST MENTOR"**.

I am also thankful to Dr. Klaus Peter Valerius for providing assistant and support to breed the animals especially PEX11 β KO mice. Special warm-hearted thanks to Dr. Wieland Stöckmann for this timely help in all times without any hesitation. I express my sincere gratitude to Dr. Barbara Ahlemeyer and Dr. Werner Kovacs for their helpful discussions in crisis periods. No work would be completed with out the help of technical staff and I owe my deep sense of gratitude to Magdalene Gottwald, Elke Richter and Andreas Klein, for all of their help in making working conditions comfortable. I am indebted to all the staff at Institute of anatomy and medical cell biology II for their whole hearted help and making my research work comfortable. I am thankful to Erike Hellmann and Silvia Heller secretaries to Prof. Baumgart-Vogt for helping me to get over all the bureaucracy matters. Special thanks to my colleague Qian Guofeng for his best companionship all the way of my research.

Acknowledgments

Friends have always been my strength and it is a delight to acknowledge all those who have been with me for various periods. Specially, I would like to address thanks to my dear wife **Manvi Porwal** for her immense love, support, suggestion and patience. I also would like to acknowledge my parents **Mr. Karnati Sathyanarayana** and **Mrs. Swarajya Laxmi**, my parent in-laws **Dr. R.K. Porwal, Mrs. Renu Porwal**, my sisters, and all family members and friends for their continuous support and encouragement through out my thesis work. Finally, special thanks to the PhD program of the Medical Faculty of the Justus Liebig University, Giessen.

**Der Lebenslauf wurde aus der elektronischen
Version der Arbeit entfernt.**

**The curriculum vitae was removed from the
electronic version of the paper.**

- ❖ Received a “**Young Scientist Travel Award 2008**” from European Life Scientist Organization (ELSO Meeting), Nice, France.

Scientific Publications:

1. **Karnati S**, Baumgart-Vogt E (2009) Peroxisomes in airway epithelia and future prospects of these organelles for pulmonary cell biology. *Histochem Cell Biol.* Apr; 131(4):447-54.
2. **Karnati S**, Baumgart-Vogt E (2008) Peroxisomes in mouse and human lung: Their involvement in pulmonary lipid metabolism. *Histochem Cell Biol.* Oct; 130(4):719-40.
3. Kilian O, Wenisch S, **Karnati S**, Baumgart-Vogt E, Hild A, Fuhrmann R, Jonuleit T, Dingeldein E, Schnettler R, Franke RP (2008) Microvasculature of bone defects filled with biodegradable nanoparticulate hydroxyapatite – an experimental study on miniature pigs. *Biomaterials.* Aug-Sep; 29(24-25):3429-37.

Scientific Publications In Progress:

1. **Karnati S**, Baumgart-Vogt E: Impaired peroxisome proliferation by knockout of PEX11 β leads to alterations in ROS metabolism in lung conducting airways. Experimental part finished - Manuscript finished and to be submitted shortly.
2. **Karnati S**, Baumgart-Vogt E: Differential expression of peroxisomal proteins during the postnatal development of the mouse lung – Manuscript in preparation.

Scientific presentations:

All abstracts reviewed and selected for oral presentations

1. **Karnati S**, Baumgart-Vogt E: Severe metabolic disturbances in Clara cells and alveolar epithelial cells due to peroxisome deficiency in the lung of PEX11 β -knockout mice (**oral presentation**). 103rd International Congress of the Anatomical Gesellschaft 2008, Innsbruck, Austria.
2. **Karnati S**, Baumgart-Vogt E: Impaired peroxisome proliferation by knockout of PEX11 β leads to alterations in ROS metabolism and cell-type specific differentiation markers in the mouse lung (**oral presentation**). 50th Symposium of the Society for Histochemistry 2008, Interlaken, Switzerland.
3. **Karnati S**, Baumgart-Vogt E: Alteration of ROS metabolism and cell type-specific differentiation markers in the lungs of PEX11 β (-/-) mice, a mouse model deficient in

peroxisome proliferation (**oral presentation**). European Respiratory Society Annual Congress (ERS) 2008, Berlin, Germany.

4. **Karnati S**, Baumgart-Vogt E: Alteration of ROS metabolism and cell type-specific differentiation markers in the lungs of PEX11 β (-/-) mice, a mouse model deficient in peroxisome proliferation (**oral presentation**). *104th International Congress of the Anatomical Gesellschaft 2009*, Antwerp, Belgium.

All abstracts reviewed and selected for poster presentations

1. **Karnati S**, Baumgart-Vogt E: Characterization of peroxisomes in alveolar type II cells of the adult mouse lung. *Annual Meeting of the German Society for Cell Biology 2005*, Heidelberg, Germany.
2. **Karnati S**, Baumgart-Vogt E: Heterogeneity of peroxisomes in distinct cell types of the adult mouse lung: Selective enrichment of peroxisomal metabolic enzymes in alveolar type II cells. *22nd Arbeitstagung der Anatomischen Gesellschaft 2005*, Würzburg, Germany.
3. **Karnati S**, Baumgart-Vogt E: Characterization of peroxisomes in alveolar type II cells of the adult mouse and human lung. *European Peroxisome Meeting 2006*, Leuven, Belgium.
4. **Karnati S**, Baumgart-Vogt E: Alteration of ROS metabolism and reduction of CC10 and T1 α in PEX11 β deficient mouse lungs. *Annual Meeting of the German Society for Cell Biology 2007*, Frankfurt, Germany.
5. **Karnati S**, Baumgart-Vogt E: Imbalance of antioxidative enzymes in PEX11 β deficient mouse lungs. *102nd International Congress of the Anatomical Gesellschaft Anatges2007*, Giessen, Germany.
6. **Karnati S**, Baumgart-Vogt E: Down-regulation of peroxisomal metabolic enzymes during transition of alveolar Type II – Type I cells. *American Thoracic Society (ATS) 2007*, San Francisco, USA.
7. **Karnati S**, Baumgart-Vogt E: Pathological consequences of peroxisome-dysfunction in the lung. *103rd International Congress of the Anatomical Gesellschaft 2008*, Innsbruck, Austria.
8. Grant P, Berg T, **Karnati S**, Nenicu A, Ahlemeyer B, Baumgart-Vogt E: A novel approach with high sensitivity to the localization of peroxisomes in tissue sections and cell cultures. *103rd International Congress of the Anatomical Gesellschaft 2008*, Innsbruck, Austria.
9. **Karnati.S**, Baumgart-Vogt E: Imbalance of antioxidative enzymes and alterations in epithelial lineage differentiation markers in the lungs of PEX11 β (-/-) mice, deficient in peroxisome proliferation. European Life Scientist Organization meeting (ELSO) 2008, Nice, France.

10. **Karnati S**, Baumgart-Vogt E: Alterations of the peroxisomal compartment during the transdifferentiation process of alveolar type II – type I cells. *25th Arbeitstagung der Anatomischen Gesellschaft 2008*, Würzburg, Germany.
11. **Karnati S**, Baumgart-Vogt E: Impaired peroxisome proliferation by knockout of PEX11 β leads to alterations in ROS metabolism and cell-type specific differentiation markers in the mouse lung. *50th Symposium of the Society for Histochemistry 2008*, Interlaken, Switzerland.

édition scientifique

VVB LAUFERSWEILER VERLAG

VVB LAUFERSWEILER VERLAG
STAUFBENBERGRING 15
D-35396 GIESSEN

Tel: 0641-5599888 Fax: -5599890
redaktion@doktorverlag.de
www.doktorverlag.de

ISBN 3-8359-5434-2



9 785835 195434 2 ©